Linear Bilateral Extended 2,2′:6′,2′′-Terpyridine: Versatile Building Block in Supramolecular Chemistry

Dissertation

zur

Erlangung der naturwissenschaftlichen Doktorwürde

(Dr. sc. nat.)

vorgelegt der

Mathematisch-naturwissenschaftlichen Fakultät

der

Universität Zürich

von

Janis Veliks

aus Lettland

Promotionskomitee

Prof. Dr. Jay S. Siegel (Vorsitz)

Prof. Dr. Kim K. Baldridge

PD Dr. Nathaniel S. Finney

Dr. Henning J. Jessen

Zürich, 2014

Die vorliegende Arbeit wurde von

der Mathematisch-naturwissenschaftlichen Fakultät

der Universität Zürich im Januar 2014

als Dissertation angenommen.

Promotionskomitee:

Prof. Dr. Jay S. Siegel (Vorsitz)

Prof. Dr. Kim K. Baldridge

PD Dr. Nathaniel S. Finney

Dr. Henning J. Jessen

Universität Zürich, 2014

CURRICULUM VITAE
Jānis VELIKS

EDUCATION:

2010 – 2014	PhD studies in Organic Chemistry at University of Zurich. PhD thesis: "*Linear Bilateral Extended 2,2′:6′,2″-Terpyridine: Versatile Building Block in Supramolecular Chemistry*", supervisor Prof. Jay S. Siegel
2008 – 2010	Graduated M.Sc. degree in Chemical Engineering at Riga Technical University, Latvia. Master's thesis "*Total Synthesis of New Furanocembranoid*", supervisor PhD Vilnis Liepins
2004 – 2008	Graduated B.Sc. degree in Chemical Engineering at Riga Technical University, Latvia. Undergraduate thesis "*Synthesis and Reactions of Substituted in Indene Ring 5-Oxo-1H-4,5-dihydroindeno[1,2-b]pyridines* ", supervisor PhD Dzintra Muceniece
2001 – 2004	Daugavpils State Gymnasium, Latvia
1993 – 2001	Daugavpils Saskaņas Primary School, Latvia

PROFESSIONAL EXPERIENCE:

2010 – 2014	University of Zürich, Institute of Organic Chemistry, doctoral research associate. Teaching Assistant, Organisch-chemische Praktikum
2008 – 2010	"Syntagon Baltic", laboratory assistant
2005 – 2008	Latvian Institute of Organic Synthesis, laboratory assistant

PUBLICATIONS:

Veliks, J.; Tseng, J.-C.; Arias, K.; Weisshar, F; Linden, A.; Siegel, J. S. Linear Bilateral Extended 2,2′:6′,2″-Terpyridine Ligands: Building Blocks for Heterometallic MOFs. *Manuscript in Preparation.*

Veliks, J.; Siegel, J. S. Three Steps in One-pot: Synthesis of Linear Bilateral Extended 2,2′:6′,2″-Terpyridine Ru(II) Complexes. *Manuscript in Preparation.*

PRESENTATIONS:

"*Towards Heterometallic Molecular Grids: Synthesis of Bipyridine and Terpyridine-Based Polytopic Ligands*", Janis Veliks, Karla Arias, Jui-Chang Tseng, Jay S. Siegel poster presented at 17th European Symposium on Organic Chemistry (Crete, Greece, 10-15 July 2011)

"*Towards Heterometallic Molecular Grids: Synthesis of Bipyridine and Terpyridine-Based Polytopic Ligands*", Janis Veliks, Karla Arias, Jui-Chang Tseng, Jay S. Siegel poster presented at Gordon Research Conference, Stereochemistry (Newport, RI, USA, July 29 - August 3, 2012)

"*Towards Heterometallic Molecular Grids: Synthesis of Bipyridine and Terpyridine-Based Polytopic Ligands*", Janis Veliks, Karla Arias, Jui-Chang Tseng, Jay S. Siegel oral

presentation at Swiss Chemical Society Fall Meeting 2012 (Zurich, ZH, Switzerland, September 13, 2012)

"*Towards the Kinetic Synthesis of the Molecular Borromean Link*", Janis Veliks, Helen Seifert, Derik K. Frantz, Anthony Linden, Jay S. Siegel poster presented at 15th International Symposium on Novel Aromatic Compounds 2013 (Taipei, Taiwan, July 28 - August 2, 2013)

"*Linear Terpyridine: Versatile Building Block in Supramolecular Chemistry*", Janis Veliks, Jay S. Siegel oral presentation at Tohoku University's Chemistry Summer School 2013 (Tohoku, Japan, August 28 - August 31, 2013)

SCHOLARSHIPS:

2009 – 2010	European Social Foundation Scholarship "Support for the Implementation of Master Studies at Riga Technical University"
2008 – 2009	Scholarship of JSC «Grindeks» Foundation for the Support of Science and Education, 2008/2009
2006 – 2007	Scholarship of JSC «Grindeks» Foundation for the Support of Science and Education, 2006/2007

Acknowledgements

Prof. Dr. Jay S. Siegel
PD Dr. Anthony Linden
Prof. Dr. Kim K. Baldridge
Dr. Henning J. Jessen
PD Dr. Nathaniel S. Finney

UZH NMR and MS Service

Dr. Jui-Chang Tseng, Dr. Karla I. Arias, Dr. Derik K. Frantz, Helen Seifert, Andrew Raub, Florian Weisshar, Dr. Andres Kaech, Peter Ueberhalt
All Siegel, Finney, Jessen and Stuparu group members past and present

My wife Ilga

Parents Regina and Ivars

Brother Maris

Grandparents Stanislavs and Anna

ABSTRACT OF THE DISSERTATION

Linear Bilateral Extended 2,2′:6′,2″-Terpyridine: Versatile Building Block in Supramolecular Chemistry

by

Janis Veliks

Doctor of Philosophy in Chemistry

University of Zurich, 2014

Professor Jay S. Siegel

The rational design and synthesis of supramolecular architectures and metal-organic frameworks (MOFs) require building blocks with defined dimensions, topology, and functions. Combination of organic ligands and metal ions allows accessing angles and topologies that are unavailable if only organic motifs are used. Therefore, there is a constant need for novel construction materials to tackle different challenging supramolecular targets.

The aim of this thesis is to study tridentate 2,2′:6′,2″-terpyridine (*terpy*) based ligands, which mimic the linear geometry of bidentate 5,5′-functionalized 2,2′-bipyridine. Therefore, the concept of *linear bilateral extended terpy* was introduced by fusing five-membered furan rings at the flanking positions of the 2,2′:6′,2″-terpyridine. In this way substituents can be placed almost perpendicular to the coordination vector of *terpy*. This ligand design allows the synthesis of metal complexes which have both octahedral geometry and topological properties of linear 2,2′-bipyridine.

At first, the synthesis of 2,6-bis(2-substituted-furo[2,3-c]pyridine-5-yl)pyridine derivatives (linear bilateral extended *terpy*), previously developed in Siegel group, was improved and optimized. The corresponding alkyl, aryl, and heteroaryl substituted ligands were successfully prepared. The synthesis of 2:1 ligand to metal complexes with metals preferring octahedral geometry (Fe^{2+}, $Ru^{2+}$and Zn^{2+}) afforded molecular “crossings” and “corners”. The X-ray crystallography showed that the flanking substituents at these complexes are spanned relative to each other with an obtuse angle, which increases in the sequence of Fe^{2+}<Ru^{2+}<Zn^{2+}. The photophysical properties of both ligands and metal complexes in solution and solid state were studied.

The Ru(II) complex of non-symmetric mixed bipyridine/terpyridine ligand with Δ-TRISPHAT^{-} counterion in dichloromethane exhibits unusual thixotropic gelation properties. The critical gelation concentration of this metallogelator is 1.13 wt% (4.8 mM) at room temperature.

Furthermore, a novel synthetic methodology towards the linear bilateral extended *terpy* Ru(II) complexes, starting from 5,5″-*bis*-(methoxymethoxy)-4,4″-*bis*-(substituted-ethynyl)-2,2′:6′,2″-terpyridines, was developed, which involves one-pot MOM cleavage, cycloisomerization, and metal complexation.

The Fe(II) containing molecular "crossing" bearing 4-pyridyl substituents at the flanking positions in the presence of Cu(I), or Ag(I) ions assembled into the 2D, or 3D heterometallic MOFs, respectively. The MOF based on Fe(II) and Ag(I) consists of a twofold interpenetrated 3D network with the diamondoid topology, whereas Fe(II), Cu(I) MOF is made of 2D honeycomb-like layers.

Finally, this thesis describes synthetic efforts towards the long-standing goal – the kinetic synthesis of the molecular Borromean link. Linear bilateral extended terpyridine ligands possess valuable geometric properties, which facilitated significant progress towards this goal. The revised route involves the synthesis of the threaded ring-in-ring complex containing functionalized linear *terpy* ligands suitable for the Eglinton reaction. The final macrocyclization step proved to be chemically feasible – the mass-spectroscopic data supports that the product with an expected molecular weight was obtained, but the formation of other topological isomers of the Borromean link cannot be excluded. Therefore, in order to prove the correct topology unambiguously, additional evidences should be provided in future. These results establish a solid base for further investigations towards the kinetic synthesis of the molecular Borromean link.

ZUSAMMENFASSUNG DER DISSERTATION

Linear bilateral erweitertes 2,2′:6′,2″-Terpyridin: Ein vielseitiger Baustein in der Supramolekularen Chemie

von

Janis Veliks

Doctor of Philosophy in Chemistry

University of Zurich, 2014

Professor Jay S. Siegel

Das rationale Design supramolekularer Architekturen und metall-organischer Gerüste (MOFs) erfordert Bausteine mit definierten Dimensionen, Topologien und Funktionen. Die Kombination organischer Liganden mit Metallionen ermöglicht Winkel und Topologien, welche nicht verfügbar wären, falls nur organische Bestandteile verwendet würden. Um verschiedene anspruchsvolle Zielverbindungen anzugehen, besteht somit ein konstanter Bedarf an neuartigen Bauteilen.

Ziel dieser Doktorarbeit ist die Untersuchung dreizähniger, auf 2,2':6',2''-Terpyridin (*terpy*) basierender Liganden, welche die lineare Geometrie zweizähniger 5,5'-funktionalisierter 2,2'-Bipyridine nachahmen. Es wurde das Konzept des *linear bilateral erweiterten terpy* eingeführt und fünfgliedrige Furanringe in die flankierenden Positionen des 2,2':6',2''-Terpyridin eingebaut. Hiermit können Substituenten fast rechtwinklig zum Koordinationsvektor des *terpy* angebracht werden. Die Bauform dieses Liganden ermöglich die Synthese von Metallkomplexen welche eine oktaedrische Geometrie und die topologischen Eigenschaften des linearen 2,2'-Bipyridin aufweisen.

In einem ersten Schritt wurde die Synthese von 2,6-bis(2-substituierte-Furo[2,3-c]pyridin-5-yl)pyridin-Derivaten, welche in der Siegel-Gruppe entwickelt worden war, optimiert. Die entsprechenden alkyl-, aryl-, und heteroarylsubstituierten Liganden wurden erfolgreich dargestellt. Die Synthese von Komplexen mit zwei Liganden pro Metall, welches die oktaedrische Geometrie bevorzugt (Fe^{2+}, Ru^{2+} und Zn^{2+}), ergab molekulare “Kreuze” und “Ecken”. Die Röntgenstrukturanalyse zeigte, dass die flankierenden Substituenten in einem stumpfen Winkel zueinander stehen, welcher in der Sequenz Fe^{2+}<Ru^{2+}<Zn^{2+} zunimmt. Die photophysikalischen Eigenschaften der Liganden und Metallkopmlexe in Lösung wurden zudem untersucht.

Der Ru(II)-Komplex nicht-symmetrischer gemischter Bipyridin/Terpyridin-Liganden mit Δ-TRISPHAT$^-$-Gegenionen in Dichlormethan wies aussergewöhnliche thixotropische

Vergelungseigenschaften auf. Die kritische Vergelungskonzentration dieses Metallogelators bei Raumtemperatur liegt bei 1.13 Gew.-% (4.8 mM).

Weiter wurde eine neuartige synthetische Methodologie in Richtung linear bilateral erweiterter *terpy*-Ru(II)-Komplexen, ausgehend von 5,5″-*bis*-(Methoxymethoxy)-4,4″-*bis*-(substituierte-ethynyl)-2,2′:6′,2″-terpyridinen, entwickelt, welche eine Eintopf-Sequenz mit der Abspaltung von MOM, der Zykloisomerisierung und der Metallkomplexierung umfasst.

Das Fe(II) enthaltende molekulare "Kreuz", das an den flankierenden Positionen 4-Pyridyl-Substituenten aufweist, assemblierte in der Anwesenheit von Cu(I)- oder Ag(I)-Ionen zu heterometallischen 2D- respektive 3D-MOFs. Der auf Fe(II) und Ag(I) basierende MOF besteht aus zweifach ineinander gewobenen 3D-Netwerken mit diamantoider Topologie, während der Fe(II)-Cu(I)-MOF aus wabenartigen 2D-Schichten besteht.

Schliesslich beschreibt diese Doktorarbeit synthetische Bemühungen in Richtung des langjährigen Ziels – die kinetische Synthese der molekularen Borromäischen Verknüpfung. Linear bilateral erweiterte Terpyridin-Liganden besitzen nützliche geometrische Eigenschaften, welche einen signifikanten Fortschritt in Richtung dieses Ziels ermöglichten. Der überarbeitete Syntheseweg schliesst die Synthese des Ring-in-Ring-Komplex mit ein, der über funktionalisierte lineare *terpy*-Liganden verfügt, die für die Eglington-Reaktion geeignet sind. Der abschliessende Makrozyklisierungsschritt erwies sich als chemisch durchführbar – die massenspektroskopischen Daten bekräftigen, dass das Produkt mit der entsprechenden molekularen Masse erhalten wurde, die Bildung anderer topologischer Isomere der Borromäischen Verknüpfung kann jedoch nicht ausgeschlossen werden. Um die korrekte Topologie eindeutig zu beweisen, müssen deshalb in Zukunft weitere Nachweise geliefert werden. Diese Resulate bilden ein solides Fundament für weitere Untersuchungen zur kinetischen Synthese der Borromäischen Verknüpfung.

Table of Contents

Chapter 1. Directional Building Blocks in Supramolecular Chemistry

1.1. Introduction

In order to build macroscopic objects, for example, a two-dimensional fence or a three-dimensional building (Figure 1.1), appropriate construction materials are needed. The design of architectures on the molecular scale also requires building blocks with defined dimensions, angles, and chemical properties.

Figure 1.1. Designed macroscopic objects: 2D fence and 3D building.[1,2]

It is important to have a library from where chemists can select the most suitable starting materials, which fulfil both the topology and function of the expected synthetic target. Biological systems are excellent examples where relatively limited amount of building blocks, like amino acids and nucleotides, act as construction materials for the synthesis of complicated nanomachines – ATP-synthase or ion pumps, efficient and specific catalytic systems – enzymes, and molecules for information storage – DNA.[3]

In 1960s-70s, supramolecular chemistry emerged from the seminal work of Lehn[4], Pedersen[5], and Cram[6]. Inspired by biochemistry and materialized by the tools of organic and inorganic chemistry, it deals with non-covalent interactions such as hydrogen-bonding, donor-acceptor, π-π interactions, metal coordination, mechanical bonding, and others.[7,8] Since the birth of this field, supramolecular chemistry has become an important driving force for creating new materials with valuable properties.[7,9-11]

Metal coordination with organic ligands is one of the most commonly used design elements, offering a vast range of interactions – from weak and labile to strong and inert[12]. Geometries of metal coordination spheres have a predictable character, which is an important feature for the design. Also, directional ligands with defined coordination sites (Figure 1.2) predetermine the geometry of assemblies. A rapidly growing field of metal-organic frameworks (MOFs) successfully applies such design principles by using metal nodes and organic spacers[13].

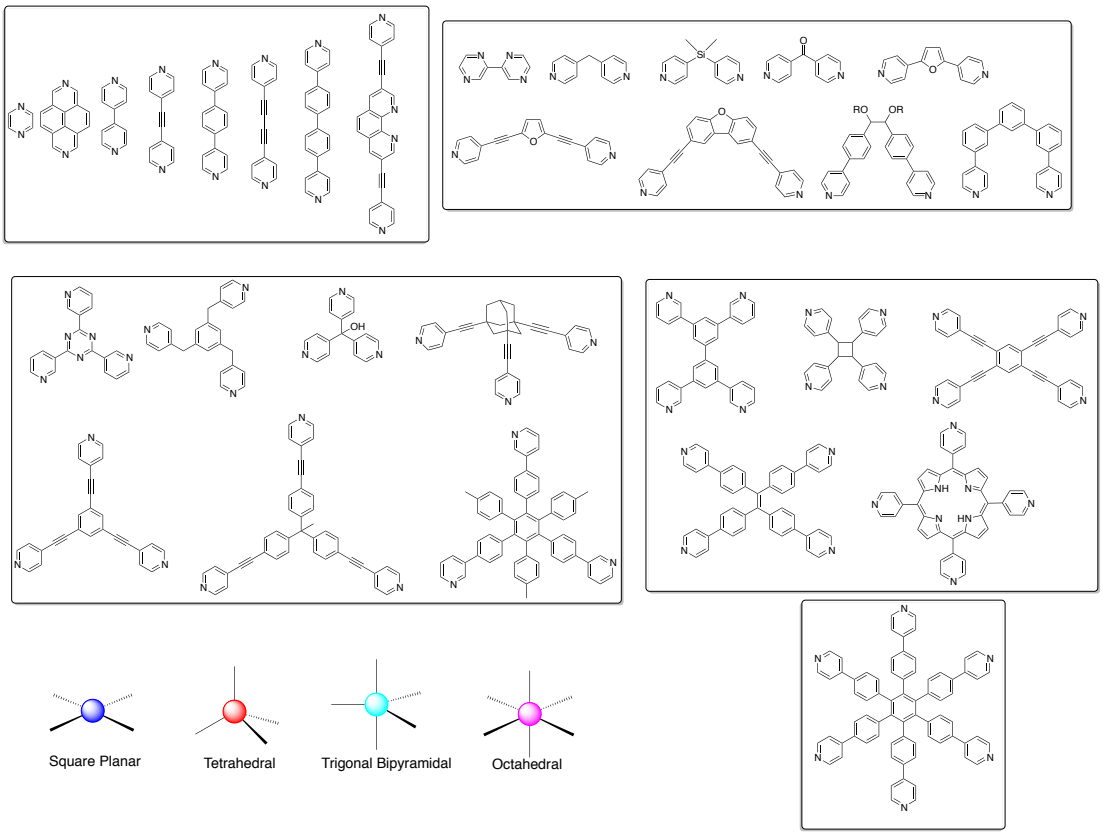

Figure 1.2. Directional pyridine based ligands and common transition metal coordination geometries.[14]

Therefore, there is a constant need for new molecules possessing defined geometry and functions. This thesis deals with the synthesis, characterization and supramolecular applications of novel tridentate ligands based on 2,6-bis(2-substituted-furo[2,3-c]pyridine-5-yl)pyridine scaffold* (Figure 1.3, B). These ligands are topological analogs of bidentate 5,5′-substituted-2,2′-bipyridines (*bipy*) – a complement to the directional "Stub", "W", "V or Λ", and "C" 2,2′:6′,2″-terpyridines (*terpy*) (Figure 1.3, A). This ligand design allows the synthesis of metal complexes which have both octahedral geometry and topological properties of linear 2,2′-bipyridine. The following work shows that such building blocks have various applications in supramolecular chemistry, like the assembly of heterometallic MOFs, thixotropic metal-organic gels, and the design element towards the synthesis of the molecular Borromean link.

* In this thesis such ligands are referred to as *linear bilateral extended terpyridines* or simply as *linear terpy*.

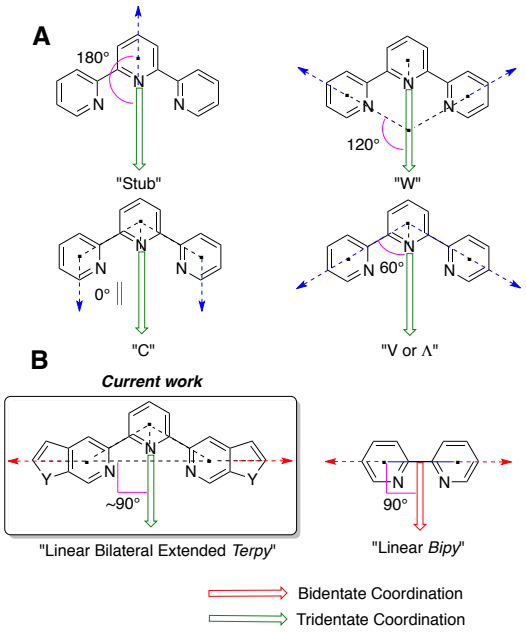

Figure 1.3. A. The "Stub", "W", "V or Λ", and "C" motifs based on *terpy*. **B.** Fused five-membered rings to *terpy* mimicking 5,5′-functionalized *bipy*.

This chapter provides a short overview of the importance of directional building blocks in supramolecular chemistry and the field of MOFs, highlighting the heterometallic MOFs. Also, the most important routes towards the synthesis of 2,2′:6′,2″-terpyridine derivatives are shortly summarized.

1.2. Thermodynamic Assembly versus Kinetic Synthesis

Depending on the strengths and stability of the non-covalent interactions, two completely different approaches towards the synthesis of supramolecular assemblies can be distinguished. *Thermodynamic assembly*[15], or as many refer to it as "self-assembly"[7,10,16], deals with the dynamic character of kinetically labile interactions (Figure 1.4). The multicomponent mixture undergoes kinetically reversible reaction, and the outcome is driven by the shift of the equilibrium towards the thermodynamically most stable product. Such approach often is extremely efficient, because it usually involves only one step, thus providing highly advanced assemblies in just one pot[17].

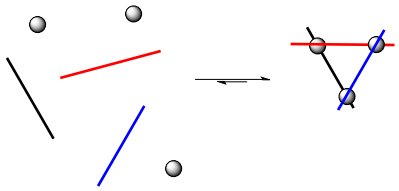

Figure 1.4. Thermodynamic assembly of the supramolecular architectures.

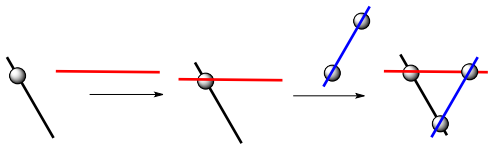

Figure 1.5. Kinetic or stepwise synthesis of the supramolecular architectures.

However, the outcome of such approach is often difficult to predict, and in many successful examples serendipity plays a crucial role[18,19]. The results are often rationalized after the actual product has been obtained.[20-22]

The *kinetic synthesis* is a diametrically opposite approach, which is based on the step-by-step construction of the supramolecular target via kinetically stable intermediates and irreversible reactions (Figure 1.5), offering the synthesis of otherwise inaccessible products[23-26]. This approach offers greater predictability, which is an important key factor for the rational design. In my opinion, such approach has more intellectual beauty than "simply mixing things together" and hoping for the positive outcome. However, multistep syntheses often have several drawbacks: they are more laborious, the total yields are lower, and sometimes a complicated purification is required. Nevertheless, both approaches require the building blocks with defined and predictable geometry in order to reach the expected synthetic targets.

1.3. Directional Building Blocks and Metal Coordination-Driven Assemblies

1.3.1. Finite Assemblies

In 1987, Lehn, Siegel et al. showed that 2,2′- bipyridine based ligands **1** and **3** in the presence of copper(I) assemble into the double-stranded helicates (Figure 1.6).[27] The proper choice of the ligand geometry and the coordination mode of metal ions resulted into a predictable assembly of components with the expected geometry.

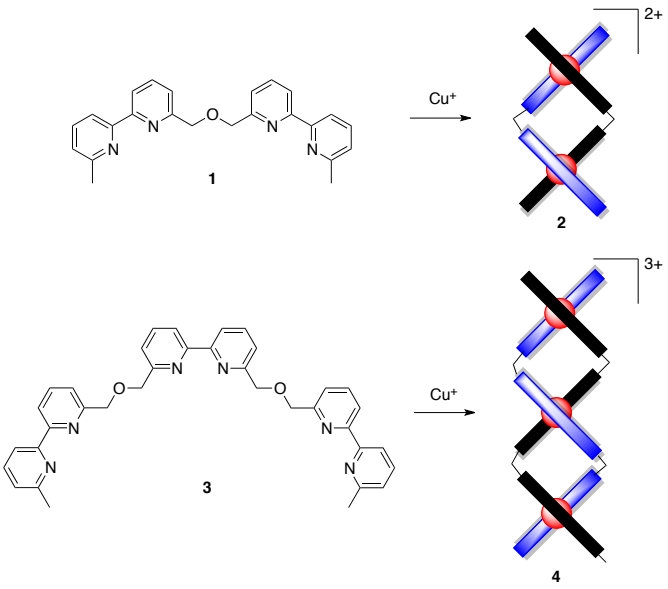

Figure 1.6. Synthesis of Cu(I) helicates.

The search for 90° angle fragments in chemistry motivated the construction of the first molecular square.[28] In 1990, Fujita et al. reported that the reaction between the square planar palladium(II) complex **5** and linear 4,4′-bipyridine (**6**) resulted in the formation of the molecular square assembly in high yield (Figure 1.7).[29,30] Later, Stang group also showed similar molecular squares based on Pt(II) complexes.[31]

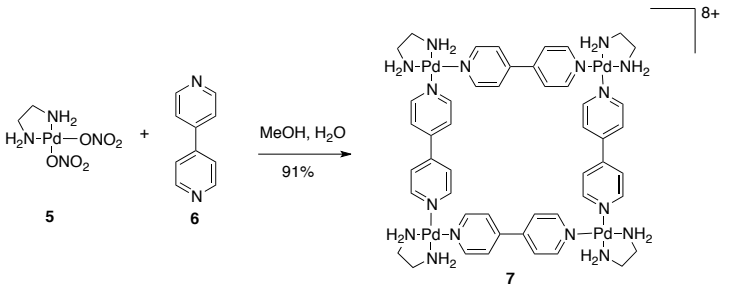

Figure 1.7. Fujita's synthesis of the Pd(II) based molecular square.

Linear ligands with perpendicular coordination sites in the presence of metal ions can form molecular grid assemblies [$n \times n$], where n is the number of coordination sites. The first example of molecular grid was reported by Osborn and coworkers in 1992 (Figure 1.8).[32] The ditopic ligand **8** in the presence of Cu(I) formed the [2×2] grid assembly **9**. Such systems were studied because of their potential application in the bottom-up nanofabrication.[33,34] Examples of [2×2] to [5×5] molecular grids are known in the literature.[35]

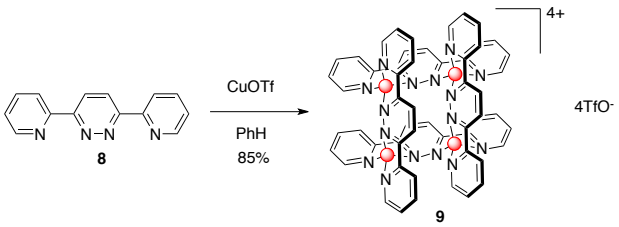

Figure 1.8. Osborn's assembly of the [2×2] molecular grid.

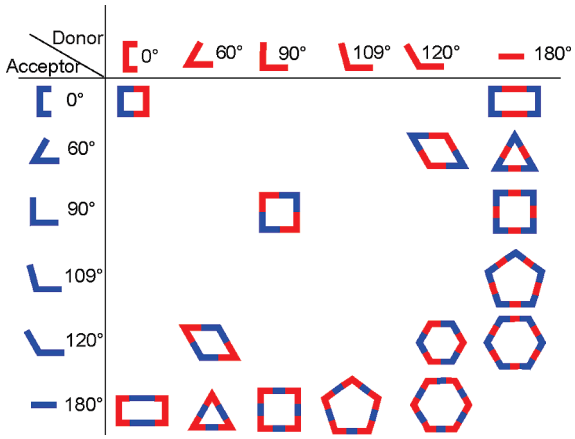

Figure 1.9. The design of 2D polygons by combination of ditopic building blocks. Adapted with permission from ref.[14]. Copyright 2013 ACS.

The design of supramolecular assemblies from directional building blocks was promoted by the work of Stang, Fujita, Raymond and others.[9,16,36] The two-dimensional molecular polygons can be designed by choosing the proper directional metal "acceptors" and organic "donors". Schematic representation of this approach is shown in Figure 1.9.

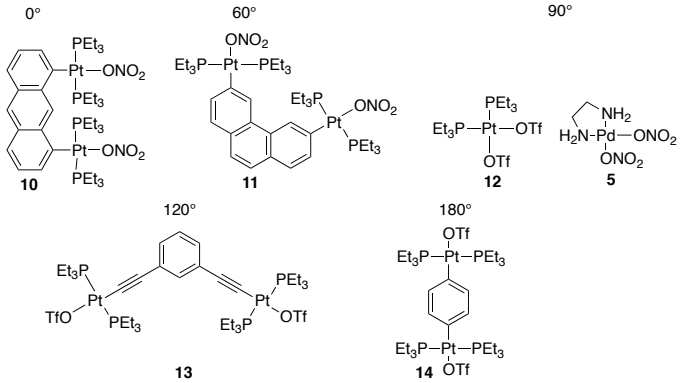

Figure 1.10. Metal-based precursors offering various angles for the construction of supramolecular assemblies.[14,28,36]

For this purpose various Pt(II) and Pd(II) containing building blocks were developed, giving access to the angles ranging from 0 ° to 180 ° (Figure 1.10).

For example, a strain-free molecular triangle can be synthesized by the combination of 180° and 60° motifs.[37] Already in 1970, attempts towards the synthesis of 2-pyridylgold(I)

(**16**) provided the triangular structure **17** – the result of serendipity rather than design (Figure 1.11).[38] Such structure fulfills both the linear coordination geometry of Au(I) and 60° angle between pyridine nitrogen and metal center.

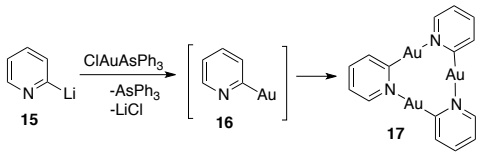

Figure 1.11. The formation of molecular triangle from 2-pyridylgold(I).

Newkome and coworkers showed a beautiful example of the rationally designed angular 2,2′:6′,2″-terpyridine based ligand **18** which assembled into molecular triangles **19** when metals preferring octahedral geometry were used (Figure 1.12).[39] Many other molecular triangles were obtained using this approach.[37,40,41]

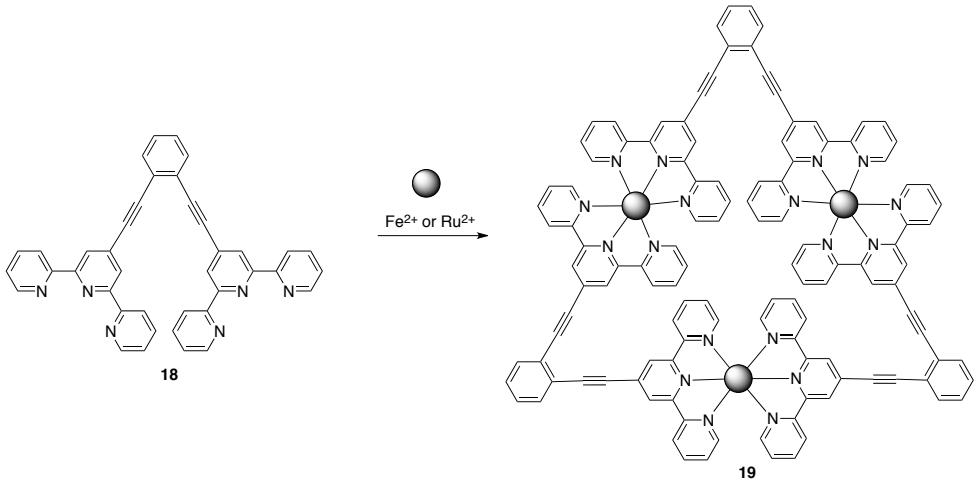

Figure 1.12. Newkome's synthesis of molecular triangle.

Similarly, the ditopic ~108° angular *terpy* ligand **20** in the presence of Fe(II), Ru(II) and Zn(II) metal ions gave the molecular pentagons **21** (Figure 1.13).[42] Hasenknopf et al.[43] and Jiang et al.[44] also reported on the other metal-organic pentagonal structures.

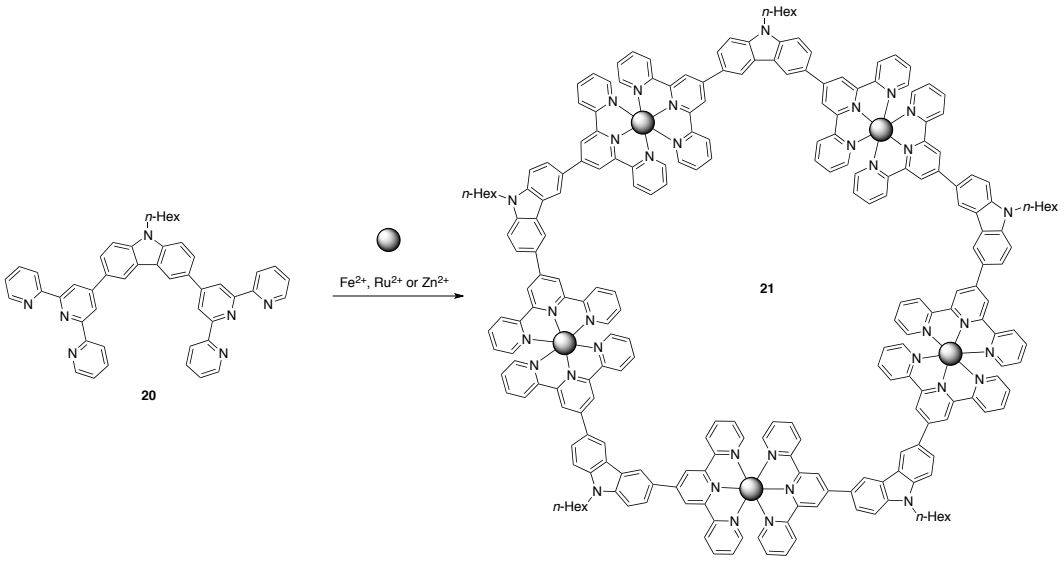

Figure 1.13. Newkome's synthesis of molecular pentagon.

Various higher molecular polygons[44], such as hexagons[45-47], less predictable heptagons[48] and octagonas[49] were also prepared using directional building blocks.

In 1988, Saalfrank et al. synthesized the first example of a metal-organic cage which was obtained serendipitously.[50] However, the rational design of three-dimensional assemblies can be tackled by the combination of ditopic and tritopic motifs, as shown in Figure 1.14.[16]

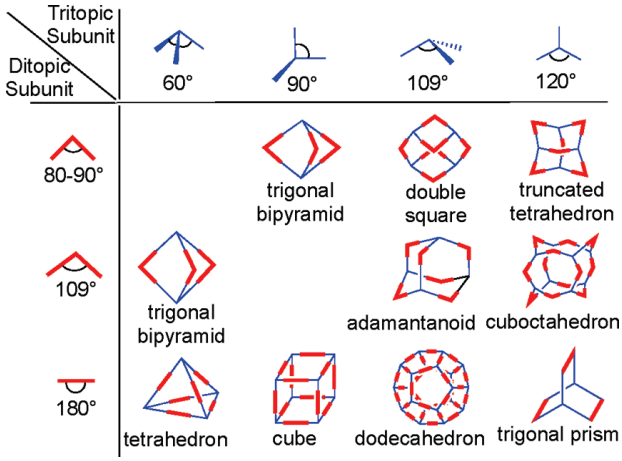

Figure 1.14. The design of 3D polyhedrons by the combination of ditopic and tritpoic building blocks. Adapted with permission from ref.[14]. Copyright 2013 ACS.

Fujita et al. showed that the three-fold symmetric directional ligand **22** in the presence of the orthogonal Pd(II) complex **5** assembles into the molecular cage **23** resembling octahedron (Figure 1.15).[51] On the other hand, the combination of the tritopic ligand **22**, the complex **5** and ditopic linear ligands (topological analogs to 4,4′-bipyridine) afforded the trigonal prismatic cages **24** which were able to incorporate aromatic guests within their cavities.[52]

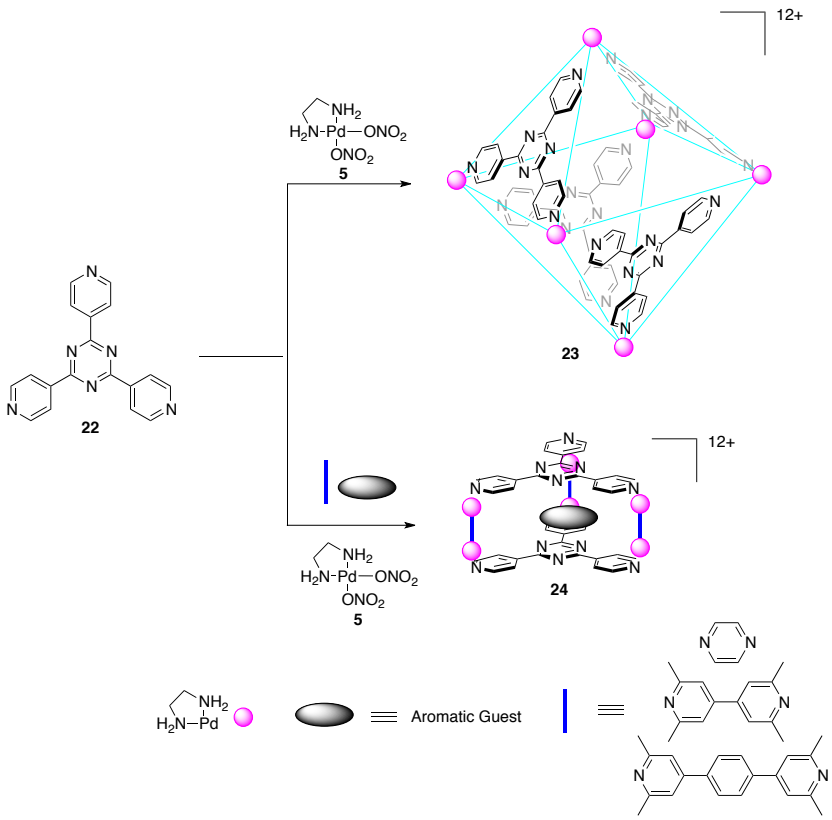

Figure 1.15. Fujita's assembly of molecular cages.

The synthesis of molecular cages opened new perspectives in such fields as host-guest chemistry[53], molecular recognition[54], reactivity modulation[55], and catalysis[56], because of their nanoscale cavities with unique environment not found in a bulk solution. Again, directional ligands play a crucial role in designing new molecular cages.[36]

1.3.2. Polymeric Assemblies

The finite metal-organic assemblies are a logical outcome of the interplay between serendipity, rational design and geometries offered by both organic and inorganic chemistry. However, infinite, polymeric networks can also be designed from the metal ions and organic ligands.

In 1990, the pioneering work by Robson and coworkers[57] initiated the new, rapidly growing field of metal-organic frameworks (MOFs) – polymeric hybrid crystalline materials consisting of organic linkers and metal nodes. They showed that the rational choice of the tetrahedral organic ligand **25** and Cu(I) ions resulted in the formation of the infinite, double-interpenetrating coordination framework with diamond-like topology (Figure 1.16).

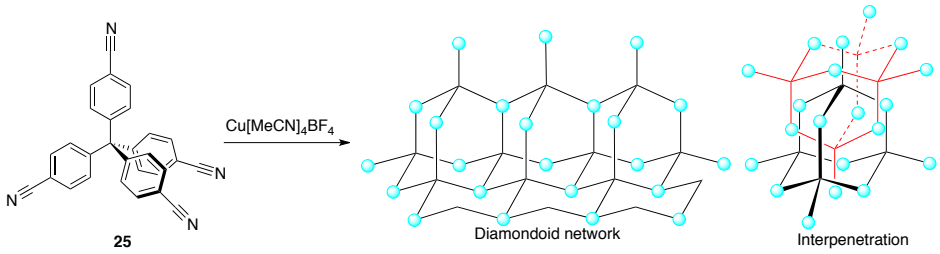

Figure 1.16. The first metal-organic framework by Robson et al.

In 1994, Fujita group synthesized the 2D MOF **26** consisting of 4,4′-bipyridine (**6**) linkers and Cd(II) metal nodes (Figure 1.17). Fujita predicted that "construction of the inner cavities mainly surrounded by organic components is attractive since the shape, size, and function of the cavity become *designable*".[58]

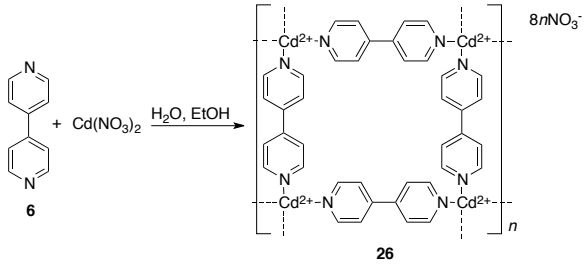

Figure 1.17. Synthesis of 2D MOF based on 4,4′-bipyridine linkers and Cd(II) metal nodes.

By replacing metal ions with inorganic clusters, Yaghi et al. revolutionized the field of MOFs in 1999. Instead of single metal ions, these metal clusters, or as they called them *secondary building units* (SBUs), can be used as rigid nodes to construct the polymeric frameworks.[59] They showed that the linear 1,4-benzenedicarboxylate linker **27** with SBU Zn_4O cluster forms a highly porous crystalline material MOF-5 with the cubic net topology (Figure 1.18). The MOF-5 remains stable even after the removal of incorporated solvent molecules and heating up to 300 °C.

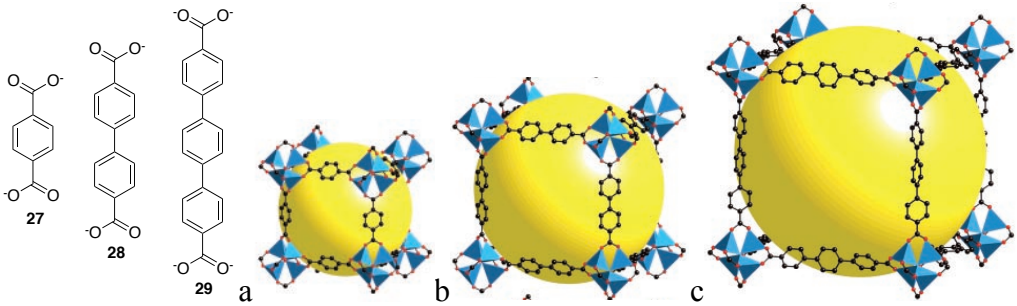

Figure 1.18. Reticular construction of MOFs by Yaghi: a) MOF-5; b) IRMOF-10; c) IRMOF-16. Adapted with permission from ref.[60] Copyright 2002 AAAS.

Yaghi group also synthesized MOFs with similar structures and topologies but with different pore sizes by simply changing the dimensions of the organic linkers such as dicarboxylates **27**, **28**, and **29** (Figure 1.18). This design principle is known as *the reticular chemistry*, and the resulting structures are called *isoreticular structures* or IRMOFs (Figure 1.18, examples a, b and c).[60,61] Since then, a huge number of different MOFs were prepared with various topologies, porosity and potential applications. Due to the high porosity of these solid, zeolite-like materials, the major focus is the search for MOFs suitable for gas adsorption, storage and separation; however, recent progress in the field showed that MOFs have huge potential also in catalysis, optoelectronics, magnetic materials, and other specific applications.[13] It follows that there is an essential need for novel organic linkers to adjust the structure, topology and function of MOFs, since the organic linkers can be easily modified and adjusted for the desired application.[14]

Most of the MOFs reported to date contain the same metal centers or clusters. In 1994, Robson et al. showed that the metal porphyrin based ligand can assemble into the MOF structure with copper centers having different oxidation states (Cu(I) and Cu(II)).[62] To date, there are significantly less examples of heterometallic MOFs reported as compared to a huge number of homometallic MOFs[63]; despite the fact, there is a growing interest in such materials. Additional metal center could not only tune the pore size and topology of a network but also bring interesting luminiscent[64], magnetic or catalytic properties[65], and improved gas adsorption[63,66-69]. However, the rapid development of this field is limited to the currently available organic ligands. The ligands for this purpose should be able to address various metal coordination modes and geometries. Most of the heterometallic MOFs reported to date contain only few types of organic ligands, and there is a clear need for novel, directional ligands. In their 2011 review article, Das et al. wrote that "construction of functional mixed metal–organic frameworks (M'MOFs) is still in an early stage".[65]

The rational approach to the synthesis of heterometallic MOFs involves preformed metalloligands. Several such ligands are shown in Figure 1.19.[70]

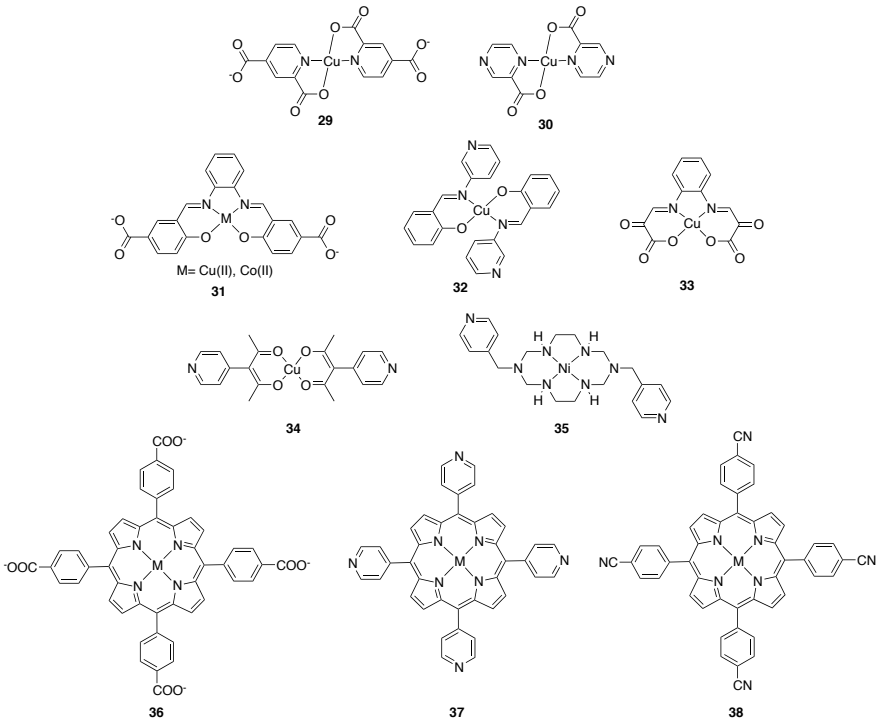

Figure 1.19. Several metalloligands used for the construction of heterometallic MOFs.

Noro et al. reported on the pyridine carboxylate based metalloligands **29** and **30**[71,72] that were used in assembly of 2D Zn(II), Cu(II) MOFs. Kitaura et al. showed the synthesis of the salen based metallo ligands **31** for the assembly of mixed 3D Zn(II),Cu(II) or Co(II) MOFs (Figure 1.20).[73]

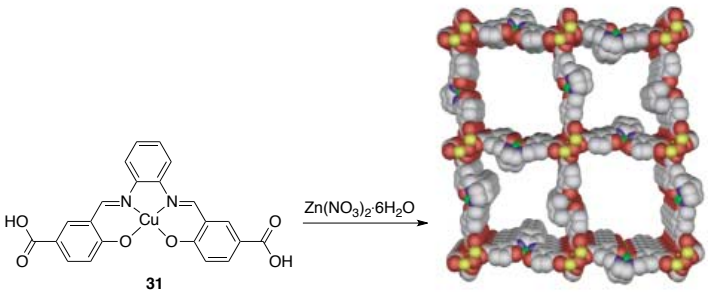

Figure 1.20. Construction of heterometallic Zn(II),Cu(II) 3D MOF. Adapted with permission from ref.[73]. Copyright 2004 WILEY-VCH Verlag GmbH & Co. KGaA, Weinheim

The polymeric 1D ladders and 2D layers containing Cu(II) and Cd(II) metal centers were prepared from the pyridine functionalized acac-type ligand **34**.[74] The interesting diketone metalloligand **33** afforded Mn(II), Cu(II) 2D framework.[75] Several porphyrine-based ligands, like **36**, **37**, and **38**, were also useful in the construction of heterometallic MOFs.[76-79]

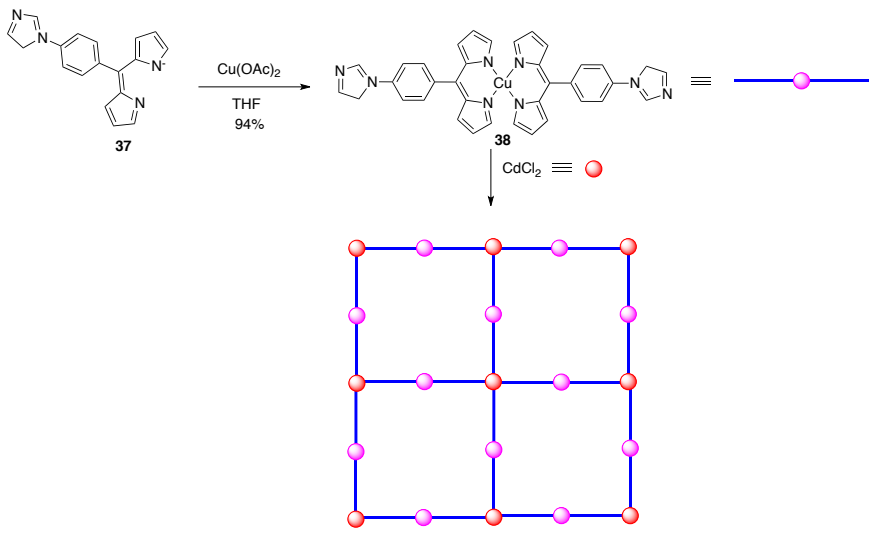

Figure 1.21. Stepwise synthesis of Cu(II), Cd(II) 2D MOF.

The principle of the stepwise construction of Cu(II), Cd(II) 2D MOF via the metalloligand **37** is depicted schematically in Figure 1.21.[80]

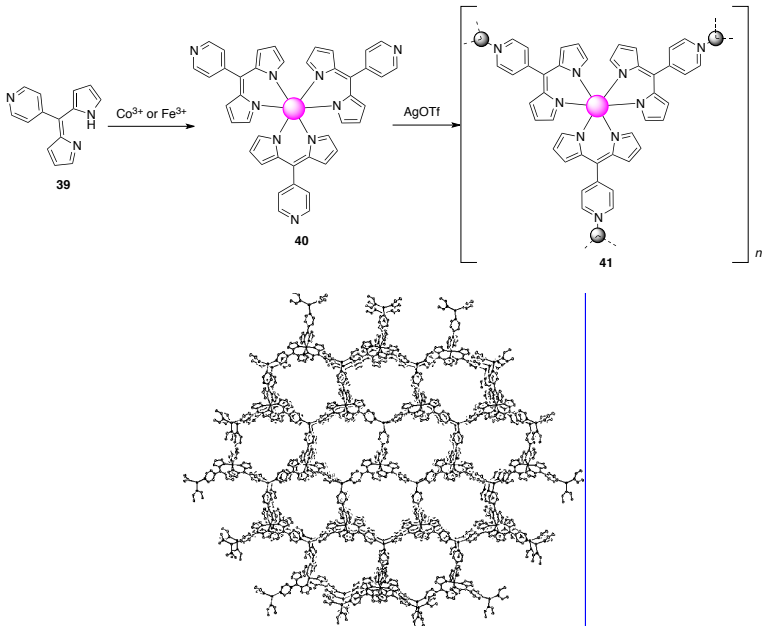

Figure 1.22. Construction of the heterometallic MOF from the three-fold symmetric metalloligand **39**. Adapted with permission from ref.[81]. Copyright 2005 American Chemical Society.

Halper and coworkers prepared interesting three-fold symmetric metalloligands **40** containing Co(II) or Fe(II), which in the presence of Ag(I) ions assembled into the heterometallic MOF (Figure 1.22).[81]

Yaghi group showed that different metal ions can also be incorporated in the already preformed MOF structure if open coordination sites are available within the framework

(Figure 1.23).[82] They successfully employed strong oxophilicity of aluminum, which allowed the construction of 2,2′-bipyridine-5,5′-dicarboxylate based MOF-253 containing Al(III) metal centers and open *bipy* coordination sites. Subsequently, the available coordination sites were metallated with $PdCl_2$. Such heterometallic porous material exhibits significantly enhanced selectivity for the adsorption of CO_2 over N_2.

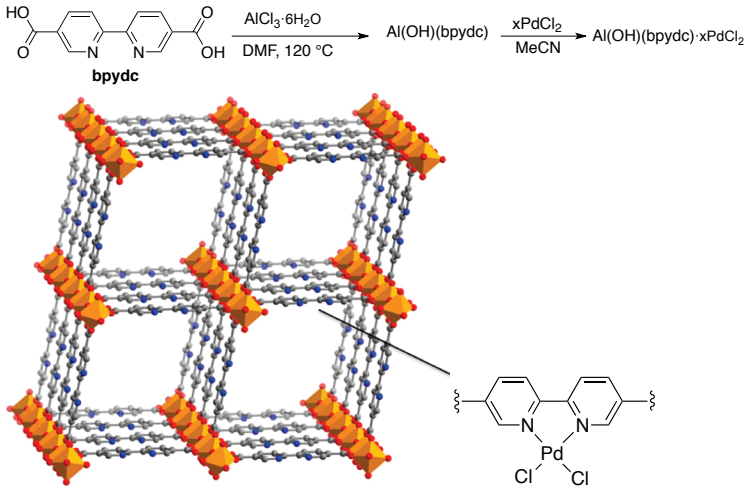

Figure 1.23. Metal insertion in 2,2′-bipyridine based MOF-253. Adapted with permission from ref.[82]. Copyright 2010 American Chemical Society.

The further development of this field strongly depends on the creation of new metalloligands addressing various coordination geometries and topologies. The current state of the heterometallic MOF field indicates that there is an urgent need for such new systems.

1.4. Synthesis of Functionalized 2,2′:6′,2″-Terpyridines

In our pursuit towards development of novel directional 2,2′:6′,2″-terpyridines based ligands, a short overview of the most common synthetic routes to 2,2′:6′,2″-terpyridines derivatives is provided below.

In 1931, Morgan and Burstall first isolated 2,2′:6′,2″-terpyridine as a side-product from the high temperature reaction of pyridine in the presence of $FeCl_3$.[83] Since then, it has become one of the most important chelating ligands with a broad spectrum of various applications.[84-86] 2,2′:6′,2″-Terpyridine derivatives are attractive design elements in supramolecular chemistry, because they are able to form 2:1 ligand to metal complexes with many transition metals preferring octahedral coordination geometry.[84,87]

There are two major synthetic strategies to the substituted 2,2′:6′,2″-terpyridine derivatives: ring construction by condensation reactions and the synthesis via cross-coupling chemistry.[86]

Several classical ring construction routes are depicted in Figure 1.24. The Kröhnke condensation[88,89] involves a reaction between the *N*-heteropyridinium salt **41** and the enone **42** in the presence of ammonium source (route A). Similarly, the condensation of the pyridyl disubstituted 1,5-diketone **44** in the presence of ammonium acetate gives the terpyridine **43** (route B).[90,91] In Jameson synthesis[92], condensation of the dithioacetal **45** with the enolate **46** (route C) affords 4′-methylthio substituted terpyridines.

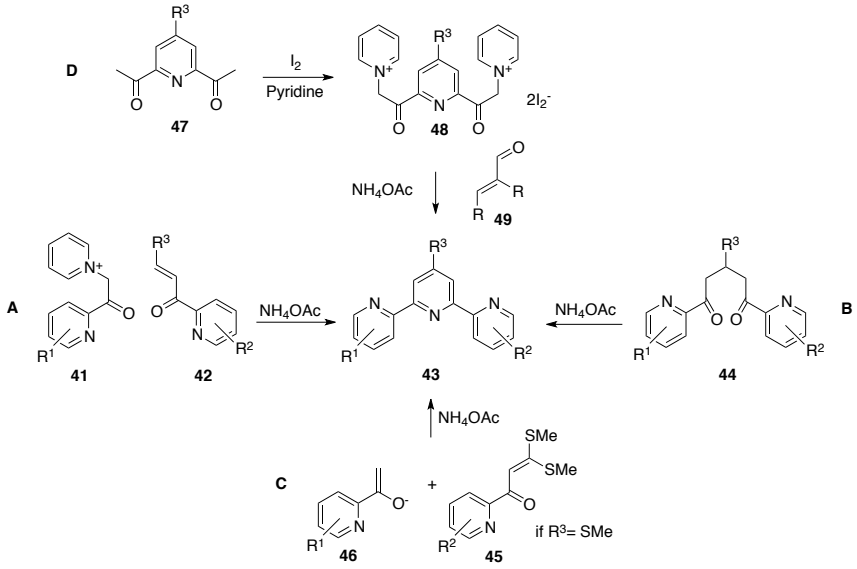

Figure 1.24. Classical synthetic routes to the 2,2′:6′,2″-terpyridine derivatives via ring construction.

Sasaki-Kröhnke synthesis[93] is based on the diketone intermediate **47** which is converted to the pyridinium iodide **48** (Figure 1.24, route D). Subsequent condensation with the α,β-unsaturated aldehyde **49** provides the terpyridine **43**. Many of these routes give moderate yields, and complicated purification is often required.

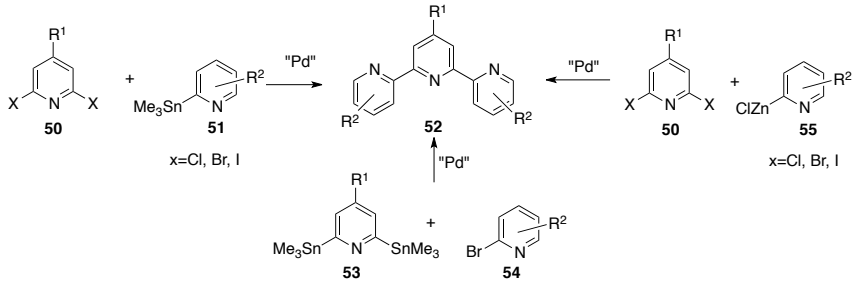

Figure 1.25. Palladium catalyzed cross-coupling routes to 2,2′:6′,2″-terpyridine derivatives.

The palladium catalyzed cross-coupling approach is a convenient and efficient strategy, providing access to various substituted terpyridines in good yields.

The palladium catalyzed Stille coupling reaction between the 2,6-dihalosubstituted pyridine **50** and the stannane **51**[94-96] provides terpyridine in good to high yields. Similarly, the

reaction of the 2,6-bis(trimethylstannyl)pyridine **53** with the 2-bromopyridine **54** proved to be efficient.[97] Negishi coupling reaction between the organozinc derivative **55** and the 2,6-dihalosubstituted pyridine **5** also leads to various *terpy* derivatives in acceptable yields and facile purification.[98,99]

Many other synthetic strategies are reported and reviewed in more detail elsewhere.[85,86]

1.5. References

(1) http://www.freepik.com/free-photo/chain-link-fence_337120.htm.

(2) http://www.freefoto.com/images.

(3) *Lehninger Principles of Biochemistry*; 6th ed.; W.H. Freeman, **2012**.

(4) Lehn, J. M. *Pure Appl. Chem.* **1978**, *50*, 871–892.

(5) Pedersen, C. J. *J. Am. Chem. Soc.* **1967**, *89*, 7017–7036.

(6) Cram, D. J.; Cram, J. M. *Science* **1974**, *183*, 803–809.

(7) Lehn, J.-M. *Supramolecular Chemistry*; VCH: Weinheim, Germany, **1995**.

(8) Schneider, H. J. *Angew. Chem. Int. Ed.* **2009**, *48*, 3924–3977.

(9) Pluth, M. D.; Bergman, R. G.; Raymond, K. N. *Acc. Chem. Res.* **2009**, *42*, 1650–1659.

(10) Lehn, J. M. *Science* **2002**, *295*, 2400–2403.

(11) Ardo, S.; Meyer, G. J. *Chem. Soc. Rev.* **2009**, *38*, 115–164.

(12) Housecroft, C.; Sharpe, A. G. *Inorg. Chem.*; 4th ed.; Prentice Hall, **2012**.

(13) Furukawa, H.; Cordova, K. E.; O'Keeffe, M.; Yaghi, O. M. *Science* **2013**, *341*, 1230444.

(14) Cook, T. R.; Zheng, Y. R.; Stang, P. J. *Chem. Rev.* **2013**, *113*, 734–777.

(15) Swiegers, G. F.; Malefetse, T. J. *Chem. Rev.* **2000**, *100*, 3483–3538.

(16) Leininger, S.; Olenyuk, B.; Stang, P. J. *Chem. Rev.* **2000**, *100*, 853–908.

(17) Holliday, B. J.; Mirkin, C. A. *Angew. Chem. Int. Ed.* **2001**, *40*, 2022–2043.

(18) Saalfrank, R. W.; Maid, H.; Scheurer, A. *Angew. Chem. Int. Ed.* **2008**, *47*, 8794–8824.

(19) Saalfrank, R. W.; Maid, H. *Chem. Commun.* **2005**, 5953–5967.

(20) Fujita, M.; Ibukuro, F.; Hagihara, H.; Ogura, K. *Nature* **1994**, *367*, 720–723.

(21) Klyatskaya, S.; Dingenouts, N.; Rosenauer, C.; Muller, B.; Hoger, S. *J. Am. Chem. Soc.***2006**, *128*, 3150–3151.

(22) Toyota, S.; Woods, C. R.; Benaglia, M.; Haldimann, R.; Wärnmark, K.; Hardcastle, K.; Siegel, J. S. *Angew. Chem. Int. Ed.* **2001**, *40*, 751–754.

(23) Loren, J. C.; Yoshizawa, M.; Haldimann, R. F.; Linden, A.; Siegel, J. S. *Angew. Chem. Int. Ed.* **2003**, *42*, 5702–5705.

(24) Uppadine, L. H.; Lehn, J. M. *Angew. Chem. Int. Ed.* **2004**, *43*, 240–243.

(25) Oliveri, C. G.; Ulmann, P. A.; Wiester, M. J.; Mirkin, C. A. *Acc. Chem. Res.* **2008**, *41*, 1618–1629.

(26) Bassani, D. M.; Lehn, J.-M.; Fromm, K.; Fenske, D. *Angew. Chem. Int. Ed.* **1998**, *37*, 2364–2367.

(27) Lehn, J. M.; Rigault, A.; Siegel, J.; Harrowfield, J.; Chevrier, B.; Moras, D. *Proc. Natl. Acad. Sci. U. S. A.* **1987**, *84*, 2565–2569.

(28) Fujita, M.; Tominaga, M.; Hori, A.; Therrien, B. *Acc. Chem. Res.* **2005**, *38*, 369–378.

(29) Fujita, M.; Yazaki, J.; Ogura, K. *J. Am. Chem. Soc.* **1990**, *112*, 5645–5647.

(30) Fujita, M.; Yazaki, J.; Ogura, K. *Tetrahedron Lett.* **1991**, *32*, 5589– 5592.

(31) Stang, P. J.; Cao, D. H. *J. Am. Chem. Soc.* **1994**, *116*, 4981–4982.

(32) Youinou, M.-T.; Rahmouni, N.; Fischer, J.; Osborn, J. A. *Angew. Chem. Int. Ed. Engl.* **1992**, *31*, 733–735.

(33) Baxter, P. N. W.; Lehn, J.-M.; Kneisel, B. O.; Fenske, D. *Chem. Commun.* **1997**, 2231–2232.

(34) Ruben, M.; Rojo, J.; Romero-Salguero, F. J.; Uppadine, L. H.; Lehn, J. M. *Angew. Chem. Int. Ed.* **2004**, *43*, 3644–3662.

(35) Dawe, L. N.; Shuvaev, K. V.; Thompson, L. K. *Chem. Soc. Rev.* **2009**, *38*, 2334–2359.

(36) Chakrabarty, R.; Mukherjee, P. S.; Stang, P. J. *Chem. Rev.* **2011**, *111*, 6810–6918.

(37) Zangrando, E.; Casanova, M.; Alessio, E. *Chem. Rev.* **2008**, *108*, 4979–5013.

(38) Vaughan, L. G. *J. Am. Chem. Soc.* **1970**, *92*, 730–731.

(39) Hwang, S. H.; Moorefield, C. N.; Fronczek, F. R.; Lukoyanova, O.; Echegoyen, L.; Newkome, G. R. *Chem. Commun.* **2005**, 713–715.

(40) Kryschenko, Y. K.; Seidel, S. R.; Arif, A. M.; Stang, P. J. *J. Am. Chem. Soc.* **2003**, *125*, 5193–5198.

(41) Murray, H. H.; Raptis, R. G.; Fackler, J. P. *Inorg. Chem.* **1988**, *27*, 26–33.

(42) Hwang, S. H.; Wang, P.; Moorefield, C. N.; Godinez, L. A.; Manriquez, J.; Bustos, E.; Newkome, G. R. *Chem. Commun.* **2005**, 4672–4674.

(43) Hasenknopf, B.; Lehn, J.-M.; Kneisel, B. O.; Baum, G.; Fenske, D. *Angew. Chem. Int. Ed. Engl.* **1996**, *35*, 1838–1840.

(44) Jiang, H.; Lin, W. *J. Am. Chem. Soc.* **2003**, *125*, 8084–8085.

(45) Newkome, G. R.; Cho, T. J.; Moorefield, C. N.; Baker, G. R.; Cush, R.; Russo, P. S. *Angew. Chem. Int. Ed.* **1999**, *38*, 3717–3721.

(46) Newkome, G. R.; Cho, T. J.; Moorefield, C. N.; Cush, R.; Russo, P. S.; Godínez, L. A.; Saunders, M. J.; Mohapatra, P. *Chem. Eur. J.* **2002**, *8*, 2946–2954.

(47) Newkome, G. R.; Cho, T. J.; Moorefield, C. N.; Mohapatra, P. P.; Godinez, L. A. *Chem. Eur. J.* **2004**, *10*, 1493–1500.

(48) Grossmann, B.; Heinze, J.; Herdtweck, E.; Köhler, F. H.; Nöth, H.; Schwenk, H.; Spiegler, M.; Wachter, W.; Weber, B. *Angew. Chem. Int. Ed. Engl.* **1997**, *36*, 387–389.

(49) Jones, P. L.; Byrom, K. J.; Jeffery, J. C.; McCleverty, J. A.; Ward, M. D. *Chem. Commun.* **1997**, 1361–1362.

(50) Saalfrank, R. W.; Stark, A.; Peters, K.; von Schnering, H. G. *Angew. Chem. Int. Ed. Engl.* **1988**, *27*, 851–853.

(51) Fujita, M.; Oguro, D.; Miyazawa, M.; Oka, H.; Yamaguchi, K.; Ogura, K. *Nature* **1995**, *378*, 469–471.

(52) Kumazawa, K.; Biradha, K.; Kusukawa, T.; Okano, T.; Fujita, M. *Angew. Chem. Int. Ed.* **2003**, *42*, 3909–3913.

(53) Maurizot, V.; Yoshizawa, M.; Kawano, M.; Fujita, M. *Dalton Trans.* **2006**, 2750–2756.

(54) Parac, T. N.; Caulder, D. L.; Raymond, K. N. *J. Am. Chem. Soc.* **1998**, *120*, 8003–8004.

(55) Yoshizawa, M.; Tamura, M.; Fujita, M. *Science* **2006**, *312*, 251–254.

(56) Fiedler, D.; Bergman, R. G.; Raymond, K. N. *Angew. Chem. Int. Ed.* **2004**, *116*, 6916–6919.

(57) Hoskins, B. F.; Robson, R. *J. Am. Chem. Soc.* **1990**, *112*, 1546–1554.

(58) Fujita, M.; Kwon, Y. J.; Washizu, S.; Ogura, K. *J. Am. Chem. Soc.* **1994**, *116*, 1151–1152.

(59) Yaghi, O. M.; Li, H.; Eddaoudi, M.; O'Keeffe, M. *Nature* **1999**, *402*, 276–279.

(60) Eddaoudi, M.; Kim, J.; Rosi, N.; Vodak, D.; Wachter, J.; O'Keeffe, M.; Yaghi, O. M. *Science* **2002**, *295*, 469–472.

(61) Delgado-Friedrichs, O.; O'Keeffe, M.; Yaghi, O. M. *Phys. Chem. Chem. Phys.* **2007**, *9*, 1035–1043.

(62) Abrahams, B. F.; Hoskins, B. F.; Michail, D. M.; Robson, R. *Nature* **1994**, *369*, 727–729.

(63) Nayak, S.; Harms, K.; Dehnen, S. *Inorg. Chem.* **2011**, *50*, 2714–2716.

(64) Bauer, C. A.; Jones, S. C.; Kinnibrugh, T. L.; Tongwa, P.; Farrell, R. A.; Vakil, A.; Timofeeva, T. V.; Khrustalev, V. N.; Allendorf, M. D. *Dalton Trans.* **2013**, DOI: 10.1039/c3dt52939h.

(65) Das, M. C.; Xiang, S.; Zhang, Z.; Chen, B. *Angew. Chem. Int. Ed.* **2011**, *50*, 10510–10520.

(66) Frigoli, M.; El Osta, R.; Marrot, J.; Medina, M. E.; Walton, R. I.; Millange, F. *Eur. J. Inorg. Chem.* **2013**, *2013*, 1138–1141.

(67) Hong, K.; Bak, W.; Moon, D.; Chun, H. *Cryst. Growth Des.* **2013**, *13*, 4066–4070.

(68) Zou, J.-Y.; Shi, W.; Xu, N.; Gao, H.-L.; Cui, J.-Z.; Cheng, P. *Eur. J. Inorg. Chem.* **2013**, DOI:10.1002/ejic.201301312.

(69) Zou, R.; Zhong, R.; Han, S.; Xu, H.; Burrell, A. K.; Henson, N.; Cape, J. L.; Hickmott, D. D.; Timofeeva, T. V.; Larson, T. E.; Zhao, Y. *J. Am. Chem. Soc.* **2010**, *132*, 17996–17999.

(70) Kitagawa, S.; Noro, S.; Nakamura, T. *Chem. Commun.* **2006**, 701–707.

(71) Noro, S.-i.; Kitagawa, S.; Yamashita, M.; Wada, T. *CrystEngComm* **2002**, *4*, 162–164.

(72) Noro, S.-i.; Kitagawa, S.; Yamashita, M.; Wada, T. *Chem. Commun.* **2002**, 222–223.

(73) Kitaura, R.; Onoyama, G.; Sakamoto, H.; Matsuda, R.; Noro, S.; Kitagawa, S. *Angew. Chem. Int. Ed.* **2004**, *116*, 2738–2741.

(74) Chen, B.; Fronczek, F. R.; Maverick, A. W. *Inorg. Chem.* **2004**, *43*, 8209–8211.

(75) Stumpf, H. O.; Pei, Y.; Kahn, O.; Ouahab, L.; Grandjean, D. *Science* **1993**, *261*, 447–449.

(76) Kosal, M. E.; Chou, J. H.; Wilson, S. R.; Suslick, K. S. *Nat. Mater.* **2002**, *1*, 118–121.

(77) Sharma, C. V. K.; Broker, G. A.; Huddleston, J. G.; Baldwin, J. W.; Metzger, R. M.; Rogers, R. D. *J. Am. Chem. Soc.* **1999**, *121*, 1137–1144.

(78) Smithenry, D. W.; Wilson, S. R.; Suslick, K. S. *Inorg. Chem.* **2003**, *42*, 7719–7721.

(79) Zhang, Z.; Zhang, L.; Wojtas, L.; Nugent, P.; Eddaoudi, M.; Zaworotko, M. J. *J. Am. Chem. Soc.* **2012**, *134*, 924–927.

(80) Beziau, A.; Baudron, S. A.; Pogozhev, D.; Fluck, A.; Hosseini, M. W. *Chem. Commun.* **2012**, *48*, 10313–10315.

(81) Halper, S. R.; Cohen, S. M. *Inorg. Chem.* **2005**, *44*, 486–488.

(82) Bloch, E. D.; Britt, D.; Lee, C.; Doonan, C. J.; Uribe-Romo, F. J.; Furukawa, H.; Long, J. R.; Yaghi, O. M. *J. Am. Chem. Soc.* **2010**, *132*, 14382–14384.

(83) Morgan, S. G.; Burstall, F. H. *J. Chem. Soc.* **1931**, 20–30.

(84) Constable, E. C. *Chem. Commun.* **1997**, 1073–1080.

(85) Hofmeier, H.; Schubert, U. S. *Chem. Soc. Rev.* **2004**, *33*, 373–399.

(86) Schubert, U. S.; Hofmeier, H.; Newkome, G. R. *Modern Terpyridine Chemistry*; Weinheim : Wiley-VCH-Verl., **2006**.

(87) Sauvage, J. P.; Ward, M. *Inorg. Chem.* **1991**, *30*, 3869–3874.

(88) Kröhnke, F. *Synthesis* **1976**, *1976*, 1–24.

(89) Potts, K. T.; Usifer, D. A.; Guadalupe, A.; Abruna, H. D. *J. Am. Chem. Soc.* **1987**, *109*, 3961–3967.

(90) Constable, E. C.; Lewis, J. *Polyhedron* **1982**, *1*, 303–306.

(91) Newkome, G. R.; Hager, D. C.; Kiefer, G. E. *J. Org. Chem.* **1986**, *51*, 850–853.

(92) Jameson, D. L.; Guise, L. E. *Tetrahedron Lett.* **1991**, *32*, 1999–2002.

(93) Sasaki, I.; Daran, J. C.; Balavoine, G. G. A. *Synthesis* **1999**, *1999*, 815–820.

(94) Stille, J. K. *Angew. Chem. Int. Ed. Engl.* **1986**, *25*, 508–524.

(95) Cárdenas, D. J.; Sauvage, J.-P. *Synlett* **1996**, *1996*, 916–918.

(96) Fallahpour, R.-A. *Synthesis* **2000**, *2000*, 1665–1667.

(97) Schubert, U. S.; Eschbaumer, C. *Org. Lett.* **1999**, *1*, 1027–1029.

(98) King, A. O.; Okukado, N.; Negishi, E.–I. *J. Chem. Soc., Chem. Commun.* **1977**, 683–684.

(99) Loren, J. C.; Siegel, J. S. *Angew. Chem. Int. Ed.* **2001**, *40*, 754–757.

Chapter 2. Linear Bilateral Extended 2,2′:6′,2′′-Terpyridine Ligands: Topological Tridentate Analogs of Bidentate 5,5′-Disubstituted 2,2′-Bipyridines

2.1. Introduction

De novo design and synthesis of functional supramolecular architectures benefit from ready access to components with well-defined assembly geometries.[1,2] A mainstay component[3] of supramolecular and materials chemistry, 2,2′:6′,2″-terpyridine[4] (*terpy*) ligands form coordination complexes with various metals and have photophysical and electrochemical properties suitable for supramolecular chemistry,[5] nanotechnology,[6] solar cells,[7] catalysis,[8] antitumor,[9] and antibacterial[10] research. A vast range of accessible *terpy* derivatives incorporate into geometrically well-defined supramolecular assemblies;[4,11] and, multi-component *terpy* assemblies, such as metal-organic frameworks (MOFs)[12] and metal-organic polyhedra (MOPs),[13] reveal properties not found in the simple sum of the parts. As such, there is a clear need for building blocks to address under-represented design geometries. Specifically, this chapter addresses the synthesis and characterization of *terpy* derivatives mimicking the linear geometry of 5,5′-functionalized 2,2′-bipyridine (*bipy* in which sites for skeletal substitution are perpendicular to the metal coordination vector (Figure 2.1, example a)).[14] Such ligands would allow the introduction of *terpy* into "linear" molecular assemblies – a complement to the "stub", "W", "V", and "C" motifs stemming from substituents at positions 4′, 4/4″, 5/5″, and 6/6″ with angles relative to the coordination vector of 180°, 120°, 60°, and 0°, respectively (Figure 1, example b).

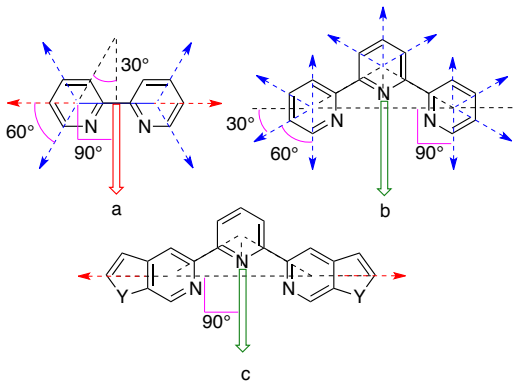

Figure 2.1. Substitution sites for a) 2,2′-bipyridine, and b) 2,2′:6′,2″-terpyridine. c) Linear bilateral sites (red arrows)[15] for 2,2′:6′,2″-terpyridine fused to five-membered rings.

Terpy based ligands form kinetically stable 2:1 ligand-to-metal complexes with Ru^{2+}, Os^{2+}, and Co^{3+}, which can easily be modified chemically and purified chromatographically. Several examples include synthesis of Borromean link precursors,[16] metal-organic dendrimers[17] and molecular grids.[18] On the other hand, *terpy* based ligands can also form kinetically labile complexes suitable for the construction of thermodynamically-driven

assemblies. Introduction of tridentate and bidentate structural units into one ligand has resulted in bifunctional molecular strings where *terpy* and 1,10-phenanthroline, connected with a flexible linker, have been used in rotoxane-based molecular machines, switches and muscles;[19] however, linear rigid-rod analogs with parallel-aligned coordination vectors for *terpy* and *bipy* would offer desirable design alternatives.

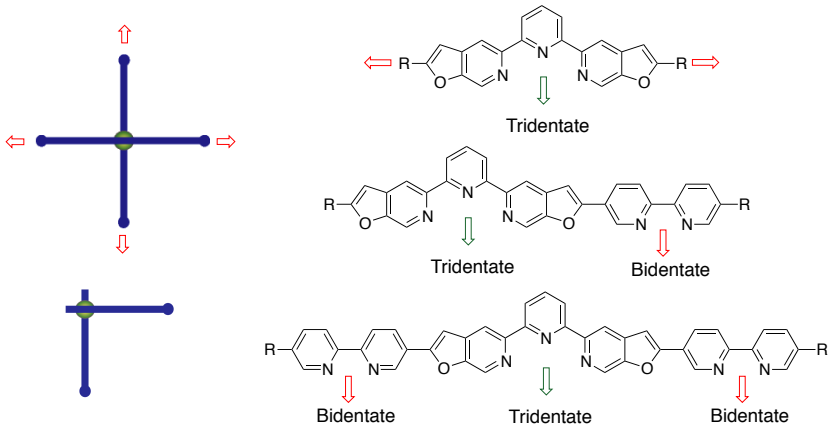

Figure 2.2. Molecular design of linear bilateral extended terpyridines.

Combination of polygons with different numbers of sides brings new topological properties to the molecular systems.[20,21] Fusion of a five-membered ring to the six-membered flanking rings of *terpy* modifies the substitution pattern (Figure 2.1, example c), specifically addressing the linear bilateral geometry mentioned above. This chapter details the practical and versatile synthesis of 2,6-bis(2-substituted-furo[2,3-c]pyridine-5-yl)pyridine-based ligands (Figure 2.2), as topological *bipy* mimics, wherein functional components can be introduced via a convergent modular strategy. Complexation of these ligands with octahedrally coordinating metal ions (Fe^{2+}, Ru^{2+}, and Zn^{2+}) gives access to terpy-based molecular "crossings" and "corners" that are potential building blocks in supramolecular chemistry. The structure and properties of these ligands are described.

2.2. Synthesis of Linear Bilateral Extended Terpyridine Ligands

2.2.1. Retrosynthesis

To access terpyridine derivatives **56** with fused five-membered rings at the flanking pyridines, one has to consider a reliable synthetic procedure where different substituents can be introduced easily. It was decided to follow the retrosynthesis proposed by Jui-Chang Tseng (Scheme 2.1). The general structure of linear terpyridine **56** leads to the opening of fused five-membered rings at a heteroatom Y, giving a disubstituted ethynyl derivative **57**. This could be

prepared using Sonogashira coupling[22] between dihalide **58** and acetylene **59**. Appropriate protection of terpyridine **60** with *ortho*-directing groups at the 5- and 5′′- positions would enable *ortho*-metalation,[23] and subsequent addition of a halide electrophile would lead to compound **58**.

Scheme 2.1. Retrosynthesis of Linear Terpyridine 56

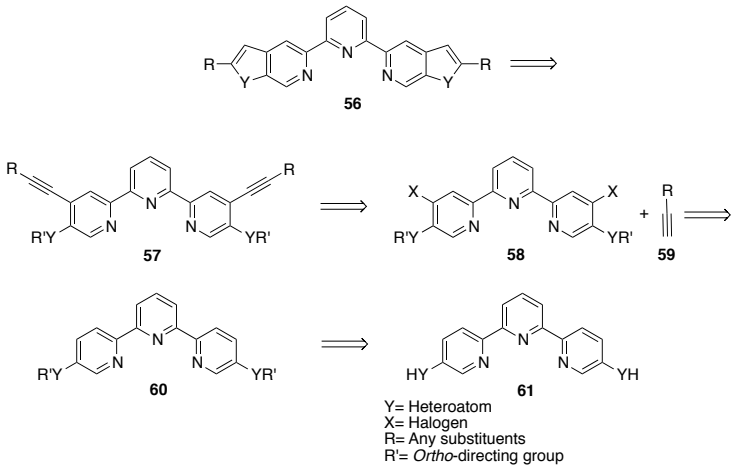

This strategy suggests an intermediate terpyridine **61** possessing YH substituents in the 5- and 5′′- positions. If heteroatom Y represents oxygen, then **61** has to be 5,5′′-hydroxy-2,2′:6′,2′′-terpyridine, thus leading to 2,6-bis(2-substituted-furo[2,3-c]pyridine-5-yl)pyridines as a new class of target ligands.

2.2.2. Synthesis of the *Terpy* Core

The pursuit of 2,6-bis(2-substituted-furo[2,3-c]pyridine-5-yl)-pyridine-based ligands motivated the development of an efficient chromatography-free synthesis of the key intermediate 4,4′′-diiodo-5,5′′-bis(methoxy-methoxy)-2,2′:6′,2′′-terpyridine (**69**). It was decided to follow the route by Jui-Chang Tseng (Scheme 2.2) which was further upscaled and optimized to avoid chromatographic purification. The route to **69** follows a Stille[24] cross-coupling strategy via **63** and **65**. Regioselective lithiation[25] of commercially available 2,5-dibromopyridine (**62**) with *n*-butyllithium and subsequent addition of 2-methoxy-4,4,5,5-tetramethyl-1,3,2-dioxaborolane gave 5-borylated pyridine **63**[26] in good yield. The precursor of the central ring, 2,6-bis(trimethylstannyl)pyridine (**65**), was synthesized in nucleophilic stannylation of 2,6-dichloropyridine (**64**) with freshly prepared $NaSnMe_3$ in good yield.[27,28] *Terpy* **66** was prepared by Stille coupling between bromide **63** and bisstannane **65** according to the procedure reported by Schlüter.[26] Oxidation/hydroxydeboronation[29] of **66** resulted in 5,5′′-dihydroxyterpyridine **67** in excellent yield.[30] These reactions were performed routinely on a 40 g to 90 g scale and have the potential for further scale-up. Subsequent deprotonation

of hydroxy groups with NaH and treatment with MOMCl (prepared *in situ*)[31] afforded *terpy* **68**, with *ortho*-directing groups at the 5,5″-positions.

Scheme 2.2. Synthesis of 4,4′′-Diiodo-5,5′′-bis(methoxymethoxy)-2,2′:6′,2′′-terpyridine (69)

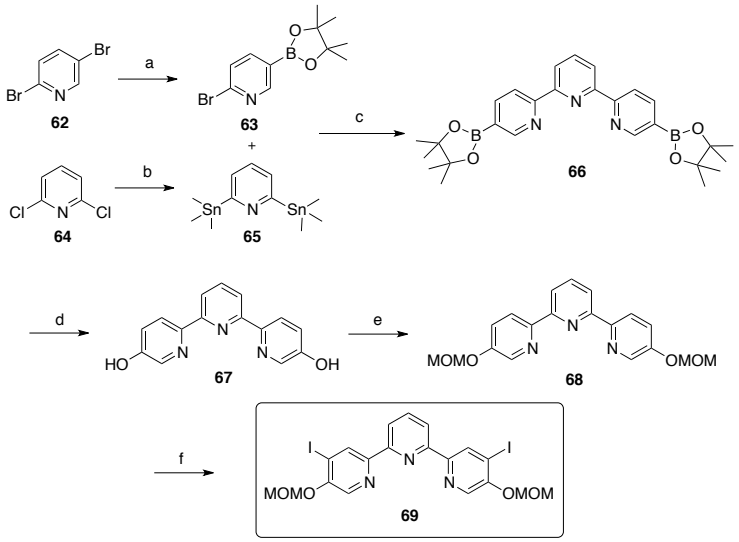

(a) *n*-BuLi, Et_2O, –78 °C, 3 h, then *B*-methoxypinacolborane, –78 °C to rt, 12 h, 83%; (b) Na, Me_3SnCl, DME, –15 °C, then **64**, –15 °C to rt, 18 h, 84%; (c) 5 mol% $Pd(PPh_3)_4$, toluene, reflux, 24 h, 56%; (d) 30% H_2O_2, aq. NaOH, THF, rt, 18 h, 96%; (e) 60% NaH, THF, DMF, 0 °C, then MOMCl/MeOAc[31], 0 °C to rt, 12 h, 96%; (f) 2.2 eq. *n*-BuLi, TMEDA, THF, –78 °C, 1 h, then 2.2 eq. I_2, –78 °C to rt, 50%.

Regioselective *ortho*-lithiation[32] with *n*-BuLi in the presence of TMEDA and subsequent quenching with iodine gave the desired diiodo-*terpy* **69**. During iodine addition, a thick precipitate formed complicating both stirring and appropriate cooling. Therefore, an optimal yield was obtained when the reaction was run on a 1–3 g scale per batch. Straightforward trituration of crude product with hot ethanol afforded pure **69**.

2.2.3. Synthesis of Acetylenes

Sonogashira coupling of alkynes with **69** introduces substituents in the flanking positions of linear terpyridine ligands. Introduction of manisyl groups improves solubility and facilitates later homologation,[33] dictated the use of 2-ethynyl-5-methoxy-1,3-dimethylbenzene **73**.[34] Standard Sonogashira coupling conditions of 4-methoxy-2,6-dimethylbromobenzene (**70**)[35] with trimethylsilylacetylene was unsatisfactory; therefore, bromide **70** was converted to the iodide **71** by lithiation and subsequent quenching with iodine (Scheme 2.3). Under optimized conditions for Sonogashira coupling, **71** reacted smoothly with trimethylsilylacetylene to produce silyl-protected acetylene **72**. Deprotection with KF in methanol gave **73** in high yield.

Manisyl substituted 5-ethynylbipyridines **77a** and **77b** were synthesized from known bromopyridines **74a**[33] and **74b**[36] (Scheme 2.4). Negishi coupling[37] with 2,5-dibromopyridine (**62**) afforded bromobipyridines **75a** and **75b**,[36] which coupled well with trimethylsilylacetylene to give **76a** and **76b**. Subsequent deprotection with KF formed ethynylbipyridines **77a** and **77b** in good yields over 2 steps.

Scheme 2.3. Synthesis of Acetylene 73

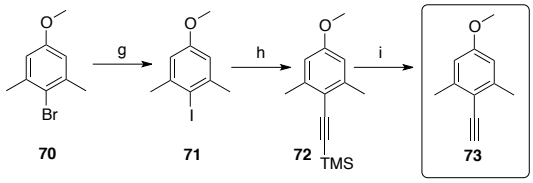

(g) *n*-BuLi, THF, –78 °C, 30 min, then I_2, –78 °C to rt, overnight, 81%; (h) trimethylsilylacetylene, 5 mol% $Pd(PPh_3)_2Cl_2$, 10 mol% CuI, toluene, Et_3N, reflux, 18 h, 95%; (i) KF, MeOH, 40 °C, 36 h, 96%.

Scheme 2.4. Synthesis of 5-Ethynyl-2,2′-bipyridines 77

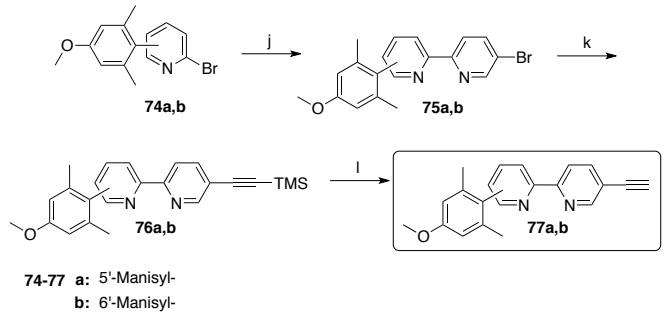

(j) 1. *n*-BuLi, THF, –78 °C, 1 h; 2. $ZnCl_2$, THF, –78 to 0 °C, 1 h; 3. **7**, 1.5 mol% $Pd(PPh_3)_4$, THF, reflux, 18 h, **75a**: 31%, **75b**: 48%[36]; (k) trimethylsilylacetylene, 10 mol% $Pd(PPh_3)_2Cl_2$, 5 mol% CuI, Et_3N, reflux, 18 h; (l) KF, MeOH, rt, 18 h, over 2 steps **77a**: 72%, **77b**: 76%.

2.2.4. Ligand Synthesis

Diiodo-*terpy* **69** proved to be an efficient building block that allowed the incorporation of various substituents in the flanking positions by straightforward cross-coupling methodology. Simple symmetric *terpy* derivatives **78a, 78b**, and **78e**, as well as a mixed variation with bipyridine **78f**, were prepared by Sonogashira coupling with an excess amount (>2 eq) of corresponding alkynes in good to high yields (Table 2.1, entries 1, 2, 5, and 6). Due to the instability of 4-ethynylpyridine,[38] **78d** was prepared in a stepwise fashion. First, bisethynyl-*terpy* **78c** was synthesized in two steps by Sonogashira coupling between **69** and trimethylsilylacetylene following one-pot deprotection of silyl groups in the presence of KF (Table 2.1, entry 3). A subsequent coupling reaction with 4-iodopyridine (**80**) under standard conditions (Table 2.1, entry 4) gave **78d** in good yield.

To incorporate two different substituents into the 4- and 4′′- positions, Sonogashira coupling was performed with 1.05 equivalents of acetylene (Table 2.1, entries 7-9), giving a statistical mixture of mono- and bis-coupled products **79a-c** and **78f-h**, respectively, as well as unreacted diiodoterpyridine **69**. These mixtures were easily separated by column chromatography, and pure monosubstituted intermediates **79a-c** were obtained.

Table 2.1. Synthesis of 78 and 79 by Sonogashira Coupling[a]

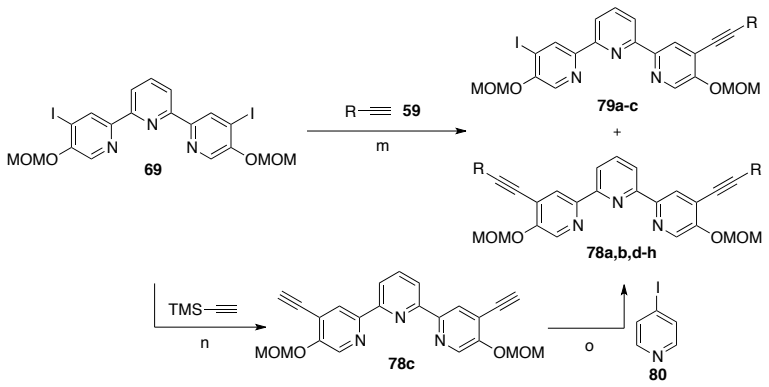

entry	R=	eq[e]	time (h)	yield (%)				
				disubst.		monosubst.		**69**[f]
1		2.5	20	**78a**	95	-	-	-
2	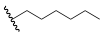	2.5	20	**78b**	92	-	-	-
3		5.0	4.5[b]/18[c]	**78c**	86	-	-	-
4		2.1[d]	20	**78d**	88	-	-	-
5		7.8	20	**78e**	85	-	-	-
6	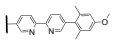	2.08	20	**78f**	90	-	-	-
7	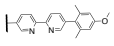	1.05	6	**78f**	18	**79a**	40	24
8	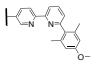	1.05	6	**78g**	17	**79b**	39	22
9		1.05	15	**78h**	15	**79c**	38	28

[a] Reaction conditions: (m) acetylene **59,** 5 mol% $Pd(PPh_3)_2Cl_2$, 10 mol% CuI, THF, Et_3N, reflux; (n) [b] trimethylsilylacetylene, 5 mol% $Pd(PPh_3)_2Cl_2$, 10 mol% CuI, THF, Et_3N, reflux, [c] then the crude mixture was subjected to TMS deprotection with KF, MeOH; (o) 1.0 eq **78c**, [d] 4-iodopyridine (**80**), 10 mol% $Pd(PPh_3)_2Cl_2$, 20 mol% CuI, THF, Et_3N, reflux. [e] Unless otherwise stated, equivalents indicated for acetylenes **59**. [f] Recovered **69**.

The non-symmetric terpyridine/bipyridine conjugates **79a** and **79b** were further subjected to coupling with manisyl acetylene **73** to give products **81a** and **81b** in good yields (Scheme 2.5).

Scheme 2.5. Synthesis of Non-symmetric Ligand Precursors 81

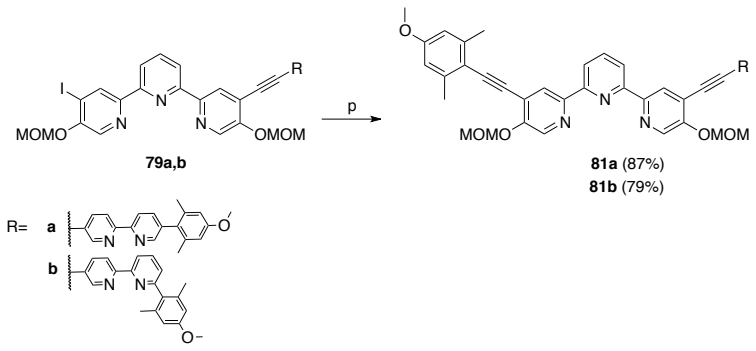

(p) Acetylene **73**, 5 mol% $Pd(PPh_3)_2Cl_2$, 10 mol% CuI, THF, Et_3N, reflux, 17-20 h.

With the library of 4,4″-disubstituted terpyridines **78a-h**, **81a** and **81b** in hand, developing general cyclization conditions to access the 2-substituted-furo[2,3-c]pyridine motif became the focus.

Table 2.2. One-pot MOM-deprotection/Cycloisomerisation of 78 and 81*a*

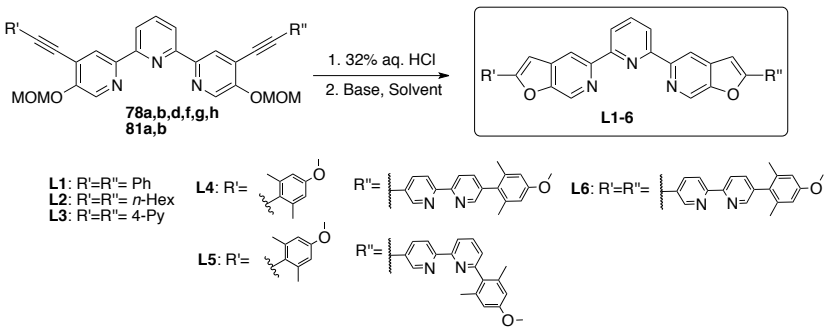

entry	SM	HCl (eq)	solvent	base	eq	time (h)	yield	
							L	(%)
1[b]	**81a**	4	MeOH	NaOMe[c]	8	20	**L4**	0
2[b]	**81a**	20	MeOH	NaOMe[c]	40	40	**L4**	5
3[b]	**81a**	42	EtOH	NaOMe[c]	85	24	**L4**	11
4[b]	**81a**	42	THF	Cs_2CO_3	60	24	**L4**	19
5	**81a**	**21**	**DMF**	**Cs_2CO_3**	**43**	**76**	**L4**	**97**
6	**81b**	21	DMF	Cs_2CO_3	43	48	**L5**	94
7	**78a**	5	DMF	Cs_2CO_3	43	48	**L1**	92
8	**78b**	5	DMF	Cs_2CO_3	43	48	**L2**	95
9	**78d**	5	DMF	Cs_2CO_3	43	48	**L3**	90
10	**78f**	10	DMF	Cs_2CO_3	15	72	**L6**	73

[a] 32% aq. HCl was added to the starting material (SM) in the indicated solvent and heated to 80 °C until the deprotection of MOM was complete (followed by LC-MS). Then the base was added, and the reaction mixture was heated to 90 °C for the corresponding time, unless otherwise stated. [b] Heated to reflux. [c] 5.4 M NaOMe in MeOH.

Conditions for acidic deprotection of the MOM group[39], followed by base-assisted cycloisomerization were tested on the mixed terpyridine/bipyridine **81a** to obtain ligand **L4**.

Various reaction conditions, like varying the acid, base, solvent, and reaction time, were tried (Table 2.2, entries 1-5). The use of HCl, Cs_2CO_3, and DMF resulted in the isolation of **L4** in high yield (Table 2.2, entry 5). These conditions also led to the isolation of **L1-L3**, **L5**, and **L6** (Table 2.2, entries 6-10) in good to high yields.

2.3. Synthesis of Molecular "Crossings" and "Corners" by Metal Complexation

A linear bilateral extended conformation of ligands can be acquired by formation of complexes with a 2:1 ligand-to-metal ratio (2:1 complexes). Initially, complexation of simple symmetric ligands **L1-L3** was tested with divalent octahedral metals (Ru^{2+}, Zn^{2+}, and Fe^{2+}) to form molecular "crossings" (Table 2.3). Ruthenium(II) complexes **[L1-L3$_2$Ru](PF$_6$)$_2$** were prepared by heating corresponding ligands with $RuCl_2(DMSO)_4$ in ethylene glycol at 120 °C,[4d] resulting in a high product yields (Table 2.3, entries 1, 4, and 7).

Table 2.3. Synthesis of Metal Complexes with Simple Symmetric Ligands L1-L3[a]

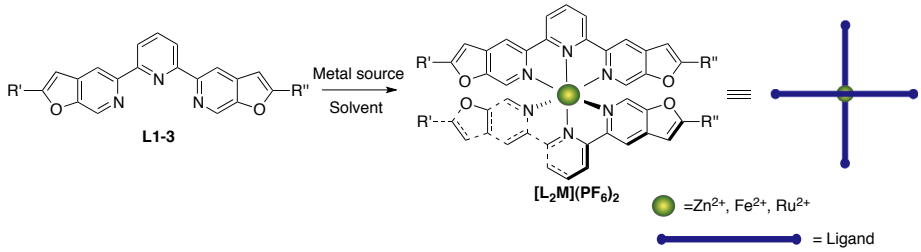

entry	ligand	R′=R″=	metal source	solvent	time (h)	T (°C)	product	Yield (%)
1	**L1**		$RuCl_2(DMSO)_4$	Ethylene glycol	18	120	**[L1$_2$Ru](PF$_6$)$_2$**	92
2			$Zn(OTf)_2$	THF/MeOH	18	rt	**[L1$_2$Zn](PF$_6$)$_2$**	94
3			$Fe(BF_4)_2$•$6H_2O$	THF/H_2O	18	rt	**[L1$_2$Fe](PF$_6$)$_2$**	90
4	**L2**	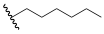	$RuCl_2(DMSO)_4$	Ethylene glycol	18	120	**[L2$_2$Ru](PF$_6$)$_2$**	99
5			$Zn(OTf)_2$	THF/MeOH	18	rt	**[L2$_2$Zn](PF$_6$)$_2$**	87
6			$Fe(BF_4)_2$•$6H_2O$	THF/H_2O	18	rt	**[L2$_2$Fe](PF$_6$)$_2$**	90
7	**L3**		$RuCl_2(DMSO)_4$	Ethylene glycol	18	120	**[L3$_2$Ru](PF$_6$)$_2$**	98
8			$Zn(OTf)_2$	THF/MeOH	48	50	**[L3$_2$Zn](PF$_6$)$_2$**	94
9			$Fe(BF_4)_2$•$6H_2O$	THF/MeCN/H_2O	18	rt	**[L3$_2$Fe](PF$_6$)$_2$**	80

[a] A solution of metal source (0.5 eq) was added to a solution of **L1-L3** (1.0 eq) and stirred at the indicated temperature. After the stated reaction time, sat. aq. KPF_6 was added to induce precipitation and the solid was collected by filtration.

Simple phenyl-substituted ligand **L1** and *n*-hexyl-substituted ligand **L2** formed 2:1 zinc(II) complexes with zinc(II) triflate in a mixture of tetrahydrofuran and methanol at room temperature (Table 2.3, entries 2 and 5). As 4-pyridyl-substituted ligand **L3** is less soluble,

heating at 50 °C was necessary to facilitate complexation, as shown in Table 2.3, entry 8. Similarly, Fe^{2+} complexes were prepared by reacting iron(II) tetrafluoroborate with the corresponding ligand in a mixture of tetrahydrofuran and water at room temperature (Table 2.3, entries 3 and 6), but, in the case of **L3**, addition of acetonitrile to the reaction mixture was necessary to improve solubility and yield (Table 2.3, entry 9). All resulting metal complexes were precipitated with aqueous KPF_6 and were obtained in good to high yield. The resulting complexes were recrystallized with diethyl ether vapor diffusion into acetonitrile or dichloromethane solutions. Kinetically stable ruthenium(II) complexes can be additionally purified by silica gel column chromatography.

Analogous to simple ligands **L1-L3**, mixed terpyridine/bipyridine ligands **L4-L6** reacted with $Zn(OTf)_2$ and $Fe(BF_4)_2 \cdot 6H_2O$ selectively at the terpyridine coordination site (Table 2.4), forming either "corner" complexes with **L4** and **L5**, or "crossing" complexes with **L6** leaving bipyridine coordination site unreacted.

Table 2.4. Synthesis of Metal Complexes with Mixed Terpyridine/Bipyridine L4-L6 Ligands[a]

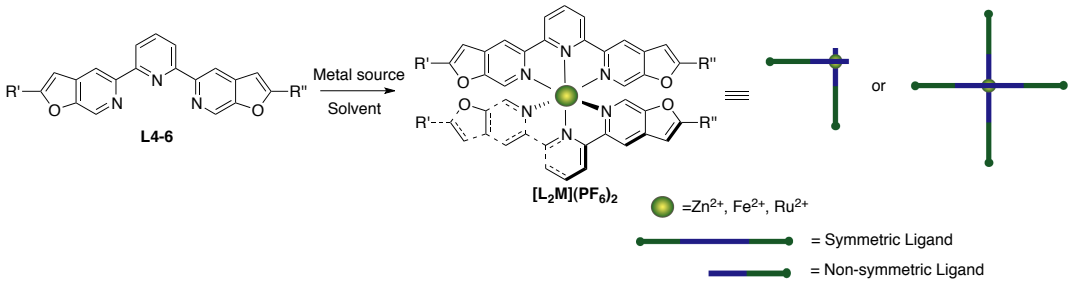

entry	ligand	R′= R″=	metal source	solvent	time (h)	T (°C)	product	Yield (%)
1	**L4**		$Zn(OTf)_2$	THF/MeOH	18	rt	**$[L4_2Zn](PF_6)_2$**	98
2			$Fe(BF_4)_2 \cdot 6H_2O$	THF/H_2O	18	rt	**$[L4_2Fe](PF_6)_2$**	97
3		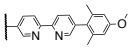	$RuCl_2(DMSO)_4$	Ethylene glycol	48	120	**$[L4_2Ru](PF_6)_2$**	-[b]
4	**L5**		$Zn(OTf)_2$	THF/H_2O	6	rt	**$[L5_2Zn](PF_6)_2$**	99
5			$Fe(BF_4)_2 \cdot 6H_2O$	THF/H_2O	6	rt	**$[L5_2Fe](PF_6)_2$**	80
6		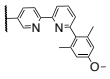	$RuCl_2(DMSO)_4$	Ethylene glycol	48	120	**$[L5_2Ru](PF_6)_2$**	-[b]
7	**L6**		$Zn(OTf)_2$	THF/MeOH	20	rt	**$[L6_2Zn](PF_6)_2$**	92
8		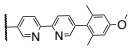	$Fe(BF_4)_2 \cdot 6H_2O$	THF/H_2O	18	rt	**$[L6_2Fe](PF_6)_2$**	80
9			$RuCl_2(DMSO)_4$	Ethylene glycol	48	120	**$[L6_2Ru](PF_6)_2$**	-[b]

[a] A solution of metal source was added to a solution of **L4-L6** and stirred at indicated temperature. After the stated reaction time, sat. aq. KPF_6 was added to induce precipitation and the solid was collected by filtration. [b] Complicated mixture, product could not be isolated.

This selectivity can be explained by the kinetic lability of Zn(II) and Fe(II) complexes and the thermodynamic stability of the highest order chelate. In contrast, the kinetically inert character of Ru(II) led to a complicated mixture of oligomers when **L4-L6** were used (Table 2.4, entries 3, 6, and 9). Isolation of the desired 2:1 complexes was not successful. Therefore, an alternative approach towards ruthenium(II) complexes was considered for the mixed ligand systems **L4-L6**. By first introducing ruthenium(II) and then functionalizing the obtained complex with bipyridine moieties, the desired "corner" and "crossing" complexes were obtained (Scheme 2.6 and 2.7).

Scheme 2.6. Indirect Synthesis Towards the Ruthenium(II) Complex with Mixed Ligand L6

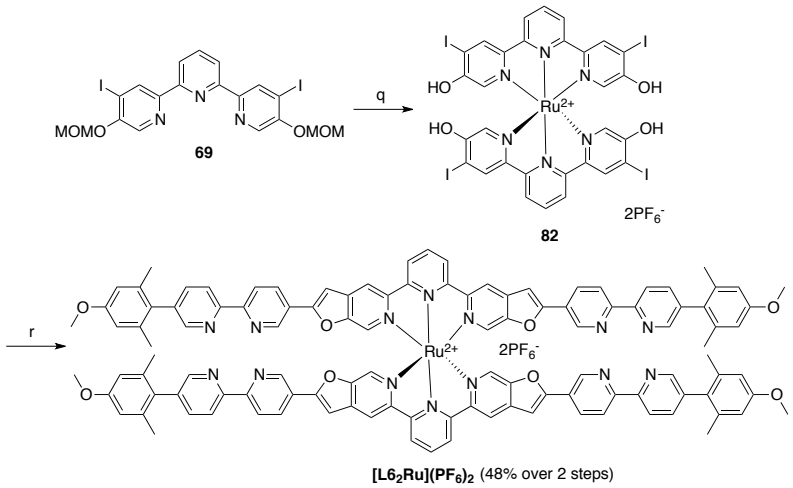

(q) 0.5 eq $RuCl_2(DMSO)_4$, ethylene glycol, 120 °C, 48 h, then aq. KPF_6; (r) 10 mol% $PdCl_2(PPh_3)_2$, 20 mol% CuI, 4.2 eq **77a**, DMF, DIPEA, 80 °C, 48 h, then aq. KPF_6.

Diiodoterpyridine **69** was subjected to complexation with 0.5 equivalents of $RuCl_2(DMSO)_4$ by heating in ethylene glycol (Scheme 2.6). Unexpectedly, during the reaction, the MOM protecting groups were cleaved, leading to the formation of compound **82**. This finding obviated harsh acidic conditions[39] for MOM-deprotection. Crude complex **82** was used in the next step, where Sonogashira cross-coupling with acetylene **77a** and *in situ* ring closure[40] afforded compound **$[L6_2Ru](PF_6)_2$** directly; thus, leading to the desired complexes in just two steps starting from **69** with a 48% overall yield.

The corresponding non-symmetric Ru(II) complexes **$[L4_2Ru](PF_6)_2$** and **$[L5_2Ru](PF_6)_2$** were prepared by a similar synthetic methodology (Scheme 2.7). Complexation of manisyl-substituted iodoterpyridine **79c** with 0.5 eq of $Ru(DMSO)_4Cl_2$ in EtOH in one step gave complexed, deprotected, and partially cyclized product **83**, which was used without further purification in the subsequent reaction. The Sonogashira coupling with ethynylbipyridine **77a** or **77b** and one-pot cyclization gave the desired complexes with 43% or 40% isolated yields over two steps, respectively.

The ^{1}H NMR spectra of **[L4$_2$Zn](PF$_6$)$_2$** and **[L4$_2$Fe](PF$_6$)$_2$** (Figure 2.3, spectra b and c) parallel that of **[L4$_2$Ru](PF$_6$)$_2$** (spectrum d). Given that **[L4$_2$Ru](PF$_6$)$_2$** is synthesized by grafting *bipy* units on to the preformed *terpy* ruthenium(II) complex **83**, it seems reasonable to conclude that Fe(II) and Zn(II) also bind at the *terpy* unit of **L4**.

Scheme 2.7. Indirect Synthesis Towards Ruthenium(II) Complex with Mixed Ligands L4 and L5

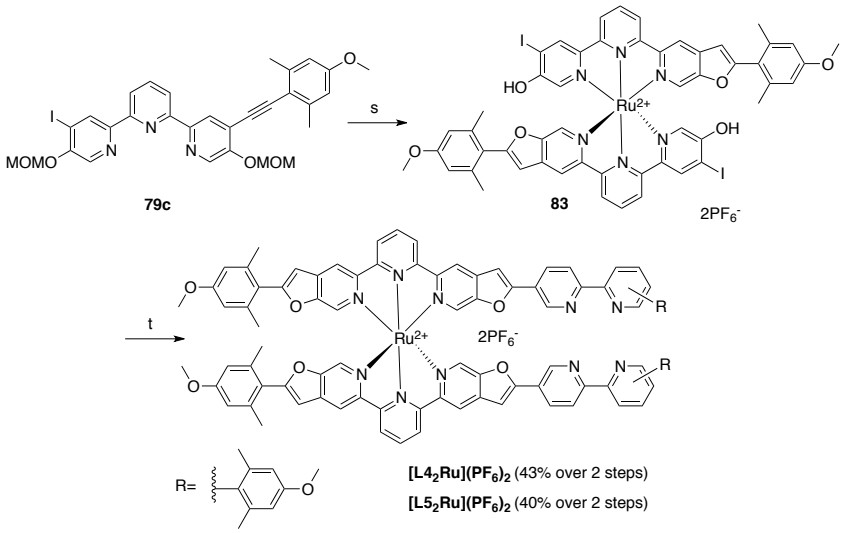

(s) 0.5 eq $RuCl_2(DMSO)_4$, EtOH, reflux, 72 h, then aq, KPF_6; (t) 5 mol% $PdCl_2(PPh_3)_2$, 10 mol% CuI, **77a** or **77b**, DMF, Et_3N, 90 °C, 24-39 h, then aq. KPF_6.

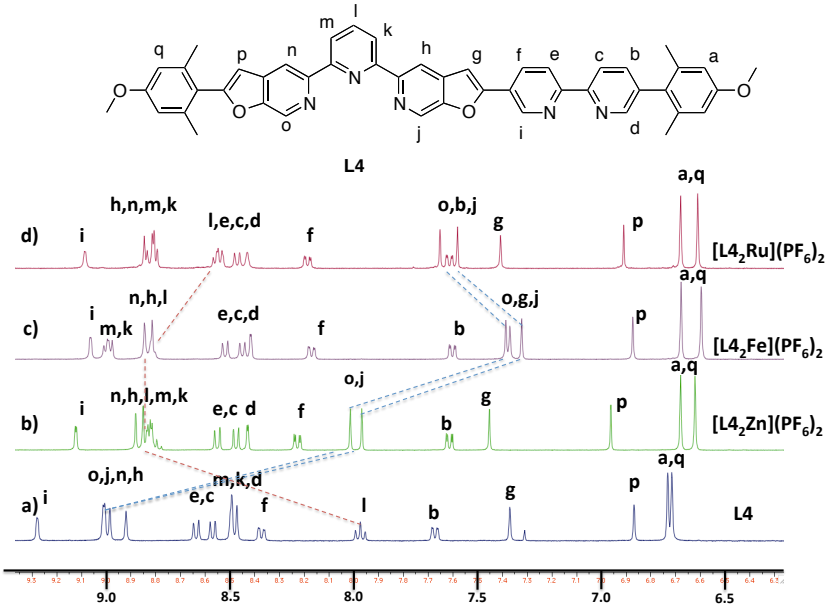

Figure 2.3. ^{1}H NMR (400 MHz, CD_2Cl_2) for the aromatic regions in **L4** and its Zn^{2+}, Fe^{2+}, and Ru^{2+} complexes.

Terpyridine transition metal complexes exhibit characteristic strong upfield shifts of the proton *o* and *j* signals (d-π* back-donation) and downfield shift for the signal of proton *l* (deshielding due to the conformational change of terpyiridine) compared to the shifts

observed for the free ligand (Figure 2.3, spectrum a). The proton signals corresponding to the bipyridine moiety are less affected. These observations hold true for all Zn^{2+}, Fe^{2+}, and Ru^{2+} complexes in the ligand series **L4–L6**.

2.4. Structure

Intermediates **78f** and **81a** give insight into the geometry of the terpyridine core and the relationship between its substituents. Single crystals suitable for X-ray crystallography were obtained from chloroform-*d* for non-symmetric *terpy* **81a** (Figure 2.4a) and from a mixture of ethyl acetate/hexane for symmetric *terpy* **78f** (Figure 2.4b). In these compounds, the *terpy* core acquires the characteristic *transoid*-conformation, thus placing 4,4″-substituents almost parallel to each other. As usual, the rings of the bipyridyl groups arrange themselves such that the N-atoms are on opposite sides of the group axis, thus avoiding short H···H contacts within the bipyridyl rings. However, for the symmetric derivative **78f** (Figure 2.4b), the N- and C-atoms in one bipyridyl group are disordered across both possible orientations that keep the N-atoms distant from one another.

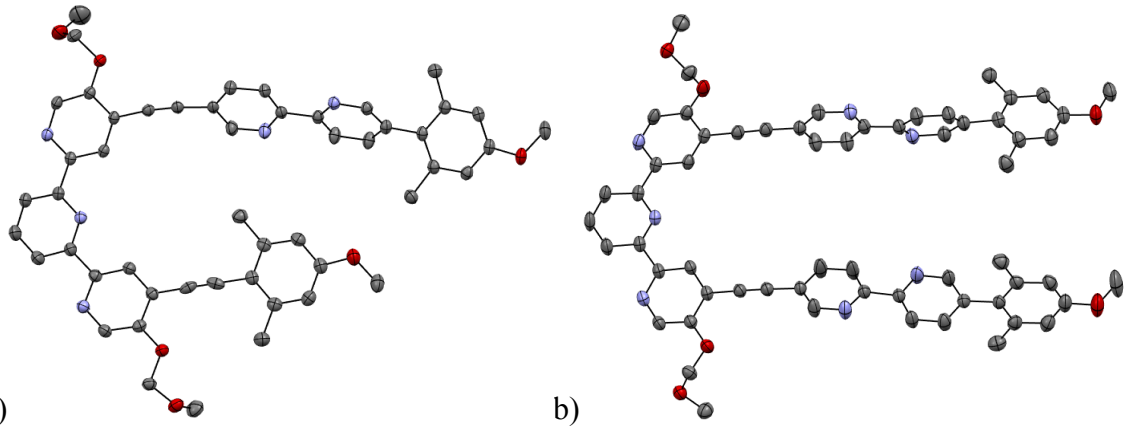

a) b)

Figure 2.4. Molecular structures of a) non-symmetric terpyridine **81a** and b) symmetric terpyridine **78f** (hydrogen atoms removed for clarity). Displacement ellipsoids (50% probability level).

Single crystals of the free ligands **L1** and **L4** suitable for X-ray crystallography were obtained by diethyl ether vapor diffusion into a saturated dichloromethane solution. In Figure 2.5, the molecular structures clearly show the presence of furo[2,3-c]pyridine-5-yl motifs linked by the central 2,6-substituted pyridine ring, thus forming the desired ligand architecture. The usual conformation of free terpyridine has a "Λ-shaped" structure with the flanking substituents placed almost perpendicular to each other, as shown on the example of **L1** (Figure 2.5a). One arm of the mixed ligand **L4** consists of furo[2,3-c]pyridine-5-yl, bipyridyl

and manisyl groups in a linear disposition and the second arm is the 2-manisyl-furo[2,3-c]pyridine-5-yl unit (Figure 2.5b). The manisyl rings in **L4** adopt a *clinal* conformation to the mean plane of the ligand, in contrast to the *periplanar* conformation of the simple phenyl substituents of **L1**. This deviation from planarity seen in crystal structure of **L4**, correlates with the much better solubility of the manisyl substituted ligands **L4-L6** in common organic solvents.

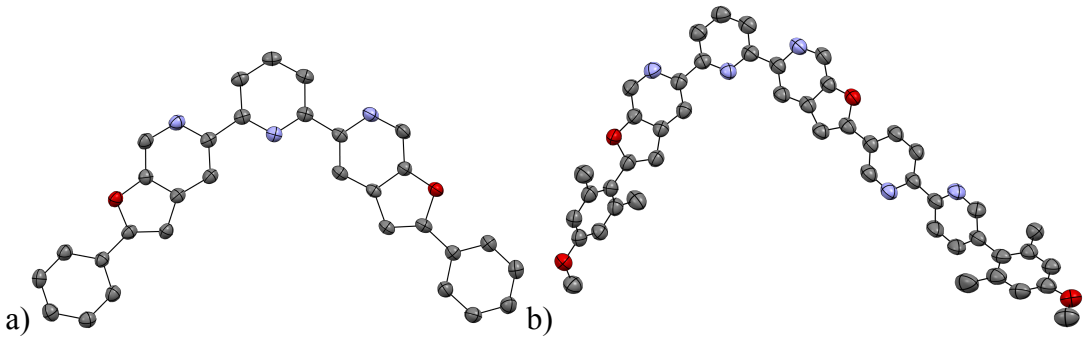

Figure 2.5. Molecular structures of a) phenyl substituted ligand **L1** b) mixed bipyridine/terpyridine ligand **L4** (hydrogen atoms removed for clarity). Displacement ellipsoids (50% probability level).

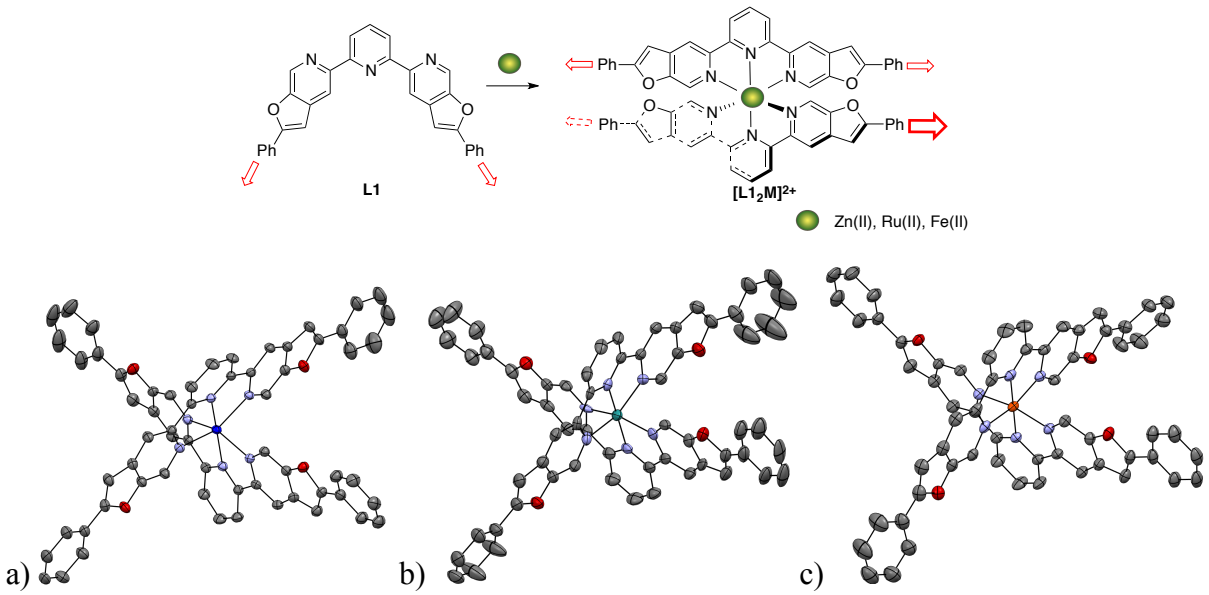

Figure 2.6. The switching of **L1** conformation from "Λ-shaped" to the "linear bilateral" and the molecular structures of a) **$[L1_2Zn](PF_6)_2$**; b) **$[L1_2Ru](PF_6)_2$**; c) **$[L1_2Fe](PF_6)_2$** (hydrogen atoms, PF_6^- and solvent molecules removed for clarity). Displacement ellipsoids (50% probability level).

The complexation of linear *terpy* ligands with metal ions preferring octahedral geometry transforms the overall ligand conformation from "Λ-shaped" to a "linear bilateral"

one, as illustrated by the molecular structures of the Fe^{2+}, Ru^{2+}, and Zn^{2+} complexes with **L1** depicted in Figure 2.6. Crystals for complexes **[L1$_2$Zn](PF$_6$)$_2$**, **[L1$_2$Ru](PF$_6$)$_2$**, and **[L1$_2$Fe](PF$_6$)$_2$** were obtained by diffusion of diethyl ether vapor into the corresponding acetonitrile solutions. These crystal structures possess triclinic symmetry and belong to space group *P-1*. In each case, the asymmetric unit consists of one cation, two PF_6^- anions, and a cavity situated about a center of inversion containing disordered solvent molecules. The three structures are essentially isostructural except that the contents of the solvent cavities may differ. The C(2)-N(2)-C(2) bite angle in these complexes increases in the order Fe^{2+} < Ru^{2+} < Zn^{2+} (atom numbers are defined in the sketch in Table 2.5).

Table 5. Selected Bite Angles and Bond Lengths of L1 Metal Complexes

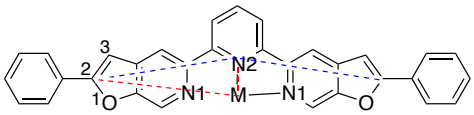

	[L1$_2$Fe](PF$_6$)$_2$	[L1$_2$Ru](PF$_6$)$_2$	[L1$_2$Zn](PF$_6$)$_2$
C(2)-N(2)-C(2) (°)[a]	142.1(3)	146.2(4)	150.1(2)
N(2)-M-C(2) (°)[b]	92.8(1)	89.9(2)	87.13(6)
M-N(1) (Å)[b]	1.971(3)	2.061(5)	2.183(2)
M-N(2) (Å)[b]	1.882(3)	1.983(4)	2.080(2)

[a] Average of two such parameters in the molecule. [b] Average of four such parameters in the molecule.

For an ideally "linear" ligand topology overall, this angle should be ~160°. The ligand in the zinc complex therefore has an almost "linear" topology, while in the iron complex it has a slightly more bent character. This trend correlates with the metal-to-nitrogen bond lengths, although that is not necessarily intuitive. An increase in the M–N2 distance would tend to decrease the bite angle, whereas increases in the M–N1 distances would open it.

2.5. Photophysical Properties

The UV/Vis spectra (Table 2.6 and Figure 2.7) of the phenyl and 4-pyridyl substituted ligands **L1** and **L3** display absorption maximum at ~300 nm in dichloromethane, while the UV/Vis spectrum of the *n*-hexyl-substituted ligand **L2** displays an absorption maximum at 239 nm and less pronounced transitions at ~300 nm. The introduction of bipyridyl groups in **L4**, **L5**, and **L6** leads to a ~36 nm bathochromic shift in the absorption maxima. These absorptions can be attributed to π-π* transitions. The simple symmetric ligands **L1** and **L2** show structured emission bands with maxima at 341 and 338 nm, respectively, and show medium quantum yields (~0.30). The ligands **L1** and **L2** display relatively short fluorescence lifetimes

(2.96 and 1.91 ns, respectively). The emission spectrum of 4-pyridyl derivative **L3** is much less featured than those of **L1** and **L2**. Its emission maximum, at 374 nm, also shows a bathochromic shift relative to **L1** and **L2**. Its quantum yield (0.14) is also significantly lower; however, the fluorescence lifetime (4.47 ns) is slightly longer compared to **L1** and **L2**.

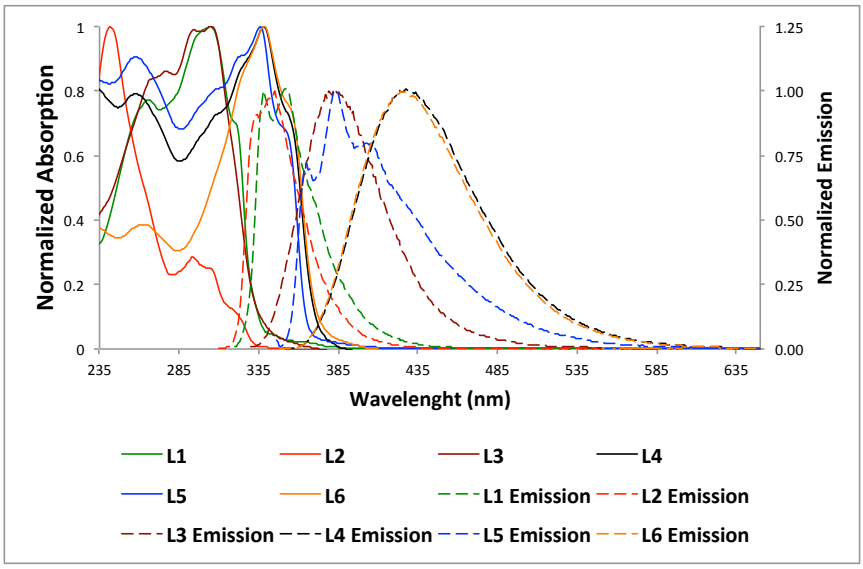

Figure 2.7. Emission and absorption spectra of ligands **L1-L6** in CH_2Cl_2 solution.

Table 2.6. Absorption and Emission Maxima, Molar Absorptivity Values (log ε), Quantum Yields (ϕ_f), and Lifetimes (τ_f) for Free Ligands L1-L6

	UV/Vis[a]		Fluorescence (solution)[a,b]				(powder)[c]	
	λ_{abs} (nm)	log ε (log(cm^{-1} mol^{-1} L))	λ_{ex} (nm)	λ_{em} (nm)	ϕ_f	τ_f (ns)	λ_{em} (nm)	ϕ_f
L1	261, **300**, 318	4.74, **4.84**, 4.68	300	341	0.27	2.96	451	0.38
L2	**239**, 287, 300	**5.12**, 4.55, 4.56	287	338	0.30	1.91	350	0.11
L3	270, 287, **300**	4.76, 4.78, **4.82**	300	374	0.14	4.47	517	0.42
L4	260, **338**	4.60, **4.73**	338	424	0.58	1.53	419	0.29
L5	258, **336**	4.69, **4.71**	336	364, **384**	0.19	2.58	461	0.13
L6	264, **338**	4.60, **5.07**	338	426	0.62	1.53	443	0.09

[a] All values were measured in CH_2Cl_2. Maximum values for λ_{abs}, λ_{em} and log ε are highlighted with bold. [b] PPO in cyclohexane (ϕ_f = 0.94) was used as the standard.[43] [c] All powder samples were measured with an integrating sphere.

The position of a manisyl group relative to the nitrogen atom strongly influences the emissive properties of *bipy* and *terpy* derivatives.[33] This observation is true for the mixed **L4**, **L5**, and **L6** ligands (Table 2.6 and Figure 2.7); when manisyl groups are placed at the *β*-position of the bipyridyl groups, as for **L4** and **L6**, broad emission bands at ~435 nm and high quantum yields (~0.60) are observed, while α-substituted analogue **L5** has structured emission band with maximum at 384 nm and relatively low quantum yield (0.19). The

compounds **L4**, **L5**, and **L6** display short lifetimes (1.53 ns, 2.58 ns, and 1.53 ns, respectively).

The solid-state (powder) emission spectra and quantum yields for ligands **L1-L6** are broad and featureless. Ligands **L1** and **L3** exhibit significantly higher quantum yields in the solid state (Table 2.6) than in solution (an increase of 0.27 to 0.38 and an increase of 0.14 to 0.42, respectively), as well as significantly red-shifted emission spectra (Δ110 nm and Δ143 nm, respectively). This suggests possible J-aggregate formation in the powder, with the fluorescence arising from exciton transitions. In contrast, the emission maximum of **L2** in powder is red-shifted only by 12 nm compared to the solution emission maximum, and the quantum yield decreases from 0.30 to 0.11. The mixed ligand **L5** shows a large bathochromic shift (Δ77 nm) but a lower quantum yield compared to that measured in solution. The solid-state quantum yields are decreased for the mixed ligands **L4** and **L6** as well, but emission maxima are less affected.

The absorption spectra of zinc(II), iron(II), and ruthenium(II) complexes with **L1-L6** (Table 2.7, Figures 2.8 and 2.9) display ligand centered (LC) transitions that are red-shifted by ~10-20 nm and of higher molar extinction coefficients relative to the parent ligands (Table 2.6). A sharp, intense band at ~330 nm appears for the metal complexes compared to the free ligands (Figures 2.8 and 2.9). Complexes with iron(II) and ruthenium(II) show characteristic lower energy bands from 360 to 600 nm and can be attributed to MLCT transitions.[41]

The MLCT bands of the iron(II) and ruthenium(II) complexes with **L1-L6** are non-luminescent at room temperature. However, excitation at the LC bands shows weak but detectable fluorescence (Table 2.7), possibly arising from an intraligand charge transfer state (ILCT).[42] The zinc(II) complexes exhibit a fluorescence comparable to that of parent ligands (Table 2.6 and 2.7), except the Zn(II) complex of *n*-hexyl-substituted **L2**. This complex has much higher quantum yield (0.63) than the free ligand (0.30).

The emission maxima of Zn(II), Fe(II), and Ru(II) complexes with **L1**, **L2**, and **L4-L6** ligands are red-shifted relative to those of the free ligands (Figures 2.8 and 2.9). However, metal complexes of 4-pyridyl-substituted **L3** show hypsochromic shift of emission maxima by ~20 nm, with respect to that of free ligand (Figure 2.8c).

The fluorescence lifetimes of the **L1-L4** metal complexes are in the range of 1.06 to 2.94 ns. The **L5** complexes with Zn(II) and Fe(II), and **L6** complex with Fe(II) display two lifetime values (Table 2.7).

The iron(II) and ruthenium(II) complexes of **L1-L6** do not show any detectible luminescence in the solid state (powder). However, zinc(II) complexes are slightly emissive, with quantum yields ranging from 0.06 to 0.17, that are significantly lower than those in

solution (Table 2.7). The only exception is zinc(II) complex of **L3**, which shows a slight increase in the quantum yield in the solid state compared to that in solution (from 0.11 to 0.16). This Zn(II) complex also exhibits a significant bathochromic shift (Δ99 nm) in the emission spectra of its powder compared to the solution.

Table 2.7. Absorption and Emission Maxima, Molar Absorptivity Values (log ε), Quantum Yields (ϕ_f), and Lifetimes (τ_f) for Metal Complexes $[L_2M](PF_6)_2$

		UV/Vis[a]		Fluorescence (solution)[a]				(powder)[e]	
L	M	λ_{abs} (nm)	log ε (log(cm^{-1} mol^{-1} L))	λ_{ex} (nm)	λ_{em} (nm)	ϕ_f	τ_f (ns)	λ_{em} (nm)	ϕ_f
L1	Ru	264, **341**, 388, 465	4.90, **5.13**, 4.60, 4.30	341	368	0.007[b]	1.74	-	-
	Zn	261, **318**, 335, 349	4.99, **5.10**, 5.09, 5.06	318	385	0.296[c]	1.85	423	0.10
	Fe	265, 316, 329, **346**, 419, 535	5.00, 5.05, 5.05, **5.12**, 4.43, 4.10	346	365	0.017[b]	1.97	-	-
L2	Ru	**250**, 329, 369, 462	**5.09**, 5.05, 4.26, 4.26	329	**348**, 366	0.001[d]	1.37	-	-
	Zn	**249**, 330, 343	**5.18**, 4.73, 4.80	330	**352**, 365	0.630[b]	1.63	374	0.11
	Fe	**252**, 336, 391, 532	**5.14**, 4.97, 4.11, 4.11	336	348, **370**	0.011[b]	1.82	-	-
L3	Ru	290, 325, **339**, 394, 464	4.88, 4.77, **4.97**, 4.39, 4.20	325	**349**, 363	0.005[b]	1.06	-	-
	Zn	261, **300**, 331, 346	4.99, **5.06**, 4.82, 4.92	300	**354**, 368	0.110[c]	1.10	453	0.16
	Fe	262, 297, 328, **344**, 424, 533	4.95, 5.03, 4.79, **5.08**, 4.28, 4.06	328	**351**, 363	0.007[c]	1.29	-	-
L4	Ru	254, **346**, 388, 463	4.94, **5.16**, 4.74, 4.37	346	465	0.003[c]	2.42	-	-
	Zn	243, **339**	5.01, **5.18**	339	487	0.573[b]	2.94	483	0.17
	Fe	253, **346**, 412, 533	4.96, **5.19**, 4.43, 4.13	346	441	0.007[b]	1.75	-	-
L5	Ru	252, **339**, 388, 465	4.93, **5.12**, 4.65, 4.32	339	443	0.001[d]	2.89	-	-
	Zn	248, **349**	4.95, **5.17**	349	497	0.097[d]	3.34 (42%), 8.03 (58%)	~500	0.05
	Fe	245, **345**, 411, 534	4.81, **5.00**, 4.25, 3.97	345	433	0.002[d]	2.37 (75%), 7.60 (25%)	-	-
L6	Ru	260, **354**, 396, 470	5.02, **5.33**, 4.96, 4.54	354	449	0.009[d]	2.18	-	-
	Zn	260, **353**	4.60, **5.07**	353	494	0.577[d]	2.06 (59%), 3.54 (41%)	501	0.06
	Fe	263, **359**, 430, 536	4.94, **5.35**, 4.64, 4.21	359	452	0.004[d]	2.25	-	-

[a] All values were measured in CH_2Cl_2. Maximum values for λ_{abs}, λ_{em} and log ε are highlighted with bold. [b] PPO in cyclohexane ($\phi_f = 0.94$); [c] DPA in cyclohexane ($\phi_f = 1.00$); [d] POPOP in cyclohexane ($\phi_f = 0.97$) were used as the standard.[43] [e] All powder samples were measured with an integrating sphere.

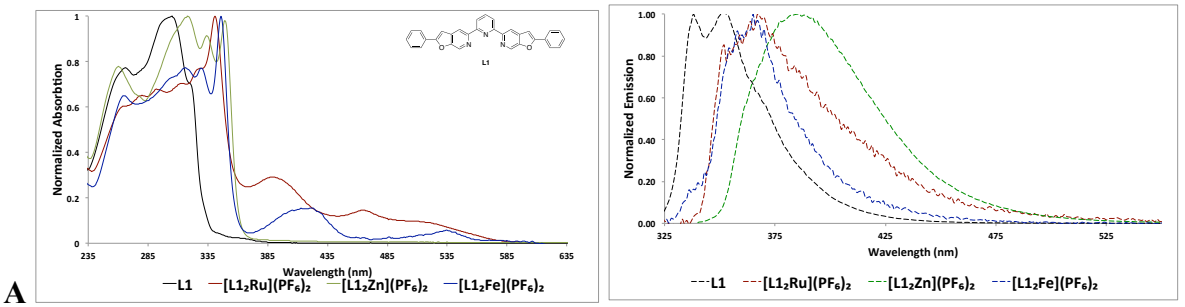

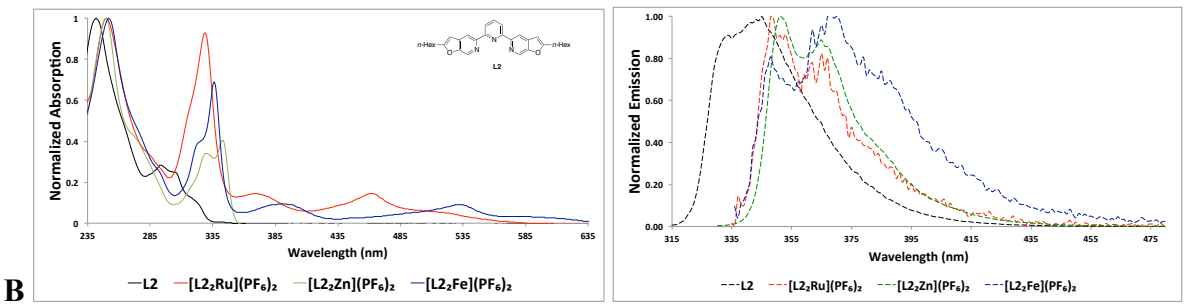

C

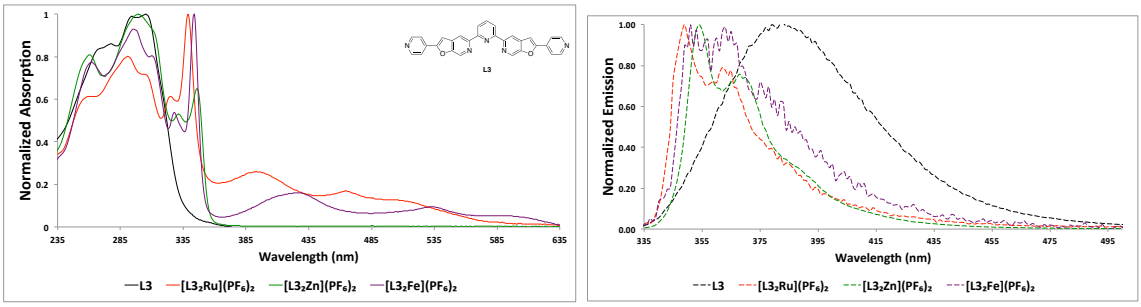

Figure 2.8. Emission and absorption spectra of ligands **L1**, **L2**, **L3** and their corresponding Zn^{2+}, Fe^{2+}, Ru^{2+} complexes in CH_2Cl_2 solution.

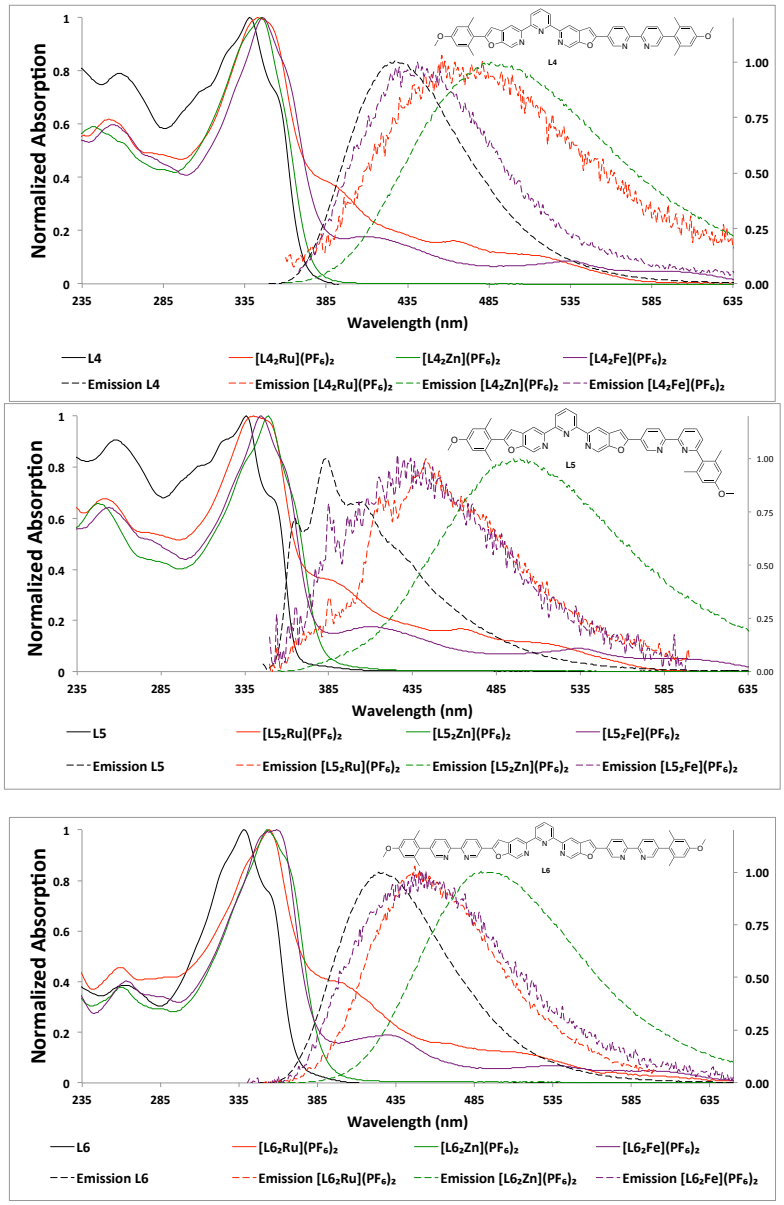

Figure 2.9. Emission and absorption spectra of ligands **L4**, **L5**, **L6** and their corresponding Zn^{2+}, Fe^{2+}, Ru^{2+} complexes in CH_2Cl_2 solution.

2.6. Thixotropic Metal-Organic Gel Based on Ru(II) Complex of L4

Gels are classified as either physical or chemical according to the nature of the interactions involved in their formation. Supramolecular gels are typically induced by aggregation of highly anisotropic 3D structures in solution which are assembled through non-covalent interactions such as hydrogen bonds, van der Waals, π-π stacking and ionic interactions. The design of metallogelators and incorporation of metals into supramolecular gels have received growing attention[44]; however, to our knowledge, no metal-organic gels containing ruthenium have been reported to date.

In our pursuit towards chiral resolution of the C_2 symmetric Ru(II) complex **[L4$_2$Ru](PF$_6$)$_2$**, a counter ion metathesis was performed, where achiral PF_6^- was exchanged with an enantiopure D_3 symmetric (Δ-TRISPHAT)$^-$ anion[45] (Figure 2.10). The comparison of ^{1}H NMR spectra (Figure 2.11) supports the formation of the **[L4$_2$Ru](Δ-TRISPHAT)$_2$** diastereomeric ion-pairs. Two sets of NMR signals can be observed in the proton spectrum of the Ru(II) complex Δ-TRISPHAT salt if compared to the corresponding PF_6^- salt. So far, separation of both diastereometrs was not successful.

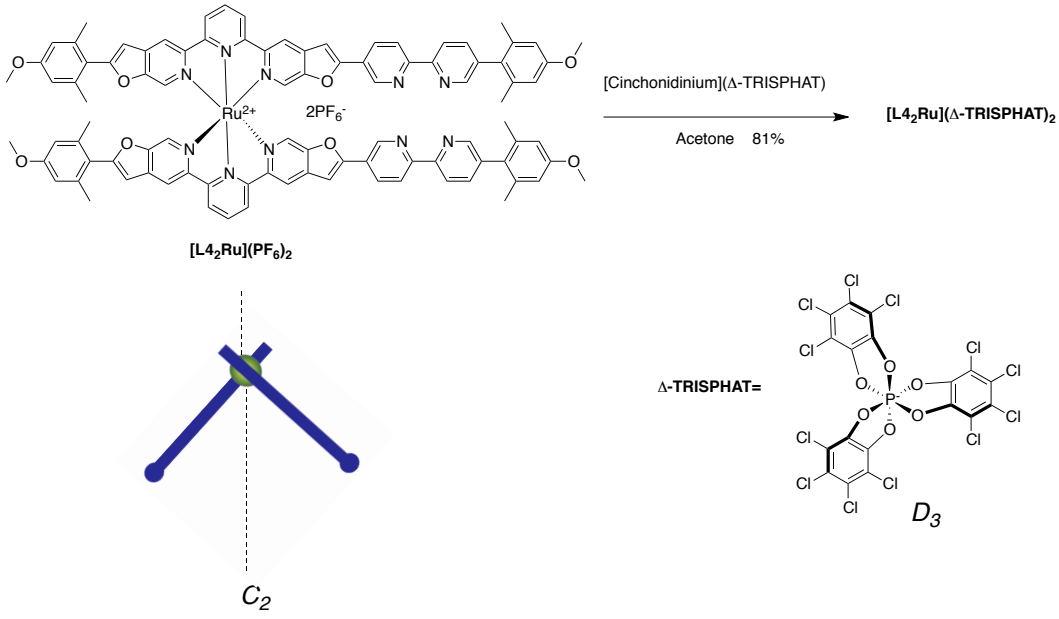

Figure 2.10. Synthesis of Ru(II) complex **[L4$_2$Ru](Δ-TRISPHAT)$_2$**.

However, attempts to separate diastereomers from dichloromethane by recrystallization resulted in an unexpected formation of a metal-organic gel (MOG), which exhibits thixotropic properties – it undergoes a reversible change from a gel into a liquid by mechanical stress (Figure 2.12). This ruthenium complex turned out to be an efficient metalogellator with critical gelation concentration 1.13 wt% (4.8 mM) at room temperature (Figure 2.13). At

higher concentrations (above 3.7 wt% (16.0 mM)) the gel forms in less than one minute, still retaining its thixotropic properties.

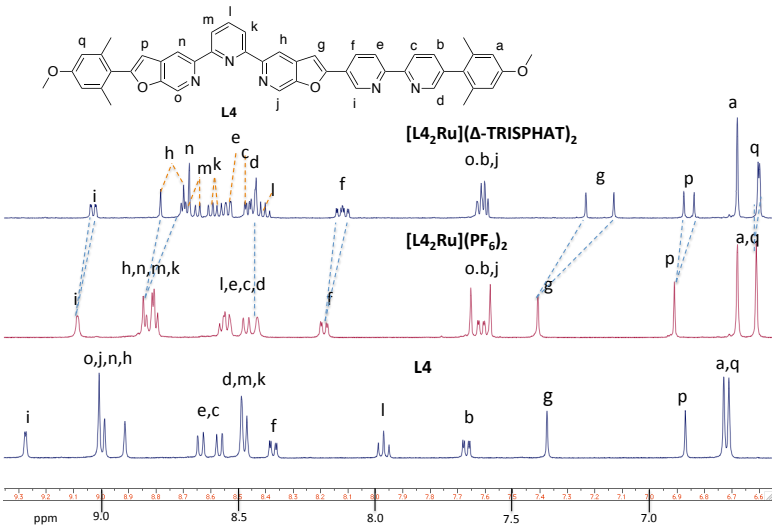

Figure 2.11. Comparison of aromatic regions in ^{1}H NMR spectra (400 MHz, CD_2Cl_2) of **L4**, **[L4$_2$Ru](PF$_6$)$_2$** and **[L4$_2$Ru](Δ-TRISPHAT)$_2$**.

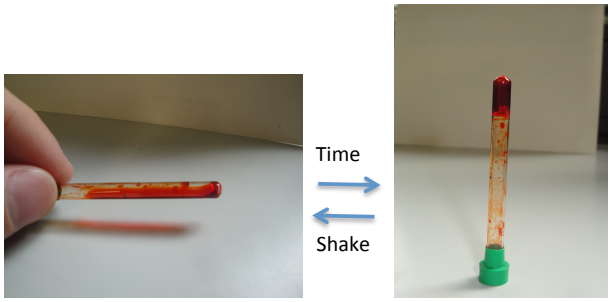

Figure 2.12. Gelation and thixotropic behaviour of **[L4$_2$Ru](Δ-TRISPHAT)$_2$** in CH_2Cl_2.

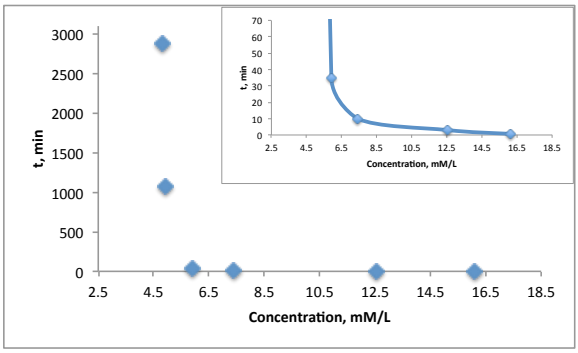

wt%	conc. mM	time, min
3.76	16.1	0.5
2.93	12.5	3
1.73	7.4	10
1.38	5.9	35
1.15	4.9	1080
1.13	4.8	2880

Figure 2.13. Time required for a gel formation vs. **[L4$_2$Ru](Δ-TRISPHAT)$_2$** conentration (wt%) in CH_2Cl_2 at room temperature.

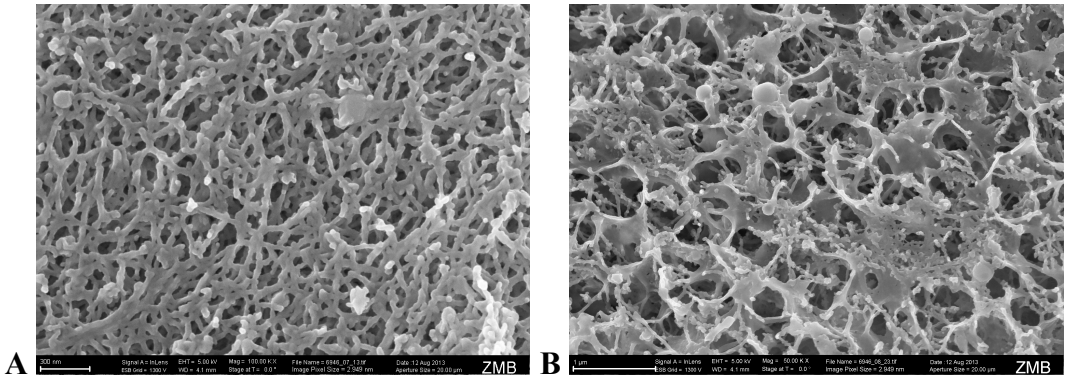

Figure 2.14. Cryo-SEM images of **[L4$_2$Ru](Δ-TRISPHAT)$_2$** in CH_2Cl_2 (3.76 wt%, 16.1 mM). **A**. Sample was applied on a carrier and immediately plunge frozen in liquid ethane; **B**. Sample was applied on a carrier, kept for ~30 sec and then frozen.

Gel morphology was determined by cryo-SEM microscopy (Figure 2.14). A 3D cross-linked fibrous structure (diameter of fibers ~30-40 nm) was observed when the gel was shaken to form a liquid, then applied on a sample carrier and immediately plunge frozen in liquid ethane. However, when the sample was kept on the carrier for gelation time and only then plunge frozen, 3D cross-linked surfaces were identified.

To gain a deeper insight into the structure of the gel and molecular interactions associated with its thixotropic properties, small and wide angle X-ray scattering (SAXS and WAXS) measurements were performed. However, this Ru(II) complex at gelation concentrations strongly absorbs X-ray photons, and it turned out to be opaque to the conventional X-ray source. A stronger X-ray source like synchrotron should be considered to study these systems.

Valuable photophysical properties of ruthenium, which have been used in photonics and light energy conversion devices[7], in combination with the ability to form a metal-organic gel and its mechanical stress responsive behavior is a promising combination of properties with huge potential in material science.

2.7. Conclusions

The concept of a linear bilateral extended terpyridine was developed by fusing five-membered rings to the flanking pyridine rings of the *terpy* ligand, thus mimicking the linear geometry of 5,5′-functionalized 2,2′-bipyridine. It was realized synthetically by developing a modular synthesis of 2,6-bis(2-substituted-furo[2,3-c]pyridine-5-yl)pyridine based ligands. This modular synthesis allowed for the introduction of alkyl, aryl, and heteroaryl

functionalities in the flanking positions of these ligands. The molecular "crossings" were synthesized by coordinating simple symmetric ligands to divalent metal cations (Fe^{2+}, $Ru^{2+}$and Zn^{2+}) forming 2:1 complexes. In the case of mixed bipyridine/terpyridine ligands, zinc(II) and iron(II) selectively form complexes at the terpyridine coordination site. The corresponding ruthenium(II) complexes were prepared through an indirect methodology. First, unfunctionalized ruthenium(II) terpyridine 2:1 complexes were prepared, then bipyridyl groups were introduced through a one-pot Sonogashira coupling with an *in situ* furan ring formation. In this way, the *terpy* and *bipy* moieties arrange themselves in a linear rod motif. These complexes resemble molecular "crossings" and "corners", depending on whether symmetric or non-symmetric starting materials were used in the reaction. X-ray crystal structures of symmetric phenyl substituted analogues showed that a proper "linear bilateral" conformation of *terpy* ligands is acquired by complexation with metal ions, so that flanking substituents are spanned relative to each other with an obtuse angle. This angle increases in the sequence of Fe^{2+}<Ru^{2+}<Zn^{2+}. The free ligands show high to medium fluorescence quantum yields that are significantly quenched by complexation with Fe^{2+} and Ru^{2+} ions. The zinc(II) complexes still retain a fluorescence efficiency similar to that of their parent ligands. The free ligands and their zinc(II) complexes exhibit solid-state emission with moderate to medium quantum yields, so could find an application as optoelectronic materials. The Ru(II) complex of non-symmetric bipyridine/terpyridine ligand **L4** in combination with Δ-TRISPHAT$^-$ counterion forms unusual thixotropic metal-organic gel in dichloromethane.

This molecular design has potential in supramolecular chemistry giving new topological features to terpyridine, which now mimics the linear geometry of 5,5′-disubstituted 2,2′-bipyridine. Terpyridine based fundamental building blocks with "crossing" and "corner" character are new tools in the hands of chemists and could inspire the creation of new designed molecular architectures.

2.8. Experimental Section

2.8.1. Materials and Methods

All reagents and solvents used for reactions were reagent grade and used without further purification unless otherwise noted. Anhydrous THF and toluene was supplied from an Mbraun solvent purification system. Analytical thin-layer chromatography was performed with Macherey–Nagel POLYGRAM SIL N-HR/UV254 or ALOX N/UV254. Flash silica gel column chromatography was performed with Merck silica gel 60 (particle size 0.040–0.063 mm). Flash alumina column chromatography was performed with deactivated (5% water) Fluka alumina (particle size 0.05–0.15 mm, pH 7.0±0.5). Melting points were recorded on a Büchi B-540 melting point apparatus. For characterization purposes, proton nuclear magnetic resonance (^{1}H-NMR) spectra were all recorded on Bruker instruments (AV-300 and ARX-300 at 300 MHz, AV2- 400 at 400 MHz, and AV-500 at 500 MHz). Chemical shifts are reported in ppm relative to $CHCl_3$ (δ 7.26), CD_2Cl_2 (δ 5.31), CD_3CN (δ 1.94) or DMSO-d_6 (2.50). Multiplicity and shape are indicated by one or more of the following abbreviations: s (singlet); d (doublet); t (triplet); q (quartet); dd (doublet of doublets); td (triplet of doublets); m (multiplet); br (broad). Carbon-13 nuclear magnetic resonance (^{13}C- NMR) spectra were recorded on Bruker instruments (ARX-300 at 75 MHz, AV2-400 at 100 MHz, and AV-500 at 125 MHz). Chemical shifts are reported relative to $CDCl_3$ (δ 77.2), CD_2Cl_2 (δ 53.8), CD_3CN (δ 1.3) or DMSO-d_6 (δ 39.5). Infrared spectroscopic data were recorded on NaCl plates as thin films, as KBr pellets or neat sample on a Perkin Elmer Spectrum One (PE) or Jasco FT/IR-4100 spectrophotometer. The intensities are given as follows: *s* = strong, *m* = medium, and *w* = weak. An Agilent 8453 UV/Vis spectrophotometer was used to record all UV/Vis spectra. Emission spectra and lifetimes (ns) were recorded on an Edinburgh Instruments FLS920 spectrometer. Solid-state quantum yields were measured using an integrating sphere accessory for FLS920 spectrometer. X-ray structures were carried out by the Laboratorium für Computerchemie und Röntgenstructuranalyse of the Institute of Organic Chemistry of the University of Zurich using a Nonius KappaCCD diffractometer with MoKα radiation (λ = 0.71037 Å).

2.8.2. Experimental Procedures

2.8.2.1. Synthesis of *Terpy* Core (69)

2-Bromo-5-(4,4,5,5-tetramethyl-1,3,2-dioxaborolan-2-yl)pyridine (63)[26]

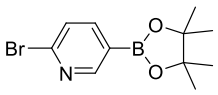

To a solution of 2,5-dibromopyridine (**62**) (22.46 g, 94.80 mmol) in Et_2O (800 mL) was added dropwise a solution of *n*-BuLi (2.50 M in hexane, 39.80 mL, 99.50 mmol) at –78 °C under N_2 atmosphere. After addition, the mixture was stirred at –78 °C for 3 h, then a solution of 2-methoxy-4,4,5,5-tetramethyl-1,3,2-dioxaborolane (15.88 g, 100.5 mmol) in Et_2O (20 mL) was introduced dropwise to the reaction mixture at –78 °C. The reaction was gradually warmed up to room temperature and stirred for 12 h, then the solvent was removed under reduced pressure. The residue was dissolved in 10% NaOH solution (200 mL) and washed with CH_2Cl_2 (100 mL × 2). The organic layers were discarded and the aqueous phase was acidified carefully to pH 1~2 with 32% HCl, then extracted with CH_2Cl_2 (200 mL × 3). The combined organic extracts were dried over $MgSO_4$, filtered and concentrated reduced pressure to afford boronic ester **63** (23.66 g, 83%) as a pale white solid.

Mp 94–95.5 °C (lit. mp 94 °C)[26]

^{1}H NMR (400 MHz, $CDCl_3$, δ): 8.67 (dd, J = 0.7, 2.0 Hz, 1H), 7.87 (dd, J = 2.0, 7.9 Hz, 1H), 7.47 (dd, J = 0.7, 7.9 Hz, 1H), 1.34 (s, 12H).

^{13}C NMR (100 MHz, $CDCl_3$, δ): 156.1 (d), 145.6 (s), 144.5 (d), 127.7 (d), 84.6 (s), 25.0 (q) *C*-Bpin was not observed in ^{13}C NMR due to line broadening of the short relaxation time and the quadrupole moment of ^{11}B (I = 3/2).

IR (film on NaCl, cm^{-1}): 2978*m*, 1578*s*, 1546*m*, 1455*m*, 1385*s*, 1357*vs*, 1142*m*, 1103*s*, 1015*m*, 857*m*, 823*m*, 742*m*, 662*m*.

MS (ESI) *m/z*: 284.1 ([M + H]$^+$); 306.1 ([M + Na]$^+$).

HRMS (ESI) *m/z*: [M + Na]$^+$ calcd for $C_{11}H_{15}NO_2BrBNa$: 306.0291; found: 306.0284.

2,6-Bis(trimethylstannyl)pyridine (65)[28]

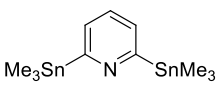

To a suspension of fresh finely chopped sodium (32.3 g, 1.40 mol, 7.38 eq) in anhydrous DME (200 mL) a solution of Me_3SnCl (94.5 g, 0.474 mol, 2.50 eq) in anhydrous DME (100 mL) was slowly added at –15 °C under N_2 atmosphere. After stirring for 3 h at –15 °C, the

pistachio green suspension of $NaSnMe_3$ in DME was introduced in 30 min., via a cannula, to a solution of 2,6-dichloropyridine (**64**) (28.07 g, 0.1897 mol, 1.00 eq) in anhydrous DME (200 mL) at –15 °C under N_2 atmosphere. The dark brown reaction mixture was stirred at –15 °C for 1 h, then gradually warmed up to room temperature and stirred for 18 h. The solvent was removed under reduced pressure, and the residue was treated with Et_2O (350 mL). The insoluble inorganic salts were filtered off through a plug of Celite (3 cm) and the cake was washed with Et_2O (300 mL). The combined filtrates were concentrated under reduced pressure to afford the crude product as dark brown oil. The crude residue was purified by vacuum distillation (0.05 mbar, 80-82 °C) to give 2,6-bis(trimethylstannyl)pyridine (**65**) (64.39 g, 84%) as colorless oil.

^{1}H NMR (400 MHz, CD_2Cl_2, δ): 7.38-7.25 (m, 3H), 0.30 (s, with Sn satellites, $^2J_{HSn}$ = 55.8/53.4 Hz, 18H).

^{13}C NMR (75 MHz, CD_2Cl_2, δ): 174.4 (s), 131.5 (d), 130.3 (d), -9.7 (q, with Sn satallites, $^1J_{CSn}$=346.9/331.6 Hz).

5,5′′-Bis(4,4,5,5-tetramethyl-1,3,2-dioxaborolan-2-yl)-2,2′:6′,2′′-terpyridine (66)[26]

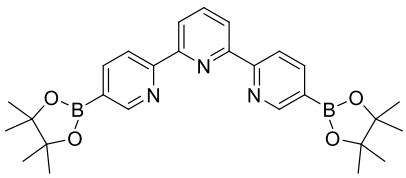

To a degassed mixture of boronic ester **63** (99.6 g, 342 mmol, 2.15 eq) and $Pd(PPh_3)_4$ (8.97 g, 7.76 mmol, 4.87 mol%) in toluene (600 mL) a solution of bisstannyl pyridine **65** (64.5 g, 159 mmol, 1.00 eq) in degassed toluene (250 mL) was added under N_2 atmosphere. The reaction mixture was heated to reflux for 24 h. The mixture was cooled to 5 °C and the resulting precipitate was collected by filtration. The solid was dissolved in CH_2Cl_2 (600 mL) and washed with 10% aqueous KF solution (500 mL × 2). The aqueous phases were extracted with CH_2Cl_2 (200 ml × 2). The combined organic phases were dried over $MgSO_4$, filtered and concentrated under reduced pressure to give diboronic ester **66** (42.26 g, 56%) as an off-white solid.

Mp 259.5–260.5 °C (lit. mp 251 °C)[26].

^{1}H NMR (400 MHz, $CDCl_3$, δ): 9.03 (dd, *J* = 0.9, 1.7 Hz, 2H), 8.59 (dd, *J* = 0.9, 7.9 Hz, 2H), 8.51 (d, *J* = 7.8 Hz, 2H), 8.23 (dd, *J* = 1.7, 7.9 Hz, 2H), 7.96 (t, *J* = 7.8 Hz, 1H), 1.39 (s, 24H).

^{13}C NMR (125 MHz, $CDCl_3$, δ): 158.3 (s) 155.6 (s), 155.2 (d), 143.3 (d), 138.0 (d), 121.9 (d), 120.4 (d), 84.3 (s), 25.0 (q) *C*-Bpin was not observed in ^{13}C NMR due to line broadening of the short relaxation time and the quadrupole moment of ^{11}B (*I* = 3/2).

IR (film on NaCl, cm^{-1}): 2977*m*, 1593*s*, 1547*m*, 1359*vs*, 1316*m*, 1142*m*, 1107*m*, 1022*m*, 857*m*, 820*m*, 765*m*, 666*m*.

MS (ESI) *m/z*: 486.3 ($[M + H]^+$); 508.3 ($[M + Na]^+$).

HRMS (ESI) *m/z*: $[M + Na]^+$ calcd for $C_{27}H_{33}N_3O_4B_2Na$: 508.2567; found: 508.2561.

5,5′′-Dihydroxy-2,2′:6′,2′′-terpyridine (67)[30]

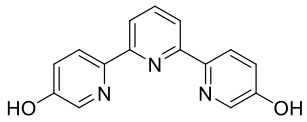

Prepared according to the modified procedure of Jui-Chang Tseng.

To a solution of diboronic ester **66** (42.16 g, 86.89 mmol, 1.000 eq) in THF (1.5 L) an aqueous solution of NaOH (6.0 M, 41.7 mL, 260 mmol, 3.00 eq) was added. After stirring the mixture for 10 min at room temperature, white precipitate formed. Then, to the resulting suspension an aqueous solution of H_2O_2 (30%, 23.6 mL, 226 mmol, 2.60 eq) was added dropwise in ~ 10 min by cooling the mixture with ice-water bath. The reaction mixture was allowed to stir at room temperature for 18 h and quenched with 10% $Na_2S_2O_3$ aqueous solution (250 mL). After complete removal of volatile organic solvents under reduced pressure, the aqueous layer was acidified with 10% HCl to pH 6–7. The resulting yellow precipitate was filtered, washed with H_2O (400 mL) and dried under high vacuum at 40 °C for 24 h to afford the dihydroxy terpyridine **67** (22.19 g, 96%) as a yellowish orange solid.

Mp 153–154 °C.

^{1}H NMR (500 MHz; DMSO-d_6, δ): 10.26 (s, 2H), 8.45 (d, J = 8.6 Hz, 2H), 8.25 (d, J = 2.7 Hz, 2H), 8.20 (d, J = 7.8 Hz, 2H), 7.95 (t, J = 7.8 Hz, 1H), 7.34 (dd, J = 8.6, 2.8 Hz, 2H).

^{13}C NMR (125 MHz, DMSO-d_6, δ): 154.8 (s), 154.4 (s), 146.6 (s), 137.9 (d), 137.4 (d), 122.9 (d), 121.5 (d), 118.4 (d).

IR (film on NaCl, cm^{-1}): 3093*br*, 1705*m*, 1565*s*, 1537*s*, 1490*m*, 1440*vs*, 1361*m*, 1283*s*, 1221*m*, 853*m*, 807*m*.

MS (ESI) *m/z*: 288.1 ($[M + Na]^+$).

HRMS (ESI) *m/z*: $[M + Na]^+$ calcd for $C_{15}H_{11}N_3O_2Na$: 288.0749; found: 288.0746.

5,5″-Bis(methoxymethoxy)-2,2′:6′,2″-terpyridine (68)

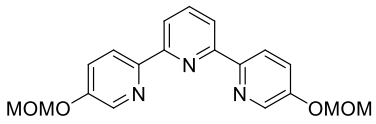

Prepared according to the modified procedure of Jui-Chang Tseng.

To a suspension of NaH (60% in oil, 3.80 g, 99.1 mmol, 3.00 eq) in anhydrous THF (120 mL) was added dropwise a solution of dihydroxy terpyridine **67** (8.76 g, 33.0 mmol, 1.00 eq) in DMF (40 mL) at 0 °C under N_2 atmosphere. After addition, the mixture was allowed to warm up and stirred at room temperature for 30 min, then cooled down to 0 °C. To this mixture was added slowly a freshly prepared solution of MOMCl in MeOAc, obtained as described in the literature from $ZnBr_2$ (3.9 mg, 1.8 mmol, 0.018 mol%) catalyzed reaction of AcCl (8.21 mL, 115.6 mmol, 3.50 eq) and $(MeO)_2CH_2$ (10.23 mL, 115.6 mmol, 3.50 eq)[31], at 0 °C under N_2 atmosphere. The reaction mixture was then warmed up to room temperature and stirred for 12 h. After slowly quenched with H_2O (200 mL) at 0 °C, the mixture was extracted with CH_2Cl_2 (200 mL × 3). The combined organic layers were dried over $MgSO_4$, filtered and concentrated under reduced pressure. The crude product was treated with hexane and collected by filtration. The residue was filtered through a short pad of silica gel eluating with hexane/EtOAc/MeOH (25:25:1) to afford terpyridine **68** (11.2 g, 96%) as a white solid.

Mp 75.5–76.5 °C.

^{1}H NMR (500 MHz, $CDCl_3$, δ): 8.53 (dd, *J* = 8.8, 0.6 Hz, 2H), 8.47 (dd, *J* = 2.9, 0.6 Hz, 2H), 8.31 (d, *J* = 7.8 Hz, 2H), 7.88 (t, *J* = 7.8 Hz, 1H), 7.51 (dd, *J* = 8.7, 2.9 Hz, 2H), 5.26 (s, 4H), 3.52 (s, 6H).

^{13}C NMR (125 MHz, $CDCl_3$, δ): 155.1 (s), 154.0 (s), 150.3 (s), 138.7 (d), 137.8 (d), 123.7 (d), 121.8 (d), 119.9 (d), 94.8 (t), 56.4 (q).

IR (film on NaCl, cm^{-1}): 2951*w*, 2908*w*, 1562*s*, 1486*m*, 1448*m*, 1283*m*, 1207*m*, 1154*m*, 1141*m*, 1077*m*, 961*vs*, 933*m*, 808*s*, 753*m*, 636*m*.

MS (ESI) *m/z*: 376.2 ($[M + Na]^+$).

HRMS (ESI) *m/z*: $[M + Na]^+$ calcd for $C_{19}H_{19}N_3O_4Na$: 376.1273; found: 376.1272.

4,4′′-Diiodo-5,5′′-bis(methoxymethoxy)-2,2′:6′,2′′-terpyridine (69)

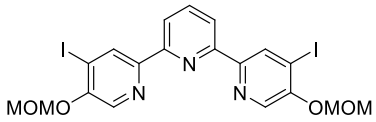

Prepared according to the modified procedure of Jui-Chang Tseng.

To a mixture of terpyridine **68** (1.10 g, 3.12 mmol, 1.00 eq) and TMEDA (0.94 mL, 6.24 mmol, 2.00 eq) in THF (70 mL) was added dropwise a solution of *n*-BuLi (2.50 M in hexane, 2.74 mL, 6.85 mmol, 2.20 eq) at –78 °C under N_2 atmosphere. The resulting deep blue mixture was allowed to stir at –78 °C for 1 h. To the mixture a solution of I_2 (1.74 g, 6.86 mmol, 2.20 eq) in THF (10 mL) was added dropwise in 20 min at –78 °C. The reaction mixture was allowed to warm to room temperature, stirred for 18 h and quenched with aqueous $Na_2S_2O_3$ (10%, 50 mL). The organic layer was separated and the aqueous phase was extracted with CH_2Cl_2 (100 mL × 3). The combined organic layers were washed with brine and dried over $MgSO_4$, filtered and evaporated under reduced pressure. The residue was suspended in EtOH (60 mL), heated to reflux and allowed to cool to room temperature. The resulting solid was collected by filtration and washed with EtOH (8 mL × 2) to give diiodo terpyridine **69** (0.94 g, 50%) as an off-white solid.

Mp 212–213 °C.

^{1}H NMR (500 MHz, $CDCl_3$, δ): 8.98 (s, 2H), 8.38 (s, 2H), 8.32 (d, *J* = 7.8 Hz, 2H), 7.89 (t, *J* = 7.8 Hz, 1H), 5.36 (s, 4H), 3.58 (s, 6H).

^{13}C NMR (125 MHz, $CDCl_3$, δ): 154.0 (s), 153.7 (s), 150.8 (s), 138.1 (d), 135.8 (d), 132.2 (d), 120.8 (d), 99.5 (s), 95.7 (t), 56.9 (q).

IR (film on NaCl, cm^{-1}): 2946*w*, 2905*w*, 1563*m*, 1480*s*, 1443*s*, 1351*m*, 1301*m*, 1265*s*, 1238*m*, 1202*m*, 1160*s*, 1037*m*, 985*vs*, 899*m*, 821*m*.

MS (ESI) *m/z*: 627.9 ([M + Na]$^+$).

HRMS (ESI) *m/z*: [M + Na]$^+$ calcd for $C_{19}H_{17}N_3O_4I_2Na$: 627.9206; found: 627.9203.

2.8.2.2. Synthesis of Acetylenes 73, 77a and 77b

2-Iodo-5-methoxy-1,3-dimethylbenzene (71)

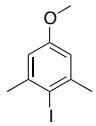

To a solution of 2-bromo-5-methoxy-1,3-dimethylbenzene (**70**) (1.00 g, 4.64 mmol, 1.00 eq) in anhydrous THF (15 mL) a solution of *n*-BuLi (2.50 M in hexane, 1.95 mL, 4.87 mmol, 1.05 eq) was added dropwise under N_2 atmosphere at -78 °C over 10 min. The resulting white suspension was stirred for 30 min. at -78 °C, then a solution of iodine (1.29 g, 5.10 mmol, 1.10 eq) in anhydrous THF was added dropwise at -78 °C over 15 min. The reaction mixture was allowed to warm up to room temperature and stirred overnight. The solvent was evaporated under reduced pressure and the residue was dissolved in CH_2Cl_2 (50 mL), washed with 10% $Na_2S_2O_3$ aqueous solution (50 mL), water and brine. The organic phase was dried over Mg_2SO_4, filtered and evaporated under reduced pressure. The residue was purified by silica gel column chromatography with hexane/ethyl acetate (99:1) to give 2-iodo-5-methoxy-1,3-dimethylbenzene (**71**)[46] (0.98 g, 81%) as a yellow oil.

^{1}H NMR (300 MHz, $CDCl_3$, δ): 6.67 (s, 2H), 3.77 (s, 3H), 2.45 (s, 6H).

^{13}C NMR (75 MHz, $CDCl_3$, δ): 159.3 (s), 143.0 (s), 113.0 (d), 97.2 (s), 55.4 (q), 29.9 (q).

IR (film on NaCl, cm^{-1}): 2996*w*, 2952*m*, 2836*m*, 1586*s*, 1464*s*, 1402*w*, 1377*w*, 1317*s*, 1275*w*, 1195*m*, 1163*s*, 1075*m*, 1030*w*, 1005*m*, 933*w*, 853*m*, 833*m*, 690*w*, 609*w*.

HRMS (EI) *m/z*: $[M]^+$ calcd for $C_9H_{11}O_1I$: 261.9854; found: 261.9854.

[(4-Methoxy-2,6-dimethylphenyl)ethynyl]trimethylsilane (72)

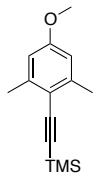

To a degassed mixture of 2-iodo-5-methoxy-1,3-dimethylbenzene (**71**) (2.00 g, 7.63 mmol, 1.00 eq), $Pd(PPh_3)_2Cl_2$ (267 mg, 0.380 mmol, 5 mol%) and CuI (145 mg, 0.760 mmol, 10 mol%) in toluene (40 mL) and triethylamine (20 mL) was added a solution of trimethylsilylacetylene (1.52 mL, 10.7 mmol, 1.40 eq) in toluene (20 mL) and triethylamine (20 mL) at 80 °C. The reaction mixture was heated to reflux for 18 h, allowed to cool to room temperature and diluted with CH_2Cl_2 (100 mL). The mixture was washed with 10% aqueous NH_4OH, water and brine. The organic phase was dried over $MgSO_4$, filtered and evaporated

under reduced pressure. The residue was purified by silica gel column chromatography with hexane/ethyl acetate (50:1) to give [(4-methoxy-2,6-dimethylphenyl)ethynyl]trimethylsilane (**72**) (1.68 g, 95%) as a pale yellow oil.

^{1}H NMR (300 MHz, $CDCl_3$, δ): 6.57 (s, 2H), 3.77 (s, 3H), 2.41 (s, 6H), 0.25 (s, 9H).

^{13}C NMR (75 MHz, $CDCl_3$, δ): 159.2 (s), 142.6 (s), 115.6 (s), 112.4 (d), 103.1 (s), 101.0 (s), 55.3 (q), 21.4 (q), 0.4 (q).

IR (film on NaCl, cm^{-1}): 3000*w*, 2959*s*, 2840*w*, 2147*s*, 1606*s*, 1575*w*, 1481*m*, 1470*m*, 1377*w*, 1321*s*, 1284*w*, 1250*m*, 1222*m*, 1194*m*, 1152*s*, 1064*m*, 943*w*, 862*s*, 786*w*, 760*m*, 698*w*, 625*w*.

HRMS (ESI) *m/z*: $[M + H]^+$ calcd for $C_{14}H_{21}OSi$: 233.13562; found: 233.13522.

2-Ethynyl-5-methoxy-1,3-dimethylbenzene (**73**)

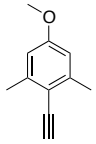

To a solution of [(4-methoxy-2,6-dimethylphenyl)ethynyl]trimethylsilane (**72**) (1.31 g, 5.64 mmol, 1.00 eq) in methanol (140 mL) KF (3.27 g, 56.4 mmol, 10.0 eq) was added. The reaction mixture was heated to 40 °C for 18 h (followed by GC/MS). After evaporation of solvent under reduced pressure, the residue was filtered through a pad of Celite eluting with diethyl ether (100 mL). The filtrate was evaporated under reduced pressure and the crude product was purified by silica gel column chromatography with hexane/ethyl acetate (95:5) to give 2-ethynyl-5-methoxy-1,3-dimethylbenzene (**73**)[34] as a white waxy solid (0.866 g, 96%).

Mp 42–44 °C.

^{1}H NMR (300 MHz, $CDCl_3$, δ): 6.59 (s, 2H), 3.78 (s, 3H), 3.42 (s, 1H), 2.43 (s, 6H).

^{13}C NMR (75 MHz, $CDCl_3$, δ): 159.3 (s) 142.8 (s), 114.5 (s), 112.5 (d), 83.9 (d), 81.5 (s), 55.3 (q), 21.4 (q).

IR (film on NaCl, cm^{-1}): 3310*s*, 3290*s*, 3001*w*, 2957*m*, 2919*m*, 2840*w*, 2144*w*, 2097*m*, 1606*s*, 1582*m*, 1481*m*, 1470*m*, 1443*m*, 1377*w*, 1320*s*, 1206*m*, 1196*m*, 1147*s*, 1062*m*, 858*m*, 840*m*, 725*w*, 680*w*.

HRMS (ESI) *m/z*: $[M + H]^+$ calcd for $C_{11}H_{13}O$: 161.09609; found: 161.09607.

5-Bromo-5′-(4-methoxy-2,6-dimethylphenyl)-2,2′-bipyridine (75a)

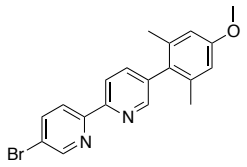

To a solution of 2-bromo-5-(4-methoxy-2,6-dimethylphenyl)pyridine (**74a**)[33] (7.20 g, 24.6 mmol, 1.00 eq) in anhydrous THF (150 mL) a solution of *n*-BuLi (2.50 M in hexane, 10.8 mL, 27.1 mmol, 1.10 eq) was added dropwise under N_2 at –78 °C over 15 min. The reaction mixture was allowed to stir for 1 h at –78 °C and then a solution of dry $ZnCl_2$ (3.70 g, 27.1 mmol, 1.10 eq) in anhydrous THF (50 mL) was added via cannula. Upon warming to room temperature, the resulting aryl zincate solution was cannulated into a solution of 2,5-dibromopyridine (**62**) (6.13 g, 25.9 mmol, 1.05 eq.) and $Pd(PPh_3)_4$ (427 mg, 0.370 mmol, 1.5 mol%) in anhydrous THF (100 mL). The reaction mixture was heated to reflux for 18 h and allowed to cool to room temperature. The resulting white precipitate was filtered off, washed with THF, and dried under reduced pressure. The dry precipitate was then suspended in a mixture of CH_2Cl_2 and a basic aqueous solution EDTA (basified using an aqueous solution of $NaHCO_3$) and stirred until all precipitate dissolve. The organic phase was separated, washed with water and brine, dried over $MgSO_4$, and evaporated under reduced pressure to give 5-bromo-5′-(4-methoxy-2,6-dimethylphenyl)-2,2′-bipyridine (**75a**) (2.84 g, 31%) as a white solid.

Mp 132–134 °C.

^{1}H NMR (400 MHz, $CDCl_3$, δ): 8.74 (d, J = 2.1 Hz, 1H) 8.47 (s, 1H), 8.44 (d, J = 8.1 Hz, 1H), 8.36 (d, J = 8.5 Hz, 1H), 7.96 (dd, J = 8.5, 2.3 Hz, 1H), 7.63 (dd, J = 8.1, 2.1 Hz, 1H), 6.71 (s, 2H), 3.83 (s, 3H), 2.06 (s, 6H).

^{13}C NMR (100 MHz, $CDCl_3$, δ): 159.1 (s), 154.7 (s), 153.6 (s), 150.4 (d), 150.2 (d), 139.6 (d), 138.6 (d), 137.9 (s), 137.2 (s), 130.3 (s), 122.4 (d), 121.2 (s), 120.8 (d), 113.2 (d), 55.3 (q), 21.3 (q).

IR (film on NaCl, cm^{-1}): 2954*w*, 2836*w*, 1607*m*, 1539*w*, 1453*vs*, 1359*w*, 1318*s*, 1275*w*, 1193*w*, 1155*s*, 1092*w*, 1075*w*, 1056*w*, 1005*m*, 837*m*, 738*w*.

HRMS (ESI) *m/z*: $[M + H]^+$ calcd for $C_{19}H_{18}BrN_2O$: 369.05970; found: 369.05953.

5-Ethynyl-5′-(4-methoxy-2,6-dimethylphenyl)-2,2′-bipyridine (77a)

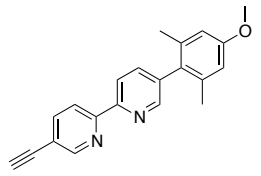

To a mixture of 5-bromo-5′-(4-methoxy-2,6-dimethylphenyl)-2,2′-bipyridine (**75a**) (2.79 g, 7.56 mmol, 1.00 eq), CuI (72 mg, 0.38 mmol, 5 mol%) and $PdCl_2(PPh_3)_2$ (0.530 g, 0.756 mmol, 10 mol%) in degassed Et_3N (150 mL) was added trimethylsilylacetylene (2.12 mL, 15.1 mmol, 2.00 eq) under N_2 atmosphere at 80 °C. The reaction mixture was heated to reflux for 19 h, allowed to cool to room temperature and evaporated to dryness under reduced pressure. The residue was redissolved in CH_2Cl_2 (100 mL), washed with 10% aqueous NH_4OH, water and brine. The organic phase was dried over $MgSO_4$, filtered and evaporated under reduces pressure. The crude residue was dissolved in MeOH (100 mL), and to the resulting mixture KF (1.32 g, 22.8 mmol, 3.00 eq) was added. The reaction mixture was stirred at room temperature for 18 h. The solvent was evaporated under reduced pressure, and the residue was filtered through a pad of Celite eluting with CH_2Cl_2 (100 mL). After evaporation of solvent, the crude product was purified by silica gel column chromatography with hexane/ethyl acetate (3:1) to give 5-ethynyl-5′-(4-methoxy-2,6-dimethylphenyl)-2,2′-bipyridine (**77a**) (1.72 g, 72%) as an off-white solid.

Mp 137.5–138.5 °C.

^{1}H NMR (500 MHz, $CDCl_3$, δ): 8.80 (dd, *J* = 2.1, 0.8 Hz, 1H), 8.49 (dd, *J* = 2.2, 0.8 Hz, 1H), 8.47 (dd, *J* = 8.1, 0.8 Hz, 1H), 8.43 (dd, *J* = 8.2, 0.8 Hz, 1H), 7.92 (dd, *J* = 8.2, 2.1 Hz, 1H), 7.64 (dd, *J* = 8.1, 2.2 Hz, 1H), 6.71 (s, 2H), 3.84 (s, 3H), 3.30 (s, 1H), 2.08 (s, 6H).

^{13}C NMR (125 MHz, $CDCl_3$, δ): 159.1 (s), 155.5 (s), 153.8 (s), 152.4 (d), 150.3 (d), 140.1 (d), 138.5 (d), 137.9 (s), 137.2 (s), 130.3 (s), 121.2 (d), 120.3 (d), 119.1 (s), 113.1 (d), 81.4 (d), 80.9 (s), 55.3 (q), 21.4 (q).

IR (film on NaCl, cm^{-1}): 3287*m*, 2955*w*, 2836*w*, 2105*vw*, 1605*m*, 1589*m*, 1461*vs*, 1318*s*, 1192*m*, 1155*s*, 1074*m*, 1056*m*, 844*m*, 746*m*.

MS (ESI) *m/z*: 315.3 ($[M + H]^+$), 337.3 ($[M + Na]^+$). HRMS (ESI) *m/z*: $[M + Na]^+$ calcd for $C_{21}H_{18}N_2ONa$: 337.1317; found: 337.1317.

5-Ethynyl-6′-(4-methoxy-2,6-dimethylphenyl)-2,2′-bipyridine (77b)

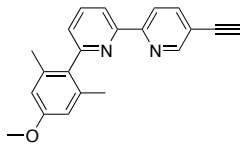

To a mixture of 5-bromo-6′-(4-methoxy-2,6-dimethylphenyl)-2,2′-bipyridine (**75b**)[36] (7.00 g, 19.0 mmol, 1.00 eq), CuI (0.181 g, 0.948 mmol, 5 mol%) and $PdCl_2(PPh_3)_2$ (1.33 g, 1.89 mmol, 10 mol%) in degassed Et_3N (150 mL) was added trimethylsilylacetylene (5.33 mL, 38.0 mmol) under N_2 atmosphere at 80 °C. The reaction mixture was heated to reflux for 18 h, allowed to cool to room temperature and evaporated to dryness under reduced pressure. The residue was redissolved in CH_2Cl_2 (200 mL), washed with aqueous 10% NH_4OH, water and brine. The organic phase was dried over $MgSO_4$, filtered and evaporated under reduces pressure. The crude residue was dissolved in MeOH (250 mL), and to the resulting mixture KF (3.50 g, 22.8 mmol, 3.23 eq) was added. The reaction mixture was stirred at room temperature for 18 h. The solvent was evaporated under reduced pressure, and the residue was filtered through a pad of Celite eluting with CH_2Cl_2 (250 mL). After evaporation of solvent, the crude product was purified by silica gel column chromatography with hexane/ethyl acetate (3:1) to give 5-ethynyl-6′-(4-methoxy-2,6-dimethylphenyl)-2,2′-bipyridine (**77b**) (4.65 g, 78%) as an off-white solid.

Mp 123.5–125 °C.

^{1}H NMR (400 MHz, $CDCl_3$, δ): 8.78 (dd, *J* = 2.1, 0.8 Hz, 1H) 8.43 (dd, *J* = 8.2, 0.8 Hz, 1H), 8.37 (dd, *J* = 7.6, 1.0 Hz, 1H), 7.87 (t, *J* = 7.6 Hz, 1H), 7.84 (dd, *J* = 8.2, 2.1 Hz, 1H), 7.24 (dd, *J* = 7.6, 1.1 Hz, 1H), 6.70 (s, 2H), 3.84 (s, 3H), 3.28 (s, 1H), 2.11 (s, 6H).

^{13}C NMR (100 MHz, $CDCl_3$, δ): 159.3 (s), 159.1 (s), 155.8 (s), 155.2 (s), 152.2 (d), 140.0 (d), 137.6 (s), 137.2 (d), 133.6 (s), 125.6 (d), 120.8 (d), 119.2 (d), 119.1 (s), 113.2 (d), 81.3 (d), 80.9 (s), 55.3 (q), 20.9 (q).

IR (film on NaCl, cm^{-1}): 3288*m*, 2954*w*, 2836*w*, 2105*w*, 1606*m*, 1585*m*, 1450*s*, 1321*m*, 1192*m*, 1157*vs*, 1070*m*, 858*m*, 819*m*, 751*m*.

MS (ESI) *m/z*: 337.2 ($[M + Na]^+$). HRMS (ESI) *m/z*: $[M + Na]^+$ calcd for $C_{21}H_{18}N_2ONa$: 337.1317; found: 337.1315.

2.8.2.3. Synthesis of Bis(ethynyl)terpyridines 78a-h, 79a-c and 81a,b

5,5′′-Bis(methoxymethoxy)-4,4′′-bis(phenylethynyl)-2,2′:6′,2′′-terpyridine (78a)

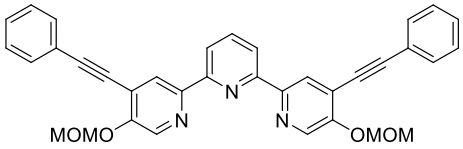

To a mixture of diiodoterpyridine **69** (300 mg, 0.496 mmol, 1.00 eq), CuI (9.4 mg, 0.050 mmol, 10 mol%) and $PdCl_2(PPh_3)_2$ (17.4 mg, 0.0248 mmol, 5 mol%) in degassed THF/Et_3N (10 mL/10 mL) was added ethynylbenzene (0.126 mL, 1.24 mmol, 2.50 eq) under N_2 atmosphere at 80 °C. The reaction mixture was heated to reflux for 20 h, allowed to cool to room temperature and evaporated to dryness under reduced pressure. The residue was redissolved in CH_2Cl_2 (30 mL), washed with 10% aqueous NH_4OH, water and brine. The organic phase was dried over $MgSO_4$, filtered and evaporated under reduces pressure. The residue was purified by neutral alumina (Brockman III) column chromatography with hexane/ethyl acetate (3:1) to give 5,5′′-bis(methoxymethoxy)-4,4′′-bis(phenylethynyl)-2,2′:6′,2′′-terpyridine (**78a**) (261 mg, 95 %) as an off-white solid.

Mp 149–151 °C.

^{1}H NMR (400 MHz, $CDCl_3$, δ): 8.72 (s, 2H), 8.60 (s, 2H), 8.36 (d, *J* = 7.8 Hz, 2H), 7.92 (t, *J* = 7.8 Hz, 1H), 7.63 (dd, *J* = 7.6, 1.7 Hz, 4H), 7.41-7.34 (m, 6H), 5.40 (s, 4H), 3.61 (s, 6H).

^{13}C NMR (100 MHz, $CDCl_3$, δ): 154.8 (s), 153.6 (s), 150.3 (s), 137.9 (d), 137.5 (d), 132.0 (d), 129.1 (d), 128.5 (d), 124.6 (d), 122.7 (s), 120.3 (d), 97.7 (s), 95.9 (t), 83.9 (s), 56.7 (q).

IR (film on NaCl, cm^{-1}): 2957*w*, 2906*w*, 2219*w*, 1600*w*, 1573*m*, 1544*w*, 1494*m*, 1484*s*, 1457*m*, 1379*m*, 1308*w*, 1268*m*, 1232*w*, 1200*m*, 1155*s*, 1077*m*, 982*s*, 921*w*, 823*w*, 757*m*, 690*w*.

MS (ESI) *m/z*: 554.3 ($[M + H]^+$); HRMS (ESI) *m/z*: $[M+Na]^+$ calcd for $C_{35}H_{27}N_3NaO_4$: 576.18938; found: 576.18905.

4,4′′-Bis(1-octynyl-1-yl)-5,5′′-bis(methoxymethoxy)-2,2′:6′,2′′-terpyridine (78b)

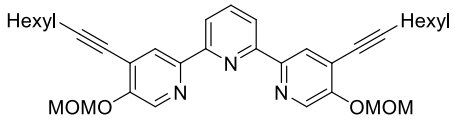

To a mixture of diiodoterpyridine **69** (300 mg, 0.496 mmol, 1.00 eq), CuI (9.4 mg, 0.050 mmol, 10 mol%) and $PdCl_2(PPh_3)_2$ (17.4 mg, 0.0248 mmol, 5 mol%) in degassed THF/Et_3N (10 mL/10 mL) was added 1-octyne (0.182 mL, 1.24 mmol, 2.50 eq) under N_2 atmosphere at

80 °C. The reaction mixture was heated to reflux for 20 h, allowed to cool to room temperature and evaporated to dryness under reduced pressure. The residue was redissolved in CH_2Cl_2 (30 mL), washed with 10% aqueous NH_4OH, water and brine. The organic phase was dried over $MgSO_4$, filtered and evaporated under reduces pressure. The residue was purified by neutral alumina (Brockman III) column chromatography with hexane/ethyl acetate (3:1) to give 4,4″-bis(1-octynyl-1-yl)-5,5″-bis(methoxymethoxy)-2,2′:6′,2″-terpyridine (**78b**) (261 mg, 92 %) as an off-white solid.

Mp 73–74 °C.

^{1}H NMR (400 MHz, $CDCl_3$, δ): 8.54 (s, 2H), 8.52 (s, 2H), 8.31 (d, *J* = 7.8 Hz, 2H), 7.88 (t, *J* = 7.8 Hz, 1H), 5.34 (s, 4H), 3.57 (s, 6H), 2.54 (t, *J* = 7.1 Hz, 4H), 1.69 (quintet, *J* = 7.4 Hz, 4H), 1.51 (quintet, *J* = 7.0 Hz, 4H), 1.39-1.31 (m, 8H), 0.91 (t, *J* = 6.8 Hz, 6H).

^{13}C NMR (100 MHz, $CDCl_3$, δ): 154.8 (s), 153.8 (s), 150.3 (s), 137.8 (d), 137.4 (d), 124.8 (d), 123.5 (s), 120.3 (d), 99.9 (s), 95.8 (t), 75.2 (s), 56.6 (q), 31.4 (t), 28.7 (t), 28.6 (t), 22.7 (t), 20.0 (t), 14.2 (q).

IR (film on NaCl, cm^{-1}): 2931*s*, 2955*s*, 2857*m*, 2235*w*, 1576*m*, 1543*w*, 1485*s*, 1456*s*, 1376*m*, 1278*m*, 1193*m*, 1154*s*, 1082*m*, 984*s*, 924*w*, 823*w*.

MS (ESI) *m/z*: 570.5 ([M + H]$^+$). HRMS (ESI) *m/z*: [M+Na]$^+$ calcd for $C_{35}H_{43}N_3NaO_4$: 592.31458; found: 592.31377.

4,4″-Diethynyl-5,5″-bis(methoxymethoxy)-2,2′:6′,2″-terpyridine (**78c**)

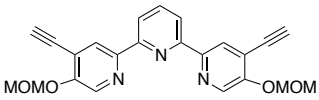

To a mixture of diiodoterpyridine **69** (908 mg, 1.50 mmol, 1.00 eq), $PdCl_2(PPh_3)_2$ (53 mg, 0.075 mmol, 5 mol%) and CuI (18 mg, 0.15 mmol, 10 mol%) in degassed THF/Et_3N (35 mL/30 mL) was added trimethylsilylacetylene (1.1 mL, 7.5 mmol, 5.0 eq) under N_2 atmosphere. The reaction mixture was heated to 80 °C for 4.5 h, filtered through Celite and the filter was washed with CH_2Cl_2 (150 ml). The filtrate was washed with 10% aqueous NH_4OH, water and brine. The organic phase was dried over $MgSO_4$, filtered and evaporated under reduces pressure. The crude residue was dissolved in CH_2Cl_2/MeOH (40 mL/40 mL) and to the resulting mixture KF (348.6 mg, 6.00 mmol) was added. The reaction mixture was stirred at room temperature for 18 h. After evaporation of solvents, the residue was treated with CH_2Cl_2 (100 mL) and filtered through a Celite plug (1 cm). The cake was washed with CH_2Cl_2 (100 mL) and the combined organic phase was concentrated in vacuo. The residue was purified by neutral alumina (Brockman III) column chromatography with hexane/ethyl

acetate (3:1) to give 4,4″-diethynyl-5,5″-bis(methoxymethoxy)-2,2′:6′,2″-terpyridine (**78c**) (516 mg, 86%) as a white solid.

Mp 167.5–169 °C.

^{1}H NMR (400 MHz, $CDCl_3$, δ): 8.64 (s, 2H), 8.60 (s, 2H), 8.33 (d, *J* = 7.8 Hz, 2H), 7.90 (t, *J* = 7.8 Hz, 1H), 5.38 (s, 4H), 3.58 (s, 6H), 3.55 (s, 2H).

^{13}C NMR (100 MHz, $CDCl_3$, δ): 154.6 (s), 154.2 (s), 150.1 (s), 138.0 (d), 137.1 (d), 125.1 (d), 121.2 (s), 120.4 (d), 95.6 (t), 85.6 (s), 78.1 (d), 56.7 (q).

IR (film on NaCl, cm^{-1}): 3179*m*, 2966*w*, 2939*w*, 2909*w*, 2105*m*, 1570*m*, 1488*m*, 1457*m*, 1369*m*, 1271*m*, 1204*m*, 1157*m*, 1079*m*, 979*vs*, 921*m*, 824*m*, 614*m*.

MS (ESI) *m/z*: 402.3 ($[M + H]^+$); 424.2 ($[M + Na]^+$). HRMS (ESI) *m/z*: $[M + Na]^+$ calcd for $C_{23}H_{19}N_3O_4Na$: 424.1273; found: 424.1273.

5,5″-Bis(methoxymethoxy)-4,4″-bis[2-(pyridine-4-yl)ethynyl]-2,2′:6′,2″-terpyridine (78d)

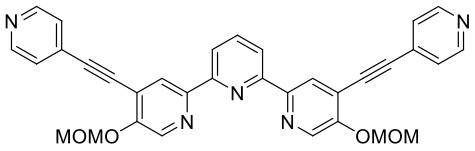

A mixture of bis-ethynyl terpyridine **78c** (401 mg, 1.00 mmol, 1.00 eq), 4-iodopyridine (**80**) (431 mg, 2.10 mmol, 2.10 eq), $PdCl_2(PPh_3)_2$ (70.2 mg, 0.100 mmol, 10 mol%) and CuI (38.2 mg, 0.200 mmol, 20 mol%) in degassed THF/ Et_3N (20 mL/20 mL) was heated to 80 °C for 20 h under N_2 atmosphere. After evaporation of solvents, the residue was redissolved in CH_2Cl_2 (100 mL), washed with 10% aqueous NH_4OH, water and brine. The organic phase was dried over $MgSO_4$, filtered and evaporated under reduces pressure. The crude product was purified by silica gel column chromatography with CH_2Cl_2/MeOH (gradient 99:1 to 9:1) to give 5,5″-bis(methoxymethoxy)-4,4″-bis[2-(pyridine-4-yl)ethynyl]-2,2′:6′,2″-terpyridine (**78d**) (489 mg, 88%) as a white solid.

Mp 174–175 °C dec.

^{1}H NMR (500 MHz, $CDCl_3$, δ): 8.68 (d, *J* = 0.6 Hz, 2H), 8.66-8.64 (m, 6H), 8.36 (d, *J* = 7.8 Hz, 2H), 7.94 (t, *J* = 7.8 Hz, 1H), 7.47-7.46 (m, 4H), 5.40 (s, 4H), 3.60 (s, 6H).

^{13}C NMR (125 MHz, $CDCl_3$, δ): 154.5 (s), 153.6 (s), 150.1 (s), 149.8 (d), 137.8 (d), 137.1 (d), 130.6 (s), 125.6 (d), 124.3 (d), 120.9 (s), 120.4 (d), 95.5 (t), 94.1 (s), 88.0 (s), 56.6 (q).

IR (film on NaCl, cm^{-1}): 2957*w*, 2831*w*, 2219*w*, 1591*s*, 1483*m*, 1456*m*, 1379*m*, 1309*m*, 1269*m*, 1201*m*, 1154*s*, 1076*m*, 974*vs*, 902*m*, 819*s*, 753*w*.

MS (ESI) *m/z*: 556.3 ([M + H]$^+$), 578.3 ([M + Na]$^+$). HRMS (ESI) *m/z*: [M + Na]$^+$ calcd for $C_{33}H_{25}N_5O_4Na$: 578.1804; found: 578.1801.

5,5″-Bis(methoxymethoxy)-4,4″-bis[2-(pyridine-3-yl)ethynyl]-2,2′:6′,2″-terpyridine (**78e**)

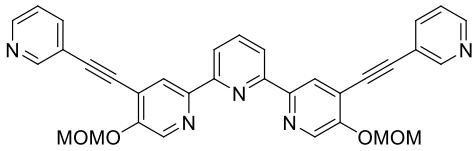

A mixture of diiodoterpyridine **69** (242 mg, 0.400 mmol, 1.00 eq), 3-ethynylpyridine (981 mg, 3.12 mmol, 7.80 eq), $PdCl_2(PPh_3)_2$ (14 mg, 0.040 mmol, 5 mol%) and CuI (7.6 mg, 0.080 mmol, 10 mol%) in degassed THF/Et_3N (40 mL/40 mL) was heated to 80 °C for 20 h under N_2 atmosphere. After evaporation of solvents, the residue was redissolved in CH_2Cl_2 (200 mL), washed with 10% NH_4OH aqueous solution, water and brine. The organic phase was dried over $MgSO_4$, filtered and evaporated under reduces pressure. The crude product was purified by silica gel column chromatography with CH_2Cl_2/MeOH (gradient 99:1 to 9:1) to give 5,5″-bis(methoxymethoxy)-4,4″-bis[2-(pyridine-3-yl)ethynyl]-2,2′:6′,2″-terpyridine (**78e**) (189 mg, 85%) as a white solid.

Mp 164–165 °C dec.

^{1}H NMR (400 MHz, $CDCl_3$, δ): 8.86 (d, *J* = 1.2 Hz, 2H), 8.69 (s, 2H), 8.63 (s, 2H), 8.61 (dd, *J* = 4.9, 1.6 Hz, 2H), 8.36 (d, *J* = 7.8 Hz, 2H), 7.93 (t, *J* = 7.9 Hz, 1H), 7.90 (dt, *J* = 7.9, 1.9 Hz, 2H), 7.34 (ddd, *J* = 7.9, 4.9, 0.7 Hz, 2H), 5.40 (s, 4H), 3.60 (s, 6H).

^{13}C NMR (125 MHz, $CDCl_3$, δ): 154.7 (s), 153.7 (s), 152.4 (d), 150.2 (s), 149.3 (d), 139.0 (d), 138.0 (d), 137.2 (d), 124.5 (d), 123.4 (d), 121.7 (s), 120.6 (d), 119.9 (s), 95.7 (t), 94.0 (s), 87.0 (s), 56.8 (q).

IR (film on NaCl, cm^{-1}): 2958*w*, 2831*w*, 2220*w*, 1570.8*m*, 1545.9*w*, 1486.0*s*, 1456.5*m*, 1408.9*w*, 1378*m*, 1308*w*, 1268*w*, 1234*w*, 1200*m*, 1155*s*, 1076*m*, 976*vs*, 923*w*, 821*w*, 703*w*.

HRMS (ESI) *m/z*: [M + H]$^+$ calcd for $C_{33}H_{26}N_5O_4$: 556.19793; found: 556.19697.

4-Iodo-4″-{2-[5′-(4-methoxy-2,6-dimethylphenyl)-2,2′-bipyridin-5-yl]ethynyl}-5,5″-bis(methoxymethoxy)-2,2′:6′,2″-terpyridine (**79a**)

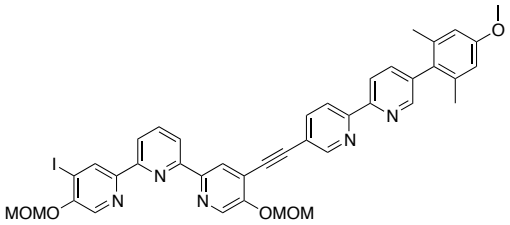

A mixture of diiodoterpyridine **69** (450 mg, 0.744 mmol, 1.00 eq), 5-ethynyl-5′-(4-methoxy-2,6-dimethylphenyl)-2,2′-bipyridine (**77a**) (245 mg, 0.781 mmol, 1.05 eq), $PdCl_2(PPh_3)_2$ (26 mg, 0.037 mmol, 5 mol%) and CuI (14 mg, 0.074 mmol, 10 mol%) in degassed THF/Et_3N (15 mL/15 mL) was heated to 80 °C for 6 h under N_2 atmosphere. The reaction mixture was diluted with CH_2Cl_2 (50 mL), washed with 10% aqueous NH_4OH, water and brine. The organic phase was dried over $MgSO_4$, filtered and evaporated under reduces pressure. The crude residue was separated by silica gel column chromatography with hexane/ethyl acetate (3:1) to give monosubstituted **79a** (225 mg, 40%), disubstituted **78f** (132 mg, 18%) and recovered starting diiodoterpyridine **69** (110 mg, 24%).

Yellowish amorphous solid, Mp 108–110 °C.

^{1}H NMR (400 MHz, $CDCl_3$, δ): 9.04 (s, 1H), 8.95 (d, *J* = 1.3 Hz, 1H), 8.69 (s, 1H), 8.64 (s, 1H), 8.52 (d, *J* = 8.2 Hz, 2H), 8.51 (s, 1H), 8.39 (s, 1H), 8.37 (dd, *J* = 7.9, 0.8 Hz, 1H), 8.34 (dd, *J* = 7.8, 0.8 Hz, 1H), 8.08 (dd, *J* = 8.2, 2.1 Hz, 1H), 7.92 (t, *J* = 7.8 Hz, 1H), 7.66 (dd, *J* = 7.9, 2.2 Hz, 1H), 6.72 (s, 2H), 5.43 (s, 2H), 5.36 (s, 2H), 3.84 (s, 3H), 3.63 (s, 3H), 3.58 (s, 3H), 2.08 (s, 6H).

^{13}C NMR (100 MHz, $CDCl_3$, δ): 159.2 (s), 155.6 (s), 154.8 (s), 154.0 (s), 153.7 (s), 153.7 (s), 152.2 (d), 150.9 (s), 150.3 (d), 150.2 (s), 139.9 (d), 138.7 (d), 138.0 (d), 137.9 (s), 137.4 (d), 137.3 (s), 135.8 (d), 132.2 (d), 130.3 (s), 124.5 (d), 121.9 (s), 121.3 (d), 120.7 (d), 120.6 (d), 120.4 (d), 119.7 (s), 113.2 (d), 99.5 (s), 95.8 (t), 95.7 (t), 94.5 (s), 87.9 (s), 56.9 (q), 56.8 (q), 55.4 (q), 21.4 (q).

IR (film on NaCl, cm^{-1}): 2956*w*, 2832*w*, 2220*w*, 1606*w*, 1569*m*, 1540*m*, 1482*m*, 1463*s*, 1451*s*, 1354*w*, 1317*m*, 1267*m*, 1235*s*, 1200*m*, 1155*vs*, 1084*m*, 976*s*, 922*w*, 845*w*, 821*w*, 733*m*.

MS (ESI) *m/z*: 792.3 ($[M + H]^+$); HRMS (ESI) *m/z*: $[M]^+$ calcd for $C_{40}H_{34}IN_5O_5$: 792.16707; found: 792.16774.

4,4″-Bis{2-[5′-(4-methoxy-2,6-dimethylphenyl)-2,2′-bipyridin-5-yl]ethynyl}-5,5″-bis(methoxymethoxy)-2,2′:6′,2″-terpyridine (78f)

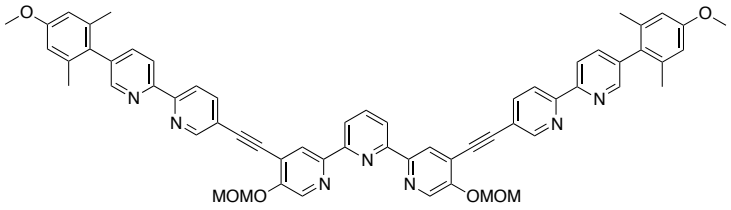

A mixture of diiodoterpyridine **69** (908 mg, 1.50 mmol, 1.00 eq), 5-ethynyl-5′-(4-methoxy-2,6-dimethylphenyl)-2,2′-bipyridine (**77a**) (981 mg, 3.12 mmol, 2.08 eq), $PdCl_2(PPh_3)_2$ (53 mg, 0.075 mmol, 5 mol%) and CuI (29 mg, 0.15 mmol, 10 mol%) in degassed THF/Et_3N (30 mL/30 mL) was heated to 80 °C for 20 h under N_2 atmosphere. The reaction mixture was diluted with CH_2Cl_2 (150 mL), washed with 10% aqueous NH_4OH, water and brine. The organic phase was dried over $MgSO_4$, filtered and evaporated under reduces pressure. The crude residue was separated by silica gel column chromatography with hexane/ethyl acetate (2:1) to give 4,4″-bis{2-[5′-(4-methoxy-2,6-dimethylphenyl)-2,2′-bipyridin-5-yl]ethynyl}-5,5″-bis(methoxymethoxy)-2,2′:6′,2″-terpyridine (**78f**) (1.325 g, 90%) as a white solid.

White crystalline solid, Mp 237–238.5 °C dec.

^{1}H NMR (400 MHz, $CDCl_3$, δ): 8.95 (d, *J* = 2.1 Hz, 2H), 8.74 (s, 2H), 8.65 (s, 2H), 8.54 (d, *J* = 8.2 Hz, 2H), 8.53 (d, *J* = 8.1 Hz, 2H), 8.47 (d, *J* = 2.2 Hz, 2H), 8.38 (d, *J* = 7.8 Hz, 2H), 8.08 (dd, *J* = 2.1, 8.2 Hz, 2H), 7.94 (t, *J* = 7.8 Hz, 1H), 7.61 (dd, *J* = 2.2, 8.1 Hz, 2H), 6.69 (s, 4H), 5.44 (s, 4H), 3.84 (s, 6H), 3.64 (s, 6H), 2.02 (s, 12H).

^{13}C NMR (125 MHz, $CDCl_3$, δ): 159.1 (s), 155.7 (s), 154.9 (s), 153.8 (s), 153.7 (s), 152.1 (d), 150.4 (s), 150.3 (d), 139.9 (d), 138.6 (d), 138.0 (d), 137.9 (s), 137.5 (d), 137.2 (s), 130.3 (s), 124.4 (d), 121.9 (s), 121.4 (d), 120.6 (d), 120.5 (d), 119.6 (s), 113.1 (d), 95.8 (t), 94.6 (s), 87.8 (s), 56.8 (q), 55.3 (q), 21.3 (q).

IR (film on NaCl, cm^{-1}): 2955*w*, 2833*w*, 2215*vw*, 1606*m*, 1573*m*, 1482*m*, 1461*vs*, 1378*m*, 1316*m*, 1268*m*, 1195*m*, 1155*vs*, 1075*m*, 976*m*, 843*m*, 746*m*.

MS (ESI) *m/z*: 1000.7 ($[M + Na]^+$); HRMS (ESI) *m/z*: $[M + Na]^+$ calcd for $C_{61}H_{51}N_7O_6Na$: 1000.3799; found: 1000.3798.

4-Iodo-4′′-{2-[6′-(4-methoxy-2,6-dimethylphenyl)-2,2′-bipyridin-5-yl]ethynyl}-5,5′′-bis(methoxymethoxy)-2,2′:6′,2′′-terpyridine (**79b**)

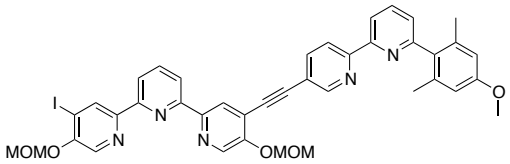

A mixture of diiodoterpyridine **69** (450 mg, 0.744 mmol, 1.00 eq), 5-ethynyl-6′-(4-methoxy-2,6-dimethylphenyl)-2,2′-bipyridine (**77b**) (245 mg, 0.781 mmol, 1.05 eq), $PdCl_2(PPh_3)_2$ (26 mg, 0.037 mmol, 5 mol%) and CuI (14 mg, 0.074 mmol, 10 mol%) in degassed THF/Et_3N (15 mL/15 mL) was heated to 80 °C for 6 h under N_2 atmosphere. The reaction mixture was diluted with CH_2Cl_2 (50 mL), washed with 10% aqueous NH_4OH, water and brine. The organic phase was dried over $MgSO_4$, filtered and evaporated under reduces pressure. The crude residue was separated by silica gel column chromatography with hexane/ethyl acetate (3:1) to give monosubstituted **79b** (230 mg, 39%), disubstituted **78g** (126 mg, 17%) and recovered starting diiodoterpyridine **69** (100 mg, 22%).

4-iodo-4''-{2-[6'-(4-methoxy-2,6-dimethylphenyl)-2,2'-bipyridin-5-yl]ethynyl}-5,5''-bis(methoxymethoxy)-2,2':6',2''-terpyridine (**79b**)

White crystalline solid, Mp 166–169 °C.

^{1}H NMR (400 MHz, $CDCl_3$, δ): 9.04 (s, 1H), 8.93 (dd, *J* = 2.0, 0.6 Hz, 1H), 8.68 (s, 1H), 8.63 (s, 1H), 8.51 (dd, *J* = 8.3, 0.6 Hz, 1H), 8.41 (dd, *J* = 7.9, 0.9 Hz, 1H), 8.39 (s, 1H), 8.37 (dd, *J* = 7.8, 0.8 Hz, 1H), 8.34 (dd, *J* = 7.8, 0.9 Hz, 1H), 8.00 (dd, *J* = 8.3, 2.0 Hz, 1H), 7.92 (t, *J* = 7.9 Hz, 1H), 7.89 (t, *J* = 7.8 Hz, 1H), 7.26 (dd, *J* = 7.9, 0.9 Hz, 1H), 6.71 (s, 2H), 5.42 (s, 2H), 5.36 (s, 2H), 3.84 (s, 3H), 3.62 (s, 3H), 3.58 (s, 3H), 2.13 (s, 6H).

^{13}C NMR (100 MHz, $CDCl_3$, δ): 159.4 (s), 159.1 (s), 156.0 (s), 155.2 (s), 154.7 (s), 154.0 (s), 153.7 (s), 152.0 (d), 150.9 (s), 150.2 (s), 139.8 (d), 138.1 (d), 137.7 (s), 137.4 (d), 137.2 (d), 135.8 (d), 133.6 (s), 132.2 (d), 125.7 (d), 124.6 (d), 122.1 (s), 121.0 (d), 120.8 (d), 120.6 (d), 119.6 (s), 119.4 (d), 113.3 (d), 99.6 (s), 95.9 (t), 95.7 (t), 94.8 (s), 87.7 (s), 56.9 (q), 56.8 (q), 55.4 (q), 20.9 (q).

IR (film on NaCl, cm^{-1}): 2957*w*, 2831*w*, 2221*vw*, 1607*m*, 1568*m*, 1542*m*, 1482*m*, 1451*s*, 1387*w*, 1354*w*, 1312*m*, 1266*m*, 1236*w*, 1200*m*, 1156*vs*, 1084*m*, 976*s*, 908*m*, 820*m*, 732*m*.

HRMS (ESI) *m/z*: $[M + H]^+$ calcd for $C_{40}H_{35}IN_5O_5$: 792.16774 ; found: 792.16789.

4,4''-bis{2-[6'-(4-methoxy-2,6-dimethylphenyl)-2,2'-bipyridin-5-yl]ethynyl}-5,5''-bis(methoxymethoxy)-2,2':6',2''-terpyridine (**78g**)

White crystalline solid, Mp 248–249.5 °C dec.

^{1}H NMR (400 MHz, $CDCl_3$, δ): 8.92 (d, *J* = 2.1 Hz, 2H), 8.69 (s, 2H), 8.64 (s, 2H), 8.48 (d, *J* = 8.3 Hz, 2H), 8.38 (d, *J* = 7.9 Hz, 2H), 8.36 (d, *J* = 7.8 Hz, 2H), 7.98 (dd, *J* = 8.3, 2.1 Hz, 2H), 7.94 (t, *J* = 7.9 Hz, 1H), 7.82 (t, *J* = 7.8 Hz, 2H), 7.22 (d, *J* = 7.6 Hz, 2H), 6.69 (s, 4H), 5.42 (s, 4H), 3.83 (s, 6H), 3.62 (s, 6H), 2.10 (s, 12H).

^{13}C NMR (125 MHz, $CDCl_3$, δ): 159.3 (s), 159.1 (s), 156.0 (s), 155.3 (s), 155.0 (s), 153.8 (s), 152.0 (d), 150.5 (s), 139.6 (d), 138.0 (d), 137.7 (s), 137.5 (d), 137.2 (d), 133.6 (s), 125.6 (d), 124.4 (d), 122.0 (s), 120.9 (d), 120.6 (d), 119.6 (s), 119.4 (d), 113.2 (d), 95.9 (t), 94.8 (s), 87.6 (s), 56.8 (q), 55.3 (q), 20.9 (q).

IR (film on NaCl, cm^{-1}): 2955*w*, 2831*w*, 2215*vw*, 1606*m*, 1567*m*, 1490*m*, 1452*s*, 1378*m*, 1311*m*, 1266*m*, 1195*m*, 1156*vs*, 1072*m*, 976*m*, 819*m*, 752*w*.

MS (ESI) *m/z*: 1000.5 ($[M + Na]^+$). HRMS (ESI) *m/z*: $[M + Na]^+$ calcd for $C_{61}H_{51}N_7O_6Na$: 1000.3799; found: 1000.3803.

4-Iodo-4′′-[2-(4-methoxy-2,6-dimethylphenyl)-ethynyl]-5,5′′-bis(methoxymethoxy)-2,2′:6′,2′′-terpyridine (**79c**)

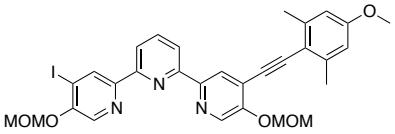

To a mixture of diiodoterpyridine **69** (450 mg, 0.744 mmol, 1.00 eq), CuI (14 mg, 0.074 mmol, 10 mol%) and $Pd(PPh_3)_2Cl_2$ (26 mg, 0.037 mmol, 5 mol%) in anhydrous THF (15 mL) was added a solution of 2-ethynyl-5-methoxy-1,3-dimethylbenzene (**73**) (125 mg, 0.781 mmol, 1.05 eq) in degassed Et_3N (15 mL) under N_2 atmosphere at 80 °C. The reaction mixture was heated to reflux for 15 h, allowed to cool to room temperature and diluted with CH_2Cl_2 (100 mL). The mixture was washed with 10% aqueous NH_4OH, water and brine. The organic phase was dried over $MgSO_4$, filtered and evaporated under reduces pressure. The residue was purified by silica gel column chromatography with hexane/ethyl acetate/MTBE (2:2:1) to give monosubstituted **79c** (179 mg, 38%), disubstituted **78h** (81 mg, 15%) and recovered starting diiodoterpyridine **69** (126 mg, 28%).

4-iodo-4''-[2-(4-methoxy-2,6-dimethylphenyl)-ethynyl]-5,5''-bis(methoxymethoxy)-2,2':6',2''-terpyridine (**79c**)

White solid, Mp 146.5–147.5 °C.

^{1}H NMR (400 MHz, $CDCl_3$, δ): 9.06 (s, 1H), 8.65 (s, 1H), 8.55 (s, 1H), 8.37 (s, 1H), 8.35 (d, *J* = 7.8 Hz, 1H), 8.31 (d, *J* = 7.8 Hz, 1H), 7.90 (t, *J* = 7.8 Hz, 1H), 6.67 (s, 2H), 5.39 (s, 2H), 5.35 (s, 2H), 3.82 (s, 3H), 3.58 (s, 3H), 3.57 (s, 3H), 2.60 (s, 6H).

^{13}C NMR (100 MHz, $CDCl_3$, δ): 160.0 (s), 154.7 (s), 153.8 (s), 153.7 (s), 153.2 (s), 150.9 (s), 150.0 (s), 142.9 (s), 138.1 (d), 137.1 (s), 135.8 (d), 132.4 (d), 124.2 (d), 123.7 (s), 120.4 (d), 114.9 (s), 112.8 (d), 99.4 (s), 96.5 (s), 95.7 (t), 95.6 (t), 90.8 (s), 56.8 (q), 56.7 (q), 55.3 (q), 21.5 (q).

IR (film on NaCl, cm^{-1}): 2956*w*, 2838*w*, 2208*w*, 1605*m*, 1581*m*, 1569*m*, 1539*m*, 1482*s*, 1453*s*, 1354*w*, 1321*s*, 1287*m*, 1269*m*, 1236*w*, 1199*m*, 1156*vs*, 1083*m*, 979*s*, 820*m*, 738*w*.

HRMS (ESI) *m/z*: $[M + H]^+$ calcd for $C_{30}H_{29}IN_3O_5$: 638.11464; found: 638.11406.

4,4″-bis[2-(4-methoxy-2,6-dimethylphenyl)-ethynyl]-5,5″-bis(methoxymethoxy)-2,2′:6′,2″-terpyridine (**78h**)

White solid, Mp 181.5–182.5 °C.

^{1}H NMR (400 MHz, $CDCl_3$, δ): 8.65 (s, 2H), 8.57 (s, 2H), 8.38 (d, *J* = 7.9 Hz, 2H), 7.94 (t, *J* = 7.9 Hz, 1H), 6.62 (s, 4H), 5.39 (s, 4H), 3.82 (s, 6H), 3.58 (s, 6H), 2.53 (s, 12H).

^{13}C NMR (100 MHz, $CDCl_3$, δ): 159.9 (s), 154.7 (s), 153.3 (s), 150.1 (s), 142.9 (s), 138.1 (d), 136.9 (d), 124.2 (d), 123.8 (s), 120.5 (d), 115.0 (s), 112.7 (d), 96.6 (s), 95.6 (t), 90.7 (s), 56.7 (q), 55.3 (q), 21.4 (q).

IR (film on NaCl, cm^{-1}): 2954*w*, 2839*w*, 2206*m*, 1605*m*, 1575*s*, 1539*w*, 1485*m*, 1456*m*, 1377*m*, 1321*s*, 1287*m*, 1266*w*, 1196*m*, 1158*vs*, 1121*w*, 1076*m*, 1059*w*, 985*s*, 922*w* 822*m*, 732*w*.

HRMS (ESI) *m/z*: $[M + H]^+$ calcd for $C_{41}H_{40}N_3O_6$: 670.29116; found: 670.29092.

4-{2-[5′-(4-Methoxy-2,6-dimethylphenyl)-2,2′-bipyridin-5-yl]ethynyl}-4″-[2-(4-methoxy-2,6-dimethylphenyl)-ethynyl]-5,5″-bis(methoxymethoxy)-2,2′:6′,2″-terpyridine (**81a**)

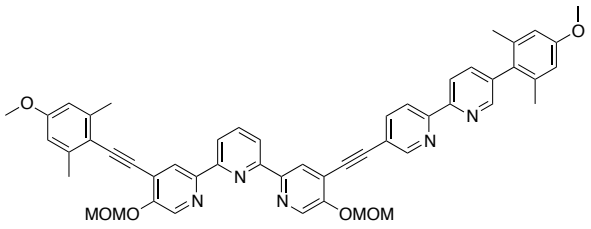

To a mixture of iodoterpyridine **69** (257 mg, 0.325 mmol, 1.00 eq), $Pd(PPh_3)_2Cl_2$ (11.4 mg, 0.016 mmol, 5 mol%) and CuI (6.2 mg, 0.032 mmol, 10 mol%) in degassed THF/Et_3N (3 mL/3 mL) was added a solution of 2-ethynyl-5-methoxy-1,3-dimethylbenzene (**73**) (57 mg, 0.36 mmol, 1.1 eq) in degassed THF/Et_3N (3 mL/3 mL) under N_2 atmosphere at 75 °C. The

reaction mixture was heated to reflux for 20 h, allowed to cool to room temperature and diluted with CH_2Cl_2 (25 mL). The mixture was washed with 10% NH_4OH aqueous solution, water and brine. The organic phase was dried over $MgSO_4$, filtered and evaporated under reduces pressure. The residue was purified by neutral alumina (Brockman III) column chromatography with hexane/ethyl acetate (3:1) to give desired product **81a** (232 mg, 87%) as an off-white solid.

Mp 177–178.5 °C.

^{1}H NMR (400 MHz, $CDCl_3$, δ): 8.92 (s, 1H), 8.75 (s, 1H), 8.69 (s, 1H), 8.64 (s, 1H), 8.57 (s, 1H), 8.55-8.51 (m, 3H), 8.37 (d, *J* = 7.8 Hz, 2H), 8.04 (d, *J* = 8.2 Hz, 1H), 7.93 (t, *J* = 7.8 Hz, 1H), 7.67 (d, *J* = 8.1 Hz, 1H), 6.73 (s, 2H), 6.61 (s, 2H), 5.43 (s, 2H), 5.39 (s, 2H), 3.84 (s, 3H), 3.75 (s, 3H), 3.63 (s, 3H), 3.58 (s, 3H), 2.56 (s, 6H), 2.09 (s, 6H).

^{13}C NMR (100 MHz, $CDCl_3$, δ): 159.9 (s), 159.2 (s), 155.6 (s), 154.9 (s), 154.6 (s), 153.8 (s), 153.6 (s), 153.2 (s), 152.1 (d), 150.4 (d), 150.3 (s), 150.2 (s), 142.8 (s), 139.8 (d), 138.6 (d), 138.0 (d), 137.9 (s), 137.4 (d), 137.3 (d), 137.1 (s), 130.3 (s), 124.7 (d), 124.1 (d), 123.6 (s), 121.8 (s), 121.3 (d), 120.4 (d), 120.4 (d), 120.2 (d), 119.7 (s), 114.9 (s), 113.2 (d), 112.8 (d), 112.7 (s), 96.5 (s), 95.8 (t), 95.5 (t), 94.2 (s), 90.8 (s), 87.9 (s), 56.8 (q), 56.7 (q), 55.4 (q), 55.3 (q), 21.5 (q), 21.4 (q).

IR (film on NaCl, cm^{-1}): 2957*m*, 2837*w*, 2208*w*, 1606*m*, 1575*s*, 1539*w*, 1486*s*, 1463*s*, 1456*s*, 1378*m*, 1320*s*, 1270*m*, 1231*w*, 1196*m*, 1157*s*, 1076*m*, 1057*w*, 982*s*, 924*m*, 907*m*, 845*m*, 822*m*, 734*m*.

HRMS (ESI) *m/z*: $[M + H]^+$ calcd for $C_{51}H_{46}N_5O_6$: 824.34426; found: 824.34373.

4-{2-[6′-(4-Methoxy-2,6-dimethylphenyl)-2,2′-bipyridin-5-yl]ethynyl}-4′′-[2-(4-methoxy-2,6-dimethylphenyl)-ethynyl]-5,5′′-bis(methoxymethoxy)-2,2′:6′,2′′-terpyridine (81b)

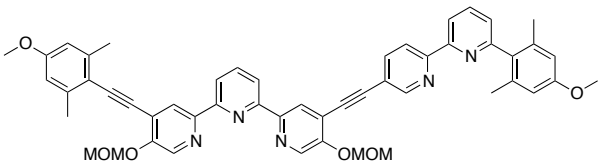

To a mixture of iodoterpyridine **69** (131 mg, 0.165 mmol, 1.00 eq), $Pd(PPh_3)_2Cl_2$ (5.8 mg, 0.0083 mmol, 5 mol%) and CuI (3.2 mg, 0.017 mmol, 10 mol%) in degassed THF/Et_3N (2.5 mL/2.5 mL) was added a solution of 2-ethynyl-5-methoxy-1,3-dimethylbenzene (**73**) (34 mg, 0.22 mmol, 1.3 eq) in degassed THF/Et_3N (2.5 mL/2.5 mL) under N_2 atmosphere at 75 °C. The reaction mixture was heated to reflux for 17 h, allowed to cool to room temperature and

diluted with CH_2Cl_2 (15 mL). The mixture was washed with 10% NH_4OH aqueous solution, water and brine. The organic phase was dried over $MgSO_4$, filtered and evaporated under reduces pressure. The residue was purified by neutral alumina (Brockman III) column chromatography with hexane/ethyl acetate (3:1) to give desired product **81b** (107 mg, 79%) as a white solid.

Mp 164–166 °C.

^{1}H NMR (400 MHz, $CDCl_3$, δ): 8.91 (s, 1H), 8.73 (s, 1H), 8.68 (s, 1H), 8.63 (s, 1H), 8.57 (s, 1H), 8.50 (d, *J* = 8.2 Hz, 1H), 8.43 (d, *J* = 8.2 Hz, 1H), 8.37 (d, *J* = 7.7 Hz, 1H), 7.99-7.87 (m, 3H), 7.29-7.25 (d, *J* = 7.1 Hz, 1H), 6.72 (s, 2H), 6.59 (s, 2H), 5.42 (s, 2H), 5.39 (s, 2H), 3.85 (s, 3H), 3.71 (s, 2H), 3.62 (s, 3H), 3.58 (s, 3H), 2.56 (s, 6H), 2.14 (s, 6H).

^{13}C NMR (100 MHz, $CDCl_3$, δ): 159.9 (s), 159.3 (s), 159.1 (s), 155.9 (s), 155.2 (s), 154.7 (s), 154.6 (s), 153.6 (s), 153.2 (s), 152.0 (d), 150.3 (s), 150.1 (s), 142.8 (s), 139.5 (d), 138.1 (s), 138.0 (d), 137.6 (s), 137.4 (d), 137.2 (d), 136.9 (d), 133.6 (s), 125.7 (d), 124.6 (d), 124.1 (d), 123.6 (s), 121.9 (s), 120.8 (d), 120.4 (d), 120.3 (d), 119.6 (s), 119.3 (d), 114.8 (s), 113.2 (d), 112.8 (d), 96.6 (s), 95.8 (t), 95.5 (t), 94.3 (s), 90.7 (s), 87.7 (s), 56.8 (q), 56.6 (q), 55.3 (q), 55.2 (q), 21.4 (q), 20.9 (q).

IR (film on NaCl, cm^{-1}): 2956*m*, 2837*w*, 2207*w*, 1605*m*, 1575*s*, 1546*w*, 1485*m*, 1455*s*, 1377*m*, 1321*s*, 1268*m*, 1233*w*, 1196*m*, 1157*vs*, 1075*m*, 982*s*, 925*w*, 821*m*, 737*w*.

HRMS (ESI) *m/z*: $[M + H]^+$ calcd for $C_{51}H_{46}N_5O_6$: 824.34426; found: 824.34402.

2.8.2.4. Synthesis of Ligands L1-L6

2,6-Bis[2-(phenyl)furo[2,3-*c*]pyridin-5-yl]pyridine (L1)

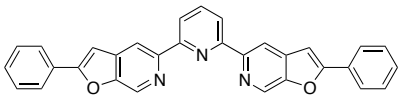

To a solution of 5,5″-bis(methoxymethoxy)-4,4″-bis(phenylethynyl)-2,2′:6′,2″-terpyridine (**78a**) (217 mg, 0.391 mmol, 1.00 eq) in DMF (10 mL) was added 32% aq. HCl (0.19 mL, 2.0 mmol, 5.0 eq). The reaction mixture was heated to 80 °C for 2 h, then Cs_2CO_3 (5.47 g, 16.8 mmol, 43.0 eq) was added portion-wise. The resulting mixture was heated to 90 °C for 48 h. Evaporation of DMF resulted in residue that was treated with water (100 ml) and the mixture was extracted with CH_2Cl_2 (100 mL × 4). The combined organic fractions were washed with water and brine, dried over $MgSO_4$, filtered and evaporated under reduced pressure. The

resulting solid was treated with hexane (20 ml), collected by filtration and washed with Et_2O (10 ml) to give desired ligand **L1** (168 mg, 92%) as an off-white solid.

Mp 294–295 °C dec.

^{1}H NMR (400 MHz, $CDCl_3$, δ): 9.02 (s, 2H), 8.98 (s, 2H), 8.48 (d, *J* = 7.8 Hz, 2H), 7.98 (t, *J* = 7.8 Hz, 1H), 7.97-7.95 (m, 4H), 7.54-7.45 (m, 6H), 7.23 (s, 2H).

^{13}C NMR (125 MHz, $CDCl_3$, δ): 160.2 (s), 155.3 (s), 152.4 (s), 149.8 (s), 138.2 (d), 137.3 (s), 132.2 (d), 130.2 (d), 129.4 (s), 129.2 (d), 125.9 (d), 120.8 (d), 113.8 (d), 101.2 (d).

IR (KBr, cm^{-1}): 2919*w*, 1606*w*, 1586*m*, 1567*m*, 1448*vs*, 1424*w*, 1399*m*, 1306*w*, 1154*w*, 1019*w*, 913*w*, 903*w*, 894*m*, 894*m*, 821*m*, 767*s*, 756*w*, 691*m*.

HRMS (ESI) *m/z*: $[M + Na]^+$ calcd for $C_{31}H_{19}N_3NaO_2$: 488.13695; found: 488.13659.

2,6-Bis[2-(hexyl)furo[2,3-*c*]pyridin-5-yl]pyridine (L2)

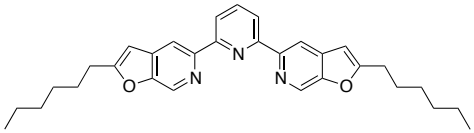

To a solution of 4,4″-bis(1-octynyl-1-yl)-5,5″-bis(methoxymethoxy)-2,2′:6′,2″-terpyridine (**78b**) (244 mg, 0.429 mmol, 1.00 eq) in DMF (10 mL) was added 32% aq. HCl (0.21 mL, 2.0 mmol, 5.0 eq). The reaction mixture was heated to 80 °C for 2 h, then Cs_2CO_3 (5.99 g, 18.4 mmol, 43 eq) was added portion-wise. The reaction mixture was heated to 90 °C for 48 h. Evaporation of DMF resulted in residue that was treated with water (100 ml) and the mixture was extracted with CH_2Cl_2 (50 mL × 3). The combined organic fractions were washed with water and brine, dried over $MgSO_4$, filtered and evaporated under reduced pressure. The crude product was purified by neutral alumina (Brockman III) column chromatography with hexane/ethyl acetate (3:1) to give desired ligand **L2** (196 mg, 95%) as a white solid.

Mp 86–87 °C.

^{1}H NMR (400 MHz, $CDCl_3$, δ): 8.82 (s, 2H), 8.78 (s, 2H), 8.40 (d, *J* = 7.8 Hz, 2H), 7.91 (t, *J* = 7.8 Hz, 1H), 6.52 (s, 2H), 2.82 (t, *J* = 7.6 Hz, 4H), 1.78 (quintet, *J* = 7.5 Hz, 4H), 1.43-1.31 (m, 12H), 0.92-0.88 (m, 6H).

^{13}C NMR (100 MHz, $CDCl_3$, δ): 164.3 (s), 155.8 (s), 152.5 (s), 149.9 (s), 137.8 (d), 136.9 (s), 131.8 (d), 120.4 (d), 113.2 (d), 102.2 (d), 31.6 (t), 29.0 (t), 28.7 (t), 27.5 (t), 22.7 (t), 14.2 (q).

IR (film on NaCl, cm^{-1}): 2933*s*, 2859*m*, 1595*s*, 1567*s*, 1455*s*, 1424*m*, 1399*m*, 1304*s*, 1285*m*, 1149*m*, 1072*w*, 1035*w*, 949*w*, 933*w*, 915*m*, 897*m*, 823*s*, 793*w*, 744*w*, 734*w*, 660*m*.

HRMS (ESI) *m/z*: $[M + H]^+$ calcd for $C_{31}H_{36}N_3O_2$: 482.28020; found: 482.28030.

2,6-Bis[2-(pyridin-4-yl)furo[2,3-*c*]pyridin-5-yl]pyridine (L3)

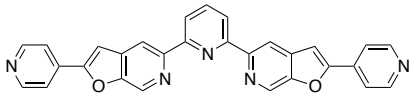

To a solution of 5,5″-bis(methoxymethoxy)-4,4″-bis[2-(pyridine-4-yl)ethynyl]-2,2′:6′,2″-terpyridine (**78d**) (117 mg, 0.211 mmol, 1.00 eq) in DMF (6 mL) was added 32% aq. HCl (0.10 mL, 3.2 mmol, 5.0 eq). The reaction mixture was heated to 80 °C for 2 h, then Cs_2CO_3 (2.94 g, 9.05 mmol, 43.0 eq) was added portion-wise. The reaction mixture was heated to 90 °C for 72 h. Evaporation of DMF resulted in residue that was treated with water (40 ml). The resulting precipitate was collected by filtration, washed with pentane (15 ml) and Et_2O (15 ml) to give desired ligand **L3** (88 mg, 90%) as an off-white solid.

Mp 335–336 °C dec.

^{1}H NMR (500 MHz, $CDCl_3$, δ): 9.04 (s, 2H), 8.95 (d, *J* = 0.8 Hz, 2H), 8.79 (dd, *J* = 4.5, 1.6 Hz, 4H), 8.48 (d, *J* = 7.8 Hz, 2H), 7.99 (t, *J* = 7.8 Hz, 1H), 7.81 (dd, *J* = 4.5, 1.6 Hz, 4H), 7.40 (d, *J* = 0.5 Hz, 2H).

^{13}C NMR (125 MHz, $CDCl_3$, δ): 156.7 (s), 155.6 (s), 152.7 (s), 150.8 (d), 150.7 (s), 138.2 (d), 136.6 (s), 136.0 (s), 133.3 (d), 120.9 (d), 119.5 (d), 113.9 (d), 104.5 (d).

IR (KBr, cm^{-1}): 3038*w*, 2919*w*, 2853*w*, 1635*w*, 1604*m*, 1568*s*, 1448*s*, 1401*s*, 13101*w*, 1296*w*, 1223*w*, 1210*w*, 1156*w*, 1037*w*, 993*w*, 916*w*, 905*m*, 895*m*, 821*vs*, 810*w*, 742*w*, 690*w*, 650*w*.

MS (ESI) *m/z*: 468.2 ($[M + H]^+$); 490.2 ($[M + Na]^+$); HRMS (ESI) *m/z*: $[M + Na]^+$ calcd for $C_{29}H_{17}N_5NaO_2$: 490.12745; found: 490.12704.

2-(4-Methoxy-2,6-dimethylphenyl)-5-(6-{2-[5′-(4-methoxy-2,6-dimethylphenyl)-2,2′-bipyridin-5-yl]furo[2,3-*c*]pyridin-5-yl}pyridin-2-yl)furo[2,3-*c*]pyridine (L4)

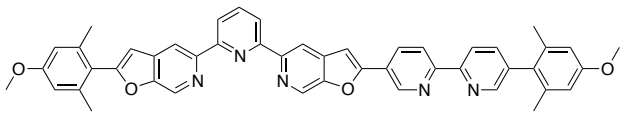

To a solution of terpyridine **81a** (231 mg, 0.281 mmol, 1.00 eq) in DMF (10 mL) was added 32% aq. HCl (0.58 mL, 5.9 mmol, 21 eq). The reaction mixture was heated to 80 °C for 5 h, then Cs_2CO_3 (3.93 g, 12.1 mmol, 43 eq) was added portion-wise. The reaction mixture was heated to 90 °C for 76 h. Evaporation of DMF resulted in residue that was treated with water (50 ml) and the mixture was extracted with CH_2Cl_2 (15 mL × 4). The combined organic fractions were washed with water and brine, dried over $MgSO_4$, filtered and evaporated under reduced pressure. The crude product was purified by neutral alumina (Brockman III) column chromatography with hexane/CH_2Cl_2/MeOH (50:50:1) to give desired product **L4** (200 mg, 97%) as a white solid.

Mp 304–305 °C dec.

^{1}H NMR (500 MHz, $CDCl_3$, δ): 9.28 (d, *J* = 2.3 Hz, 1H), 9.03 (s, 1H), 9.01 (s, 1H), 8.97 (s, 1H), 8.94 (s, 1H), 8.62 (d, *J* = 8.3 Hz, 1H), 8.56 (d, *J* = 8.3 Hz, 1H), 8.53 (d, *J* = 2.2 Hz, 1H), 8.49 (d, *J* = 7.8 Hz, 1H), 8.48 (d, *J* = 7.8 Hz, 1H), 8.37 (dd, *J* = 8.3, 2.3 Hz, 1H), 7.99 (t, *J* = 7.8 Hz, 1H), 7.68 (dd, *J* = 8.0, 2.2 Hz, 1H), 7.35 (s, 1H), 6.84 (s, 1H), 6.73 (s, 2H), 6.73 (s, 2H), 3.86 (s, 3H), 3.85 (s, 3H), 2.29 (s, 6H), 2.09 (s, 6H).

^{13}C NMR (125 MHz, $CDCl_3$, δ): 160.5 (s), 159.8 (s), 159.1 (s), 156.9 (s), 156.8 (s), 155.7 (s), 155.6 (s), 153.7 (s), 152.7 (s), 152.4 (s), 150.6 (s), 150.4 (d), 149.8 (s), 146.7 (d), 140.3 (s), 138.6 (d), 138.1 (d), 138.0 (s), 137.3 (s), 136.8 (s), 136.5 (s), 133.7 (d), 132.8 (d), 132.3 (d), 130.3 (s), 125.4 (s), 122.1 (s), 121.3 (d), 121.1 (d), 120.7 (d), 120.6 (d), 113.7 (d), 113.6 (d), 113.3 (d), 113.1 (d), 106.5 (d), 102.7 (d), 55.4 (q), 55.3 (q), 21.4 (q), 21.0 (q).

IR (KBr, cm^{-1}): 2923*w*, 1607*s*, 1570*m*, 1447*s*, 1460*s*, 1402*m*, 1319*m*, 1193*w*, 1154*vs*, 1063*w*, 1012*w*, 826*w*, 653*w*.

HRMS (ESI) *m/z*: $[M + H]^+$ calcd for $C_{47}H_{37}N_5O_4$: 736.29183; found: 736.29141.

2-(4-Methoxy-2,6-dimethylphenyl)-5-(6-{2-[6′-(4-methoxy-2,6-dimethylphenyl)-2,2′-bipyridin-5-yl]furo[2,3-*c*]pyridin-5-yl}pyridin-2-yl)furo[2,3-*c*]pyridine (L5)

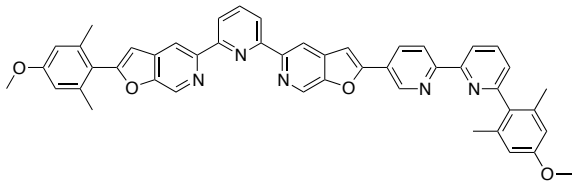

To a solution of terpyridine **81b** (51.6 mg, 0.0604 mmol, 1.00 eq) in DMF (2 mL) was added 32% aq. HCl (0.069 mL, 0.22 mmol, 21 eq). The reaction mixture was heated to 80 °C for 4 h, then Cs_2CO_3 (844 mg, 2.60 mmol, 43.0 eq) was added portion-wise. The reaction mixture was heated to 90 °C for 48 h. Evaporation of DMF resulted in residue that was treated with water (20 ml) and the mixture was extracted with CH_2Cl_2 (15 mL × 4). The combined organic fractions were washed with water and brine, dried over $MgSO_4$, filtered and evaporated under reduced pressure. The crude product was purified by neutral alumina (Brockman III) column chromatography with hexane/CH_2Cl_2/MeOH (50:50:1) to give desired product **L5** (43.3 mg, 94%) as a white solid.

Mp 300–301 °C dec.

^{1}H NMR (400 MHz, $CDCl_3$, δ): 9.23 (s, 1H), 8.99 (s, 1H), 8.94 (s, 1H), 8.93 (s, 2H), 8.59 (d, *J* = 8.3 Hz, 1H), 8.47 (s, 1H), 8.47-8.41 (m, 2H), 8.24 (d, *J* = 8.4 Hz, 1H), 7.96 (t, *J* = 7.8 Hz, 1H), 7.89 (t, *J* = 7.7 Hz, 1H), 7.28-7.26 (m, 2H), 6.82 (s, 1H), 6.72 (s, 4H), 3.85 (s, 3H), 3.85 (s, 3H), 2.28 (s, 6H), 2.14 (s, 6H).

^{13}C NMR (100 MHz, $CDCl_3$, δ): 160.5 (s), 159.4 (s), 159.1 (s), 157.2 (s), 156.9 (s), 156.0 (s), 155.6 (s), 155.2 (s), 152.7 (s), 152.5 (s), 150.7 (s), 150.2 (s), 146.5 (d), 140.3 (s), 137.9 (d), 137.7 (s), 137.2 (d), 136.5 (s), 136.4 (s), 133.6 (s), 133.5 (d), 132.8 (d), 132.5 (d), 125.7 (d), 125.4 (s), 122.3 (s), 121.5 (d), 120.7 (d), 120.5 (d), 119.2 (d), 113.6 (d), 113.5 (d), 113.3 (d), 113.2 (d), 106.4 (d), 102.5 (d), 55.4 (q), 55.3 (q), 21.0 (q), 20.9 (q).

IR (KBr, cm^{-1}): 2925*w*, 1606*s*, 1568*m*, 1448*vs*, 1401*w*, 1319*m*, 1195*w*, 1154*s*, 1071*w*, 821*w*, 651*w*.

HRMS (ESI) *m/z*: $[M + H]^+$ calcd for $C_{47}H_{37}N_5O_4$: 736.29183; found: 736.29186.

2,6-Bis{2-[5′-(4-methoxy-2,6-dimethylphenyl)-2,2′-bipyridin-5-yl]furo[2,3-*c*]pyridin-5-yl}pyridine (**L6**)

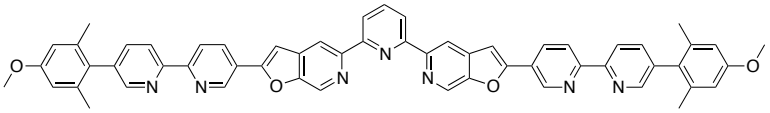

To a solution of terpyridine **78f** (185 mg, 0.190 mmol, 1.00 eq) in DMF (10 mL) was added 32% aq. HCl (0.19 mL, 1.9 mmol, 10 eq). The reaction mixture was heated to 80 °C for 4 h, then Cs_2CO_3 (926 mg, 2.84 mmol, 15.0 eq) was added portion-wise. The reaction mixture was heated to 90 °C for 72 h. Evaporation of DMF resulted in residue that was treated with water (20 ml) and the mixture was extracted with CH_2Cl_2 (20 mL × 4). The combined organic fractions were washed with water and brine, dried over $MgSO_4$, filtered and evaporated under reduced pressure. The crude product was treated with acetone and collected by filtration to give desired product **L6** (123 mg, 73%) as a yellow solid.

Mp >330 °C dec.

^{1}H NMR (400 MHz, $CDCl_3$, δ): 9.26 (dd, *J* = 2.2, 0.7 Hz, 2H), 9.00 (s, 2H), 8.93 (s, 2H), 8.61 (dd, *J* = 8.3, 0.7 Hz, 2H), 8.55 (dd, *J* = 8.0, 0.8 Hz, 2H), 8.53 (dd, *J* = 2.2, 0.8 Hz, 2H), 8.46 (d, *J* = 7.8 Hz, 2H), 8.34 (dd, *J* = 8.3, 2.2 Hz, 2H), 7.97 (t, *J* = 7.8 Hz, 1H), 7.68 (dd, *J* = 8.0, 2.2 Hz, 2H), 7.32 (s, 2H), 6.73 (s, 4H), 3.85 (s, 6H), 2.09 (s, 12H).

^{13}C NMR (125 MHz, $CDCl_3$, δ): 159.2 (s), 156.9 (s), 156.8 (s), 155.6 (s), 153.7 (s), 152.7 (s), 150.6 (s), 150.4 (d), 146.7 (d), 138.6 (d), 138.1 (d), 138.0 (s), 137.3 (s), 136.4 (s), 133.7 (d) 132.9 (d), 130.3 (s), 125.4 (s), 121.2 (d), 121.1 (d), 120.7 (d), 113.6 (d), 113.1 (d), 102.6 (d), 55.3 (q), 21.4 (q).

IR (film on NaCl, cm^{-1}): 2921*w*, 1605*s*, 1570*m*, 1460*vs*, 1448*s*, 1316*m*, 1274*w*, 1193*w*, 1155*vs*, 1078*w*, 1061*w*, 1012*w*, 998*w*, 905*w*, 844*w*, 820*m*, 733*w*, 648*w*.

HRMS (ESI) *m/z*: $[M + 2H]^{2+}$ calcd for $C_{57}H_{45}N_7O_4$: 445.67610; found: 445.67560.

2.8.2.5. Preparation of Zn^{2+}, Fe^{2+} and Ru^{2+} Complexes of Ligands L1-L6

Zn[2,6-bis(2-phenylfuro[2,3-*c*]pyridin-5-yl)pyridine]-2PF_6 ([$L1_2Zn$](PF_6)$_2$)

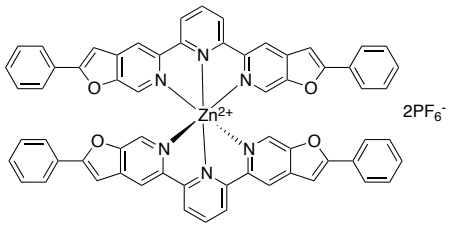

To a solution of ligand **L1** (25.0 mg, 0.0537 mmol, 1.00 eq) in THF (12 mL) a solution of $Zn(OTf)_2$ (9.78 mg, 0.0264 mmol, 0.50 eq) in MeOH (2.2 mL) was added dropwise in 5 minutes at room temperature. The reaction mixture was stirred for 18 h at room temperature. To the mixture saturated aq. KPF_6 was added and the resulting yellow precipitate was filtered over Celite, washed with water, Et_2O, hexane and redissolved with acetonitrile. The solvent was evaporated to give desired Zn complex (**[$L1_2Zn$](PF_6)$_2$**) (32.3 mg, 94%) as a yellow solid. Single crystals suitable for X-ray diffraction analysis were obtained by slow vapor diffusion of Et_2O into an acetonitrile solution of (**[$L1_2Zn$](PF_6)$_2$**).

Mp >370 °C dec.

^{1}H NMR (500 MHz, CD_3CN, δ): 8.84 (s, 2H), 8.81-8.76 (m, 3H), 8.02 (s, 2H), 7.87-7.82 (m, 4H), 7.48-7.44 (m, 6H), 7.37 (s, 2H).

^{13}C NMR (125 MHz, CD_3CN, δ): 163.7 (s), 153.5 (s), 151.0 (s), 144.9 (d), 142.5 (s), 140.4 (s), 132.1 (d), 131.7 (d), 129.9 (d), 128.6 (s), 126.6 (d), 123.0 (d), 116.3 (d), 102.0 (d).

IR (KBr, cm^{-1}): 3116*w*, 3065*w*, 1616*m*, 1583*w*, 1478*w*, 1454*s*, 1425*w*, 1324*m*, 1177*w*, 1021*w*, 959*w*, 842*vs*, 767*w*, 687*w*, 558*s*.

HRMS (ESI) *m/z*: $[M]^{2+}$ calcd for $C_{62}H_{38}N_6O_4Zn$: 497.11175; found: 497.11197.

Fe[2,6-bis(2-phenylfuro[2,3-*c*]pyridin-5-yl)pyridine]-2PF_6 ([$L1_2Fe$](PF_6)$_2$)

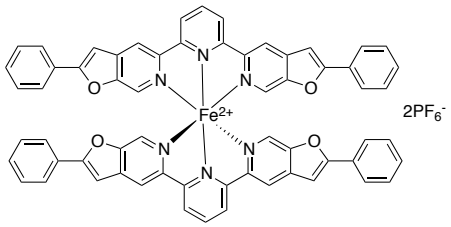

To a solution of ligand **L1** (25.0 mg, 0.0537 mmol, 1.00 eq) in THF (12 mL) a solution of $Fe(BF_4)_2 \cdot 6H_2O$ (9.06 mg, 0.0269 mmol, 0.500 eq) in water (2.2 mL) was added dropwise in 5 minutes at room temperature. The dark purple reaction mixture was stirred for 18 h at room

temperature. To the mixture saturated aq. KPF_6 was added and the resulting dark purple precipitate was filtered over Celite, washed with water, Et_2O, hexane and redissolved with acetonitrile. The solvent was evaporated to give desired Fe complex **$[L1_2Fe](PF_6)_2$** (30.8 mg, 90 %) as a dark purple solid. Single crystals suitable for X-ray diffraction analysis were obtained by slow vapor diffusion of Et_2O into an acetonitrile solution of **$[L1_2Fe](PF_6)_2$**.

Mp >370 °C dec.

^{1}H NMR (500 MHz, CD_3CN, δ): 8.96 (d, *J* = 8.1 Hz, 2H), 8.80 (t, *J* = 8.1 Hz, 1H), 8.78 (s, 2H), 7.78-7.75 (m, 4H), 7.45-7.41 (m, 6H), 7.34 (s, 2H), 7.24 (s, 2H).

^{13}C NMR (125 MHz, CD_3CN, δ): 162.52 (s) 161.1 (s), 152.6 (s), 151.6 (s), 138.8 (d), 138.5 (s), 136.7 (d), 131.5 (d), 129.6 (d), 128.2 (s), 126.4 (d), 122.6 (d), 116.9 (d), 101.7 (d).

IR (KBr, cm^{-1}): 3116*w*, 3086*w*, 1622*m*, 1585*w*, 1564*w*, 1459*s*, 1449*s*, 1320*m*, 1278*w*, 1252*w*, 1174*w*, 1020*w*, 841*vs*, 766*m*, 746*w*, 687*m*, 558*s*.

HRMS (ESI) *m/z*: $[M]^{2+}$ calcd for $C_{62}H_{38}N_6O_4Fe$: 493.11473; found: 493.11390.

Ru[2,6-bis(2-phenylfuro[2,3-*c*]pyridin-5-yl)pyridine]-2PF_6 ($[L1_2Ru](PF_6)_2$)

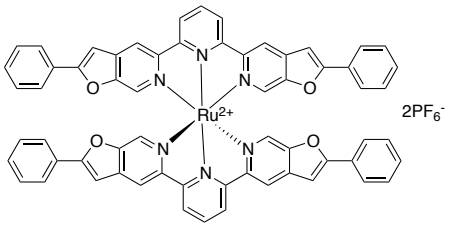

A suspension of ligand **L1** (25.0 mg, 0.0537 mmol, 1.00 eq) and $Ru(DMSO)_4Cl_2$ (13.0 mg, 0.0269 mmol, 0.500 eq) in ethylene glycol (15 ml) was heated to 120 °C for 18 h. The reaction mixture was allowed to cool to room temperature and a saturated aq. KPF_6 solution was added. The resulting red precipitate was filtered over Celite, washed with water, Et_2O, hexane and redissolved with acetonitrile. The solvent was evaporated and the residue was purified by silica gel column chromatography with acetonitrile/H_2O/aq. KPF_6 (97:3:0.3), reprecipitated with a saturated aq. KPF_6 solution and collected by filtration. The red solid was washed with water and Et_2O to give desired complex **$[L1_2Ru](PF_6)_2$** (32.5 mg, 92%) as a dark red solid. Single crystals suitable for X-ray diffraction analysis were obtained by slow vapor diffusion of Et_2O into an acetonitrile solution of **$[L1_2Ru](PF_6)_2$**.

Mp >350 °C dec.

^{1}H NMR (500 MHz, CD_3CN, δ): 8.82 (s, 2H), 8.80 (d, *J* = 8.2 Hz, 2H), 8.50 (t, *J* = 8.2 Hz, 1H), 7.83-7.80 (m, 4H), 7.68 (s, 2H), 7.48-7.46 (m, 6H), 7.34 (s, 2H).

^{13}C NMR (125 MHz, CD_3CN, δ): 163.1 (s), 156.8 (s), 152.9 (s), 152.8 (s), 137.9 (s), 137.0 (d), 136.8 (d), 131.9 (d), 130.2 (d), 128.9 (s), 126.9 (d), 123.2 (d), 117.9 (d), 102.4 (d).

IR (KBr, cm^{-1}): 3116*w*, 3069*w*, 1621*m*, 1585*w*, 1567*w*, 1485*w*, 1459*s*, 1447*s*, 1385*w*, 1313*w*, 1278*w*, 1176*w*, 1020*w*, 842*vs*, 767*w*, 687*w*, 558*s*.

HRMS (ESI) *m/z*: $[M]^{2+}$ calcd for $C_{62}H_{38}N_6O_4Ru$: 516.10018; found: 516.09979.

Zn[2,6-bis(2-hexylfuro[2,3-*c*]pyridin-5-yl)pyridine]-PF_6 ($[L2_2Zn](PF_6)_2$)

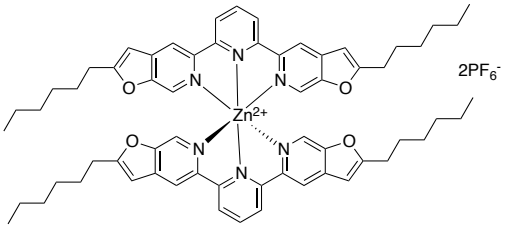

To a solution of ligand **L2** (15.0 mg, 0.0311 mmol, 1.00 eq) in THF (3 mL) a solution of $Zn(OTf)_2$ (5.66 mg, 0.0156 mmol, 0.500 eq) in MeOH (1.3 mL) was added dropwise in 5 minutes at room temperature. The reaction mixture was stirred for 18 h at room temperature. To the mixture saturated aq. KPF_6 was added and the resulting yellow precipitate was filtered over Celite, washed with water, Et_2O, hexane and redissolved with acetonitrile. The solvent was evaporated to give desired Zn complex (**$[L2_2Zn](PF_6)_2$**) (17.8 mg, 87%) as a yellow solid. Recrystallization by slow vapor diffusion of Et_2O into a CH_2Cl_2 solution of (**$[L2_2Zn](PF_6)_2$**) gives yellow needles.

Mp 257–258 °C dec.

^{1}H NMR (500 MHz, CD_2Cl_2, δ): 8.75-8.71 (m, 3H), 8.68 (s, 2H), 7.75 (s, 2H), 6.70 (s, 2H), 2.74 (t, *J* = 7.6 Hz, 4H), 1.64 (quintet, *J* = 7.4 Hz, 4H), 1.29-1.20 (m, 12H), 0.81 (t, *J* = 6.8 Hz, 6H).

^{13}C NMR (125 MHz, CD_2Cl_2, δ): 169.46 (s), 153.2 (s), 150.6 (s), 144.9 (d), 141.5 (s), 140.3 (s), 130.7 (d), 122.3 (d), 115.5 (d), 103.2 (d), 31.6 (t), 29.0 (t), 28.9 (t), 27.4 (t), 22.7 (t), 14.1 (q).

IR (film on NaCl, cm^{-1}): 3125*w*, 2931*m*, 2859*w*, 1620*w*, 1587*m*, 1485*w*, 1456*s*, 1429*w*, 1324*s*, 1257*w*, 1182*w*, 1158*w*, 959*w*, 900*w*, 841*vs*, 740*w*, 665*w*, 558*m*.

HRMS (ESI) *m/z*: $[M]^{2+}$ calcd for $C_{62}H_{70}N_6O_4Zn$: 513.23695; found: 513.23769.

Fe[2,6-bis(2-hexylfuro[2,3-*c*]pyridin-5-yl)pyridine]-PF_6 ($[L2_2Fe](PF_6)_2$)

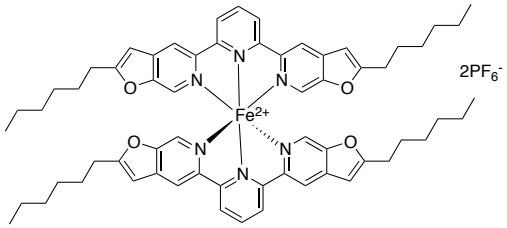

To a solution of ligand **L2** (15.0 mg, 0.0311 mmol, 1.00 eq) in THF (3 mL) a solution of $Fe(BF_4)_2 \cdot 6H_2O$ (5.26 mg, 0.0156 mmol, 0.500 eq) in water (1.3 mL) was added dropwise in 5 minutes at room temperature. The dark purple reaction mixture was stirred for 18 h at room temperature. To the mixture saturated aq. KPF_6 was added and the resulting dark purple precipitate was filtered over Celite, washed with water, Et_2O, hexane and redissolved with acetonitrile. The solvent was evaporated to give desired Fe complex **$[L2_2Fe](PF_6)_2$** (18.4 mg, 90 %) as a dark purple solid. Recrystallization by slow vapor diffusion of Et_2O into a CH_2Cl_2 solution of **$[L2_2Fe](PF_6)_2$** gives dark purple blocks.

Mp 299–300 °C dec.

^{1}H NMR (500 MHz, CD_2Cl_2, δ): 8.87 (d, J = 7.9 Hz, 2H) 8.74 (t, J = 8.0 Hz, 1H), 8.64 (s, 2H), 7.11 (s, 2H), 6.61 (s, 2H), 2.68 (t, J = 7.6 Hz, 4H), 1.62-1.52 (m, 4H), 1.27-1.17 (m, 12H), 0.80 (t, J = 6.9 Hz, 6H).

^{13}C NMR (125 MHz, CD_2Cl_2, δ):168.3 (s), 161.1 (s), 152.6 (s), 150.8 (s), 138.6 (s), 138.5 (d), 135.5 (d), 122.0 (d), 116.4 (d), 103.1 (d), 31.6 (t), 28.9 (t), 28.6 (t), 27.4 (t), 22.7 (t), 14.0 (q).

IR (film on NaCl, cm^{-1}): 3123*w*, 2931*m*, 2860*w*, 1624*w*, 1585*m*, 1456*s*, 1320*m*, 1259*w*, 1157*w*, 904*w*, 841*vs*, 749*w*, 674*w*, 558*m*.

HRMS (ESI) *m/z*: $[M]^{2+}$ calcd for $C_{62}H_{70}FeN_6O_4$: 509.23993; found: 509.23943.

Ru[2,6-bis(2-hexylfuro[2,3-*c*]pyridin-5-yl)pyridine]-PF_6 ($[L2_2Ru](PF_6)_2$)

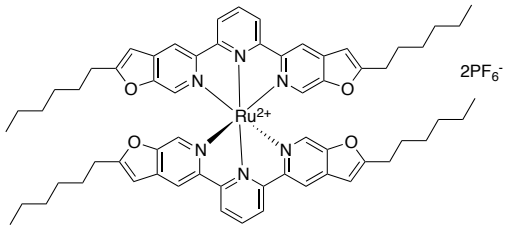

A suspension of ligand **L2** (25.0 mg, 0.0519 mmol, 1.00 eq) and $Ru(DMSO)_4Cl_2$ (12.6 mg, 0.0260 mmol, 0.500 eq) in ethylene glycol (15 ml) was heated to 120 °C for 18 h. The reaction mixture was allowed to cool to room temperature and a saturated aq. KPF_6 solution

was added. The resulting red precipitate was filtered over Celite, washed with water, Et_2O, hexane and redissolved with acetonitrile. The solvent was evaporated to give desired Ru complex (**[L2$_2$Ru](PF$_6$)$_2$**) (34.8 mg, 99%) as a dark red solid.

Mp >320 °C dec.

^{1}H NMR (500 MHz, CD_2Cl_2, δ): 8.68 (d, *J* = 8.2 Hz, 2H) 8.63 (s, 2H), 8.45 (t, *J* = 8.2 Hz, 1H), 7.38 (s, 2H), 6.64 (d, *J* = 0.7 Hz, 2H), 2.70 (t, *J* = 7.5 Hz, 4H), 1.59 (quintet, *J* = 7.5 Hz, 4H), 1.28-1.18 (m, 12H), 0.80 (t, *J* = 6.9 Hz, 6H).

^{13}C NMR (125 MHz, CD_2Cl_2, δ): 168.6 (s), 156.1 (s), 152.4 (s), 151.2 (s), 137.6 (s), 136.5 (d), 135.0 (d), 122.1 (d), 117.0 (d), 103.1 (d), 31.6 (t), 28.9 (t), 28.7 (t), 27.4 (t), 22.7 (t), 14.1 (q).

IR (film on NaCl, cm^{-1}): 3125*w*, 2931*m*, 2859*w*, 1623*w*, 1584*m*, 1493*w*, 1455*s*, 1314*m*, 1259*w*, 1156*w*, 903*w*, 840*vs*, 740*w*, 557*m*.

HRMS (ESI) *m/z*: $[M]^{2+}$ calcd for $C_{62}H_{70}RuN_6O_4$: 532.22539; found: 532.22467.

Zn[2,6-bis(2-(pyridin-4-yl)furo[2,3-*c*]pyridin-5-yl)pyridine]-PF$_6$ ([L3$_2$Zn](PF$_6$)$_2$)

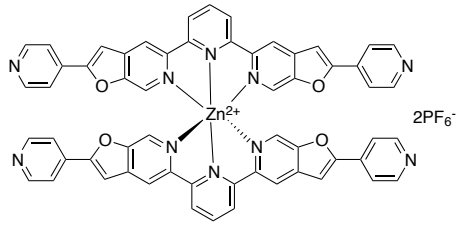

To a solution of ligand **L3** (12.0 mg, 0.0257 mmol, 1.00 eq) in THF (12 mL) a solution of $Zn(OTf)_2$ (4.67 mg, 0.0156 mmol, 0.500 eq) in MeOH (1.1 mL) was added dropwise in 5 minutes at room temperature. The reaction mixture was stirred for 48 h at room temperature. To the mixture saturated aq. KPF_6 was added and the resulting yellow precipitate was filtered over Celite, washed with water, Et_2O, hexane and redissolved with acetonitrile. The solvent was evaporated to give desired Zn complex **[L3$_2$Zn](PF$_6$)$_2$** (15.5 mg, 94%) as a yellow solid. Recrystallization by slow vapor diffusion of Et_2O into an acetonitrile solution of **[L3$_2$Zn](PF$_6$)$_2$** gives yellow block.

Mp >350 °C dec.

^{1}H NMR (500 MHz, CD_3CN, δ) 8.93 (d, *J* = 0.9 Hz, 2H), 8.85-8.83 (m, 2H), 8.80-8.76 (m, 1H), 8.69-8.68 (m, 4H), 8.12 (d, *J* = 0.8 Hz, 2H), 7.73-7.71 (m, 4H), 7.63 (d, *J* = 0.7 Hz, 2H).

^{13}C NMR (125 MHz, CD_3CN, δ): 161.1 (s), 154.0 (s), 151.8 (d), 151.2 (s), 145.2 (d), 143.2 (s), 139.9 (s), 136.0 (s), 133.5 (d), 123.6 (d), 120.5 (d), 117.3 (d), 105.7 (d).

IR (KBr, cm^{-1}): 2921*w*, 1611*m*, 1582*w*, 1599*w*, 1452*m*, 1414*w*, 1384*w*, 1325*m*, 1179*w*, 1046*w*, 835*vs*, 690*w*, 558*s*.

HRMS (ESI) *m/z*: $[M]^{2+}$ calcd for $C_{58}H_{34}N_{10}O_4Zn$: 499.10225; found: 499.10186.

Fe[2,6-bis(2-(pyridin-4-yl)furo[2,3-*c*]pyridin-5-yl)pyridine]-PF_6 ($[L3_2Fe](PF_6)_2$)

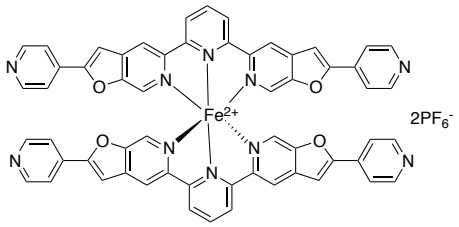

To a suspension of ligand **L3** (100 mg, 0.214 mmol, 1.00 eq) in a mixture of THF (21 mL) and MeCN (2 mL) under N_2 atmosphere a solution of $Fe(BF_4)_2 \cdot 6H_2O$ (36.1 mg, 0.107 mmol, 0.500 eq) in water (9 mL) was added dropwise in 5 minutes at room temperature. The dark purple reaction mixture was stirred for 18 h at room temperature. To the mixture saturated aq. KPF_6 was added and the resulting dark purple precipitate was filtered over Celite, washed with water, Et_2O, hexane and redissolved with acetonitrile. The solvent was evaporated to give a dark purple solid. Recrystallization by slow vapor diffusion of Et_2O into an acetonitrile solution of crude product afforded dark purple blocks of **$[L3_2Fe](PF_6)_2$** that were collected by filtration (0.109 mg, 80%).

Mp >350 °C dec.

^{1}H NMR (500 MHz, CD_3CN, δ): 8.99 (d, *J* = 8.1 Hz, 2H), 8.86 (s, 2H), 8.81 (t, *J* = 8.1 Hz, 1H), 8.64 (d, *J* = 5.8 Hz, 4H), 7.64 (d, *J* = 6.0 Hz, 4H), 7.53 (s, 2H), 7.47 (s, 2H).

^{13}C NMR (125 MHz, CD_3CN, δ): 161.5 (s), 159.8 (s), 153.2 (s), 152.6 (s), 151.7 (d), 139.3 (d), 138.6 (d), 138.1 (s), 135.8 (s), 123.5 (d), 120.3 (d), 117.9 (d), 105.6 (d).

IR (KBr, cm^{-1}): 2923*w*, 1611*m*, 1577*w*, 1455*m*, 1414*w*, 1384*w*, 1321*w*, 1174*w*, 1043*w*, 844*vs*, 690*w*, 558*m*.

HRMS (ESI) *m/z*: $[M]^{2+}$ calcd for $C_{58}H_{34}N_{10}O_4Fe$: 495.10522; found: 495.10475.

Ru[2,6-bis(2-(pyridin-4-yl)furo[2,3-*c*]pyridin-5-yl)pyridine]-PF_6 ($[L3_2Ru](PF_6)_2$)

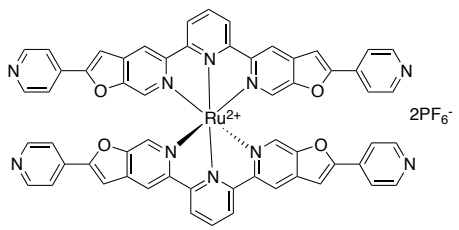

A suspension of ligand **L3** (12.0 mg, 0.0257 mmol, 1.00 eq) and $Ru(DMSO)_4Cl_2$ (6.22 mg, 0.0129 mmol, 0.500 eq) in ethylene glycol (10 ml) was heated to 120 °C for 18 h. The reaction mixture was allowed to cool to room temperature and a saturated aq. KPF_6 solution was added. The resulting red precipitate was filtered over Celite, washed with water, Et_2O, hexane and redissolved with acetonitrile. The solvent was evaporated to give desired Ru

complex **[L3$_2$Ru](PF$_6$)$_2$** (16.7 mg, 98%) as a dark red solid. Recrystallization by slow vapor diffusion of Et_2O into an acetonitrile solution of **[L3$_2$Ru](PF$_6$)$_2$** gives dark red blocks.

Mp >350 °C dec.

^{1}H NMR (400 MHz, CD_3CN, δ): 8.88 (d, *J* = 0.7 Hz, 2H), 8.82 (d, *J* = 8.2 Hz, 2H), 8.68-8.66 (m, 4H), 8.53 (t, *J* = 8.2 Hz, 1H), 7.76 (s, 2H), 7.68-7.67 (m, 4H), 7.57 (d, *J* = 0.7 Hz, 2H).

^{13}C NMR (125 MHz, CD_3CN, δ): 160.1 (s), 156.7 (s), 153.1 (s), 153.0 (s), 151.6 (d), 138.0 (d), 137.2 (s), 137.2 (d), 136.0 (s), 123.5 (d), 120.4 (d), 118.6 (d), 105.8 (d).

IR (KBr, cm^{-1}): 2922*w*, 1609*m*, 1576*w*, 1455*s*, 1414*w*, 1313*w*, 1177*w*, 1042*w*, 990*w*, 845*vs*, 690*w*, 558*w*.

HRMS (ESI) *m/z*: $[M]^{2+}$ calcd for $C_{58}H_{34}N_{10}O_4Ru$: 518.09061; found: 518.09079.

Zn[2-(4-methoxy-2,6-dimethylphenyl)-5-(6-{2-[5′-(4-methoxy-2,6-dimethylphenyl)-2,2′-bipyridin-5-yl]furo[2,3-*c*]pyridin-5-yl}pyridin-2-yl)furo[2,3-*c*]pyridine]$_2$-2PF$_6$ ([L4$_2$Zn](PF$_6$)$_2$)

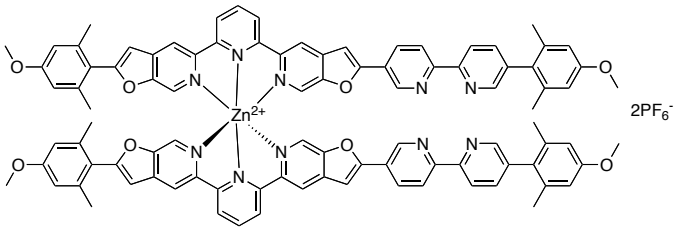

To a solution of ligand **L4** (24.0 mg, 0.0326 mmol, 1.00 eq) in THF (6 mL) a solution of $Zn(OTf)_2$ (5.93 mg, 0.0163 mmol, 0.500 eq) in MeOH (2 mL) was added dropwise in 5 minutes at room temperature. The reaction mixture was stirred for 18 h at room temperature. To the mixture saturated aq. KPF_6 was added and the resulting yellow precipitate was filtered over Celite, washed with water, Et_2O, hexane and redissolved with acetonitrile. The solvent was evaporated to give desired Zn complex **[L4$_2$Zn](PF$_6$)$_2$** (29.3 mg, 98%) as a yellow solid. Recrystallization by slow vapor diffusion of Et_2O into an acetonitrile solution of **[L4$_2$Zn](PF$_6$)$_2$** gives yellow precipitate.

Mp 286–289 °C dec.

^{1}H NMR (400 MHz, CD_2Cl_2, δ): 9.12 (d, *J* = 1.6 Hz, 2H), 8.88 (d, *J* = 0.5 Hz, 2H), 8.85-8.78 (m, 8H), 8.55 (d, *J* = 8.5 Hz, 2H), 8.48 (d, *J* = 8.1 Hz, 2H), 8.43 (d, *J* = 1.4 Hz, 2H), 8.23 (dd, *J* = 8.4, 2.3 Hz, 2H), 8.01 (s, 2H), 7.97 (s, 2H), 7.61 (dd, *J* = 8.1, 2.2 Hz, 2H), 7.45 (d, *J* = 0.5 Hz, 2H), 6.96 (d, *J* = 0.7 Hz, 2H), 6.68 (s, 4H), 6.62 (s, 4H), 3.79 (s, 6H), 3.76 (s, 6H), 2.08 (s, 12H), 2.01 (s, 12H).

^{13}C NMR (100 MHz, CD_2Cl_2, δ): 164.4 (s), 161.4 (s), 161.3 (s), 159.4 (s), 158.3 (s), 153.5 (s), 153.5 (s), 153.3 (s), 150.8 (s), 150.7 (d), 150.6 (s), 147.2 (d), 145.2 (d), 142.3 (s), 141.7 (s),

140.5 (s), 140.1 (s), 140.1 (s), 138.8 (d), 138.1 (s), 137.9 (s), 134.5 (d), 131.7 (d), 131.5 (d), 130.5 (s), 124.1 (s), 122.8 (d), 122.7 (d), 121.4 (d), 121.2 (d), 120.7 (s), 116.4 (d), 116.1 (d), 113.7 (d), 113.3 (d), 107.5 (d), 103.0 (d), 55.6 (q), 55.5 (q), 21.3 (q), 20.9 (q).

IR (film on NaCl, cm^{-1}): 2919*w*, 1603*s*, 1455*vs*, 1321*s*, 1283*w*, 1193*w*, 1155*m*, 1063*w*, 959*w*, 842*vs*, 558*w*.

HRMS (ESI) *m/z*: $[M]^{2+}$ calcd for $C_{94}H_{74}N_{10}O_8Zn$: 767.24858; found: 767.24808.

Fe[2-(4-methoxy-2,6-dimethylphenyl)-5-(6-{2-[5′-(4-methoxy-2,6-dimethylphenyl)-2,2′-bipyridin-5-yl]furo[2,3-*c*]pyridin-5-yl}pyridin-2-yl)furo[2,3-*c*]pyridine]$_2$-2PF$_6$ ([L4$_2$Fe](PF$_6$)$_2$)

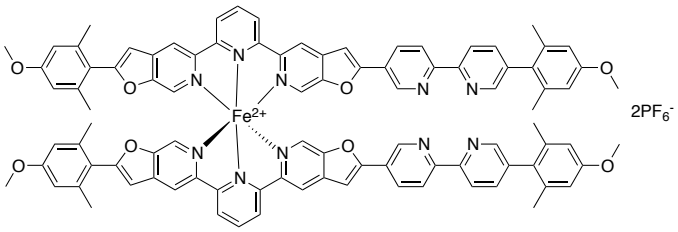

To a solution of ligand **L4** (24.0 mg, 0.0326 mmol, 1.00 eq) in THF (6 mL) a solution of $Fe(BF_4)_2 \cdot 6H_2O$ (5.50 mg, 0.0163 mmol, 0.500 eq) in water (2 mL) was added dropwise in 5 minutes at room temperature. The dark purple reaction mixture was stirred for 48 h at room temperature. To the mixture saturated aq. KPF_6 was added and the resulting dark purple precipitate was filtered over Celite, washed with water, Et_2O, hexane and redissolved with acetonitrile. The solvent was evaporated to give desired Fe complex **[L4$_2$Fe](PF$_6$)$_2$** (28.3 mg, 97%) as a dark purple solid. Recrystallization by slow vapor diffusion of Et_2O into an acetonitrile solution of **[L4$_2$Fe](PF$_6$)$_2$** gives dark purple blocks.

Mp >330 °C dec.

^{1}H NMR (400 MHz, CD_2Cl_2, δ): 9.06 (d, *J* = 1.6 Hz, 2H), 9.01-8.98 (m, 4H), 8.87-8.78 (m, 6H), 8.52 (d, *J* = 8.4 Hz, 2H), 8.45 (d, *J* = 8.1 Hz, 2H), 8.42 (d, *J* = 1.6 Hz, 2H), 8.17 (dd, *J* = 8.4, 2.0 Hz, 2H), 7.60 (dd, *J* = 8.1, 2.0 Hz, 2H), 7.39 (s, 2H), 7.37 (s, 2H), 7.32 (s, 2H), 6.87 (s, 2H), 6.68 (s, 4H), 6.60 (s, 4H), 3.79 (s, 6H), 3.75 (s, 6H), 2.02 (s, 12H), 2.01 (s, 12H).

^{13}C NMR (100 MHz, CD_2Cl_2, δ): 163.3 (s), 161.7 (s), 161.3 (s), 161.2 (s), 161.0 (s), 160.4 (s), 159.4 (s), 158.2 (s), 153.4 (s), 152.9 (s), 152.7 (s), 151.7 (s), 151.0 (s), 150.7 (d), 147.2 (d), 140.5 (s), 139.1 (d), 138.8 (d), 138.4 (s), 138.1 (s), 137.9 (s), 136.6 (d), 136.2 (d), 134.4 (d), 130.5 (s), 123.9 (s), 122.5 (d), 122.5 (d), 121.4 (d), 121.2 (d), 120.4 (s), 117.1 (d), 116.9 (d), 113.7 (d), 113.3 (d), 107.3 (d), 102.8 (d), 55.6 (q), 55.5 (q), 21.3 (q), 20.8 (q).

IR (film on NaCl, cm^{-1}): 2919*w*, 1603*s*, 1455*vs*, 1318*s*, 1281*w*, 1193*w*, 1154*s*, 1063*w*, 841*vs*, 558*w*.

HRMS (ESI) *m/z*: $[M]^{2+}$ calcd for $C_{94}H_{74}N_{10}O_8Fe$: 763.25153; found: 763.25054.

Ru[4-iodo-6′-(2-(4-methoxy-2,6-dimethylphenyl)furo[2,3-*c*]pyridin-5-yl)-2,2′-bipyridin-5-ol]$_2$-2PF$_6$ (83)

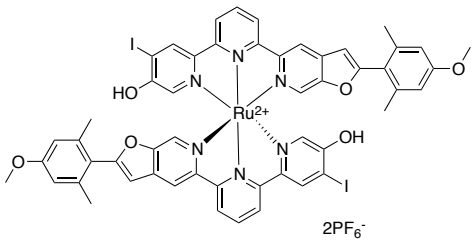

A suspension of 4-iodo-4″-[2-(4-methoxy-2,6-dimethylphenyl)-ethynyl]-5,5″-bis(methoxymethoxy)-2,2′:6′,2″-terpyridine (**79c**) (148 mg, 0.232 mmol, 1.00 eq) and $Ru(DMSO)_4Cl_2$ (56.3 mg, 0.116 mmol, 0.500 eq) in ethanol (44 ml) was heated to reflux for 72 h. The reaction mixture was allowed to cool to room temperature and a saturated aq. KPF_6 solution was added. The resulting red precipitate was filtered over Celite, washed with water, Et_2O, hexane and redissolved with acetonitrile. The solvent was evaporated to give Ru complex **83** (171 mg, crude yield 99%) as a dark red solid that was used without further purification in the subsequent reaction.

Mp >350 °C dec.

^{1}H NMR (500 MHz, CD_3CN, δ): 8.71 (br. s, 1H), 8.68 (br. s, 1H), 8.57-8.47 (m, 2H), 8.29-8.21 (m, 1H), 7.29 (br. s, 1H), 6.92 (s, 1H), 6.68 (br. s, 2H), 6.44 (br. s, 1H), 3.76 (s, 3H), 2.02 (s, 6H).

^{13}C NMR (125 MHz, CD_3CN, δ):162.0 (s), 160.9 (s), 155.4 (s), 154.3 (s), 151.9 (s), 151.4 (s), 140.2 (s), 138.0 (d), 136.4 (s), 135.5 (d), 134.0 (d), 121.8 (d), 120.5 (d), 116.6 (d), 113.2 (d), 106.8 (d), 55.0 (q), 19.7 (q).

IR (film on NaCl, cm^{-1}): 3647*w*, 3584*w*, 3440*br*, 3086*w*, 2922*w*, 2844*w*, 2194*w*, 1604*m*, 1575*w*, 1455*vs*, 1381*w*, 1318*s*, 1193*w*, 1154*m*, 1068*w*, 842*vs*, 738*w*, 623*w*, 558*m*.

HRMS (ESI) *m/z*: $[M-H]^+$ calcd for $C_{52}H_{39}I_2N_6O_6Ru$: 1199.00723; found: 1199.00725.

Ru[2-(4-methoxy-2,6-dimethylphenyl)-5-(6-{2-[5′-(4-methoxy-2,6-dimethylphenyl)-2,2′-bipyridin-5-yl]furo[2,3-*c*]pyridin-5-yl}pyridin-2-yl)furo[2,3-*c*]pyridine]$_2$-2PF$_6$ ([L4$_2$Ru](PF$_6$)$_2$)

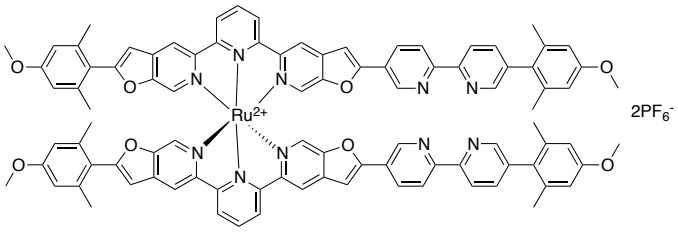

A mixture of a crude complex **83** (130 mg, 0.0873 mmol, 1.00 eq), 5-ethynyl-5′-(4-methoxy-2,6-dimethylphenyl)-2,2′-bipyridine (**77a**) (56.2 mg, 0.179 mmol, 2.05 eq), $PdCl_2(PPh_3)_2$ (3.1 mg, 0.0044 mmol, 5 mol%) and CuI (1.7 mg, 0.0087 mmol, 10 mol%) in degassed DMF/Et_3N (20 mL/12 mL) was heated to 90 °C for 24 h under N_2 atmosphere. The reaction mixture was allowed to cool to room temperature and the solvent was evaporated under reduced pressure. The residue was redissolved in CH_2Cl_2, washed with 10% NH_4OH aqueous solution, water and brine. The organic phase was dried over $MgSO_4$, filtered and evaporated under reduces pressure. The crude residue was purified by silica gel column chromatography with acetonitrile/CH_2Cl_2/H_2O/aq. KPF_6 (140:100:8:3). The first red band was collected and the solvent was evaporated under reduced pressure. The residue was redissolved in CH_2Cl_2 and filtered through a pad of Celite. The filtrate was evaporated under reduced pressure to give desired Ru complex **[L4$_2$Ru](PF$_6$)$_2$** (70 mg, 43% from **79c** over 2 steps) as a dark red solid.

Mp >350 °C dec.

^{1}H NMR (400 MHz, CD_2Cl_2, δ): 9.09 (d, *J* = 1.1 Hz, 2H), 8.85-8.79 (m, 8H), 8.57-8.53 (m, 4H), 8.47 (d, *J* = 8.1 Hz, 2H), 8.43 (s, 2H), 8.19 (dd, *J* = 8.4, 2.1 Hz, 2H), 7.65 (s, 2H), 7.61 (dd, *J* = 8.2, 2.0 Hz, 3H), 7.58 (s, 2H), 7.41 (s, 2H), 6.91 (s, 2H), 6.68 (s, 4H), 6.61 (s, 4H), 3.79 (s, 6H), 3.76 (s, 6H), 2.05 (s, 12H), 2.01 (s, 12H).

^{13}C NMR (100 MHz, CD_2Cl_2, δ): 163.6 (s), 161.4 (s), 160.7 (s), 159.4 (s), 158.2 (s), 156.2 (s), 156.1 (s), 153.5 (s), 152.7 (s), 152.5 (s), 152.1 (s), 151.4 (s), 150.7 (s), 147.1 (d), 140.5 (s), 138.8 (d), 138.1 (s), 137.9 (s), 137.5 (s), 136.9 (d), 136.0 (d), 135.7 (d), 134.4 (d), 130.5 (s), 124.0 (s), 122.7 (d), 122.6 (d), 121.4 (d), 121.2 (d), 120.5 (s), 117.8 (d), 117.5 (d), 113.7 (d), 113.3 (d), 107.4 (d), 102.9 (d), 55.6 (q), 55.5 (q), 21.3 (q), 20.9 (q).

IR (film on NaCl, cm^{-1}): 2920*w*, 1603*s*, 1456*vs*, 1315*s*, 1278*w*, 1192*w*, 1154*s*, 1062*w*, 999*w*, 841*vs*, 557*m*.

HRMS (ESI) *m/z*: $[M]^{2+}$ calcd for $C_{94}H_{74}N_{10}O_8Ru$: 786.23642; found: 786.23519.

Zn[2-(4-methoxy-2,6-dimethylphenyl)-5-(6-{2-[6′-(4-methoxy-2,6-dimethylphenyl)-2,2′-bipyridin-5-yl]furo[2,3-*c*]pyridin-5-yl}pyridin-2-yl)furo[2,3-*c*]pyridine]$_2$-2PF$_6$ ([L5$_2$Zn](PF$_6$)$_2$)

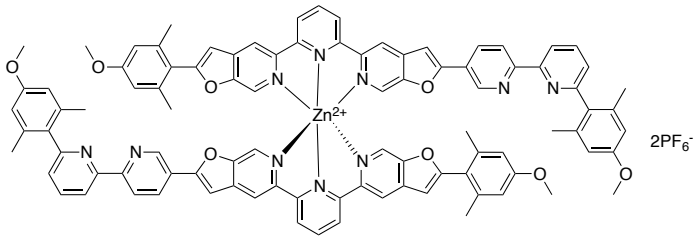

To a solution of ligand **L5** (5.08 mg, 0.00690 mmol, 1.00 eq) in THF (1 mL) a solution of $Zn(OTf)_2$ (1.25 mg, 0.00345 mmol, 0.500 eq) in water (0.4 mL) was added dropwise in 1 minutes at room temperature. The reaction mixture was stirred for 6 h at room temperature. To the mixture saturated aq. KPF_6 was added and the resulting yellow precipitate was filtered over Celite, washed with water, Et_2O, hexane and redissolved with acetonitrile. The solvent was evaporated to give desired Zn complex **[L5$_2$Zn](PF$_6$)$_2$** (6.23 mg, 99%) as a yellow solid. Recrystallization by slow vapor diffusion of Et_2O into an acetonitrile solution of **[L5$_2$Zn](PF$_6$)$_2$** gives yellow precipitate.

Mp 270–272 °C dec.

^{1}H NMR (400 MHz, CD_2Cl_2, δ): 9.11 (s, 2H), 8.84-8.79 (m, 10H), 8.49 (d, *J* = 8.6 Hz, 2H), 8.37 (d, *J* = 7.5 Hz, 2H), 8.15 (dd, *J* = 8.4, 2.2 Hz, 2H), 7.98 (s, 2H), 7.95 (s, 2H), 7.87 (t, *J* = 7.8 Hz, 3H), 7.42 (s, 2H), 7.26 (dd, *J* = 7.7, 0.6 Hz, 2H), 6.95 (s, 2H), 6.66 (s, 4H), 6.62 (s, 4H), 3.80 (s, 6H), 3.76 (s, 5H), 2.08 (s, 12H), 2.04 (s, 12H).

^{13}C NMR (125 MHz, CD_2Cl_2, δ): 164.3 (s), 161.4 (s), 161.2 (s), 159.6 (s), 159.3 (s), 158.4 (s), 154.9 (s), 153.4 (s), 153.2 (s), 150.7 (s), 150.5 (s), 147.0 (d), 145.1 (d), 142.1 (s), 141.6 (s), 140.4 (s), 140.0 (s), 140.0 (s), 137.8 (s), 137.6 (d), 134.3 (d), 133.6 (s), 131.6 (d), 131.4 (d), 126.3 (d), 124.1 (s), 122.7 (d), 122.6 (d), 121.4 (d), 120.6 (s), 119.5 (d), 116.3 (d), 116.0 (d), 113.6 (d), 113.2 (d), 107.4 (d), 102.8 (d), 55.5 (q), 55.5 (q), 20.8 (q), 20.7 (q).

IR (film on NaCl, cm^{-1}): 2921*w*, 1603*s*, 1582*m*, 1454*vs*, 1322*s*, 1284*w*, 1193*w*, 1155*m*, 1070*w*, 841*vs*, 558*w*.

HRMS (ESI) *m/z*: $[M]^{2+}$ calcd for $C_{94}H_{74}N_{10}O_8Zn$: 767.24858; found: 767.24783.

Fe[2-(4-methoxy-2,6-dimethylphenyl)-5-(6-{2-[6′-(4-methoxy-2,6-dimethylphenyl)-2,2′-bipyridin-5-yl]furo[2,3-*c*]pyridin-5-yl}pyridin-2-yl)furo[2,3-*c*]pyridine]$_2$-2PF$_6$ ([L5$_2$Fe](PF$_6$)$_2$)

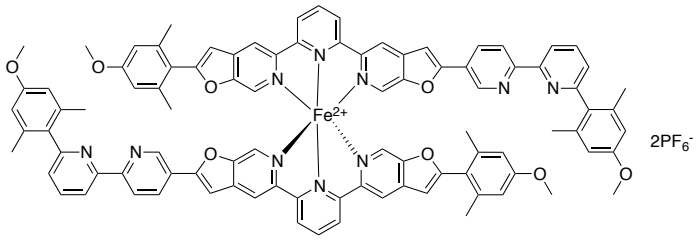

To a solution of ligand **L5** (5.18 mg, 0.00704 mmol, 1.00 eq) in THF (3 mL) a solution of $Fe(BF_4)_2 \cdot 6H_2O$ (1.88 mg, 0.00352 mmol, 0.500 eq) in water (0.4 mL) was added dropwise in 1 minutes at room temperature. The dark purple reaction mixture was stirred for 6 h at room temperature. To the mixture saturated aq. KPF_6 was added and the resulting dark purple precipitate was filtered over Celite, washed with water, Et_2O, hexane and redissolved with acetonitrile. The solvent was evaporated to give desired Fe complex **[L5$_2$Fe](PF$_6$)$_2$** (5.11 mg, 80%) as a dark purple solid. Recrystallization by slow vapor diffusion of Et_2O into an acetonitrile solution of **[L5$_2$Fe](PF$_6$)$_2$** gives dark purple precipitate.

Mp >320 °C dec.

^{1}H NMR (500 MHz, CD_2Cl_2, δ): 9.05 (s, 2H), 8.99-8.92 (m, 4H), 8.85-8.74 (m, 6H), 8.47 (d, *J* = 7.6 Hz, 2H), 8.36 (d, *J* = 7.7 Hz, 2H), 8.10 (d, *J* = 7.5 Hz, 2H), 7.87 (t, *J* = 7.5 Hz, 2H), 7.35 (s, 2H), 7.33 (s, 2H), 7.30 (s, 2H), 7.25 (d, *J* = 7.6 Hz, 2H), 6.86 (s, 2H), 6.66 (s, 4H), 6.59 (s, 4H), 3.80 (s, 6H), 3.75 (s, 6H), 2.03 (s, 12H), 2.01 (s, 12H).

^{13}C NMR (125 MHz, CD_2Cl_2, δ): 163.2 (s), 161.3 (s), 161.1 (s), 160.9 (s), 160.3 (s), 159.6 (s), 159.3 (s), 158.4 (s), 154.9 (s), 152.8 (s), 152.6 (s), 151.5 (s), 150.9 (s), 147.0 (d), 140.4 (s), 139.0 (d), 138.2 (s), 137.8 (s), 137.6 (d), 136.5 (d), 136.1 (d), 134.2 (d), 133.6 (s), 126.3 (d), 123.9 (s), 122.4 (d), 122.4 (d), 121.4 (d), 120.3 (s), 119.5 (d), 117.0 (d), 116.8 (d), 113.6 (d), 113.2 (d), 107.2 (d), 102.7 (d), 55.5 (q), 55.5 (q), 20.8 (q), 20.7 (q).

IR (film on NaCl, cm^{-1}): 2921*w*, 1604*s*, 1455*vs*, 1318*s*, 1282*w*, 1193*w*, 1155*m*, 1070*w*, 841*vs*, 558*w*.

HRMS (ESI) *m/z*: $[M]^{2+}$ calcd for $C_{94}H_{74}FeN_{10}O_8$: 763.25153; found: 763.25106.

Ru[2-(4-methoxy-2,6-dimethylphenyl)-5-(6-{2-[6′-(4-methoxy-2,6-dimethylphenyl)-2,2′-bipyridin-5-yl]furo[2,3-*c*]pyridin-5-yl}pyridin-2-yl)furo[2,3-*c*]pyridine]$_2$-2PF$_6$ ([L5$_2$Ru](PF$_6$)$_2$)

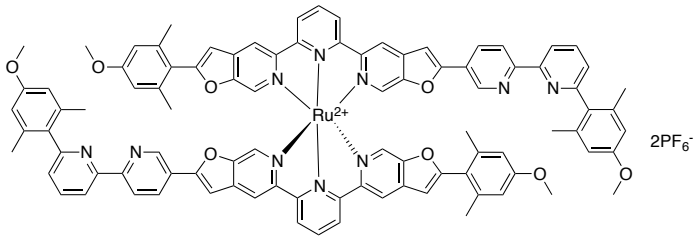

A mixture of a crude complex **83** (15.7 mg, 0.0105 mmol, 1.00 eq), 5-ethynyl-6′-(4-methoxy-2,6-dimethylphenyl)-2,2′-bipyridine (**77b**) (6.79 mg, 0.0216 mmol, 2.05 eq), $PdCl_2(PPh_3)_2$ (0.37 mg, 0.00053 mmol, 5 mol%) and CuI (0.20 mg, 0.0011 mmol, 10 mol%) in degassed DMF/Et_3N (2 mL/2 mL) was heated to 90 °C for 39 h under N_2 atmosphere. The reaction mixture was allowed to cool to room temperature and the solvent was evaporated under reduced pressure. The residue was redissolved in CH_2Cl_2, washed with 10% NH_4OH aqueous solution, water and brine. The organic phase was dried over $MgSO_4$, filtered and evaporated under reduces pressure. The crude residue was purified by silica gel column chromatography with acetonitrile/CH_2Cl_2/H_2O/aq. KPF_6 (140:100:8:3). The first red band was collected and the solvent was evaporated under reduced pressure. The residue was redissolved in CH_2Cl_2 and filtered through a pad of Celite. The filtrate was evaporated under reduced pressure to give desired Ru complex **[L5$_2$Ru](PF$_6$)$_2$** (7.8 mg, 40% from **79c** over 2 steps) as a dark red solid.

Mp >350 °C dec.

^{1}H NMR (400 MHz, CD_2Cl_2, δ): 9.07 (s, 2H), 8.81-8.74 (m, 8H), 8.53-8.44 (m, 4H), 8.36 (d, *J* = 7.5 Hz, 2H), 8.10 (d, *J* = 7.3 Hz, 2H), 7.86 (t, *J* = 7.8 Hz, 2H), 7.63 (s, 2H), 7.57 (s, 2H), 7.38 (s, 2H), 7.25 (d, *J* = 7.5 Hz, 2H), 6.91 (s, 2H), 6.67 (s, 4H), 6.60 (s, 4H), 3.81 (s, 6H), 3.75 (s, 6H), 2.04 (s, 12H), 2.03 (s, 12H).

^{13}C NMR (125 MHz, CD_2Cl_2, δ): 163.5 (s), 161.2 (s), 160.5 (s), 159.5 (s), 159.4 (s), 158.1 (s), 156.1 (s), 155.9 (s), 154.7 (s), 152.6 (s), 152.4 (s), 152.0 (s), 151.3 (s), 147.0 (d), 140.4 (s), 137.8 (d), 137.4 (s), 137.3 (s), 136.8 (d), 135.9 (d), 135.6 (d), 134.2 (d), 133.4 (s), 126.4 (d), 124.0 (s), 122.6 (d), 122.5 (d), 121.4 (d), 120.4 (s), 119.6 (d), 117.7 (d), 117.5 (d), 113.6 (d), 113.2 (d), 107.3 (d), 103.0 (d), 55.5 (q), 55.5 (q), 20.8 (q), 20.7 (q).

IR (film on NaCl, cm^{-1}): 2921*w*, 1604*s*, 1455*vs*, 1313*m*, 1291*w*, 1193*w*, 1156*m*, 1070*w*, 842*vs*, 558*w*.

HRMS (ESI) *m/z*: $[M]^{2+}$ calcd for $C_{94}H_{74}N_{10}O_8Ru$: 786.23642; found: 786.23652.

Zn[2,6-bis{2-[5′-(4-methoxy-2,6-dimethylphenyl)-2,2′-bipyridin-5-yl]furo[2,3-*c*]pyridin-5-yl}pyridine]-2PF$_6$ ([L6$_2$Zn](PF$_6$)$_2$)

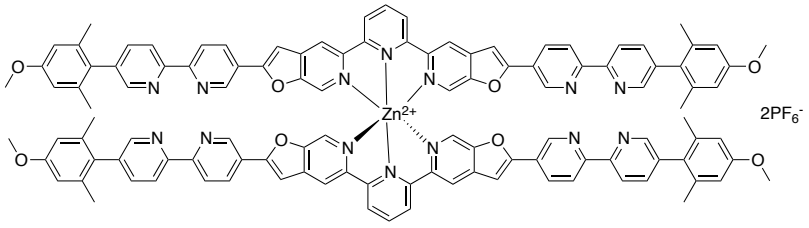

To a solution of ligand **L6** (15.2 mg, 0.0171 mmol, 1.00 eq) in THF (12 mL) a solution of $Zn(OTf)_2$ (3.10 mg, 0.00854 mmol, 0.500 eq) in water (1.4 mL) was added dropwise in 5 minutes at room temperature. The reaction mixture was stirred for 18 h at room temperature. To the mixture saturated aq. KPF_6 was added and the resulting yellow precipitate was filtered over Celite, washed with water, Et_2O, hexane and redissolved with acetonitrile. The solvent was evaporated to give desired Zn complex **[L6$_2$Ru](PF$_6$)$_2$** (16.8 mg, 92%) as a yellow solid. Recrystallization by slow vapor diffusion of Et_2O into an acetonitrile solution of **[L6$_2$Ru](PF$_6$)$_2$** gives yellow precipitate.

Mp >350 °C dec.

^{1}H NMR (400 MHz, CD_2Cl_2, δ): 9.13 (s, 2H), 8.91-8.84 (m, 5H), 8.57 (d, *J* = 8.5 Hz, 2H), 8.48 (d, *J* = 7.7 Hz, 2H), 8.43 (s, 2H), 8.23 (d, *J* = 8.5 Hz, 2H), 8.05 (s, 2H), 7.62 (d, *J* = 7.7 Hz, 2H), 7.45 (s, 2H), 6.68 (s, 4H), 3.79 (s, 6H), 2.01 (s, 12H).

^{13}C NMR (125 MHz, CD_2Cl_2, δ): 161.5 (s), 159.3 (s), 158.2 (s), 153.5 (s), 153.4 (s), 150.6 (d), 150.6 (s), 147.1 (d), 145.2 (d), 142.2 (s), 140.1 (s), 138.8 (d), 138.0 (s), 137.9 (s), 134.4 (d), 131.8 (d), 130.4 (s), 124.0 (s), 122.9 (d), 121.3 (d), 121.1 (d), 116.4 (d), 113.2 (d), 102.9 (d), 55.4 (q), 21.3 (q).

IR (film on NaCl, cm^{-1}): 2909*w*, 2841*w*, 1602*m*, 1454*s*, 1430*w*, 1322*m*, 1276*w*, 1192*w*, 1155*m*, 1062*w*, 1012*w*, 959*w*, 842*vs*, 747*w*, 558*m*.

HRMS (ESI) *m/z*: $[M]^{2+}$ calcd for $C_{114}H_{86}ZnN_{14}O_8$: 921.30168; found: 921.30007.

Fe[2,6-bis{2-[5′-(4-methoxy-2,6-dimethylphenyl)-2,2′-bipyridin-5-yl]furo[2,3-*c*]pyridin-5-yl}pyridine]-2PF$_6$ ([L6$_2$Fe](PF$_6$)$_2$)

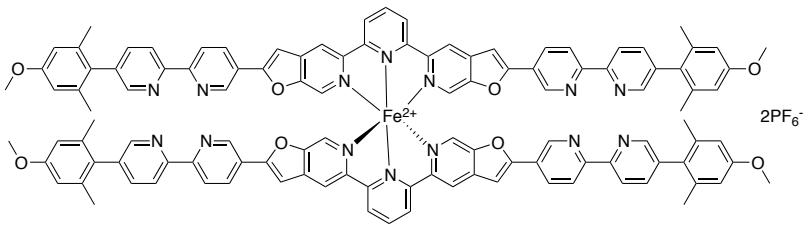

To a solution of ligand **L6** (15.0 mg, 0.0169 mmol, 1.00 eq) in THF (15 mL) a solution of $Fe(BF_4)_2{\cdot}6H_2O$ (2.84 mg, 0.00842 mmol, 0.500 eq) in water (1.1 mL) was added dropwise in

5 minutes at room temperature. The dark purple reaction mixture was stirred for 6 h at room temperature. To the mixture saturated aq. KPF_6 was added and the resulting dark purple precipitate was filtered over Celite, washed with water, Et_2O, hexane and redissolved with acetonitrile. The solvent was evaporated to give desired Fe complex **$[L6_2Fe](PF_6)_2$** (14.4 mg, 80%) as a dark purple solid. Recrystallization by slow vapor diffusion of Et_2O into an acetonitrile solution of **$[L6_2Fe](PF_6)_2$** gives dark purple precipitate.

Mp >350 °C dec.

^{1}H NMR (400 MHz, CD_2Cl_2, δ): 9.08-9.03 (m, 4H), 8.90 (t, *J* = 7.8 Hz, 1H), 8.86 (s, 2H), 8.52 (d, *J* = 8.5 Hz, 2H), 8.45 (d, *J* = 8.1 Hz, 2H), 8.41 (s, 2H), 8.17 (d, *J* = 8.5 Hz, 2H), 7.60 (d, *J* = 8.1 Hz, 2H), 7.43 (s, 2H), 7.36 (s, 2H), 6.67 (s, 4H), 3.79 (s, 6H), 2.00 (s, 12H).

^{13}C NMR (100 MHz, CD_2Cl_2, δ): 161.0 (s), 160.5 (s), 159.4 (s), 158.2 (s), 153.4 (s), 152.9 (s), 151.6 (s), 150.7 (d), 147.2 (d), 139.2 (s), 138.8 (s), 138.4 (d), 138.1 (s), 137.9 (s), 136.7 (d), 134.4 (d), 130.5 (s), 123.9 (s), 122.8 (d), 121.4 (d), 121.2 (d), 117.2 (d), 113.3 (d), 102.8 (d), 55.5 (q), 21.3 (q).

IR (film on NaCl, cm^{-1}): 2914*w*, 2841*w*, 1601*m*, 1456*s*, 1318*m*, 1276*w*, 1192*w*, 1155*m*, 1062*w*, 1012*w*, 840*vs*, 749*w*, 558*m*.

HRMS (ESI) *m/z*: $[M]^{2+}$ calcd for $C_{114}H_{86}FeN_{14}O_8$: 917.80621; found: 917.80624.

Ru[5,5′′-dihydroxy-4,4′′-diiodo-2,2′:6′,2′′-terpyridine]-2PF_6 (82)

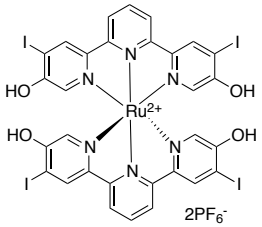

A suspension of diiodoterpyridine **69** (333 mg, 0.550 mmol, 1.00 eq) and $Ru(DMSO)_4Cl_2$ (133 mg, 0.275 mmol, 0.500 eq) in ethylene glycol (60 ml) was heated to 120 °C for 48 h. To the hot reaction mixture a saturated aq. KPF_6 solution was added till the first precipitate forms. The mixture was allowed to cool to room temperature. After dilution with water, the resulting orange precipitate was collected by filtration, washed with water, Et_2O, ethanol and CH_2Cl_2. Drying under high vacuum resulted in desired Ru complex **82** (319 mg, crude yield 89%) as an orange solid, that is insoluble in water and common organic solvents and was used without further purification in the subsequent reaction.

Mp >350 °C dec.

IR (KBr, cm^{-1}): 3407*br*, 3077*m*, 2927*m*, 1573*m*, 1551*m*, 1509*m*, 1449*vs*, 1378*m*, 1299*s*, 1228*w*, 1170*w*, 1053*w*, 846*s*, 689*w*, 614*w*, 561*m*.

HRMS (ESI) *m/z*: $[M]^{2+}$ calcd for $C_{30}H_{18}I_4N_6O_4Ru$ calcd for: 568.8379; found: 567.82914.

Ru[2,6-bis{2-[5′-(4-methoxy-2,6-dimethylphenyl)-2,2′-bipyridin-5-yl]furo[2,3-*c*]pyridin-5-yl}pyridine]-2PF$_6$ ([L6$_2$Ru](PF$_6$)$_2$)

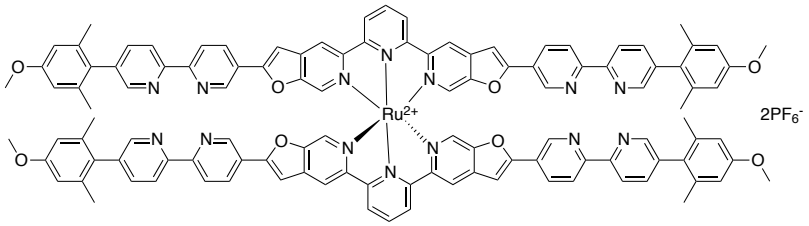

A mixture of crude **82** (40.0 mg, 0.0308 mmol, 1.00 eq), 5-ethynyl-5′-(4-methoxy-2,6-dimethylphenyl)-2,2′-bipyridine (**77a**) (40.7 mg, 0.129 mmol, 4.20 eq), $PdCl_2(PPh_3)_2$ (2.2 mg, 0.0031 mmol, 10 mol%) and CuI (1.2 mg, 0.0062 mmol, 20 mol%) in degassed DMF/DIPEA (7 mL/7 mL) was heated to 80 °C for 48 h under N_2 atmosphere. The reaction mixture was allowed to cool to room temperature and the solvent was evaporated under reduced pressure. The residue was treated with EtOAc, collected by filtration and purified by silica gel column chromatography with acetonitrile/CH_2Cl_2/H_2O/aq. KPF_6 (140:100:8:3). The first red band was collected and the solvent was evaporated under reduced pressure. The residue was redissolved in CH_2Cl_2 and filtered through a pad of Celite. The filtrate was evaporated under reduced pressure to give desired complex **[L6$_2$Ru](PF$_6$)$_2$** (36 mg, 48% from **69** over 2 steps) as a dark red solid.

Mp >350 °C dec.

^{1}H NMR (500 MHz, CD_2Cl_2, δ): 9.08 (d, *J* = 2.1 Hz, 2H), 8.94 (s, 2H), 8.93 (d, *J* = 9.8 Hz, 2H), 8.62 (t, *J* = 8.1 Hz, 1H), 8.53 (d, *J* = 8.5 Hz, 2H), 8.45 (d, *J* = 8.2 Hz, 2H), 8.41 (d, *J* = 1.7 Hz, 2H), 8.18 (dd, *J* = 8.4, 2.2 Hz, 2H), 7.69 (s, 2H), 7.61 (dd, *J* = 8.1, 2.1 Hz, 2H), 7.43 (s, 2H), 6.67 (s, 4H), 3.78 (s, 6H), 2.00 (s, 12H).

^{13}C NMR (125 MHz, CD_2Cl_2, δ): 160.8 (s), 159.4 (s), 158.2 (s), 156.0 (s), 153.4 (s), 152.7 (s), 152.0 (s), 150.7 (d), 147.1 (d), 138.8 (d), 138.1 (s), 137.9 (s), 137.5 (s), 137.1 (d), 136.0 (d), 134.4 (d), 130.5 (s), 123.9 (s), 122.9 (d), 121.4 (d), 121.2 (d), 117.9 (d), 113.3 (d), 102.9 (d), 55.5 (q), 21.3 (q).

IR (film on NaCl, cm^{-1}): 2920*w*, 2836*w*, 1600*m*, 1454*vs*, 1383*w*, 1315*m*, 1276*w*, 1192*w*, 1155*m*, 1061*w*, 1011*w*, 999*w*, 841*vs*, 558*m*.

HRMS (ESI) *m/z*: $[M]^{2+}$ calcd for $C_{114}H_{86}N_{14}O_8Ru$: 940.28954; found: 940.28944.

Ru[2-(4-methoxy-2,6-dimethylphenyl)-5-(6-{2-[5′-(4-methoxy-2,6-dimethylphenyl)-2,2′-bipyridin-5-yl]furo[2,3-*c*]pyridin-5-yl}pyridin-2-yl)furo[2,3-*c*]pyridine]$_2$-(Δ-TRISPHAT)$_2$ ([L4$_2$Ru](Δ-TRISPHAT)$_2$)

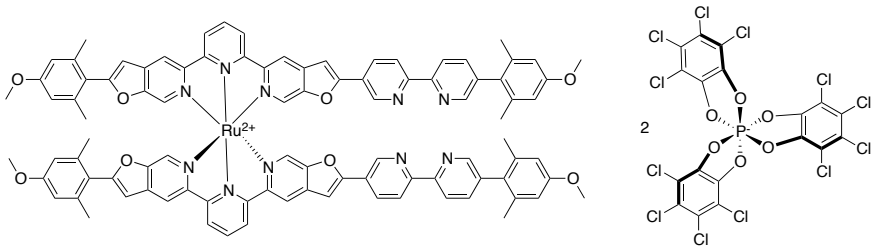

To a solution of **[L4$_2$Ru](PF$_6$)$_2$** (6.3 mg, 1.0 eq, 0.0034 mmol) in CH_2Cl_2 (0.5 mL) a solution of [cinhonidinium](Δ-TRISPHAT) (7.6 mg, 2.1 eq, 0.0071) in acetone (1.1 mL) was added. The mixture was stirred for 10 min. at room temperature. The resulting red suspension was evaporated, dissolved in minimum amount of CH_2Cl_2 applied on the Al_2O_3 column (deactivated with 5wt % H_2O) and eluted with eluent gradient (CH_2Cl_2:MeOH 999:1 to 99:1). The collected red bands were evaporated under reduced pressure to give desired diastereomeric mixture **[L4$_2$Ru](Δ-TRISPHAT)$_2$** (8.5 mg, 81%) as a red solid.

Mp >300 °C dec.

^{1}H NMR (500 MHz, CD_2Cl_2, δ): 9.05 (d, *J* = 2.1 Hz, 2H), 9.03 (d, *J* = 2.2 Hz, 2H), 8.79 (s, 2H), 8.71 (d, *J* = 8.3 Hz, 2H), 8.71 (s, 2H), 8.69 (s, 4H), 8.66 (d, *J* = 8.3 Hz, 2H), 8.61 (d, *J* = 8.0 Hz, 2H), 8.58 (d, *J* = 8.0 Hz, 2H), 8.55 (dd, *J* = 1.5, 8.5 Hz, 4H), 8.47 (dd, *J* = 2.7, 8.1 Hz, 4H), 8.44 (s, 4H), 8.44-8.40 (m, 4H), 8.14 (dd, *J* = 2.5, 8.5 Hz, 2H), 8.12 (dd, *J* = 2.3, 8.4 Hz, 2H), 7.66-7.60 (m, 12H), 7.24 (s, 2H), 7.14 (s, 2H), 6.89 (s, 2H), 6.85 (s, 2H), 6.69 (s, 8H), 6.62 (s, 4H), 6.61 (s, 4H), 3.80 (s, 12H), 3.77 (s, 12H), 2.03 (s, 12H), 2.03 (s, 24H), 2.02 (s, 12H).

^{13}C NMR (125 MHz, CD_2Cl_2, δ): 161.6, 161.1, 161.0, 159.6, 158.5, 157.5, 157.4, 156.3, 156.2, 156.2, 153.5, 152.7, 152.5, 152.0, 151.3, 150.9, 147.2, 142.4, 142.3, 140.6, 139.0, 138.3, 138.1, 137.6, 137.5, 137.0, 136.9, 135.9, 134.6, 130.6, 123.7, 123.2, 122.7, 122.6, 122.5, 122.3, 122.2, 121.6, 121.3, 120.3, 118.0, 117.8, 117.6, 117.5, 114.6, 114.5, 113.9, 113.4, 107.5, 104.0, 102.8, 102.7, 55.8, 55.7, 21.5, 21.1, 21.0.

IR (film on NaCl, cm^{-1}): 2961*m*, 2921*m*, 2852*m*, 1599*m*, 1454*vs*, 1390*m*, 1314*m*, 1263*w*, 1237*w*, 1193*w*, 1155*w*, 1009*w*, 992*s*, 833*m*, 818*m*, 719*w*, 674*m*, 622*w*.

HRMS (ESI) *m/z*: $[M]^{2+}$ calcd for $C_{94}H_{74}N_{10}O_8Ru$: 786.2375; found: 786.2363; $[M+(\Delta\text{-TRISPHAT})+H]^{2+}$ calcd for $C_{112}H_{75}Cl_{12}N_{10}O_{14}PRu$: 1168.0250; found: 1168.0241.

2.9. References

(1) (a) Stang, P. J. *Chem. Eur. J.* **1998**, *4*, 19–27. (b) Leininger, S.; Olenyuk, B.; Stang, P. J. *Chem. Rev.* **2000**, *100*, 853−908. (c) Chakrabarty, R.; Mukherjee, P. S.; Stang, P. J. *Chem. Rev*. **2011**, *111*, 6810–6918.

(2) (a) Fujita, M.; Kwon, Y. J.; Washizu, S.; Ogura, K. *J. Am. Chem. Soc*. **1994***, 116,* 1151–1152. (b) Fujita, M.; Tominaga, M.; Hori, A.; Therrien, B. *Acc. Chem. Res*. **2005**, *38*, 371–380.

(3) (a) Lehn, J.-M. *Angew. Chem. Int. Ed. Engl.* **1988**, *27*, 89–112. (b) F. Vögtle, *Supramolecular Chemistry*, Wiley, Chichester, **1991**. (c) Lehn, J.-M. *Supramolecular Chemistry-Concepts and Perspectives*, VHC, Weinheim*,* **1995**. (d) Safont-Sempere, M. M.; Fernàndez, G.; Würthner, F. *Chem. Rev*. **2011**, *111*, 5784–5814.

(4) (a) Morgan, S. G.; Burstall, F. H. *J. Chem. Soc.* **1931**, 20–30. (b) Morgan, S. G.; Burstall, F. H. *J. Chem. Soc.* **1937**, 1649–1655. (b) Hofmeier, H.; Schubert, U. S. *Chem. Soc. Rev.* **2004**, *33*, 373–399. (c) Schubert, U. S.; Hofmeier, H.; Newkome, G. R. *Modern Terpyridine Chemistry*, Wiley-VCH, Weinheim, **2006**.

(5) (a) Sauvage, J.-P.; Ward, M. *Inorg. Chem.* **1991**, *30*, 3869–3874. (b) Benaglia, M.; Ponzini, F.; Woods, C. R.; Siegel, J. S. *Org. Lett*. **2001**, *3*, 967–969. (c) Constable, E. C. *Chem. Soc. Rev.* **2007**, *36*, 246–253. (d) Coronado, E.; Galan-Mascaros, J. R.; Gaviña, P.; Mart-Gastal-do, C.; Romero, F. M.; Tatay, S. *Inorg. Chem.* **2008**, *47*, 5197–5203.

(6) (a) Norsten, T. B.; Frankamp, B. L.; Rotello, V. M. *Nano Lett*. **2002**, *12*, 1345–1348. (b) Dong, T.-Y.; Hunag, C.-L.; Chen, C.-P.; Lin, M.-C. *J. Organomet. Chem*. **2007**, *692*, 5147–5155. (c) Winter, A.; Hager, M. D.; Newkome, G. R.; Schubert, U. S. *Adv. Mater.* **2011**, *23*, 5728–5748.

(7) (a) O'Regan, B.; Grätzel, M. *Nature* **1991**, *353*, 737–740. (b) Ardo, S.; Meyer, G. J. *Chem. Soc. Rev*. **2009**, *38*, 115–164.

(8) Winter, A.; Newkome, G. R.; Schubert, U. S. *ChemCatChem* **2011**, *3*, 1384–1406.

(9) (a) Lowe, G.; Droz, A. S.; Park, J. J.; Weaver, G. W. *Bioorg. Chem.* **1999**, *27*, 477–486. (b) Becker, K.; Herold-Mende, C.; Park, J. J.; Lowe, G.; Schirmer, R. H. *J. Med. Chem.* **2001**, *44*, 2784–2792. (c) Dobroschke, M.; Geldmacher, Y.; Ott, I.; Harlos, M.; Kater, L.; Wagner, L.; Gust, R.; Sheldrick, W. S.; Prokop, A. *ChemMedChem* **2009**, *4*, 177–187. (d) Jeong, B.-S.; Choi, H.; Kwak, Y.-S.; Lee, E.-S. *Bull. Korean Chem. Soc.* **2011**, *32*, 3566–3570.

(10) (a) Jain, A.; Winkel, B. S. J.; Brewer, K. J. *J. Inorg. Biochem.* **2007**, *101*, 1525–1528. (b) Anthonysamy, A.; Balasubramanian, S.; Shanmugaiah, V.; Mathivanan, N. *Dalton Trans*. **2008**, 2136–2143.

(11) (a) Fallahpour, R.-A. *Synthesis* **2003**, 155–184. (c) Heller, M.; Schubert, U. S. *Eur. J. Org. Chem.* **2003**, 947–961. (b) Gavina, P.; Tatay, S. *Tetrahedron Lett.* **2006**, *47*, 3471–3473.

(12) (a) Hoskins, B. F.; Robson, R. *J. Am. Chem. Soc.* **1990***, 112*, 1546–1554. (b) Férey, G. *Chem. Soc. Rev.* **2008***, 37*, 191–214. (c) Farha, O. K.; Hupp, J. T. *Acc. Chem. Res.* **2010**, *43*, 1166–1175. (d) Juan-Alcaniz, J.; Gascon, J.; Kapteijn, F. *J. Mater. Chem*. **2012**, *22*, 10102–10118.

(13) (a) Li, H.; Eddaoudi, M.; O'Keeffe, M.; Yaghi, O. M. *Nature* **1999***, 402*, 276–279. (b) Perry, J. J.; Perman, J. A.; Zaworotko, M. J. *Chem. Soc. Rev.* **2009***, 38*, 1400–1417.

(14) For the first synthesis of 2,2′-bipyridine and reviews, see: (a) Blau, F. *Monatsh. Chem*. **1889**, *10*, 375–388. (b) Kaes, C.; Katz, A.; Hosseini, M. W. *Chem. Rev.* **2000**, *100*, 3553–3590. (c) Balzani, V.; Bergamini, G.; Marchioni, F.; Ceroni, P. *Coord. Chem. Rev.* **2006**, *250*, 1254–1266.

For the examples of 5,5′-functionalized 2,2′-bipyridines, see: (d) Khatyr, A.; Ziessel, R. *J. Org. Chem*. **2000**, *65*, 7814–7824. (e) Matthews, C. J.; Elsegood, M. R. J.; Bernardinelli, G.; Clegg, W.; Williams, A. F. *Dalton Trans.* **2004**, 492–497.

(15) The term "linear bilateral extended 2,2′:6′,2″-terpyridine" was chosen to describe *terpy* based scaffold represented in Fig. 1., example c., because it mimics the linear or extended geometry of 5,5′-disubstituted 2,2′-bipyridine and has "two-sided" or *bilateral* character. For definition of "bilateral," see: *The Oxford English Dictionary. 7th ed.* OUP, Oxford, **2005**.

(16) Loren, J. C.; Yoshizawa, M.; Haldimann, R. F.; Linden, A.; Siegel, J. S. *Angew. Chem. Int. Ed.* **2003**, *42*, 5702–5705.

(17) Constable, E. C. *Chem. Commun*. **1997**, 1073–1080.

(18) Bassani, D. M.; Lehn, J.-M.; Fromm, K.; Fenske, D. *Angew. Chem. Int. Ed.* **1998**, *37*, 2364–2367.

(19) (a) Armaroli, N.; Balzani, V.; Collin, J.-P.; Gaviña, P.; Sauvage, J.-P.; Ventura, B. *J. Am. Chem. Soc.* **1999**, *121,* 4397–4408. (b) Collin, J.-P.; Dietrich-Buchecker, C.; Gaviña, P.; Jimenez-Molero, M. C.; Sauvage, J.-P. *Acc. Chem. Res*. **2001**, *34*, 477–487. (c) Durot, S.; Reviriego, F.; Sauvage, J.-P. *Dalton Trans*. **2010**, *39*, 10557–10570.

(20) Siegel, J. S. *Nature* **2012**, *486*, 327–328.

(21) (a) Yasui, Y.; Frantz, D. K.; Siegel, J. S. *Org. Lett*. **2006**, *8*, 4989–4992. (b) Frantz, D. K.; Sullivan, A. A.; Yasui, Y.; Linden, A.; Baldridge, K. K.; Siegel, J. S. *Org. Biomol. Chem*. **2009**, *7*, 2347–2352. (c) Frantz, D. K.; Linden, A.; Baldridge, K. K.; Siegel, J. S. *J. Am. Chem. Soc*. **2012**, *134*, 1528−1535.

(22) Sonogashira, K.; Tohda, Y.; Hagihara, N. *Tetrahedron Lett.* **1975**, *50*, 4467–4470.

(23) (a) Gilman, H.; Bebb, R. L. *J. Am. Chem. Soc*. **1939**, *61*, 109. (b) Wittig, G.; Fuhrman, G. *Chem. Ber*. **1940**, *73*, 1197. (c) Snieckus, V. *Chem. Rev*. **1990**, *90*, 879–933.

(24) Stille, J. K. *Angew. Chem. Int. Ed. Engl.* **1986**, *25*, 508–524.

(25) Parham, W. E.; Piccirilli, R. M. *J. Org. Chem*. **1977**, *42*, 257–260.

(26) Lehmann, U.; Henze, O.; Schlüter, A. D. *Chem. Eur. J.* **1999**, *5*, 854–859.

(27) Schubert, U. S.; Eschbaumer. *Org. Lett*. **1999**, *1*, 1027–1029.

(28) (a) Yamamoto, Y.; Yanagi, A. *Chem. Pharm. Bull.* **1982**, *30*, 1731–1737. (b) Silbestri, G. F.; Lo Fiego, M. J.; Lockhart, M. T.; Chopa, A. B. *J. Organomet. Chem.* **2010**, *695*, 2578–2585.

(29) Voisin, A. S.; Bouillon, A.; Lancelot, J.-C.; Rault, S. *Tetrahedron* **2005**, *61*, 1417–1421.

(30) (a) Belfrekh, N.; Dietrich-Buchecker, C.; Sauvage, J.-P. *Inorg. Chem.* **2000**, *39*, 5169–5172. (b) Curphey, T. J.; Hoffman, E. J.; McDonald, C. *Chem. Ind.* **1967**, *7*, 1138.

(31) Berliner, M. A.; Belecki, K. *J. Org. Chem.* **2005**, *70*, 9618–9621.

(32) (a) Winkle, M. R.; Ronald, R. C. *J. Org. Chem*. **1982**, *47*, 2101–2108. (b) Le Strat, F.; Harroween, D. C.; Maddaluno, J. *J. Org. Chem*. **2005**, *70*, 489–498. (c) Azzouz, R.; Bischoff, L.; Fruit, C.; Marsais, F. *Synlett* **2006**, 1908–1912.

(33) Manisole = 3,5-dimethylanisole; manisyl = 4-methoxy-2,6-dimethylphenyl. Loren, J. C.; Siegel, J. S. *Angew. Chem. Int. Ed.* **2001**, *40*, 754–757.

(34) (a) Yates, K.; Mandrapilias, G. *J. Org . Chem.* **1980**, *45*, 3902–3906. (b) Shijun. Z.; Jensen, C.; Sheng, L.; Amane, M.; Hyunsik, C. W.O. Patent 2,010,141,758, Dec 9, 2010.

(35) (a) Goerth, F. C.; Rucker, M.; Eckhardt, M.; Brueckner, R. *Eur. J. Org. Chem*. **2000**, *14*, 2605–2612. (b) Zysman-Colman, E.; Arias, K.; Siegel, J. S. *Can. J. Chem*. **2009**, *87*, 440–447.

(36) Arias, K. I.; Zysman-Colman, E.; Loren, J. C.; Linden, A.; Siegel, J. S. *Chem. Commun.* **2011**, *47*, 9588–9590.

(37) (a) Negishi, E. *J. Org. Chem*. **1977**, *42*, 1821–1823. (b) Negishi, E.; Takahashi, T. *Org. Synth*. **1988**, *66*, 67–74.

(38) Rubinsztajn, S.; Fife, W. K.; Zeldin, M. *Tetrahedron Lett*. **1992**, *33*, 1821–1824.

(39) (a) Auerback, J.; Weinreb, S. M. *J. Chem. Soc., Chem. Commun*. **1974**, 298–299. (b) Meyers, A. I.; Durandetta, J. L.; Munavu, R. *J. Org. Chem*. **1975**, *40*, 2025–2029.

(40) (a) Arcadi, A.; Cacchi, S.; Marinelli, F. *Synthesis* **1986**, 749–751. (b) Kundu, N. G.; Pal, M.; Mahanty, J. S.; De, M. *J. Chem. Soc., Perkin Trans. 1* **1997**, 2815–2820. (c) Arcadi, A.; Cacchi, S.; Di Giuseppe, S.; Fabrizi, G.; Marinelli, F. *Synlett* **2002**, *3*, 453–457.

(41) Kalyanasundaram, K. *Photochemistry of Polypyridine and Porphyrin Complexes*, Academic Press, London, **1992**.

(42) Klosterman, J. K.; Linden, A.; Frantz, D. K.; Siegel, J. S. *Dalton Trans*. **2010**, *39*, 1519–1531.

(43) Boens, N.; Qin, W.; Basaric, N.; Hofkens, J.; Ameloot, M.; Pouget, J.; Lefevre, J.-P.; Valeur, B.; Gratton, E.; vandeVen, M.; Silva, N. D.; Engelborghs, Y.; Willaert, K.; Sillen, A.; Rumbles, G.; Phillips, D.; Visser, A. J. W. G.; van Hoek, A.; Lakowicz, J. R.; Malak, H.; Gryczynski, I.; Szabo, A. G.; Krajcarski, D. T.; Tamai, N.; Miura, A. *Anal. Chem*. **2007**, *79*, 2137−2149.

(44) (a) Piepenbrock, M. O.; Lloyd, G. O.; Clarke, N.; Steed, J. W. *Chem Rev* **2010**, *110*, 1960–2004. (b) Zhang, J.; Su, C.-Y. *Coord. Chem. Rev.* **2013**, *257*, 1373–1408.

(45) Favarger, F.; Goujon-Ginglinger, C.; Monchaud, D.; Lacour, J. *J. Org. Chem.* **2004**, *69*, 8521–8524.

(46) Goldschmidt, S.; Suchanek, L. *Chem. Ber.* **1957**, *90*, 19–28.

Chapter 3. Three Steps in One-pot: Synthesis of Linear Bilateral Extended 2,2′:6′,2″-Terpyridine Ru(II) Complexes

3.1. Introduction

Ability of tridentate 2,2′:6′,2″-terpyridine (*terpy*) ligands to form kinetically stable complexes with ruthenium(II), and their interesting photophysical and electrochemical properties have been extensively utilized in various fields. The characteristic strong metal-ligand coordinative bonds have been an attractive tool as a design element in supramolecular chemistry.[1-4] Dye sensitized solar cells developed by Gratzel[5] have drawn a special attention to polypyridine ruthenium complexes[6]. In previous chapter the concept of topologically linear bilateral extended *terpy* ligands was introduced as potential building blocks in supramolecular chemistry. It has been shown that octahedral metal complexes of tridentate 2,2′:6′,2″-terpyridine fused with five-membered furans rings mimic the topology of tetrahedral metal complexes of bidentate 5,5′-functionalized 2,2′-bipyridine (*bipy*) (Figure 3.1). An efficient one-pot acidic MOM-deprotection and base assisted cycloisomerization allowed accessing alkyl, aryl and heteroaryl substituted linear bilateral extended *terpy* derivatives. However, functional groups labile to the base or acid are incompatible under above described conditions. Therefore, a synthetic methodology to obtain these ligands or metal complexes directly under the neutral conditions would be of great importance (Figure 3.2). To extend accessibility to the linear bilateral *terpy* ligands, we focused on the available synthetic methodologies for the furo[2,3-c]pyridine functionlaity, as this is the key structural element for these systems.

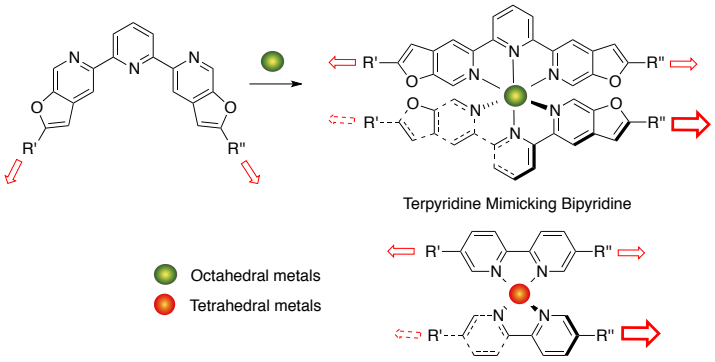

Figure 3.1. Linear bilateral extended 2,2′:6′,2″-terpyridine mimicking the topology of bidentate 5,5′-functionalized 2,2′-bipyridine.

In 1987, Fràter *et al* showed that furo[2,3-c]pyridine forms as a side product of Claisen rearrangement of 2-propynyl(3-pyridiyl)ethers at high temperature.[7] Since then many other methodologies have been developed[8-13]. So far the most efficient protocol involves palladium catalyzed cross-coupling reaction between 3-hydroxy-4-halopyridine and acetylene with *in situ* cyclization to form fused furan ring, which was first discovered and further extended by Marinelli *et al*.[14-16] Although it has been reported that ruthenium

($CpRuCl(PPh_3)_2$) catalyzed cycloisomerizations of 2-ethynylpehnols give benzofuranes via formation of ruthenium vinlydenes[17], to our knowledge, no ruthenium catalyzed synthesis of furo[2,3-c]pyridines is known to date. Given the fact that ruthenium is powerful catalyst in cycloisomerization reactions[18,19] and based on the results described in the previous chapter, it was expected that the formation of 2,6-*bis*-(2-substituted-furo[2,3-*c*]pyridin-5-yl)pyridine scaffold could take place in course of the complexation reaction of 5,5″-bis-(methoxymethoxy)-4-(2-substituted-ethynyl)-2,2′:6′,2″-terpyridine with $Ru(DMSO)_4Cl_2$. (Figure 3.2). In this chapter, the new methodology is described that provides access to linear bilateral extended 2,2′:6′,2″-terpyridine Ru(II) complexes via one-pot MOM cleavage, cycloisomerization and metal complexation of 5,5″-*bis*-(methoxymethoxy)-4,4″-*bis*-(substituted-ethynyl)-2,2′:6′,2″-terpyridines.

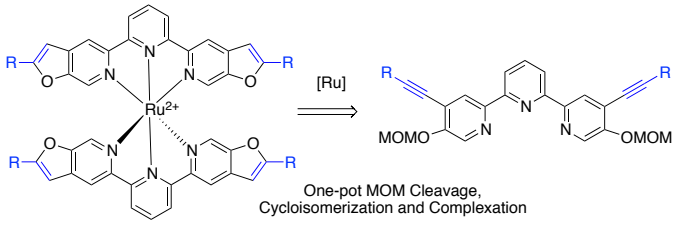

Figure 3.2. The one-pot strategy for the synthesis of linear bilateral extended 2,2′:6′,2″-terpyridine Ru(II) complexes from 5,5″-*bis*-(methoxymethoxy)-4,4″-*bis*-(substituted-ethynyl)-2,2′:6′,2″-terpyridines.

3.2. Results and Discussion

3.2.1. Synthesis of bisethynyl-substituted terpyridine substrates 78

Initially, several substrates bearing different functional groups were prepared in order to test one-pot synthesis of Ru(II) complexes of linear bilateral extended terpyridine ligands. The 4,4″-diethynyl 5,5″-diMOM substituted terpyridines **78** were efficiently prepared from the diiodoterpyridine **69**. The Sonogashira coupling[20] reaction between terpyridine **69** and excess of various acetylenes **59** gave disubstituted ethynylterpyridines **78** bearing aryl, haloaryl, amide, ester, heteroaryl, nitrile and alkyl groups with good to high yields (Table 3.1). The Miyaura borylation[21] of dibromo derivative **78j** afforded pinacolboronate **78o** in a good yield. (Scheme 3.1).

Table 1. Synthesis of Acetylenes 78

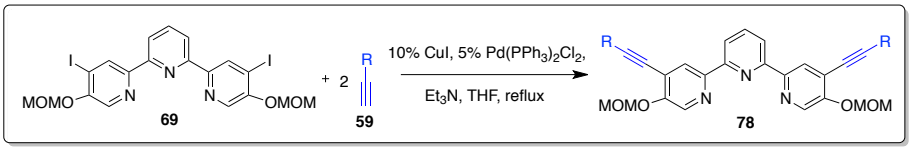

entry	R=	eq	time (h)	product	yield (%)
1	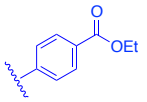	2.5	18	**78i**	83
2	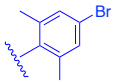	2.2	18	**78j**	64
3	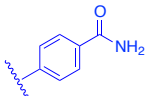	2.4	18	**78k**	85
4		2.5	20	**78a**	95
5		7.8	20	**78e**	85
6	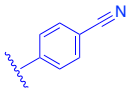	2.4	18	**78l**	85
7	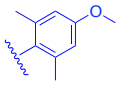	2.3	8	**78h**	91
8	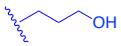	2.4	18	**78n**	71

Scheme 1. Synthesis of Pinacol Boronate 78o

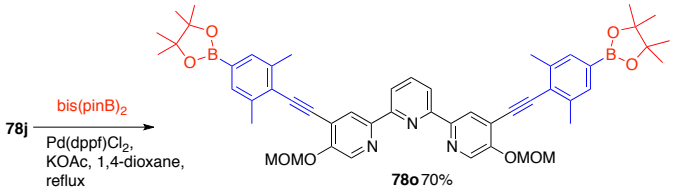

3.2.2. One-pot MOM Cleavage, Cyclization and Ru(II) Complexation

Attempts to obtain Ru(II) complex **[L7$_2$Ru](PF$_6$)$_2$** functionalized with ester groups via free ligand **84** with following complexation were not successful (Scheme 3.2). The hydrolysis of ester groups during the one-pot acidic MOM deporotection and base assisted cycloisomerization of **78i** did not give the desired diester **84**, instead the ~2:1 mixture of acid and monoester was formed. This motivated to test diester **78i** as the first substrate for the neutral one-pot preparation of complex **[L7$_2$Ru](PF$_6$)$_2$**.

Scheme 3.2. Unsuccessful synthesis of $[L7_2Ru](PF_6)_2$

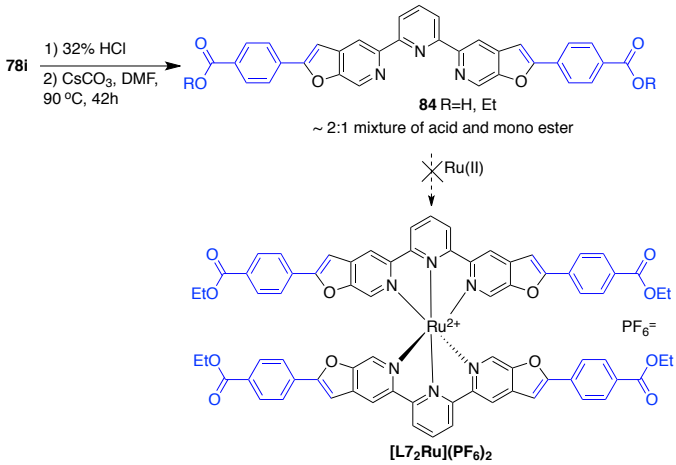

The diethyl ester **78i** and 0.5 equivalents of $Ru(DMSO)_4Cl_2$ were heated in ethylene glycol to 120 °C for 48 hours (Scheme 3.3). According to ESI-MS, the formation of the 2:1 ligand to Ru(II) complex was observed, in addition, the molecular ion clearly showed that MOM protecting groups were cleaved in the course of the reaction.

Scheme 3.3. Synthesis of *bis*-[2,6-*bis*-(2-Substituted-furo[2,3-*c*]pyridin-5-yl)pyridine] Ru(II)-2PF_6 Complexes $[L_2Ru](PF_6)_2$ [a]

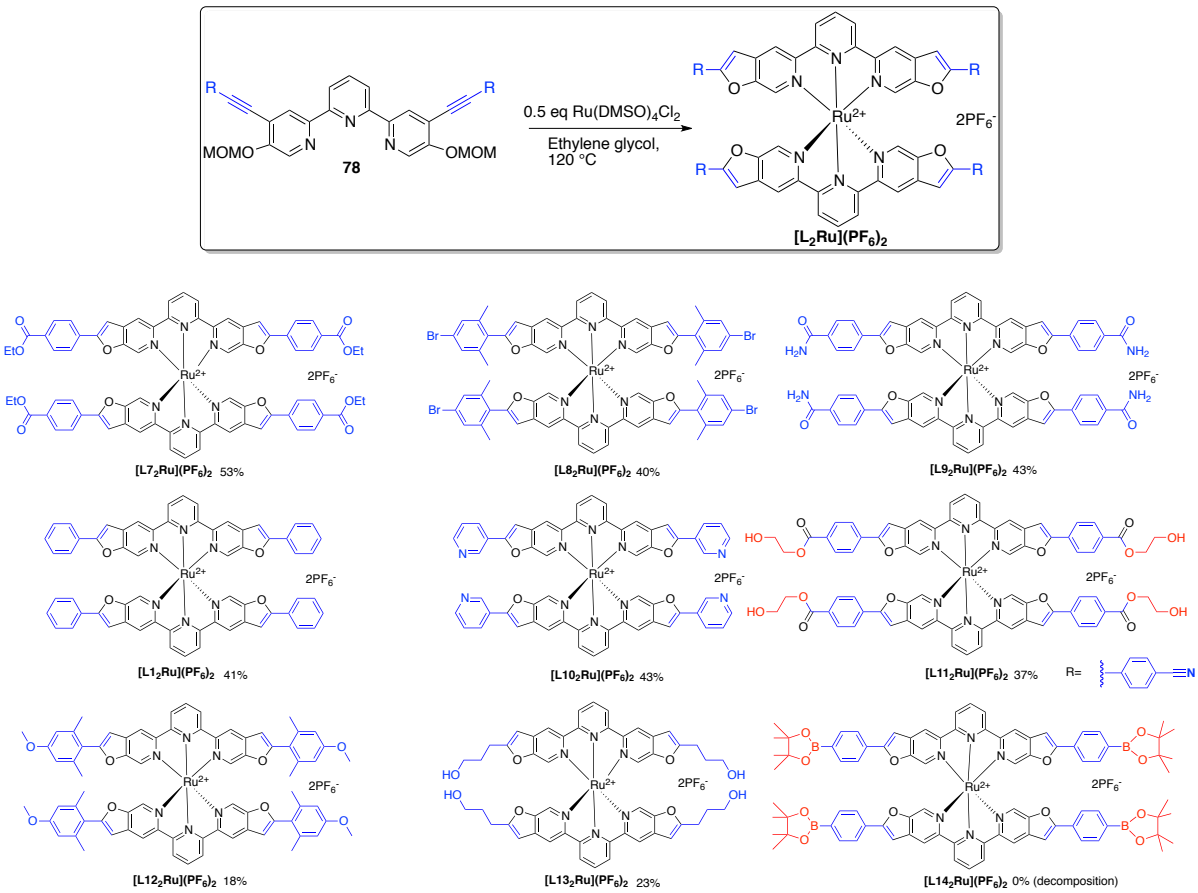

[a] The terpyridine **78** (0.02 mmol) and $Ru(DMSO)_4Cl_2$ (0.01 mmol) were heated in ethylene glycol (8 ml) to 120 °C under N_2 for 24 to 48 h. The crude product was precipitated with aq. KPF_6 and purified by silica gel column chromatography.

The crude reaction mixture was subjected to chromatographic separation to isolate the red band, which suggested the presence of bis-*terpy* Ru(II) species. The ^{1}H and ^{13}C NMR spectra allowed to distinguish whether the newly formed product remains as a diacetylene or performs cyclization to give furo[2,3-c]pyridine moieties. In comparison to the ^{1}H NMR spectrum of diacetylene **78i**, a new singlet appears at 7.47 ppm in the spectrum of the complex **[L7$_2$Ru](PF$_6$)$_2$**, which is characteristic for H at the C3 position of a furo[2,3-c]pyridine fragment. The characteristic signals for the disubstituted ethynyl group are absent in ^{13}C NMR of **[L7$_2$Ru](PF$_6$)$_2$**, but a new CH signal appears at 104.3 ppm (multiplicity determined from DEPT90 and DEPT135 experiments), which corresponds to the C3 position of the furan ring. Overall, spectral data are compatible with the previously reported Ru(II) complexes of linear bilateral extended terpyridines and support the formation of product **[L7$_2$Ru](PF$_6$)$_2$**.

To test the scope of the reaction, various diacetylenes **78** were used for obtaining one-pot MOM deprotection, furan cyclization and Ru(II) complexation products **[L$_2$Ru](PF$_6$)$_2$** (Scheme 3.3).

The diacetylenes **78a,e,i-k** give the desired products **[L1,7-10$_2$Ru](PF$_6$)$_2$** in 40-53 % yields. Unexpectedly, nitrile groups of **78l** underwent solvolysis to give ethylene glycol ester **[L11$_2$Ru](PF$_6$)$_2$**. This is an interesting example of the reaction where four transformations take place in one-pot. The substrates with electron donating groups give low yields of the desired complexes, as shown with the examples of **[L12$_2$Ru](PF$_6$)$_2$** and **[L13$_2$Ru](PF$_6$)$_2$**. It should be noted that pinacol boronate **78o** decomposed under the reaction conditions and no desired product **[L14$_2$Ru](PF$_6$)$_2$** was obtained.

A plausible mechanism for the Ru(II) catalyzed MOM deprotection and cycloizomerization is proposed in Scheme 3.4. Initially, Ru(II) species act as Lewis acid activating an ether bond of the methoxymethoxy (OMOM) group in order to promote the substitution with ethylene glycol **A**. The formed Ru pyridine-3-olate species **B** are converted to 4-ethynyl-3-hydroxy-pyridyl intermediate **C** in the presence of previously generated acid. Ruthenium coordinates to the acetylene group activating it for the 5-endo-dig cyclization **D** to give a fused furan ring. Further, the organoruthenium intermediate is converted to the desired furopyridine motif **E**. Presumably, after the catalytic cycle Ru(II) species are trapped by *terpy* affording the desired complexes **[L$_2$Ru](PF$_6$)$_2$**.

Scheme 3.4. Proposed Mechanism for Ru(II) Catalyzed MOM Cleavage and Cycloisomerization of 78

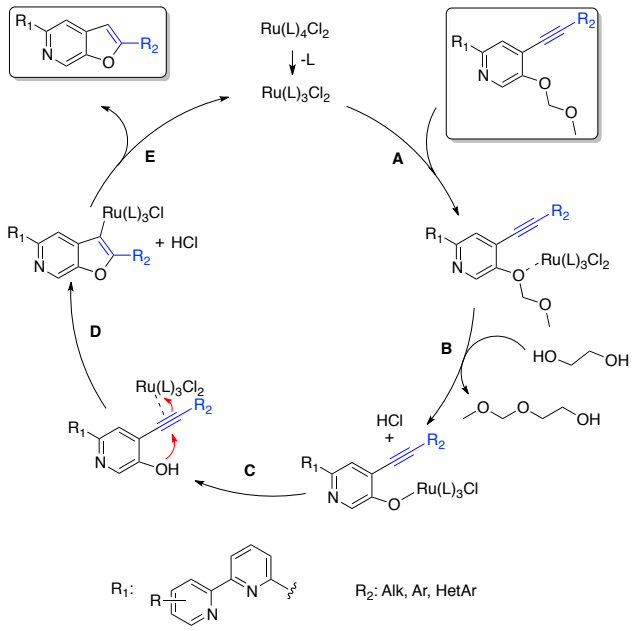

The diethyl ester **[L7$_2$Ru](PF$_6$)$_2$**, prepared by the above-mentioned methodology, can be further used to obtain an interesting, water-soluble zwitterionic complex **[L15$_2$Ru](PF$_6$)$_2$**, which has four terminal carboxylate groups (Scheme 3.5). Such molecular "crossing" with carboxylate groups could be interesting building block for the synthesis of MOFs.

Scheme 3.5. Synthesis of Zwitterionic Ru(II) Complex [L15$_2$Ru](PF$_6$)$_2$

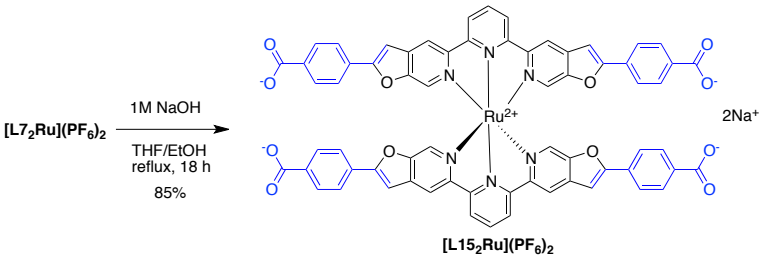

3.2.3. Photophysical Properties

The photophysical properties of ruthenium complexes **[L$_2$Ru](PF$_6$)$_2$** are summarized in Table 3.2. The UV-vis spectra of **[L$_2$Ru](PF$_6$)$_2$** display pronounced ligand centered (LC) absorptions with maxima at ~330-341 nm and characteristic lower energy MLCT bands (400-509 nm) (Figure 3.3). The MLCT bands of **[L$_2$Ru](PF$_6$)$_2$** are non-luminescent at room temperature. However, excitation at the LC bands of **[L7$_2$Ru](PF$_6$)$_2$**, **[L1$_2$Ru](PF$_6$)$_2$** and **[L9-12$_2$Ru](PF$_6$)$_2$** show weak but detectable emission (Figure 3.4).

Table 3.2. Absorption and Emission Maxima, Molar Absorptivity Values (log ε), Quantum Yields (ϕ_f), and Lifetimes (τ_f) for $[L_2Ru](PF_6)_2$

	UV/Vis[a]		Fluorescence [a]		
	λ_{abs} (nm)	log ε (log(cm^{-1} mol^{-1} L))	λ_{em} (nm)	ϕ_f, % [b]	τ_f (ns)
$[L7_2Ru](PF_6)_2$	256, 311, 324, 330, **341**, 399, 466, 503	4.86, 5.10, 5.06, 5.01, **5.21**, 4.59, 4.35, 4.27	383	0.04	4.60
$[L8_2Ru](PF_6)_2$	200, 256, 318sh, **330**, 376, 461, 494	5.11, 5.01, 4.89, **5.09**, 4.37, 4.22, 4.00	- [c]	- [c]	- [c]
$[L9_2Ru](PF_6)_2$	218, 256, 312, 325, **340**, 396, 465, 509	4.61, 4.71, 4.90, 4.89, **5.02**, 4.51, 4.36, 4.30	379, **399**	0.01	4.20
$[L1_2Ru](PF_6)_2$	258, 291, 307, 324, **338**, 389, 464, 506	4.90, 5.01, 4.99, 4.98, **5.16**, 4.57, 4.30, 3.73	349	0.06	3.22
$[L10_2Ru](PF_6)_2$	256, 291, 306, 323, **337**, 391, 464, 509	4.89, 4.99, 4.97, 4.90, **5.11**, 4.49, 4.27, 4.12	359	0.17	4.58
$[L11_2Ru](PF_6)_2$	256, 311, 324, **341**, 400, 465, 506	4.75, 5.00, 4.97, **5.09**, 4.50, 4.27, 4.20	380	<0.01 [d]	- [d]
$[L12_2Ru](PF_6)_2$	242, 274, 288, **330**, 372, 462, 508	5.02, 4.86, 4.83, **5.08**, 4.45, 4.22, 3.98	364	<0.01 [d]	- [e]
$[L13_2Ru](PF_6)_2$	**247**, 326, 366, 461, 499	**4.99**, 4.97, 4.23, 4.16, 3.85	- [c]	- [c]	- [c]
$[L15_2Ru](PF_6)_2$ [f]	258, 297, 313, 326, **341**, 390, 466, 508	4.52, 4.66, 4.69, 4.70, **4.79**, 4.26, 4.00, 3.90	- [c]	- [c]	- [c]

[a] All values measured in MeCN unless otherwise stated. [b] Measured with an integrating sphere. [c] Nonluminescence at rt. [d] Below the detection limit. [e] Due to the low emission cannot be measured reliably. [f] Measured in the 1:1 mixture of MeCN:H_2O.

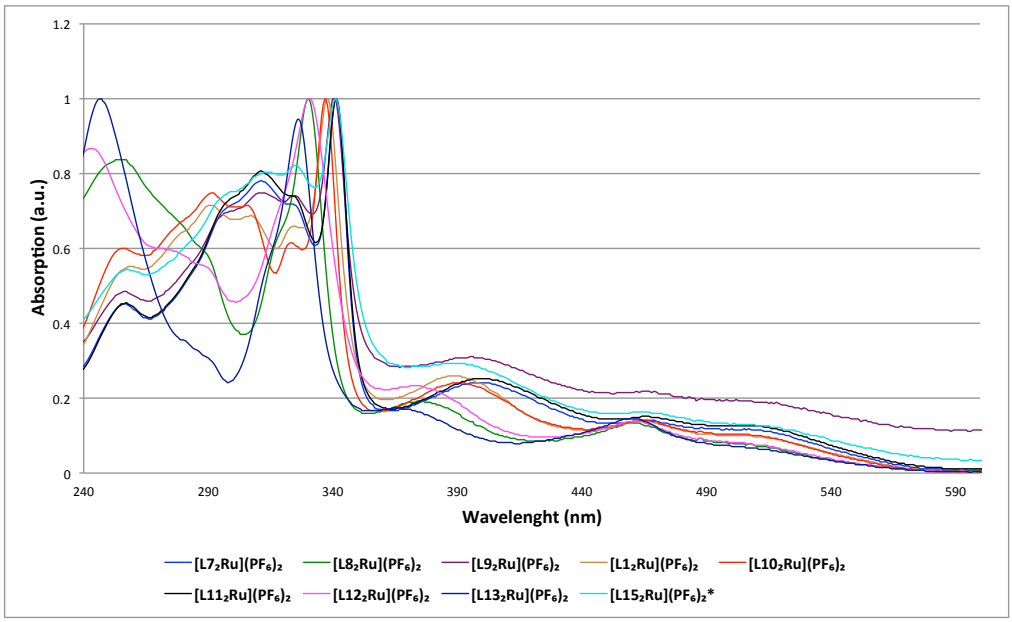

Figure 3.3. Absorption and emission spectra of complexes **$[L_2Ru](PF_6)_2$** in MeCN solution. * Measured in the 1:1 mixture of MeCN:H_2O.

The fluorescence quantum yields of these complexes are very low and range from 0.01% to 0.17%. The emission for **$[L11_2Ru](PF_6)_2$** and **$[L12_2Ru](PF_6)_2$** can be observed; however, quantum yields could not be reliably measured due to the low values. The

fluorescence lifetimes for complexes **[L1$_2$Ru](PF$_6$)$_2$**, **[L7$_2$Ru](PF$_6$)$_2$**, and **[L9-10$_2$Ru](PF$_6$)$_2$** are in the range of 4.3-4.6 ns.

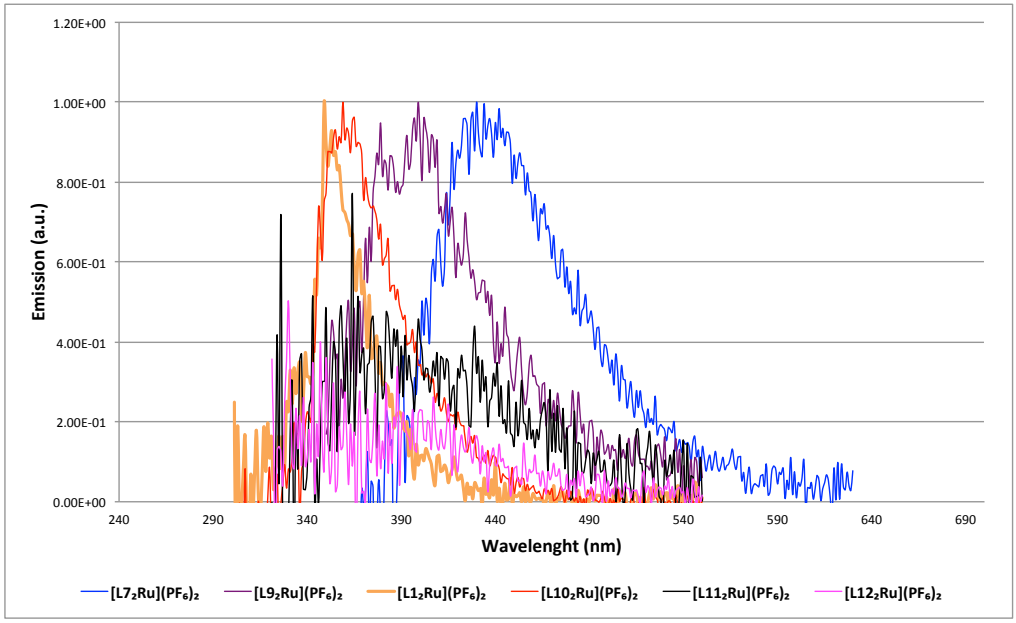

Figure 3.4. Absorption and emission spectra of complexes **[L$_2$Ru](PF$_6$)$_2$** in MeCN solution.

3.3. Conclusions

In summary, a novel one-pot MOM deprotection, cycloisomerization and complexation reaction has been developed, which provided an access to linear bilateral extended 2,2′:6′,2″-terpyridine Ru(II) complexes starting form 5,5”-bis-(methoxymethoxy)-4-(2-substituted-ethynyl)-2,2′:6′,2”-terpyridine. These new reaction conditions broaden the scope to access linear bilateral extended terpyridine Ru(II) complexes. Especially, this method provides a direct access to Ru(II) complexes bearing such base labile groups like esters.

3.4. Experimental Section

3.4.1. Materials and Methods

All reagents and solvents used for reactions were reagent grade and used without further purification unless otherwise noted. Commercial chemicals where used as received without special purification. Acetylenes **59i**[22], **59j**[23], **59k**[24] and **59l**[25] were prepared according to the literature procedures. Anhydrous THF and toluene was supplied from an Mbraun solvent purification system. Analytical thin-layer chromatography was performed with Macherey–Nagel POLYGRAM SIL N-HR/UV254 or ALOX N/UV254. Flash silica gel column chromatography was performed with Merck silica gel 60 (particle size 0.040–0.063 mm). Flash alumina column chromatography was performed with deactivated (5% water) Fluka alumina (particle size 0.05–0.15 mm, pH 7.0±0.5). Melting points were recorded on a Büchi B-540 melting point apparatus. For characterization purposes, proton nuclear magnetic resonance (^{1}H-NMR) spectra were all recorded on Bruker instruments (AV-300 and ARX-300 at 300 MHz, AV2- 400 at 400 MHz, and AV-500 at 500 MHz). Chemical shifts are reported in ppm relative to $CHCl_3$ (δ 7.26), CD_3CN (δ 1.94) or DMSO-d_6 (δ 2.50). Multiplicity and shape are indicated by one or more of the following abbreviations: s (singlet); d (doublet); t (triplet); q (quartet); dd (doublet of doublets); td (triplet of doublets); m (multiplet); br (broad). Carbon-13 nuclear magnetic resonance (^{13}C-NMR) spectra were recorded on Bruker instruments (ARX-300 at 75 MHz, AV2-400 at 100 MHz, and AV-500 at 125 MHz). Chemical shifts are reported relative to $CDCl_3$ (δ 77.2), CD_3CN (δ 1.3) or DMSO-d_6 (δ 39.5). Infrared spectroscopic data was recorded on NaCl plates as thin films or as KBr pellets on a Perkin Elmer Spectrum One (PE) and the intensities are given as follows: *s* = strong, *m* = medium, and *w* = weak. An Agilent 8453 UV/Vis spectrophotometer was used to record all UV/Vis spectra. Emission spectra and lifetimes (ns) were recorded on an Edinburgh Instruments FLS920 spectrometer. Quantum yields were measured using an integrating sphere accessory for FLS920 spectrometer. ESI-HRMS spectra were recorded at the MS Facility of the Institute of Organic Chemistry of the University of Zurich.

3.4.2. Experimental Procedures

General Procedure for the Synthesis of 78

To a mixture of diiodoterpyridine **69** (1.0 mmol), CuI (0.1 mmol) and $PdCl_2(PPh_3)_2$ (0.05 mmol) in degassed THF/Et_3N (10 mL/10 mL) was added acetylene **59** (amount indicated below) under N_2 atmosphere at 80 °C. The reaction mixture was heated to reflux till completion (followed by TLC), allowed to cool to room temperature and evaporated to dryness under reduced pressure. The residue was redissolved in CH_2Cl_2 (30 mL), washed with 10% aqueous NH_4OH, water and brine. The organic phase was dried over $MgSO_4$, filtrated and evaporated under reduces pressure. And purified as indicated below.

*diethyl 4,4''-(5,5''-bis-(methoxymethoxy)-2,2':6',2''-terpyridine-4,4''-diyl)-bis-(ethyne-2,1-diyl)-dibenzoate (**78i**)*. Ethyl 4-ethynylbenzoate (**59i**) (2.5 mmol). Purified by neutral Al_2O_3 (deact. with 5% w/w H_2O) column chromatography with hexane/EtOAc (3:1).

White solid; 579 mg (yield 83%).

Mp 159–161 °C.

IR (film on NaCl, cm^{-1}): 2980*w*, 2216*w*, 1718*s*, 1606*m*, 1572*w*, 1484*m*, 1456*m*, 1404*w*, 1379*m*, 1308*m*, 1273*vs*, 1233*m*, 1199*m*, 1158*m*, 1105*m*, 1074*m*, 1020*w*, 987*m*, 922*w*, 905*w*, 855*w*, 820*w*, 767*m*, 694*w*.

^1H NMR (500 MHz, $CDCl_3$, δ): 8.69 (s, 2H), 8.62 (s, 2H), 8.36 (d, *J* = 7.8 Hz, 2H), 8.05 (AA′BB′ spin system, 4H), 7.93 (t, *J* = 7.8 Hz, 1H), 7.68 (AA′BB′ spin system, 4H), 5.41 (s, 4H), 4.41 (q, *J* = 7.0 Hz, 4H), 3.61 (s, 6H), 1.42 (t, *J* = 7.0 Hz, 6H).

^{13}C NMR (125 MHz, $CDCl_3$, δ): 166.0, 154.6, 153.8, 150.2, 138.1, 137.2, 132.0, 131.0, 129.7, 127.1, 124.7, 122.4, 120.7, 96.9, 95.9, 86.4, 61.4, 56.8, 14.5.

HRMS (ESI) *m/z* $[M+H]^+$ calcd for $C_{41}H_{36}N_3O_8$ 698.24969, found 698.24925.

*5,5''-bis-(methoxymethoxy)-4,4''-bis-((4-bromo-2,6-dimethylphenyl)ethynyl)-2,2':6',2''-terpyridine (**78j**)*. 5-Bromo-2-ethynyl-1,3-dimethylbenzene (**59j**) (2.2 mmol). Purified by neutral Al_2O_3 (deact. with 5% w/w H_2O) column chromatography with hexane/EtOAc (gradient 3:1 to 1:1).

A light yellow solid; 491 mg (yield 64%).

Mp 181–184 °C.

IR (film on NaCl, cm^{-1}): 2953*w*, 2919*w*, 2853*w*, 2211*w*, 1572*m*, 1538*w*, 1485*m*, 1454*w*, 1376*w*, 1306*w*, 1262*m*, 1202*m*, 1202*w*, 1155*s*, 1086*m*, 1073*m*, 991*vs*, 921*w*, 902*w*, 854*w*, 838*w*, 817*m*, 777*w*, 724*w*, 606*w*.

^{1}H NMR (400 MHz, $CDCl_3$, δ): 8.65 (s, 2H), 8.59 (s, 2H), 8.36 (d, *J* = 7.8 Hz, 2H), 7.93 (t, *J* = 7.8 Hz, 1H), 7.25 (s, 4H), 5.39 (s, 4H), 3.57 (s, 6H), 2.50 (s, 12H).

^{13}C NMR (100 MHz, $CDCl_3$, δ): 154.8, 153.4, 150.2, 142.7, 138.1, 137.0, 130.1, 124.2, 123.0, 122.7, 121.6, 120.5, 95.5, 94.7, 92.9, 56.7, 21.0.

HRMS (ESI) *m/z* $[M+H]^+$ calcd for $C_{39}H_{34}Br_2N_3O_4$ 766.09106, found 766.09145.

*4,4″-(5,5″-bis-(methoxymethoxy)-2,2′:6′,2″-terpyridine-4,4″-diyl)-bis-(ethyne-2,1-diyl)-dibenzamide (**78k**)*. 4-Ethynylbenzamide (**59k**) (2.4 mmol). The reaction mixture was evaporated to dryness under reduced pressure. The residual solid was treated with 10% aqueous NH_4OH, filtered and washed with water. The crude product was heated to reflux with EtOH/THF (400/40 mL), allowed to cool to room temperature and the solid was collected by filtration.

Off-white solid; 544 mg (yield 85%). Mp >300 °C.

IR (KBr, cm^{-1}): 3406*s*, 3190*m*, 2954*w*, 2924*w*, 2849*w*, 1655*s*, 1611*s*, 1573*w*, 1555*w*, 1514*w*, 1483*w*, 1457*m*, 1409*m*, 1382*s*, 1304*w*, 1269*w*, 1251*w*, 1120*w*, 1157*m*, 1074*m*, 985*m*, 923*w*, 907*w*, 853*w*, 818*w*, 769*w*.

^{1}H NMR (400 MHz, DMSO-d_6, δ): 8.70 (s, 2H), 8.68 (s, 2H), 8.35 (d, *J* =7.8 Hz, 2H), 8.09 (t, *J* =7.8 Hz, 1H), 8.08 (br. s, 2H), 7.97-7.95 (AA′BB′ spin system, 4H), 7.77-7.75 (AA′BB′ spin system, 4H), 7.50 (br. s, 2H), 5.51 (s, 4H), 3.53 (s, 6H).

^{13}C NMR (125 MHz, DMSO-d_6, δ): 167.0, 154.2, 153.2, 149.0, 138.5, 137.6, 134.8, 131.6, 127.9, 124.2, 123.4, 121.0, 120.2, 96.7, 95.3, 85.3, 56.2.

HRMS (ESI) *m/z* $[M+H]^+$ calcd for $C_{37}H_{30}N_5O_6$: 640.21906; found: 640.21907.

*5,5″-bis-(methoxymethoxy)-4,4″-bis-(phenylethynyl)-2,2′:6′,2″-terpyridine (**78a**)*. Phenyl acetylene (**59a**) (2.5 mmol). Purified by neutral Al_2O_3 (deact. with 5% w/w H_2O) column chromatography. Eluent hexane/EtOAc 3:1.

Off-white solid; 526 mg (yield 95 %).

Mp 149–151 °C.

IR (film on NaCl, cm^{-1}): 2957*w*, 2906*w*, 2219*w*, 1600*w*, 1573*m*, 1544*w*, 1494*m*, 1484*s*, 1457*m*, 1379*m*, 1308*w*, 1268*m*, 1232*w*, 1200*m*, 1155*s*, 1077*m*, 982*s*, 921*w*, 823*w*, 757*m*, 690*w*.

^{1}H NMR (400 MHz, $CDCl_3$, δ): 8.72 (s, 2H), 8.60 (s, 2H), 8.36 (d, *J* = 7.8 Hz, 2H), 7.92 (t, *J* = 7.8 Hz, 1H), 7.63 (dd, *J* = 7.6, 1.7 Hz, 4H), 7.41-7.34 (m, 6H), 5.40 (s, 4H), 3.61 (s, 6H).

^{13}C NMR (100 MHz, $CDCl_3$, δ): 154.8, 153.6, 150.3, 137.9, 137.5, 132.0, 129.1, 128.5, 124.6, 122.7, 120.3, 97.7, 95.9, 83.9, 56.7.

HRMS (ESI) *m/z* $[M+Na]^+$ calcd for $C_{35}H_{27}N_3NaO_4$ 576.18938, found 576.18905.

*5,5″-bis(methoxymethoxy)-4,4″-bis[2-(pyridine-3-yl)ethynyl]-2,2′:6′,2″-terpyridine (**78e**)*. 3-Ethynylpyridine (**59e**) (7.8 mmol). Purified by silica gel column chromatography with CH_2Cl_2/MeOH (gradient 99:1 to 9:1).

White solid; 472 mg (yield 85%).

Mp 164–165 °C dec.

IR (film on NaCl, cm^{-1}): 2958*w*, 2831*w*, 2220*w*, 1571*m*, 1546*w*, 1486*s*, 1457*m*, 1409*w*, 1378*m*, 1308*w*, 1268*w*, 1234*w*, 1200*m*, 1155*s*, 1076*m*, 976*vs*, 923*w*, 821*w*, 703*w*.

^1H NMR (400 MHz, $CDCl_3$, δ): 8.86 (d, *J* = 1.2 Hz, 2H), 8.69 (s, 2H), 8.63 (s, 2H), 8.61 (dd, *J* = 4.9, 1.6 Hz, 2H), 8.36 (d, *J* = 7.8 Hz, 2H), 7.93 (t, *J* = 7.9 Hz, 1H), 7.90 (dt, *J* = 7.9, 1.9 Hz, 2H), 7.34 (ddd, *J* = 7.9, 4.9, 0.7 Hz, 2H), 5.40 (s, 4H), 3.60 (s, 6H).

^{13}C NMR (125 MHz, $CDCl_3$, δ): 154.7, 153.7, 152.4, 150.2, 149.3, 139.0, 138.0, 137.2, 124.5, 123.4, 121.7, 120.6, 119.9, 95.7, 94.0, 87.0, 56.8.

HRMS (ESI) *m/z* $[M+H]^+$ calcd for $C_{33}H_{26}N_5O_4$: 556.19793; found: 556.19697.

*4,4″-(5,5″-bis-(methoxymethoxy)-2,2′:6′,2″-terpyridine-4,4″-diyl)-bis-(ethyne-2,1-diyl)dibenzonitrile (**78l**)*. 4-Ethynylbenzonitrile (**59l**) (2.4 eq). Purified by neutral Al_2O_3 (deact. with 5% w/w H_2O) column chromatography with hexane/EtOAc (1:1).

White solid; 513 mg (yield 85%).

Mp 232–233 °C.

IR (film on NaCl, cm^{-1}): 2952*w*, 2916*w*, 2845*w*, 2226*s*, 1605*m*, 1573*m*, 1504*w*, 1482*m*, 1457*w*, 1380*m*, 1309*m*, 1270*m*, 1200*w*, 1156*m*, 983*s*, 900*s*, 839*s*.

^1H NMR (500 MHz, $CDCl_3$, δ): 8.64 (s, 2H), 8.63 (s, 2H), 8.35 (d, *J* = 7.7 Hz, 2H), 7.94 (t, *J* = 7.8 Hz, 1H), 7.71-7.66 (AA′BB′ spin system, 8H), 5.40 (s, 4H), 3.60 (s, 6H).

^{13}C NMR (125 MHz, $CDCl_3$, δ): 154.9, 153.8, 150.4, 138.1, 137.4, 132.5, 132.3, 127.5, 124.3, 121.3, 120.7, 118.4, 112.6, 95.8, 95.4, 87.9, 56.8.

HRMS (ESI) *m/z* $[M+H]^+$ calcd for $C_{37}H_{26}N_5O_4$: 604.19793; found: 604.19798.

*4,4″-bis-[2-(4-methoxy-2,6-dimethylphenyl)-ethynyl]-5,5″-bis(methoxymethoxy)-2,2′:6′,2″-terpyridine (**78h**)*. 2-Ethynyl-5-methoxy-1,3-dimethylbenzene (**73**) (2.3 mmol). Purified by silica gel column chromatography with CH_2Cl_2/MeOH (95:5).

Off-white solid; 609 mg (yield 91%). Mp 182–183 °C.

IR (film on NaCl, cm^{-1}): 2952*w*, 2902*w*, 2836*w*, 2190*w*, 1603*m*, 1573*s*, 1484*m*, 1453*m*, 1377*m*, 1315*m*, 1303*s*, 1283*m*, 1228*m*, 1194*m*, 1155*s*, 1119*m*, 1086*m*, 1073*m*, 1058*m*, 990*s*,

921*m*, 897*m*, 853*m*, 818*m*, 732*m*, 661*w*, 602*m*.

^{1}H NMR (400 MHz, $CDCl_3$, δ): 8.65 (s, 2H), 8.57 (s, 2H), 8.38 (d, *J* = 7.9 Hz, 2H), 7.94 (t, *J* = 7.9 Hz, 1H), 6.62 (s, 4H), 5.39 (s, 4H), 3.81 (s, 6H), 3.58 (s, 6H), 2.53 (s, 12H).

^{13}C NMR (125 MHz, $CDCl_3$, δ): 159.9, 154.7, 153.3, 150.1, 142.9, 138.1, 136.9, 124.2, 123.8, 120.5, 115.0, 112.7, 96.6, 95.6, 90.7, 56.7, 55.3, 21.4.

HRMS (ESI) *m/z* $[M+H]^+$ calcd for $C_{41}H_{40}N_3O_6$: 670.29116; found: 670.29071.

*5,5''-(5,5''-bis-(methoxymethoxy)-2,2':6',2''-terpyridine-4,4''-diyl)dipent-4-yn-1-ol (**78n**).*

Pent-4-yn-1-ol (**59n**) (2.4 mmol). Purified by neutral Al_2O_3 (deact. with 5% w/w H_2O) column chromatography with CH_2Cl_2/MeOH (95:5).

White amorphous solid; 367 mg (71%).

Mp 144–145 °C.

IR (film on NaCl, cm^{-1}): 3332*br*, 2940*w*, 2919*w*, 2233*w*, 1567*w*, 1544*w*, 1487*m*, 1459*m*, 1378*m*, 1276*m*, 1193*m*, 1153*s*, 1083*m*, 978*vs*, 924*m*;

^{1}H NMR (400 MHz, $CDCl_3$, δ): 8.56 (s, 2H), 8.54 (d, *J* = 0.5 Hz, 2H), 8.31 (d, *J* =7.8 Hz, 2H), 7.89 (t, *J* = 7.8 Hz, 1H), 5.34 (s, 4H), 3.89 (t, *J* =6.1 Hz, 4H), 3.57 (s, 6H), 2.68 (t, *J* =6.8 Hz, 4H), 2.17 (br. s, 2H), 1.95 (tt, *J* = 6.1, 6.8 Hz, 4H).

^{13}C NMR (125 MHz, $CDCl_3$, δ): 154.8, 153.9, 150.3, 137.9, 137.3, 124.8, 122.9, 120.3, 98.7, 95.7, 77.4, 77.2, 76.9, 75.9, 61.9, 56.7, 31.3, 16.8.

HRMS (ESI) *m/z* $[M+H]^+$ calcd for $C_{29}H_{32}N_3O_6$: 518.22856; found: 518.22837.

Synthesis of 78o

*4,4''-bis((2,6-dimethyl-4-(3,3,4,4-tetramethylborolan-1-yl)phenyl)ethynyl)-5,5''-bis(methoxymethoxy)- 2,2':6',2''-terpyridine (**78o**).*

Prepared according to the Miyaura borylation[21] from (**78j**) as follows:

In a dry 50 mL 2 necked flask to a mixture of dibromide **78j** (100 mg, 1.0 eq, 0.131 mmol), bis(pinacolato)diboron (72.8 mg, 2.2 eq, 0.286 mmol), potassium acetate (51.2 mg, 4.0 eq, 0.528 mmol) and $Pd(dppf)Cl_2$ (10.7 mg, 10 mol%, 0.0131 mmol) under N_2 atmosphere dry 1,4-dioxane (12 mL) was added. The reaction mixture was heated to reflux for 18 h, allowed to cool to room temperature and the solvent was evaporated under reduced pressure. The crude mixture was purified by silica gel column chromatography with hexane:EtOAc:CH_2Cl_2 (3:1:3).

White amorphous solid; 79 mg (yield 70%). Mp 80–86 (waxy solid) °C. IR (film on NaCl, cm^{-1}): 2977*w*, 2919*w*, 2849*w*, 2207*w*, 1607*w*, 1575*w*, 1483*m*, 1455*m*, 1364*vs*, 1314*w*, 1260*w*, 1237*m*, 1199*w*, 1146*s*, 1074*m*, 985*s*, 853*m*, 740*w*, 740*w*; ^{1}H NMR (400 MHz, $CDCl_3$, δ): 8.63 (s, 2H), 8.60 (s, 2H), 8.37 (d, *J* = 7.8 Hz, 2H), 7.93 (t, *J* = 7.8 Hz, 1H), 7.55 (s, 4H), 5.40 (s, 4H), 3.58 (s, 6H), 2.57 (s, 12H), 1.37 (s, 24H). ^{13}C NMR (75 MHz, $CDCl_3$, δ): 155.1, 153.5, 150.3, 140.0, 137.0, 136.9, 133.1, 129.9, 125.3, 123.9, 122.9, 120.5, 95.9, 95.4, 93.0, 84.1, 56.7, 25.0, 21.0. HRMS (ESI) *m/z* $[M+H]^+$ calcd for $C_{51}H_{58}B_2N_3O_8$: 862.44204; found: 862.44228.

General Procedure for One-pot Synthesis of $[L_2Ru](PF_6)_2$

A mixture of diethynyl terpyridine **78** (0.02 mmol) and $Ru(DMSO)_4Cl_2$ (0.01 mmol) in ethylene glycol (8 mL) was heated to 120 °C under N_2 atmosphere for the indicated time. The mixture was allowed to cool to room temperature and aqueous KPF_6 was added. The resulting deep-red precipitate was collected by filtration on Celite, washed with water, Et_2O, hexane and redissolved with acetonitrile into a clean flask. The solvent was evaporated to give a deep-red residue, which was purified by silica gel column chromatography. The combined fractions containing product **$[L_2Ru](PF_6)_2$** were evaporated under reduced pressure. Dissolved in minimum amount of acetonitrile and reprecipitated with aq. KPF_6 solution. A red solid was collected by filtration on Celite, washed with water, Et_2O and redissolved with acetonitrile into a clean flask. Solvent evaporated under reduced pressure to give **$[L_2Ru](PF_6)_2$**.

*Ru[diethyl 4,4'-(5,5'-(pyridine-2,6-diyl)bis(furo[2,3-c]pyridine-5,2-diyl))dibenzoate]$_2$-2PF_6 (**$[L7_2Ru](PF_6)_2$**)*. The reaction mixture was heated for 24 h. Eluent acetonitrile/H_2O/aq. KPF_6/CH_2Cl_2 (97:3:0.3:100). The first red band was collected.

Dark red solid; 17.0 mg (yield 53%).

Mp >282 dec °C.

IR (film on NaCl, cm^{-1}): 2983*w*, 2918*w*, 2849*w*, 1714*s*, 1613*m*, 1456*s*, 1412*w*, 1368*w*, 1279*s*, 1182*w*, 1108*m*, 1016*m*, 842*vs*, 773*w*, 699*w*, 558*m*.

^{1}H NMR (500 MHz, CD_3CN, δ): 8.86 (s, 4H), 8.81 (d, *J* = 8.2 Hz, 4H), 8.52 (t, *J* = 8.2 Hz, 2H), 8.07-8.05 (AA′BB′ spin system, 8H), 7.91-7.89 (AA′BB′ spin system, 8H), 7.73 (s, 4H), 7.47 (s, 4H), 4.32 (q, *J* = 7.1 Hz, 8H), 1.34 (t, *J* = 7.1 Hz, 12H).

^{13}C NMR (125 MHz, CD_3CN, δ): 166.4, 161.7, 156.8, 153.2, 153.0, 137.7, 137.5, 137.1, 133.3, 132.8, 131.0, 126.9, 123.4, 118.3 (overlapping with CD_3CN), 104.3, 62.2, 14.5.

HRMS (ESI) *m/z*: $[M]^{2+}$ calcd for $C_{74}H_{54}N_6O_{12}Ru$: 660.14262; found: 660.14224.

*Ru[2,6-bis(2-(4-bromo-2,6-dimethylphenyl)furo[2,3-c]pyridin-5-yl)pyridine]$_2$-2PF$_6$ (**[L8$_2$Ru](PF$_6$)$_2$**)*. The reaction mixture was heated for 48 h. Eluent gradient acetonitrile/H_2O/aq. KPF_6/CH_2Cl_2 (97:3:0.3:0 to 97:5:1:100). The first red band was collected.
Dark red solid; 14.0 mg (yield 40 %).
Mp >370 dec. °C.
IR (film on NaCl, cm^{-1}): 2921*w*, 2853*w*, 1623*w*, 1592*m*, 1452*s*, 1311*w*, 1249*w*, 1148*w*, 1001*w*, 913*w*, 843*vs*, 740*w*, 559*m*.
^{1}H NMR (500 MHz, CD_3CN, δ): 8.85 (s, 4H), 8.75 (d, *J* = 8.2 Hz, 4H), 8.44 (t, *J* = 8.2 Hz, 2H), 7.72 (s, 4H), 7.35 (s, 8H), 7.06 (s, 4H), 2.04 (s, 24H).
^{13}C NMR (125 MHz, CD_3CN, δ): 161.3, 156.8, 153.0, 152.7, 141.8, 137.7, 137.2, 136.8, 131.6, 128.4, 125.0, 123.2, 118.1 (overlapping with CD_3CN), 108.3, 20.3.
HRMS (ESI) *m/z*: $[M]^{2+}$ calcd for $C_{70}H_{50}Br_4N_6O_4Ru$: 727.98196; found: 727.98320.

*Ru[4,4'-(5,5'-(pyridine-2,6-diyl)bis(furo[2,3-c]pyridine-5,2-diyl))dibenzamide]$_2$-2PF$_6$ (**[L9$_2$Ru](PF$_6$)$_2$**)*. The reaction mixture was heated for 48 h. The crude product was dissolved in minimum amount of wet acetonitrile and charged on a silica gel column (insoluble in dry acetonitrile). Eluent acetonitrile/H_2O/aq. KPF_6 (90:10:5). The first red band was collected.
Dark red solid; 12.8 mg (yield 43%).
Mp >334 dec. °C.
IR (KBr, cm^{-1}): 3441*br*, 1667*s*, 1619*m*, 1599*m*, 1555*w*, 1456*m*, 1411*w*, 1384*s*, 1315*w*, 1282*w*, 1176*w*, 1014*w*, 912*w*, 848*vs*, 804*w*, 774*w*, 558*w*.
^{1}H NMR (500 MHz, CD_3CN+D_2O, δ): 8.87 (s, 4H), 8.82 (d, *J* = 8.3 Hz, 4H), 8.49 (t, *J* = 8.3 Hz, 2H), 8.16-7.99 (m, 8H), 7.87 (s, 16H), 7.71 (s, 4H), 7.47 (s, 4H).
^{13}C NMR (125 MHz, CD_3CN+D_2O, δ): 170.1, 161.8, 156.7, 153.1, 152.9, 137.7, 137.3, 137.1, 136.1, 131.8, 129.4, 126.9, 123.4, 118.2 (overlapping with CD_3CN), 104.02.
HRMS (ESI) *m/z*: $[M]^{2+}$ calcd for $C_{66}H_{42}N_{10}O_8Ru$: 602.11098; found: 602.11118.

*Ru[2,6-bis(2-phenylfuro[2,3-c]pyridin-5-yl)pyridine]$_2$-2PF$_6$ (**[L1$_2$Ru](PF$_6$)$_2$**)*. The reaction mixture was heated for 48 h. Eluent acetonitrile/H_2O/aq. KPF_6 (97:3:0.3). The first red band was collected.
Dark red solid; 10.8 mg (yield 41 %).
Mp >350 dec °C.
IR (KBr, cm^{-1}): 3116*w*, 3069*w*, 1621*m*, 1585*w*, 1567*w*, 1485*w*, 1459*s*, 1447*s*, 1385*w*, 1313*w*, 1278*w*, 1176*w*, 1020*w*, 842*vs*, 767*w*, 687*w*, 558*s*. ^{1}H NMR (500 MHz, CD_3CN, δ): 8.82 (s, 2H), 8.80 (d, *J* = 8.2 Hz, 2H), 8.50 (t, *J* = 8.2 Hz, 1H), 7.83-7.80 (m, 4H), 7.68 (s, 2H), 7.48-

7.46 (m, 6H), 7.34 (s, 2H). ^{13}C NMR (125 MHz, CD_3CN, δ): 163.1, 156.8, 152.9, 152.8, 137.9, 137.0, 136.8, 131.9, 130.2, 128.9, 126.9, 123.2, 117.9, 102.4.
HRMS (ESI) *m/z*: $[M]^{2+}$ calcd for $C_{62}H_{38}N_6O_4Ru$: 516.10018; found: 516.09979.

*Ru[2,6-bis(2-(pyridin-3-yl)furo[2,3-c]pyridin-5-yl)pyridine]$_2$-2PF$_6$ (**[L10$_2$Ru](PF$_6$)$_2$**)*. The reaction mixture was heated for 48 h. Eluent acetonitrile/H_2O/aq. KPF_6 (90:10:5). The first red band was collected.
Dark red solid; 11.4 mg (yield 43%).
Mp >278 dec. °C.
IR (KBr, cm^{-1}): 2921*s*, 2851*m*, 1659*m*, 1632*m*, 1469*w*, 1449*m*, 1407*m*, 1309*w*, 1014*w*, 913*m*, 872*w*, 840*s*, 798*m*, 700*m*, 557*m*.
^{1}H NMR (500 MHz, CD_3CN, δ): 9.01 (d, *J* = 1.8 Hz, 4H), 8.86 (s, 4H), 8.81 (d, *J* = 8.2 Hz, 4H), 8.61 (dd, *J* = 1.6, 4.8 Hz, 4H), 8.52 (t, *J* = 8.2 Hz, 2H), 8.10 (dt, *J* = 1.9, 8.13 Hz, 4H), 7.73 (s, 4H), 7.45 (s, 4H), 7.44 (dd, *J* = 4.8, 7.9 Hz, 4H).
^{13}C NMR (125 MHz, CD_3CN, δ): 160.6, 156.8, 153.1, 153.0, 152.4, 148.0, 137.6, 137.5, 137.0, 134.0, 125.3, 125.0, 123.4, 118.3 (overlapping with CD_3CN), 103.8.
HRMS (ESI) *m/z*: $[M]^{2+}$ calcd for $C_{58}H_{34}N_{10}O_4Ru$: 518.09061; found: 518.09128.

*Ru[bis(2-hydroxyethyl) 4,4'-(5,5'-(pyridine-2,6-diyl)bis(furo[2,3-c]pyridine-5,2-diyl))dibenzoate]$_2$-2PF$_6$ (**[L11$_2$Ru](PF$_6$)$_2$**)*. The reaction mixture was heated for 48 h. Eluent acetonitrile/H_2O/aq. KPF_6/CH_2Cl_2 (35:2:1:19). The second red band was collected.
Dark red solid; 12.4 mg (yield 37%).
Mp >330 dec. °C.
IR (KBr, cm^{-1}): 3431*br*, 2923*w*, 2852*w*, 1717*s*, 1620*m*, 1586*w*, 1456*s*, 1411*w*, 1374*w*, 1313*w*, 1278*s*, 1182*w*, 1125*w*, 1077*w*, 1015*w*, 846*s*, 773*w*, 558*m*.
^{1}H NMR (500 MHz, CD_3CN, δ): 8.85 (s, 4H), 8.81 (d, *J* = 8.2 Hz, 4H), 8.52 (t, *J* = 8.2 Hz, 2H), 8.11-8.09 (AA′BB′ spin system, 8H), 7.92-7.91 (AA′BB′ spin system, 8H), 7.73 (s, 4H), 7.48 (s, 4H), 4.32 (t, *J* = 4.8 Hz, 8H), 3.78 (t, *J* = 4.8 Hz, 8H), 2.98 (br. s, 4H).
^{13}C NMR (125 MHz, CD_3CN, δ): 166.4, 161.7, 156.8, 153.2, 153.0, 137.7, 137.5, 137.1, 133.1, 132.9, 131.1, 126.9, 123.4, 118.3 (overlapping with CD_3CN), 104.4, 67.9, 60.8.
HRMS (ESI) *m/z*: $[M]^{2+}$ calcd for $C_{74}H_{54}N_6O_{16}Ru$: 692.13248; found: 692.13168.

*Ru[2,6-bis(2-(4-methoxy-2,6-dimethylphenyl)furo[2,3-c]pyridin-5-yl)pyridine]$_2$-2PF$_6$ (**[L12$_2$Ru](PF$_6$)$_2$**)*. The reaction mixture was heated for 48 h. Eluent acetonitrile/H_2O/aq. KPF_6 (97:3:0.3). The first red band was collected.

Dark red solid; 5.6 mg (yield 18%).

Mp >283 dec. °C.

IR (film on NaCl, cm^{-1}): 2918*w*, 1604*m*, 1455*s*, 1384*w*, 1313*m*, 1291*w*, 1192*w*, 1153*w*, 1067*w*, 1003*w*, 840*vs*, 809*w*, 737*w*, 558*w*.

^{1}H NMR (500 MHz, CD_3CN, δ): 8.83 (s, 4H), 8.75 (d, *J* = 8.2 Hz, 4H), 8.43 (t, *J* = 8.2 Hz, 2H), 7.69 (s, 4H), 6.98 (s, 4H), 6.70 (s, 8H), 3.77 (s, 12H), 2.04 (s, 24H).

^{13}C NMR (125 MHz, CD_3CN, δ): 163.0, 161.9, 156.9, 153.0, 152.6, 141.2, 137.5, 137.3, 136.8, 123.1, 121.5, 117.8, 114.3, 107.8, 56.0, 20.7.

HRMS (ESI) *m/z*: $[M]^{2+}$ calcd for $C_{74}H_{62}N_6O_8Ru$: 632.18409; found: 632.18350.

Ru[3,3'-(5,5'-(pyridine-2,6-diyl)bis(furo[2,3-c]pyridine-5,2-diyl))dipropan-1-ol]$_2$-2PF$_6$ ***([L13$_2$Ru](PF$_6$)$_2$)***. The reaction mixture was heated for 18 h. Eluent acetonitrile/H_2O/aq. KPF_6/CH_2Cl_2 (35:2:1:19). The first red band was collected.

Dark red solid; 5.8 mg (yield 23%).

Mp >206 dec. °C.

IR (film on NaCl, cm^{-1}): 3401*br*, 2918*w*, 1623*w*, 1583*m*, 1455*s*, 1313*m*, 1256*m*, 1174*w*, 1058*w*, 1028*m*, 947*m*, 936*m*, 897*m*, 841*vs*, 808*m*, 558*m*.

^{1}H NMR (500 MHz, CD_3CN, δ): 8.68 (d, *J* = 8.1 Hz, 4H), 8.67 (s, 4H), 8.39 (t, *J* = 8.1 Hz, 2H), 7.48 (s, 4H), 6.70 (s, 4H), 3.44 (t, *J* = 5.2 Hz, 8H), 2.78 (t, *J* = 7.5 Hz, 8H), 2.58 (br. s, 4H), 1.76 (quintuplet, *J* = 6.5 Hz, 8H).

^{13}C NMR (125 MHz, CD_3CN, δ): 168.6, 156.7, 152.9, 152.4, 137.9, 136.5, 136.3, 122.9, 117.5, 103.6, 61.2, 30.9, 25.5.

HRMS (ESI) *m/z*: $[M]^{2+}$ calcd for $C_{50}H_{46}N_6O_8Ru$: 480.12116; found: 480.12126.

Synthesis of [L15$_2$Ru](PF$_6$)$_2$

Ru[Na 4,4'-(5,5'-(pyridine-2,6-diyl)bis(furo[2,3-c]pyridine-5,2-diyl))dibenzoate]$_2$-2PF$_6$ ***([L15$_2$Ru](PF$_6$)$_2$)***.

To a suspension of **[L7$_2$Ru](PF$_6$)$_2$** (13.1 mg, 1.0 eq, 0.00813 mmol) in a 1:1 mixuture of EtOH/THF (8 mL) was added aqueous 1 M NaOH (81 μL, 10 eq, 0.081 mmol). The reaction mixture was heated to reflux for 18 h. The hot reaction mixture was filtered off to collect red solid, which was rinsed with few drops of abs. EtOH and dried under vacuum.

Red solid; 8.6 mg (yield 85 %).

Mp >200 dec. °C.

IR (KBr, cm^{-1}): 2927*w*, 2853*w*, 1596*m*, 1574*s*, 1551*m*, 1456*m*, 1385*s*, 1308*w*, 1279*w*, 1092*w*, 1013*w*, 846*w*, 789*w*.

^{1}H NMR (500 MHz, CD_3CN + 5% D_2O, δ): 9.07 (s, 4H), 9.02 (d, *J* = 8.32 Hz, 4H), 8.53 (t, *J* = 8.32 Hz, 2H), 7.88-7.86 (AA′BB′ spin system, 8H), 7.83 (s, 4H), 7.78-7.76 (AA′BB′ spin system, 8H), 7.59 (s, 4H).

^{13}C NMR (125 MHz, CD_3CN + 5% D_2O) 169.9, 161.9, 158.7, 155.8, 152.4, 152.0, 142.3, 137.2, 136.3, 130.4, 128.7, 125.8, 123.1, 117.7, 102.7.

HRMS (ESI) *m/z*: $[M+4H-2Na]^{2+}$ calcd for $C_{66}H_{38}N_6O_{12}Ru$: 604.07991; found: 604.07974.

3.5. References

(1) Schubert, U. S.; Hofmeier, H.; Newkome, G. R. *Modern Terpyridine Chemistry*; Weinheim : Wiley-VCH-Verl., **2006**.

(2) Baranoff, E.; Collin, J. P.; Flamigni, L.; Sauvage, J. P. *Chem. Soc. Rev.* **2004**, *33*, 147–155.

(3) Sauvage, J. P.; Collin, J. P.; Chambron, J. C.; Guillerez, S.; Coudret, C.; Balzani, V.; Barigelletti, F.; De Cola, L.; Flamigni, L. *Chem. Rev.* **1994**, *94*, 993–1019.

(4) Hofmeier, H.; Schubert, U. S. *Chem. Soc. Rev.* **2004**, *33*, 373–399.

(5) O'Regan, B.; Grätzel, M. *Nature* **1991**, *353*, 737–740.

(6) Ardo, S.; Meyer, G. J. *Chem. Soc. Rev.* **2009**, *38*, 115–164.

(7) Bruhn, J.; Zsindely, J.; Schmid, H.; Fràter, G. *Helv. Chim. Acta* **1978**, *61*, 2542–2559.

(8) Shiotani, S.; Morita, H. *J. Heterocycl. Chem.* **1982**, *19*, 1207–1209.

(9) Morita, H.; Shiotani, S. *J. Heterocycl. Chem.* **1986**, *23*, 549–552.

(10) Sabot, C.; Oueis, E.; Brune, X.; Renard, P. Y. *Chem. Commun.* **2012**, *48*, 768–770.

(11) Cho, S. Y.; Kim, S. S.; Park, K.-H.; Kang, S. K.; Choi, J.-K.; Hwang, K.-J.; Yum, E. K. *Heterocycles* **1996**, 549–552.

(12) Kitamura, T.; Tsuda, K.; Fujiwara, Y. *Tetrahedron Lett.* **1998**, *39*, 5375–5376.

(13) Le Strat, F.; Harrowven, D. C.; Maddaluno, J. *J. Org. Chem.* **2005**, *70*, 489–498.

(14) Arcadi, A.; Marinelli, F.; Cacchi, S. *Synthesis* **1986**, *1986*, 749–751.

(15) Arcadi, A.; Cacchi, S.; Di Giuseppe, S.; Fabrizi, G.; Marinelli, F. *Synlett* **2002**, *2002*, 453–457.

(16) Arcadi, A.; Cacchi, S.; Di Giuseppe, S.; Fabrizi, G.; Marinelli, F. *Org. Lett.* **2002**, *4*, 2409–2412.

(17) Varela-Fernández, A.; González-Rodríguez, C.; Varela, J. s. A.; Castedo, L.; Saá, C. *Org. Lett.* **2009**, *11*, 5350–5353.

(18) Michelet, V.; Toullec, P. Y.; Genet, J. P. *Angew. Chem., Int. Ed.* **2008**, *47*, 4268–4315.

(19) Trost, B. M.; Rhee, Y. H. *J. Am. Chem. Soc.* **2002**, *124*, 2528–2533.

(20) Sonogashira, K.; Tohda, Y.; Hagihara, N. *Tetrahedron Lett.* **1975**, *16*, 4467.

(21) Ishiyama, T.; Murata, M.; Miyaura, N. *J. Org. Chem.* **1995**, *60*, 7508–7510.

(22) Duggan, M. E.; Duong, L. T.; Fisher, J. E.; Hamill, T. G.; Hoffman, W. F.; Huff, J. R.; Ihle, N. C.; Leu, C.-T.; Nagy, R. M.; Perkins, J. J.; Rodan, S. B.; Wesolowski, G.; Whitman, D. B.; Zartman, A. E.; Rodan, G. A.; Hartman, G. D. *J. Med. Chem.* **2000**, *43*, 3736–3745.

(23) Pearson, D. L.; Tour, J. M. *J. Org. Chem.* **1997**, *62*, 1376–1387.

(24) Nguyen, N. H.; Apriletti, J. W.; Baxter, J. D.; Scanlan, T. S. *J. Am. Chem. Soc.* **2005**, *127*, 4599–4608.

(25) Richardson, C.; Reed, C. A. *J. Org. Chem.* **2007**, *72*, 4750–4755.

Chapter 4. Heterometallic MOFs based on Linear Bilateral Extended 2,2′:6′,2′′-Terpyridine

4.1. Introduction

Rational design and assembly of supramolecular architectures require building blocks with defined geometries and topology.[1] The pioneering work of Robson in 1990 showed that organic ligands and metal centers can act as "spacers and nodes" for constructing extended polymeric frameworks.[2] Such design principles are successfully applied in the rapidly growing field of metal-organic frameworks (MOFs)[3-6] with a major focus on creating novel porous materials for gas adsorption, storage[7-9], and seperation[10]. However, synthesis and investigation of MOFs can also address specific properties required in such fields as catalysis[11,12], specific recognition[13], NLO optical[14], luminescent[15], spin crossover and magnetic materials[16-20], and medicine[21-23]. A rigid and defined framework can be a platform for embedding complexity and still maintaining predictable structure.[24] The MOFs are mostly prepared by solvothermal synthesis, but room temperature synthesis by slow diffusion of reactants can also be efficient.[25,26]

The inorganic nodes bring rigidity, define topology, and offer geometries unavailable when using only organic molecules. However, further success and advance in the field of MOFs strongly depend on the development of versatile organic linkers because that is where the function, dimensions and properties can be tuned and adjusted most efficiently.

In the previous chapters, the synthesis and metal complexation of a novel class of ligands – linear bilateral extended 2,2′:6′,2″-terpyridines (*terpy*) was described. These are topological tridentate analogs of bidentate 5,5′-disubstituted 2,2′-bipyridines, which form molecular crossings upon complexation with metals preferring octahedral geometry. The flanking positions can be used for introducing directional groups that open the doors to assembly of extended network structures. This chapter describes assembly of 2D and 3D heterometallic MOFs based on 4-pyridyl substituted Fe(II) molecular crossing **L3** in the presence of metals preferring tetrahedral geometry (Cu(I) and Ag(I)).

4.2.Results and Discussion

4.2.1. Synthesis of 2D and 3D Heterometallic MOFs

A solution of $AgPF_6$ in ethanol was layered over a solution of the 4-pyridyl substituted **$[L3_2Fe](PF_6)_2$** complex in acetonitrile. A small amount of cyclohexane between the layers was used to slow down the diffusion process. In a few days needle-like crystals formed which over two weeks transformed into dark purple blocks that were separated by filtration to give

$[L3_2FeAg]_n(PF_6)_{3n}$ (Scheme 4.1). The structure of the product was elucidated by single crystal X-ray analysis.

Scheme 4.1. Synthesis of 3D MOF $[L3_2FeAg]_n(PF_6)_{3n}$

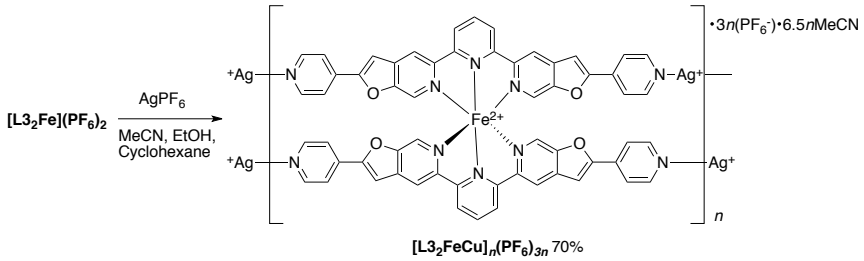

$[L3_2FeCu]_n(PF_6)_{3n}$ 70%

Similarly, a $[Cu(CH_3CN)_4]PF_6$ solution was slowly diffused into the acetonitrile solution of **$[L3_2Fe](PF_6)_2$**, using small amount of cyclohexane between the layers. Dark purple block-like crystals were obtained over three weeks, and the resulting product **$[L3_2FeCu(MeCN)]_n(PF_6)_{3n}$** was separated by filtration (Scheme 4.2). The X-ray structure could be only partially solved due to the insufficient diffraction and crystal quality.

Scheme 4.2. Synthesis of 2D MOF $[L3_2FeCu(MeCN)]_n(PF_6)_{3n}$

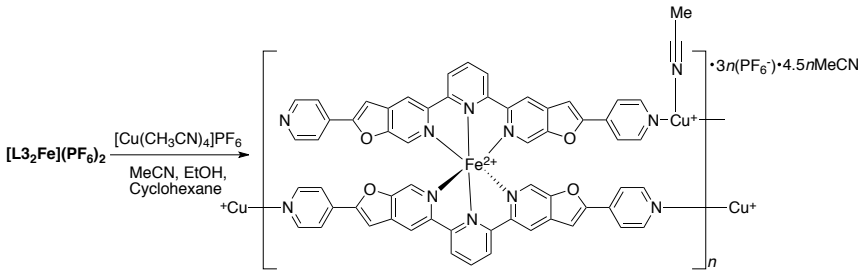

$[L3_2FeCu(MeCN)]_n(PF_6)_{3n}$ 47%

4.2.2. Structure

The crystals of **$[L3_2FeAg]_n(PF_6)_{3n}$** and **$[L3_2FeCu(MeCN)]_n(PF_6)_{3n}$** used for single crystal X-ray analysis where kept in the mother liquor to avoid decomposition, which happens due to quick loss of crystallization solvent.

The X-ray crystal structure of **$[L3_2FeAg]_n(PF_6)_{3n}$** was elucidated in space group *P-1*. The results of structural analysis are presented in Figures 4.1 and 4.2. The cationic structure of **$[L3_2FeAg]_n(PF_6)_{3n}$** is a three-dimensional interpenetrating polymer.

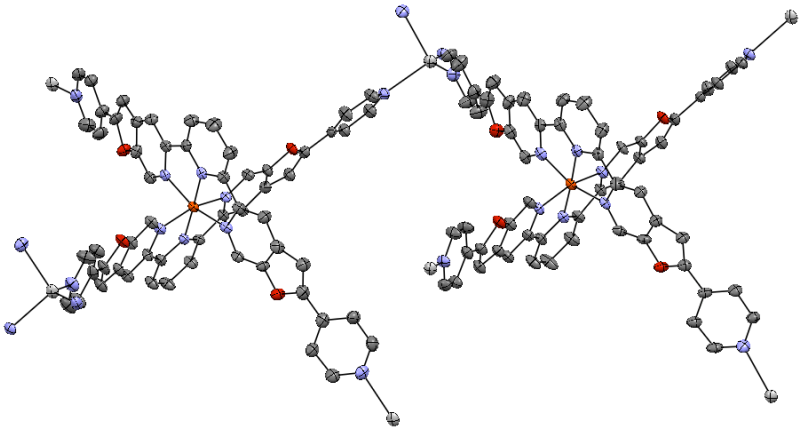

Figure 4.1. ORTEP drawing (50% probability) of the cation in $\mathbf{[L3_2FeAg]_n(PF_6)_{n3}}$. (Color code: Fe, brown; Ag, silver; N, light blue; O, red; C, dark gray; P, orange; F, light green) Hydrogen atoms and PF_6^- removed for clarity.

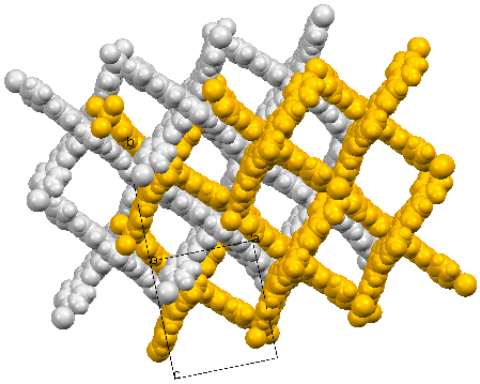

Figure 4.2. Packing of $\mathbf{[L3_2FeAg]_n(PF_6)_{3n}}$. The cationic structure consists of two interpenetrating 3D networks related by inversion symmetry (color defined by symmetry operations). Hydrogen atoms, PF_6^- and disordered solvent molecules removed for clarity.

The symmetry operators connecting the asymmetric unit to adjacent units within the polymer all involve unit cell translations. However, the space group also contains inversion symmetry, which means that the inversion related version of the polymer has no bonds connecting it to the original polymer, but they do interweave with one another. The asymmetric unit contains two repeats of the chemically unique portion of the polymeric cation, six disordered PF_6^- anions and a cavity situated about a center of inversion containing disordered solvent molecules. The 3D framework structure can be interpreted as consisting of layers held together by coordination bonds between 4-pyridyl groups and silver atoms. One such layer is shown in Figure 4.3, examples **A**, **B** and **C**. The layer down the *c* axis is represented in example **A**, where a squeezed honeycomb network can be seen consisting of 6-membered rings with alternating Ag(I) and Fe(II) nodes.

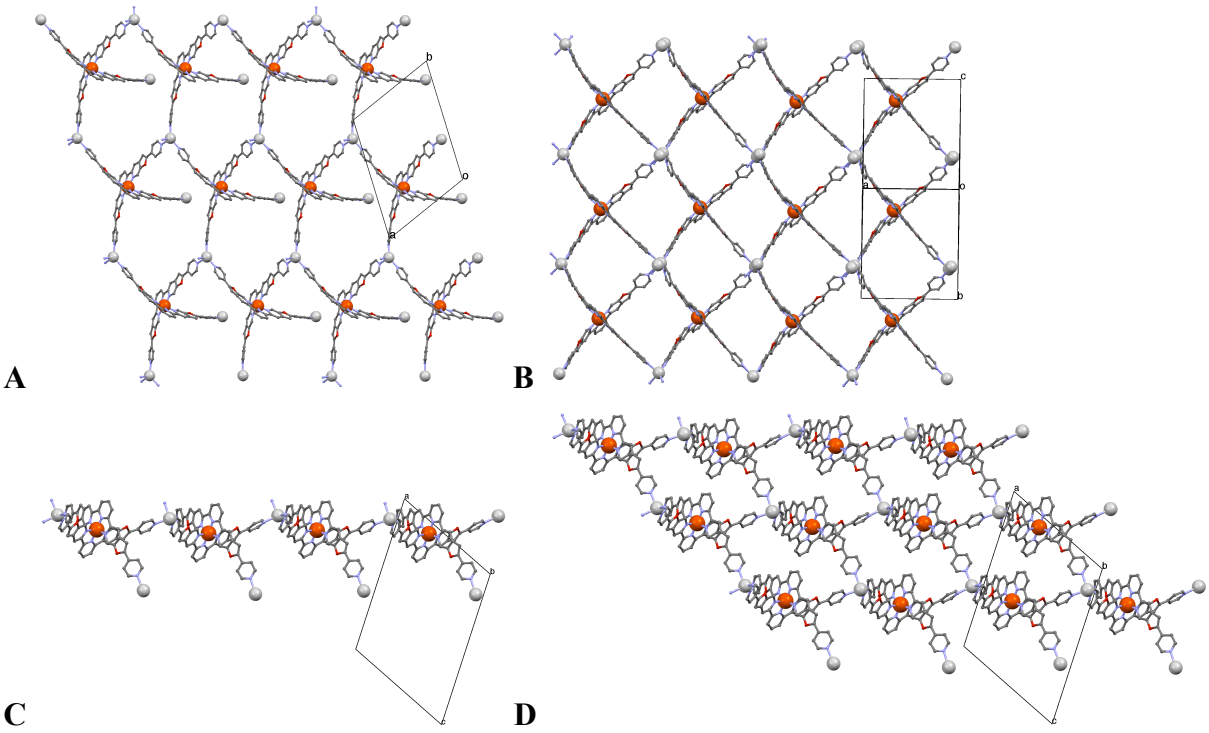

Figure 4.3. Ball and stick representation of cationic network $\mathbf{[L3_2FeAg]_{\mathit{n}}(PF_6)_{\mathit{n}3}}$. **A.** One layer view down *c* axis **B.** One layer view down the edge *ao*. **C.** One layer view down *b* axis. **D.** Three layers view down *b* axis.

Example **C** represents one layer from side view (down *b* axis), whereas example **D** shows three layers stacked on top of each other and connected through N-Ag bonds. When the network is observed from the perspective showed in Figure 4.3, example **B** and Figure 4.2, rectangular channels can be seen with alternating silver and iron atoms at the corners. The distances Ag(1)-Ag(2) and Fe(1)-Fe(2) are 16.9095(6) and 16.7399(8) Å, respectively. This causes significant voids and channels within the structure. Each unit cell contains one centrosymmetric cavity which comprises 31.5% of the total volume.

Topology of the cationic network of $\mathbf{[L3_2FeAg]_n(PF_6)_{3n}}$ is represented in Figure 4.4. The structure of the iron(II) based molecular "crossings" reveal that the furo[2,3-*c*]pyridine arms of the ligand are significantly tilted; therefore, angle between N atoms of both flanking 4-pyridiyl groups and central ring of *terpy* N(4)-N(2)-N(5) is 134.43(5)°. This can be represented schematically as tetrahedron to define net topology (Figure 4.4). Distorted adamantane units within 3D polymeric network can be recognized from the crystal structure. The nodes of this framework are tetrahedral silver(I) centers (Figure 4.4, light blue balls) and octahedral iron(II) centers (purple balls), where four arms of molecular "crossing" act as linkers. The overall topology of the network can be assigned as **dia-b** net.[29,30] The inversion

related network is interpenetrated in a characteristic manner for the diamondoid type networks.[2]

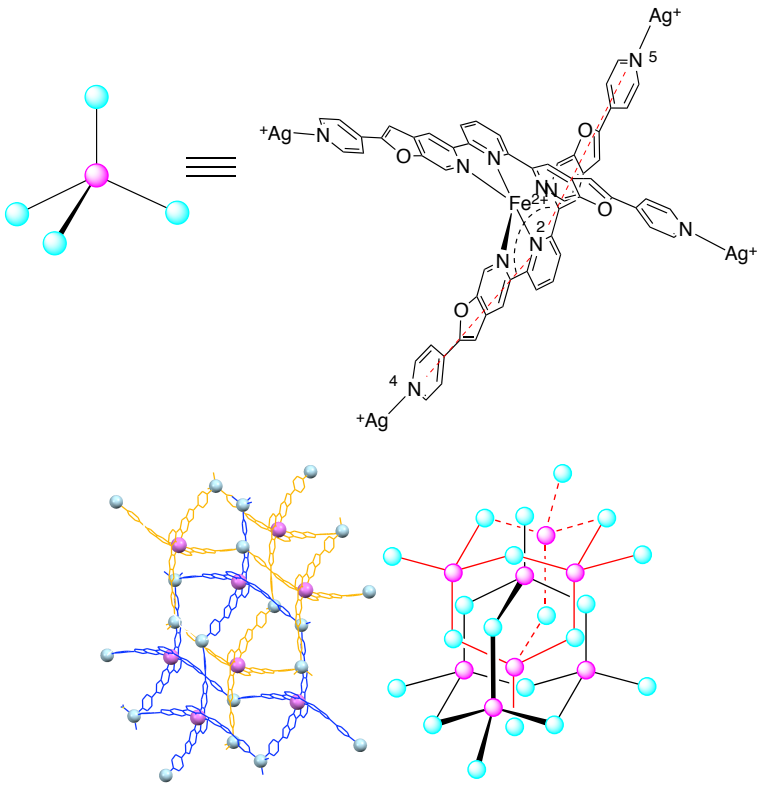

Figure 4.4. The diamondoid net (**dia-b**) topology of **$[L3_2FeAg]_n(PF_6)_{3n}$** and interpenetration.

The schematic representation of the molecular structure of **$[L3_2FeCu(MeCN)]_n(PF_6)_{3n}$** solved in space group *P-1* is shown in Figures 4.5 and 4.6. Given the poor quality of data, care must be taken when analyzing the structure.

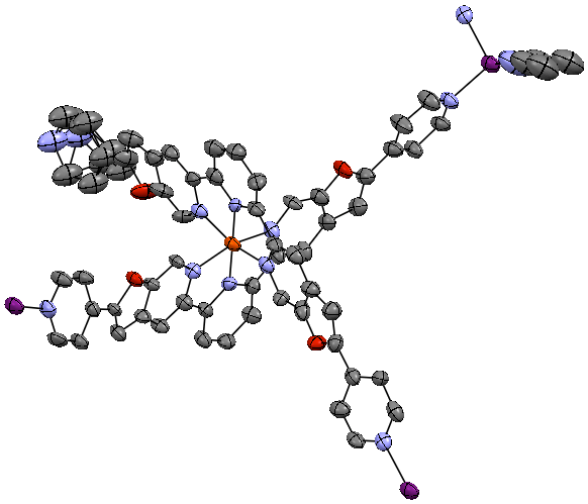

Figure 4.5. Schematic representation of the molecular structure of **$[L3_2FeCu(MeCN)]_n(PF_6)_{3n}$**. Model of the cation drawn as thermal ellipsoids (50% probability). Both MeCN molecule bound to the Cu center and the uncoordinated pyridine ring are severely disordered. (Color code: Fe, brown; Cu, purple; N, light blue; O, red; C, dark gray). Hydrogen atoms and PF_6^- removed for clarity.

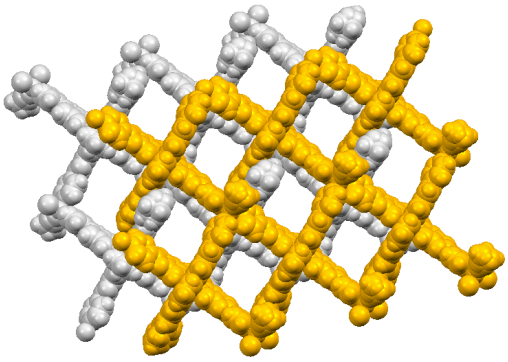

Figure 4.6. Space filling representation of **[L3$_2$FeCu(MeCN)]$_n$(PF$_6$)$_{3n}$**. Two inversion symmetry related 2D polymeric layers (color defined by symmetry operations). Hydrogen atoms, PF_6^- and disordered solvent molecules removed for clarity.

The structure could not been definitely solved due to the insufficient diffraction and crystal quality. The asymmetric unit should contain 3 PF_6^- anions; instead, only 2.5 per unit could be assigned. Nevertheless, atom connectivity of cationic network can be modeled based on X-ray diffraction data. This shows that Fe(II) based molecular "crossings" in the presence of Cu(I) assemble into the structure similar to that of **[L3$_2$FeAg]$_n$(PF$_6$)$_{3n}$** (Figure 4.6). However, one coordination site of tetrahedral Cu(I) center is occupied with solvent molecule – presumably acetonitrile, but this cannot be definitely assigned from X-ray data. ^{1}H NMR spectrum of vacuum dried and re-dissolved crystals in MeCN-d_6 supports the presence of acetonitrile in the sample but it could also originate from co-crystallized solvent. However, if the starting material $[Cu(CH_3CN)_4]PF_6$ is taken in consideration, it is reasonable to assume that one of the four coordination sites of Cu(I) center contains MeCN ligand. This does not allow one of four 4-pyridyl groups, which is severely disordered, to be coordinated to the copper atom. Therefore, **[L3$_2$FeCu(MeCN)]$_n$(PF$_6$)$_{3n}$** structure consists of stacked 2D polymeric sheets or layers. Two such inversion symmetry related cationic layers are shown in Figure 4.6. One individual layer is drawn from different perspectives in Figure 4.7, examples **A**, **B**, and **C**. The layer down the *a* axis is represented in example **A**, where the honeycomb network topology can bee seen with 6-membered rings containing alternating Cu(I) and Fe(II) nodes. Figure 4.6 and Figure 4.7, example **B**, reveal a perspective were rectangular-shaped channels can be observed – similar to those of **[L3$_2$FeAg]$_n$(PF$_6$)$_{3n}$** structure. The comparison of one and three layers from side view (down *c* axis) is shown in the Figure 4.7, example **C** and **D**.

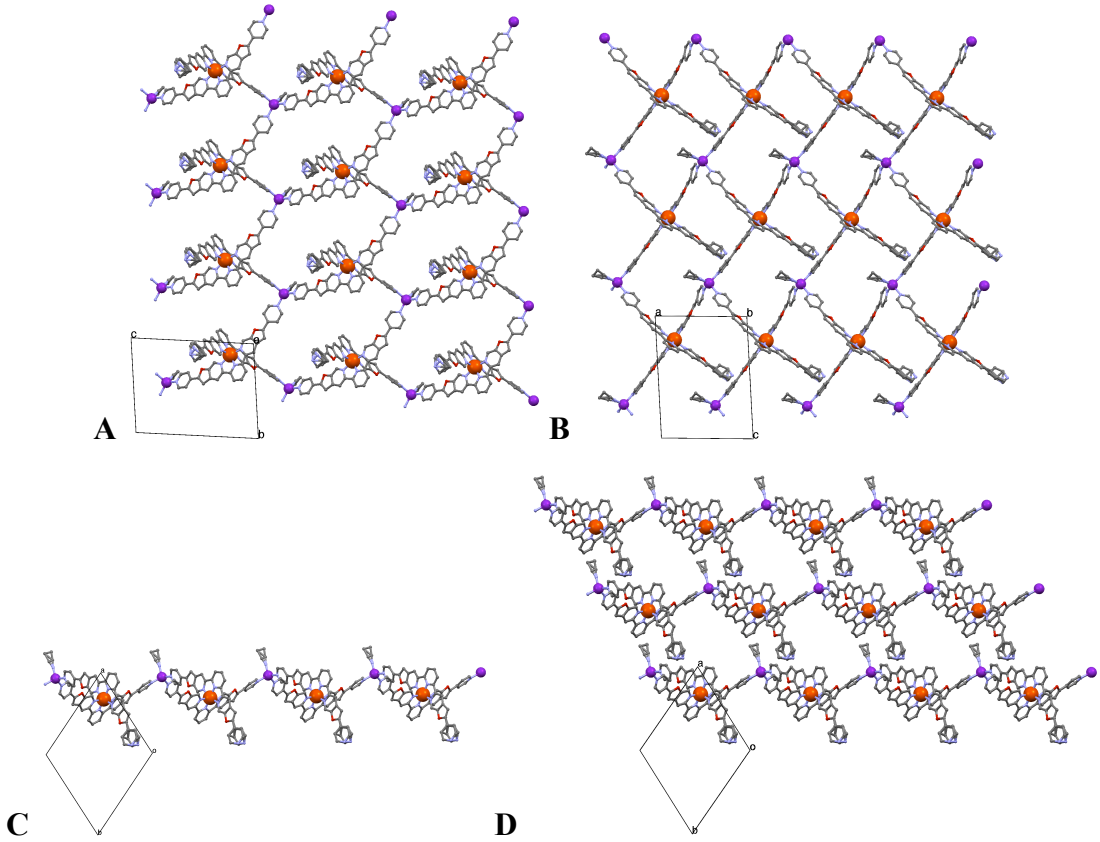

Figure 4.7. Ball and stick representation of cationic network $\mathbf{[L3_2FeCu(MeCN)]_n(PF_6)_{3n}}$. **A.** One layer view down *a* axis **B.** One layer view down *b* axis. **C.** One layer view down *c* axis. **D.** Three independent layers view down *c* axis.

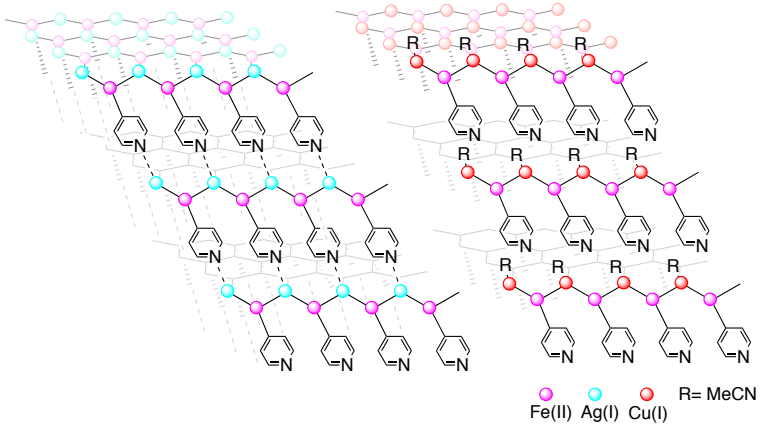

Figure 4.8. Schematic representation of 3D structure of $\mathbf{[L3_2FeAg]_n(PF_6)_{3n}}$ and 2D layered structure of $\mathbf{[L3_2FeCu(MeCN)]_n(PF_6)_{3n}}$.

The ionic radius for Ag^+ is larger than that of Cu^+ ion[31], which results in longer coordination bonds between pyridine nitrogen and silver than those of N-Cu. The N-Ag bonds of $\mathbf{[L3_2FeAg]_n(PF_6)_{3n}}$ joining layers are more elongated than those that are in the plane of layers. Taking into consideration similarities between both structures, it can be concluded that one of four pyridine rings in $\mathbf{[L3_2FeCu(MeCN)]_n(PF_6)_{3n}}$ is simply not able to reach enough distance

to coordinate to Cu(I) center due to sterical considerations. This is represented schematically in Figure 4.8. Therefore, selecting different metal ions one can tailor either fully coordinated 3D network, or 2D network leaving uncoordinated pyridines. Such heterometallic 2D layers with free pyridine arms might be of interest for surface chemistry and assembly of 2D crystals.

4.2.3. Properties

Compounds **$[L3_2FeAg]_n(PF_6)_{3n}$** and **$[L3_2FeCu(MeCN)]_n(PF_6)_{3n}$** are insoluble in alcohols, Et_2O, hydrocarbons, and dichloromethane, whereas they readily dissolve in acetonitrile and acetone. The ^1H and ^{13}C NMR spectra of vacuum dried and dissolved crystals of **$[L3_2FeAg]_n(PF_6)_{3n}$** and **$[L3_2FeCu(MeCN)]_n(PF_6)_{3n}$** in acetonitrile-$d_3$ are similar to that of **$[L3_2Fe](PF_6)_2$**. However, proton signals of 4-pyridyl groups are slightly shifted due to the presence of Ag(I) or Cu(I) ions. UV-vis spectra of **$[L3_2FeAg]_n(PF_6)_{3n}$** and **$[L3_2FeCu(MeCN)]_n(PF_6)_{3n}$** for dissolved crystals in acetonitrile are shown in Figures 4.9 and 4.10. There is no observable difference in absorption spectra of both compounds, and they are superimposable with the spectrum of **$[L3_2Fe](PF_6)_3$** in acetonitrile. The spectra of **$[L3_2FeAg]_n(PF_6)_{3n}$** and **$[L3_2FeCu(MeCN)]_n(PF_6)_{3n}$** exhibit strong ligand centered absorptions with maxima at 294 nm and weaker absorptions at lower energy that can be attributed to MLCT transitions. All the above mentioned observations suggest that the corresponding polymeric structures observed in solid state disassociate in acetonitrile solution due to the weak coordination of Cu(I) and Ag(I) to the 4-pyridyl groups. This can also be seen in the mass spectra (ESI) of the dissolved **$[L3_2FeAg]_n(PF_6)_{3n}$** and **$[L3_2FeCu(MeCN)]_n(PF_6)_{3n}$** in acetonitrile, where only discrete species, like $[Ag]^+$, $[Ag+MeCN]^+$ and $[L3_2Fe]^{2+}$ for **$[L3_2FeAg]_n(PF_6)_{3n}$** and, similarly, $[Cu+MeCN]^+$, $[Cu+2MeCN]^+$ and $[L3_2Fe]^{2+}$ for **$[L3_2FeCu(MeCN)]_n(PF_6)_{3n}$** can be seen (Figure 4.11 and 4.12). Nevertheless, this proves that Ag(I) and Cu(I) species were incorporated in both crystalline materials.

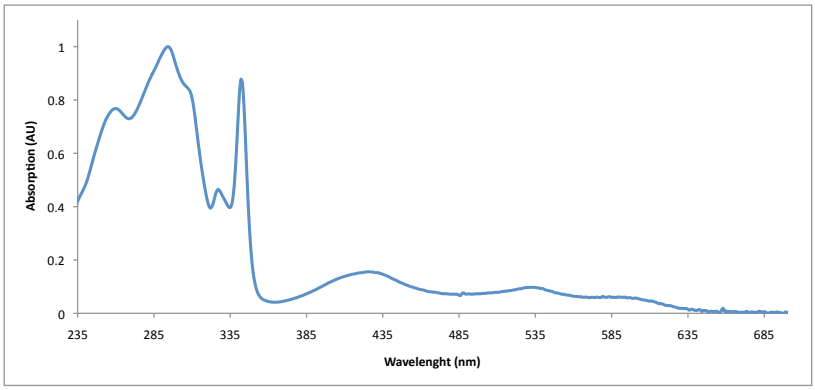

Figure 4.9. UV-vis of **$[L3_2FeAg]_n(PF_6)_{3n}$** in acetonitrile (λ_{max}= 294 nm, log ε = 5.12 $cm^{-1}mol^{-1}L$).

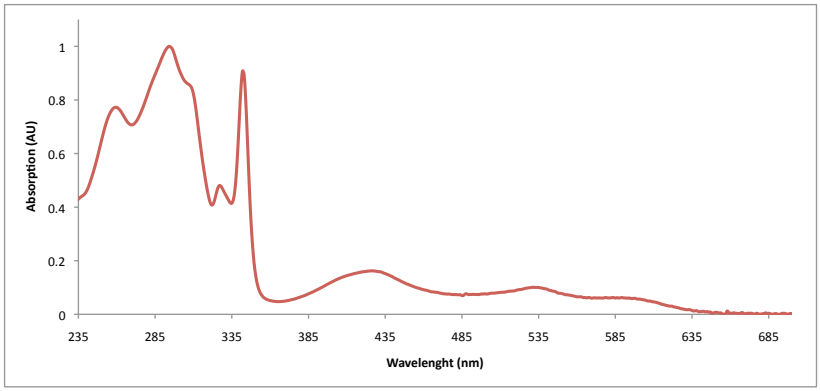

Figure 4.10. UV-vis of **$[L3_2FeCu(MeCN)]_n(PF_6)_{3n}$** in acetonitrile ($\lambda_{max}$= 294 nm, log ε = 5.12 $cm^{-1}mol^{-1}L$).

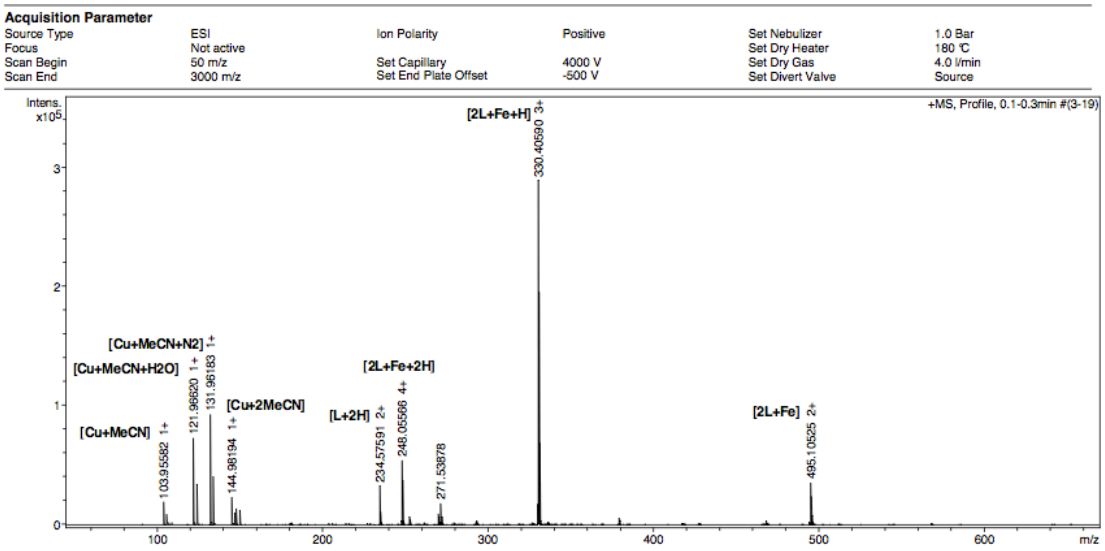

Figure 4.11. HRMS (ESI). Crystals of **$[L3_2FeCu(MeCN)]_n(PF_6)_{3n}$** dissolved in acetonitrile.

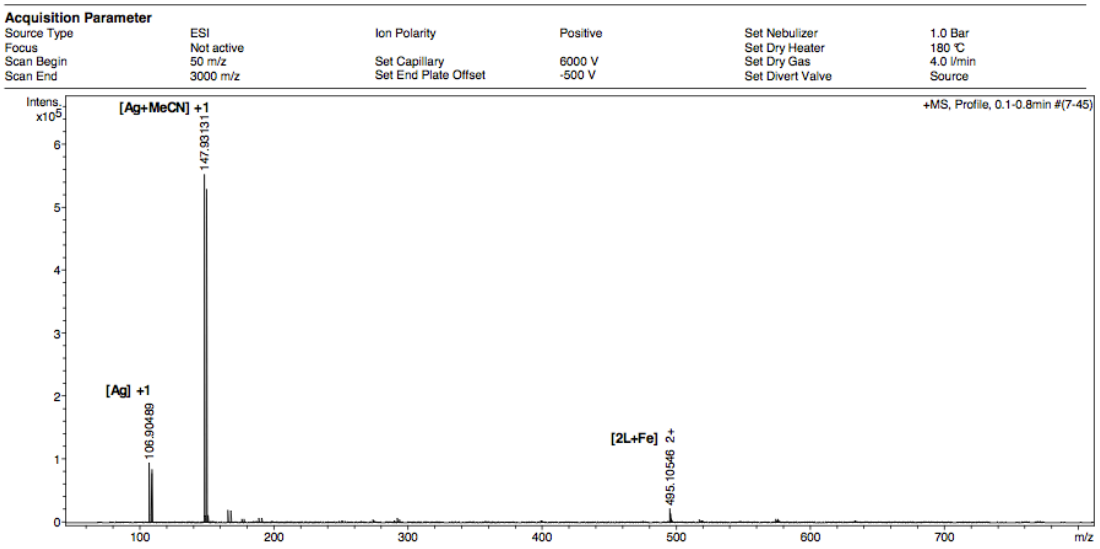

Figure 4.12. HRMS (ESI). Crystals of **$[L3_2FeAg]_n(PF_6)_{3n}$** dissolved in acetonitrile.

4.3. Conclusions

In summary, it has been shown that the linear bilateral extended *terpy* based Fe(II) "crossings" functionalized with 4-pyridiyl groups are able to assemble into the 3D or 2D MOFs by using metals preferring tetrahedral coordination geometry (Ag(I) and Cu(I), respectively). Substitution of flanking positions of linear bilateral extended *terpy* with directional functional groups allows constructing supramolecular assemblies and extended networks.

Given the fact that the convenient synthesis of the previously mentioned ligands has been developed, various functional groups can be easily introduced to address other supramolecular interactions like hydrogen, donor-acceptor, coordination bonding as well as strong metal-carboxylate bonds extensively utilized in the field of MOFs.

Therefore, linear bilateral extended *terpy* based fundamental building blocks with "crossing" and "corner" character are new tools in the hands of chemists and could inspire the creation of new designed molecular architectures.

4.4. Experimental Section

4.4.1. Materials and Methods

All reagents and solvents used for reactions were reagent grade and used without further purification unless otherwise noted. Commercial chemicals where used as received without special purification. Melting points were recorded on a Büchi B-540 melting point apparatus. For characterization purposes, proton nuclear magnetic resonance (^{1}H-NMR) spectra were all recorded on Bruker instruments (AV2- 400 at 400 MHz, and AV-500 at 500 MHz). Chemical shifts are reported in ppm relative to CD_3CN (δ 1.94). Carbon-13 nuclear magnetic resonance (^{13}C-NMR) spectra were recorded on Bruker instrument (AV-500 at 125 MHz). Chemical shifts are reported relative to CD_3CN (δ 1.3). Infrared spectroscopic data was recorded on Jasco FT/IR-4100 spectrophotometer. An Agilent 8453 UV/Vis spectrophotometer was used to record all UV/Vis spectra. ESI-HRMS spectra were recorded at the MS Facility of the Institute of Organic Chemistry of the University of Zurich.

4.4.2. Experimental Procedures

Synthesis of Heterometallic 3D MOF $[L3_2FeAg]_n(PF_6)_{3n}$

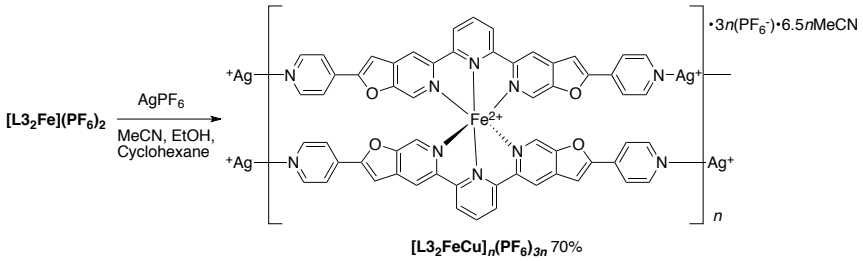

A solution of $AgPF_6$ (0.91 mg, 2.0 eq, 0.0036 mmol) in ethanol (0.5 mL) was layered over a solution of **$[L3_2Fe](PF_6)_2$** (2.31 mg, 1.0 eq, 0.00180 mmol) in acetonitrile (0.5 mL). A small amount of cyclohexane (~0.05 ml) between the layers was used to slow down the diffusion process. In few days needle-like crystals formed which over 2 weeks transformed into the dark purple blocks. A supernatant was removed with pipette and the crystals were washed with additional amount of EtOH (x2), then collected by filtration to give **$[L3_2FeAg]_n(PF_6)_{3n}$** (1.94 mg, 70%). The crystals for the single crystal X-ray diffraction analysis where kept in the mother liquor to avoid solvent loss.

The analytical sample for characterization was dried under vacuum at rt for 8 h:

Mp > dec 250° C.

^{1}H NMR (500 MHz, CD_3CN, δ): 8.99 (d, *J* = 8.2 Hz, 4H), 8.87 (s, 4H), 8.81 (t, *J* = 8.2 Hz, 2H), 8.66-8.64 (AA′BB′ spin system, 8H), 7.66-7.65 (AA′BB′ spin system, 4H), 7.54 (d, *J* = 0.9 Hz, 4H), 7.48 (s, 4H).

^{13}C NMR (125 MHz, CD_3CN, δ): 161.6, 159.8, 153.3, 152.6, 151.8, 139.4, 138.7, 138.2, 135.9, 123.5, 120.4, 118.0, 105.7.

FT-IR (neat, cm^{-1}): 3115*w*, 3078*w*, 3041*w*, 1607*m*, 1578*m*, 1450*m*, 1415*m*, 1320*m*, 1259*w*, 1225*w*, 1174*w*, 1041*w*, 991*w*, 918*w*, 834*s*, 808*s*, 746*m*, 689*m*, 661*m*, 555*m*.

HRMS (ESI) (solvent MeCN) *m/z*: $[Ag]^+$ calcd for Ag: 106.90454; found: 106.90489; $[Ag+MeCN]^+$ calcd for C_2H_3AgN: 147.93131; found: 147.93109; $[L3_2Fe]^{2+}$ calcd for $C_{58}H_{34}FeN_{10}O_4$: 495.10522; found: 495.10546; (**$[L3_2FeAg]_n(PF_6)_{3n}$** disassociates in MeCN, but $[Ag]^+$ and $[Ag+MeCN]^+$ species besides $[L3_2Fe]^{2+}$ in the mass spectrum support incorporation of silver ions in the product).

Crystallographic Data of **$[L3_2FeAg]_n(PF_6)_{3n}\cdot 6.5n$MeCN**

Crystallised from	MeCN / EtOH/Cyclohexane
Empirical formula	$C_{142}H_{107}Ag_2F_{36}Fe_2N_{33}O_8P_6$
Formula weight [g mol^{-1}]	3600.82
Crystal colour, habit	dark purple, prism
Crystal dimensions [mm]	0.10 × 0.25 × 0.35
Temperature [K]	160(1)
Crystal system	triclinic
Space group	$P\bar{1}$ (#2)
Z	2
Reflections for cell determination	39813
2θ range for cell determination [°]	4 − 55
Unit cell parameters *a* [Å]	17.3266(2)
b [Å]	21.9786(3)
c [Å]	23.2172(2)
α [°]	99.5900(10)
β [°]	108.8320(10)
γ [°]	107.2280(10)
V [$Å^3$]	7649.13(15)
F(000)	3628

D_x [g cm^{-3}]	1.563
μ(Mo $K\alpha$) [mm^{-1}]	0.611
Scan type	ω
$2\theta_{(max)}$ [°]	54.7
Transmission factors (min; max)	0.811; 1.000
Total reflections measured	86017
Symmetry independent reflections	31245
R_{int}	0.032
Reflections with $I > 2\sigma(I)$	23483
Reflections used in refinement	31245
Parameters refined; restraints	1858; 7163
Final $R(F)$ [$I > 2\sigma(I)$ reflections]	0.0749
$wR(F^2)$ (all data)	0.2252
Weights:	$w = [\sigma^2(F_o^2) + (0.1380P)^2 + 8.9667P]^{-1}$ where $P = (F_o^2 + 2F_c^2)/3$
Goodness of fit	1.095
Final Δ_{max}/σ	0.002
$\Delta\rho$ (max; min) [e Å^{-3}]	5.42; -1.51
$\sigma(d_{(C-C)})$ [Å]	0.005 – 0.007

Synthesis of Heterometallic 2D MOF $[L3_2FeCu(MeCN)]_n(PF_6)_{3n}$

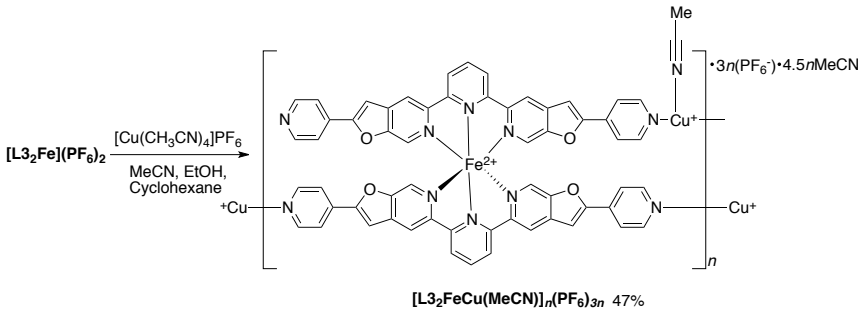

$[L3_2FeCu(MeCN)]_n(PF_6)_{3n}$ 47%

A solution of **$[L3_2Fe](PF_6)_2$** (4.75 mg, 1.0 eq, 0.00371 mmol) under N_2 in degassed acetonitrile (0.5 mL) was layered over a solution of $[Cu(CH_3CN)_4]PF_6$ (3.16 mg, 2.0 eq, 0.00742 mmol) in degassed EtOH (0.5 mL). A small amount of cyclohexane (~0.05 ml) between the layers was used to slow down the diffusion process. Over 3 weeks purple block like crystals formed. A supernatant was removed with pipette and the crystals were washed with additional amount of EtOH (x2), then collected by filtration to give

[L3$_2$FeCu(MeCN)]$_n$(PF$_6$)$_{3n}$ (2.67 mg, 47%). The crystals for the single crystal X-ray diffraction analysis where kept in the mother liquor to avoid solvent loss.

The analytical sample for characterization was dried under vacuum at rt for 6 h:

Mp > dec 300° C.

^{1}H NMR (400 MHz, CD_3CN, δ): 8.99 (d, *J* = 8.0 Hz, 4H), 8.87 (s, 4H), 8.81 (t, *J* = 7.99 Hz, 2H), 8.66-8.64 (AA′BB′ spin system, 8H), 7.6-7.65 (AA′BB′ spin system, 8H), 7.54 (s, 4H), 7.48 (s, 4H), 1.96 (s, 12H, corresponds to 4 CH_3CN molecules).

^{13}C NMR (125 MHz, CD_3CN, δ): 161.6, 159.8, 153.2, 152.6, 151.7, 139.4, 138.6, 138.1, 135.9, 123.5, 120.4, 117.9, 105.6.

FT-IR (neat, cm^{-1}): 3109*w*, 3047*w*, 1607*m*, 1570*m*, 1541*w*, 1450*m*, 1414*m*, 1318*m*, 1255*w*, 1178*w*, 1161*w*, 1042*w*, 988*w*, 962*w*, 917*w*, 837*s*, 740*w*, 690*m*, 655*m*, 556*s*.

HRMS (ESI) (solvent MeCN) *m/z*: $[Cu+MeCN]^+$ calcd for C_2H_3CuN: 103.95560; found: 106.90489; $[Cu+2MeCN]^+$ calcd for $C_4H_6CuN_2$: 144.98215; found: 144.98194. $[L3_2Fe+H]^{3+}$ calcd for $C_{58}H_{35}FeN_{10}O_4$: 330.40526; found: 330.40590; $[L3_2Fe]^{2+}$ calcd for $C_{58}H_{34}FeN_{10}O_4$: 495.10522; found: 495.10525; (**[L3$_2$FeCu(MeCN)]$_n$(PF$_6$)$_{3n}$** disassociates in MeCN, but the presence of $[Cu+MeCN]^+$ and $[Cu+2MeCN]^+$ species besides $[L3_2Fe]^{2+}$ species in the mass spectrum support the incorporation of copper ions in the product).

Crystallographic Data of **[L3$_2$FeCu(MeCN)]$_n$(PF$_6$)$_{3n}$·4.5*n*MeCN**

Crystallised from	MeCN / EtOH/Chex
Empirical formula	$C_{69}H_{50.5}CuF_{18}FeN_{15.5}O_4P_3$
Formula weight [g mol^{-1}]	1715.03
Crystal colour, habit	dark purple, prism
Crystal dimensions [mm]	0.20 × 0.25 × 0.28
Temperature [K]	160(1)
Crystal system	triclinic
Space group	$P\bar{1}$ (#2)
Z	2
Reflections for cell determination	20758
2θ range for cell determination [°]	5 − 57

Unit cell parameters	a [Å]	14.9414(2)
	b [Å]	15.3956(2)
	c [Å]	18.3235(2)
	α [°]	94.4451(12)
	β [°]	91.6360(11)
	γ [°]	113.0082(14)
	V [Å^3]	3860.05(9)
F(000)		1734
D_x [g cm^{-3}]		1.475
μ(Mo $K\alpha$) [mm^{-1}]		0.626
Scan type		ω
$2\theta_{(max)}$ [°]		56.7
Transmission factors (min; max)		0.820; 1.000
Total reflections measured		44801
Symmetry independent reflections		16211
R_{int}		0.033
Reflections with $I > 2\sigma(I)$		12223
Reflections used in refinement		16211
Parameters refined; restraints		1028; 1021
Final $R(F)$ [$I > 2\sigma(I)$ reflections]		0.0643
	$wR(F^2)$ (all data)	0.2069
Weights:	$w = [\sigma^2(F_o^2) + (0.1266P)^2 + 1.64P]^{-1}$ where $P = (F_o^2 + 2F_c^2)/3$	
Goodness of fit		1.084
Final Δ_{max}/σ		0.002
$\Delta\rho$ (max; min) [e Å^{-3}]		1.01; -0.80
$\sigma(d_{(C-C)})$ [Å]		0.004 – 0.009

4.5. References

(1) Lehn, J.-M. *Supramolecular chemistry: Concepts and perspectives*; VCH: Weinheim, **1995**.

(2) Hoskins, B. F.; Robson, R. *J. Am. Chem. Soc.* **1990**, *112*, 1546–1554.

(3) Yaghi, O. M.; Li, H.; Eddaoudi, M.; O'Keeffe, M. *Nature* **1999**, *402*, 276–279.

(4) Yaghi, O. M.; O'Keeffe, M.; Ockwig, N. W.; Chae, H. K.; Eddaoudi, M.; Kim, J. *Nature* **2003**, *423*, 705–714.

(5) Furukawa, H.; Cordova, K. E.; O'Keeffe, M.; Yaghi, O. M. *Science* **2013**, *341*, 1230444.

(6) Rosi, N. L.; Eckert, J.; Eddaoudi, M.; Vodak, D. T.; Kim, J.; O'Keeffe, M.; Yaghi, O. M. *Science* **2003**, *300*, 1127–1129.

(7) Getman, R. B.; Bae, Y. S.; Wilmer, C. E.; Snurr, R. Q. *Chem. Rev.* **2012**, *112*, 703–723.

(8) Sumida, K.; Rogow, D. L.; Mason, J. A.; McDonald, T. M.; Bloch, E. D.; Herm, Z. R.; Bae, T. H.; Long, J. R. *Chem. Rev.* **2012**, *112*, 724–781.

(9) Suh, M. P.; Park, H. J.; Prasad, T. K.; Lim, D. W. *Chem. Rev.* **2012**, *112*, 782–835.

(10) Li, J. R.; Sculley, J.; Zhou, H. C. *Chem. Rev.* **2012**, *112*, 869–932.

(11) Fujita, M.; Kwon, Y. J.; Washizu, S.; Ogura, K. *J. Am. Chem. Soc.* **1994**, *116*, 1151–1152.

(12) Lee, J.; Farha, O. K.; Roberts, J.; Scheidt, K. A.; Nguyen, S. T.; Hupp, J. T. *Chem. Soc. Rev.* **2009**, *38*, 1450–1459.

(13) Li, Q.; Zhang, W.; Miljanic, O. S.; Sue, C. H.; Zhao, Y. L.; Liu, L.; Knobler, C. B.; Stoddart, J. F.; Yaghi, O. M. *Science* **2009**, *325*, 855–859.

(14) Liang, L. L.; Ren, S. B.; Zhang, J.; Li, Y. Z.; Du, H. B.; You, X. Z. *Dalton Trans.* **2010**, *39*, 7723–7726.

(15) Cui, Y.; Yue, Y.; Qian, G.; Chen, B. *Chem. Rev.* **2012**, *112*, 1126–1162.

(16) Dirtu, M. M.; Rotaru, A.; Gillard, D.; Linares, J.; Codjovi, E.; Tinant, B.; Garcia, Y. *Inorg. Chem.* **2009**, *48*, 7838–7852.

(17) Garcia, Y.; Ksenofontov, V.; Mentior, S.; Dirtu, M. M.; Gieck, C.; Bhatthacharjee, A.; Gutlich, P. *Chem. Eur. J.* **2008**, *14*, 3745–3758.

(18) Garcia, Y.; Kahn, O.; Rabardel, L.; Chansou, B.; Salmon, L.; Tuchagues, J. P. *Inorg. Chem.* **1999**, *38*, 4663–4670.

(19) Halder, G. J.; Kepert, C. J.; Moubaraki, B.; Murray, K. S.; Cashion, J. D. *Science* **2002**, *298*, 1762–1765.

(20) Niel, V.; Thompson, A. L.; Munoz, M. C.; Galet, A.; Goeta, A. E.; Real, J. A. *Angew. Chem., Int. Ed.* **2003**, *42*, 3760–3762.

(21) Keskin, S.; Kızılel, S. *Ind. Eng. Chem. Res.* **2011**, *50*, 1799–1812.

(22) Liu, D.; Huxford, R. C.; Lin, W. *Angew. Chem., Int. Ed.* **2011**, *50*, 3696–3700.

(23) Ma, Z.; Moulton, B. *Coordin. Chem. Rev.* **2011**, *255*, 1623–1641.

(24) Deng, H.; Doonan, C. J.; Furukawa, H.; Ferreira, R. B.; Towne, J.; Knobler, C. B.; Wang, B.; Yaghi, O. M. *Science* **2010**, *327*, 846–850.

(25) Tranchemontagne, D. J.; Hunt, J. R.; Yaghi, O. M. *Tetrahedron* **2008**, *64*, 8553–8557.

(26) Stock, N.; Biswas, S. *Chem. Rev.* **2012**, *112*, 933–969.

(29) O'Keeffe, M.; Yaghi, O. M. *Chem. Rev.* **2012**, *112*, 675–702.

(30) Reticular Chemistry Structure Resource, http://rcsr.anu.edu.au/nets/dia-b

(31) Shannon, R. D. *Acta Crystallogr., Sect. A: Found. Crystallogr.* **1976**, *32*, 751–767.

Chapter 5. Towards Kinetic Synthesis of the Molecular Borromean Link

5.1. Introduction

Human mind is free in its ability to imagine and comprehend complex ideas, concepts, and geometrical shapes. The art and science are the mirrors of this freedom where human being is trying to crash the unsurpassable border between his mind and the physical world, in which we all are inevitably enclosed. Human imagination far exceeds the limitations of the real world – luckily, there are many people who are brave enough to step outside of what we can see, smell, hear, and feel. Our convenient 3D space, perception of time and matter is challenged by modern physics, mathematics, and chemistry. The quantum physics shows that the laws that apply to familiar macroscopic objects are not applicable to the atomic and subatomic particles[1]. Mathematics can open the doors to other dimensions.[2] Whereas chemistry, the discipline of the science, which is privileged to transform the matter on the molecular scale, allows the creation of new forms of matter – substances that have never existed before[3]. This is where humans can surpass nature; however, to my mind, this is an ambiguous statement, because we are a part of nature. Let us leave this question to philosophy – other discipline celebrating the freedom of the human mind[4]. The field of chemistry allows the pure imagination of the human mind to be materialized on the molecular level. History has shown that fundamental research driven by pure curiosity creates a basis for the benefit of the whole society. Chemistry of "unnatural" products allows the creation of substances with new properties non-existent in nature[5,6].

5.1.1. Chemistry and Topology

Chemistry of topologically complex molecules deals with the structures whose abstract graphs cannot be represented in 2D plane. A graph without any embedding that can be represented in the plane is said to be *nonplanar*[7]. Topologically complex DNA superstructures and proteins with nonplanar graphs are known to occur in biology[8,9]; however, in chemistry this is an extremely uncommon phenomenon and requires special synthetic design[10]. Most molecules have abstract graphs with zero crossings of edges. Even such molecule as fullerene, which is known to have a ball-shaped structure[11,12], from the perspective of topology, has a simple abstract graph, which can be represented in 2D plane (Figure 5.1), assuming that the bonds are flexible edges and the carbon atoms are nodes.

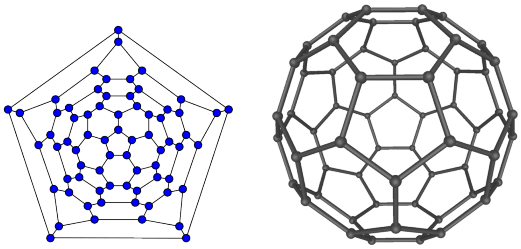

Figure 5.1. The planar topology of fullerene[13,14].

Mathematics and knot theory inspire chemists to look for topologically complex shapes.[7] The *knot* can be defined as "a simple closed polygonal (or smooth) curve embedded in 3-space"[15], whereas *link* is considered to be a combination of knots. Therefore, in mathematical sense all knots are based on a circle (unknot) (Figure 5.2, A). The simplest is a trefoil knot that exhibits three crossings, which is the smallest possible number (Figure 5.2, B). The simplest nontrivial knot consists of two interlocked rings (unknots), which is called Hopf link (Figure 5.2, C).[16] In three-dimensional space abstract graphs of both trefoil knot and Hopf link cannot be represented in plane; however, higher order dimensions could allow the transformation of these into separate unknots.[17]

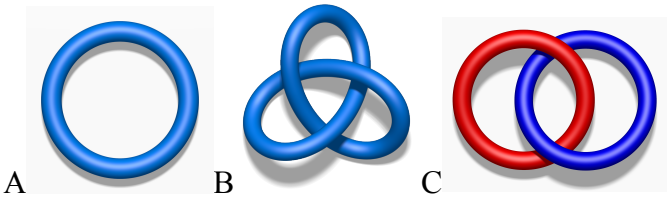

Figure 5.2. A. Unknot[18]; B. Trefoil knot[19]; C. Hopf Link[20].

This kind of graphs are called *extrinsically nonplanar*. In 1930, Kuratowsky proved that only K_5 and $K_{3,3}$ graphs (Figure 5.3) can be *intrinsically nonplanar*, or truly topologically nonplanar.[21] However, from the perspective of chemical topology both intrinsic and extrinsic graphs are of great interest to the field. Incredible progress of chemical science in recent decades has allowed many of these theoretical shapes to be materialized on the molecular level.

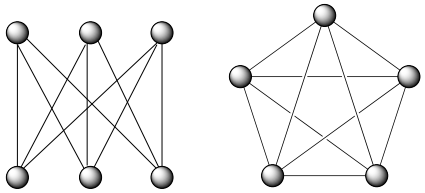

Figure 5.3. Intrinsically nonplanar graphs $K_{3,3}$ and K_5.

In 1961, Wasserman reported the first compound where description of the topology was important.[22] Macrocyclization of diethyl tetratriacontanedioate in the presence of large deuterated cycloalkane provided statistical byproducts, and one of them consisted of two mutually interlocked rings (Figure 5.4). The identity of the product was established by chemical methods. In chemistry, such molecules with Hopf link topology are known as *catenanes*. This shift of paradigm has inspired the construction of other molecules of topological importance.

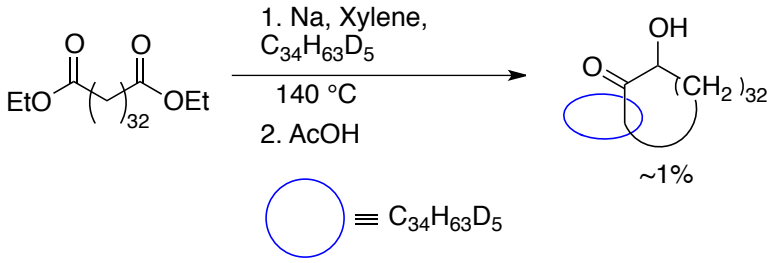

Figure 5.4. Wasserman's statistical synthesis of catenanes.

In order to obtain topologically interesting targets, the major focus became the development of more efficient and directed synthetic strategies.

In 1965, Schill published the first successful directed synthesis of catenane.[23,24] This approach was based on the properly functionalized templating core, which allowed the construction of interlocked macrocycles around it (Figure 5.5).

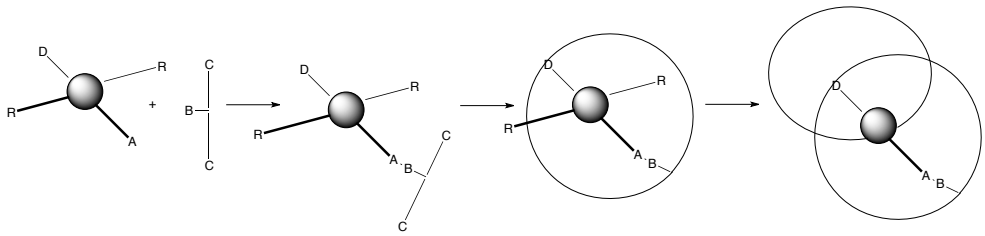

Figure 5.5. Schematic representation of Schill's directed synthesis of catenane.

Frisch and Wasserman envisioned the Möbius ladder approach towards various knotted and catenated structures. Different number of twists and rungs in the Möbius ladder could result in interesting topological consequences.[25] The first successful synthesis of the Möbius strip was reported by Walba[26], where the ladder with three rungs after macrocyclization afforded the mixture of the topologically desired product, as well as a conventional ring structure (Figure 5.6). However, attempts to obtain knotted or linked structures by cleavage of the rungs were not successful.

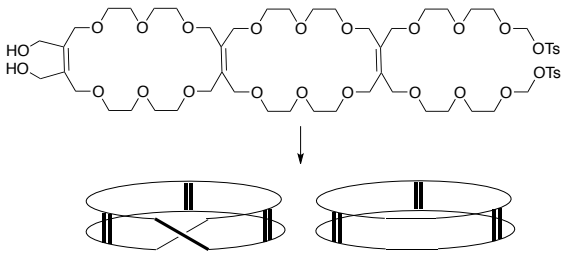

Figure 5.6. Walba's synthesis of the Möbius strip via three rung ladder.

The first molecule possessing the intrinsically nonplanar graph K_5 (Figure 5.3) was synthesized independently by Simmons and Paquette in 1981.[27,28] The $K_{3,3}$ molecules were prepared by Walba[29] and Siegel[30].

In 1983, Sauvage reported the first successful metal templated synthesis of catenanes, which was a real breakthrough in chemical topology.[31,32] The complexation of two phenatroline ligands with copper(I) and subsequent alkylation/macrocyclization afforded metallo-catenane (Figure 5.7). The removal of metal ions liberated free catenanes.

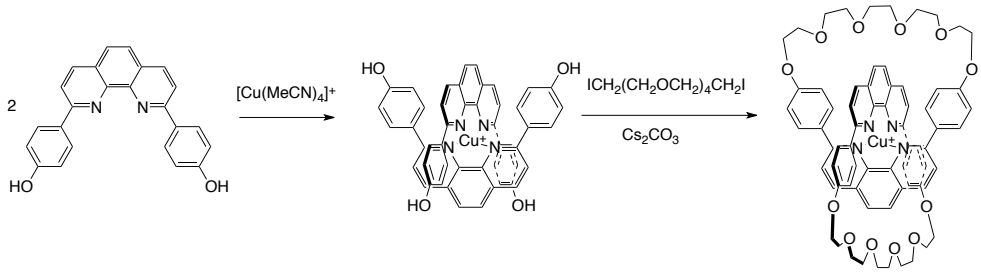

Figure 5.7. Sauvage's metal template synthesis of catenane.

Such approach stimulated the synthesis of various supramolecular architectures[33,34] like rotaxanes[35], knots and polycatenanes[10], molecular grids[36], ladders and helicates[37]. Also, other supramolecular interactions, like hydrogen and donor-acceptor, were successfully utilized for various topologically interesting targets.[38] Leigh developed the active metal template strategy which is based on the principle that metal ions can be both the template and catalyst for macrocyclization at the same time.[39,40]

The work presented in this chapter also deals with the control of the topology based on the metal templation.

5.1.2. The Borromean Link

The knot theory reveals a fascinating example of the nontrivial link consisting of three interlocked loops with remarkable topological properties – no two loops are mutually linked;

however, the combination of all three generates a linked structure. Cleavage of one loop results in separation of other two.

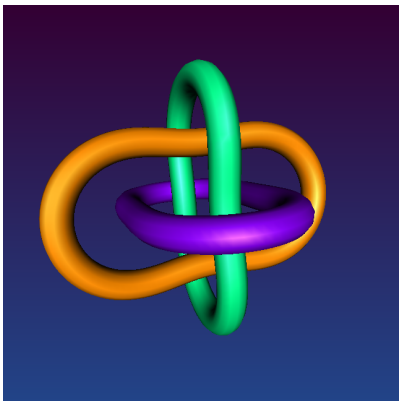

Figure 5.8. The Borromean link.[41]

Such link is known as *the Borromean Link* (Figure 5.8), which is named after the family crest of the Borromeos, an Italian family from the Renaissance[42]. The Rolfsen notation[43] for this link is 6_2^3, where six stands for the minimal amount of crossings in its reduced representation, superscript describes the number of loops involved, and subscript is the index distinguishing between the links with the same number of components. The above-mentioned topological property can also exist for links with more than three rings, and these are called *Brunnian Links*. Another interesting feature of the Borromean link is that it is topologically achiral in its reduced presentation, even when all rings are oriented.[17]

In 1961, Wasserman was the first to suggest that a molecule with the Borromean link topology could theoretically form in the macrocyclization reaction as a statistical side product.[25] Afterwards, many other more rational approaches were offered. In 1985, Walba proposed a strategy which anticipated that three-stranded braid bound with two rungs, after cyclization and cleavage, could theoretically form the Borromean link (Figure 5.9).[17]

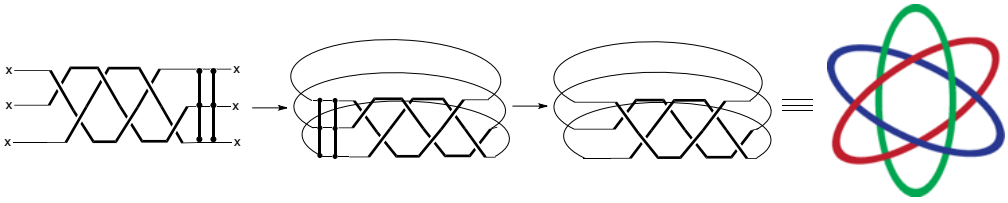

Figure 5.9. Three-stranded braid approach towards the Borromean link.

The Borromean link can be represented in various embeddings. The three most common representations are shown in Figure 5.10 [44]. Since the chemical synthesis deals not only with the topology of the molecular graph but also with the real molecular structure in 3D space, a

particular embedding should be taken into consideration to develop a reasonable synthetic strategy.

The most common is S_6 symmetric Venn diagram[45] depicted in Figure 5.10, example A.

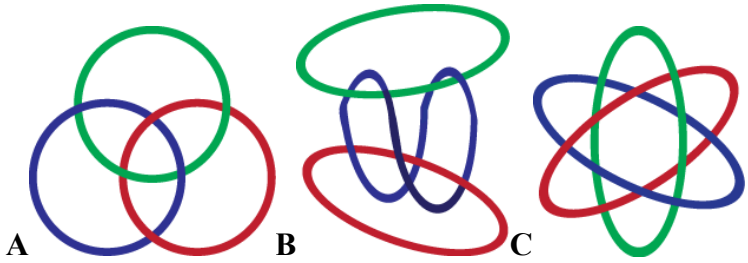

Figure 5.10. The Borromean Link. **A**. *Venn diagram*; **B**. *Chain rings*; **C**. *Orthogonal rings*.

In 2003, Loren, Yoshizawa and Siegel proposed retrosynthetic strategies towards these three Borromean link representations. A careful inspection of the Venn diagram reveals that it can be derived from the trefoil knot motif – triskelion (Figure 5.11).[46,47] The retrosynthesis of chain rings leads to the properly functionalized rack structure (Figure 5.12).[44]

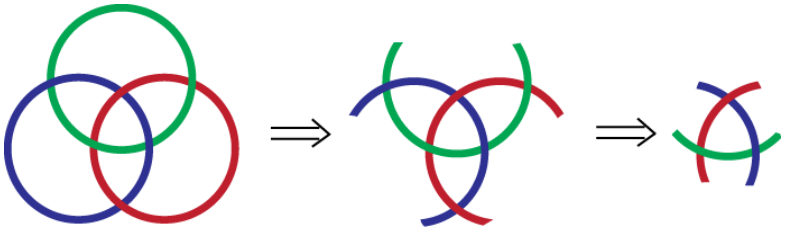

Figure 5.11. Schematic retrosynthesis of the Venn diagram leading to the triskelion motif.

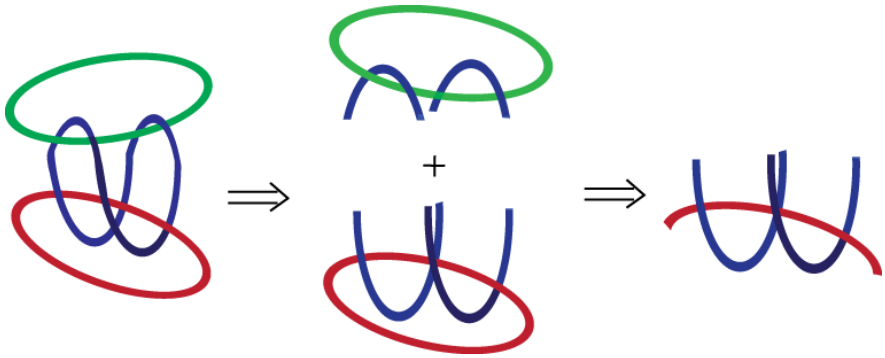

Figure 5.12. Schematic retrosynthesis of chain rings.

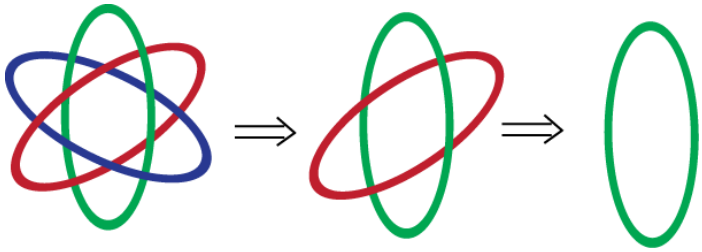

Figure 5.13. Schematic retrosynthesis of the orthogonal ring.

However, the orthogonal representation of the Borromean link could be obtained in a stepwise ring-by-ring synthesis (Figure 5.13).

The nucleobases form base-pairs in a controllable manner[48] – the necessary template for the synthesis of topologically complex structures. In 1997, Seeman and coworkers showed that the proper choice of complimentary DNA strands after ligation formed the first structure possessing the Borromean topology on the molecular scale (Figure 5.14).[49] This DNA superstructure is derived from the Venn diagram by replacing each crossing with 1.5 turns of double helix. The correct topology was supported by a selective scission of only one ring. The digestion products were analyzed by the gel electrophoresis, which supported the liberation of two separate rings besides the breakdown products of the first ring.

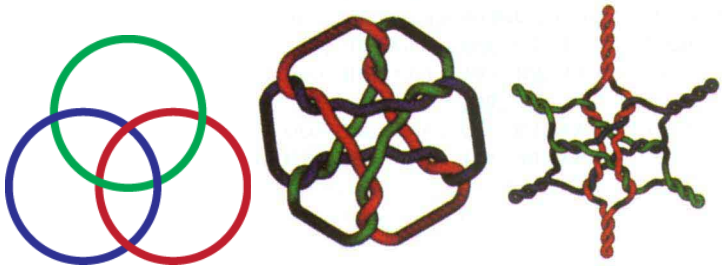

Figure 5.14. Seeman's DNA superstructure with the Borromean topology. Adapted with permission from ref.[48]. Copyright Macmillan Publishers Ltd (1997).

The spontaneous assembly, or sometimes called "programmed behavior",[5,50] is a powerful approach towards the complex supramolecular targets. In 2004, Stoddart group employed the thermodynamic assembly of the Borromean link zinc(II) complex by exploiting the reversible character of the imine bond formation and templating character of the Zn(II) ions[51]. They were able to obtain S_6 symmetric structure that resembles the Venn diagram representation of the Borromean link (Figure 5.15). After reduction of the imine bonds and removal of zinc ions the free nanoscale Borromean link can be liberated.[52] This one pot synthesis is a landmark of chemical topology and directed assembly process.

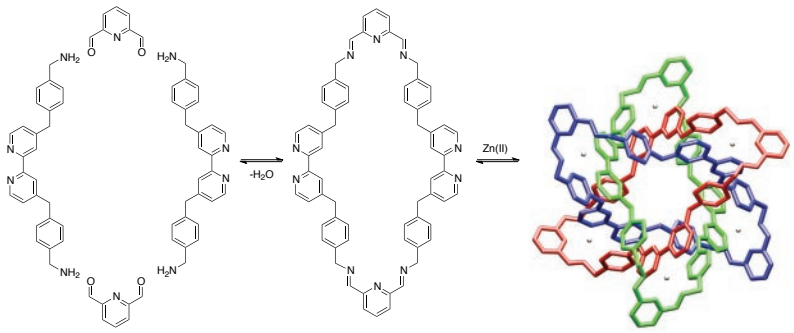

Figure 5.15. Stoddart's synthesis of the Borromean link. Adapted with permission from ref. [51]. Copyright AAAS (2004).

Stoddart group also challenged the topologically achiral nature of the Borromean link by using enantiomerically pure starting materials. They were able to assemble the chiral version of the Borromean link Zn(II) complex which possesses C_1 symmetry (Figure 5.16).[53] The chirality results from the particular embedding of the molecular graph in 3D space; however, form the point of view of topology, the abstract graph of this structure still remains achiral.

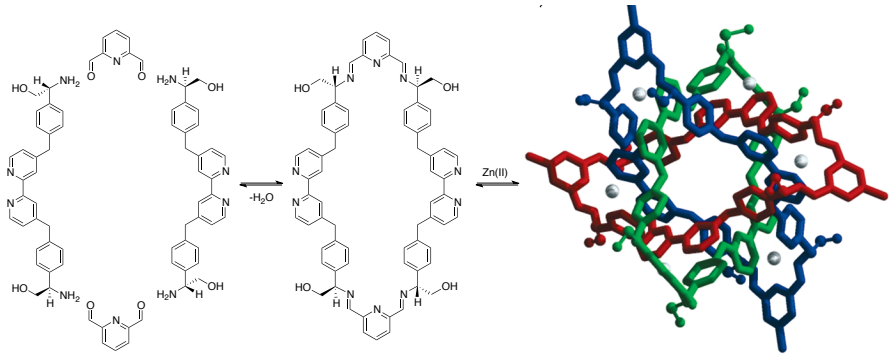

Figure 5.16. Stoddart's synthesis of the chiral Borromean Link. Adapted with permission from ref.[53]. Copyright John Wiley & Sons Inc (2006).

5.1.3. Attempts Towards the Borromean Link in Siegel Group

In 2003, Loren et al. reported on the synthetic attempts towards the stepwise construction of the molecular Borromean link.[44] The retrosynthesis of this approach is depicted in Figure 5.17. It was anticipated that the reaction of the macrocycle **I**, posessing endocyclic coordination sites, with the heteroleptic metal complex **H** could form the threaded macrocycle **G**.

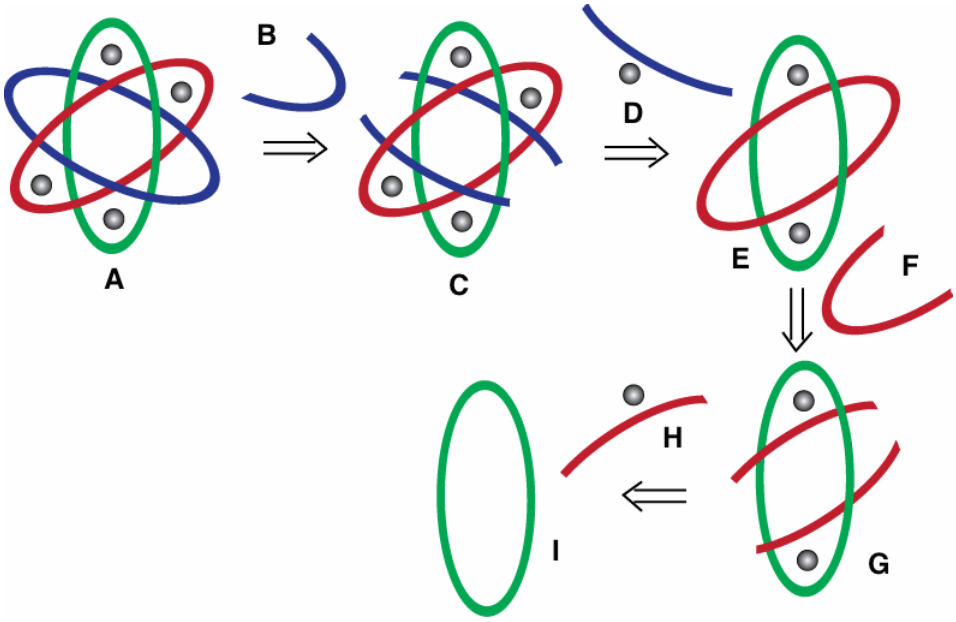

Figure 5.17. Lorens's and Yoshizawa's approach towards the Borromean link.

It was expected that **G** together with the cap **F** could be further converted to the ring-in-ring complex **E**. Subsequently, another threading with **D** would afford the macrocyclic complex **C**. The third and the final ring could be constructed by coupling the cap **B** with the threaded macrocycle **C** to give the Borromean link metal complex **A**.[54]

The synthesis was started from the manisyl substituted terpyridine **85a** which upon several functional group transformations was converted to the ethynyl substituted terpyridine **85c** (Scheme 5.1). Complexation with Cu(II) and the subsequent Eglinton reaction gave the macrocycle **87** in high yield. Then hydrogenation of the triple bonds gave the macrocycle **88** – the key intermediate for the further development of this synthetic strategy.

Scheme 5.1. Lorens's and Yoshizawa's Synthesis of Ru(II) Ring-in-ring Complex 91

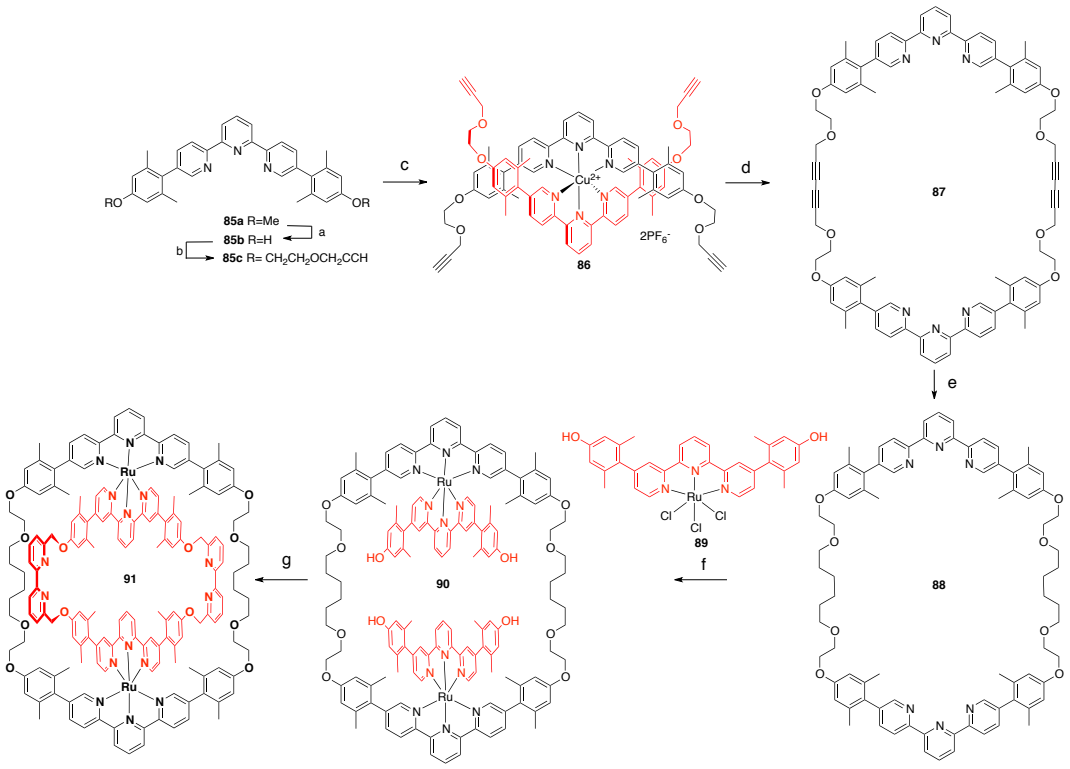

Reaction conditions: a) Py-HCl, 185 °C, 4 h, 97%. b) Cs_2CO_3, $TsO(CH_2)_2OCH_2CCH$ (2.2eq), DMF, 80 °C, 10 h, 69%. c) $Cu(OAc)_2 \cdot H_2O$ (0.5 eq), EtOH, rt, 1 h. d) $Cu(OAc)_2 \cdot H_2O$ (10.0 eq), EtOH (high dil.), reflux, 72 h, 91%. e) H_2, 80 psi, 10% Pd-carbon, 1:1 EtOH:CH_2Cl_2, 6 h, 91%. f) 198 (2.1 eq), 2:2:1 CH_2Cl_2:EtOH:ethylene glycol, reflux, 12 h, 65%. g) 6,6′-bisbromomethyl-2,2′-biypyridine (2.1 eq), Cs_2CO_3, ACN, 72 h, 49%.

Furthermore, threading of the ring **88** with the $RuCl_3$ complex of the "W"-shaped terpyridine **89** gave the Ru(II) complex **90**. The distance between both phenolic hydroxyl groups on the opposite ligands is ~8 Å. This allowed to perform alkylation of **90** with two equivalents of 6,6′-bisbromomethyl-2,2′-biypyridine, affording the ring-in-ring complex **91**.[44] Unfortunately, all attempts to introduce the third ring fragment by complexation with copper were not

successful. Loren suggested that the problematic threading might be caused by the *transoid* conformation of uncomplexed 2,2′-bipydidine (*bipy*) coordination site.

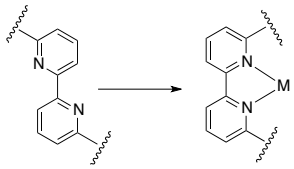

The metal complexation would switch the conformation of *bipy* to *cisoid*, thus causing a significant strain to the whole macrocyclic system (Figure 5.18, A.).[54]

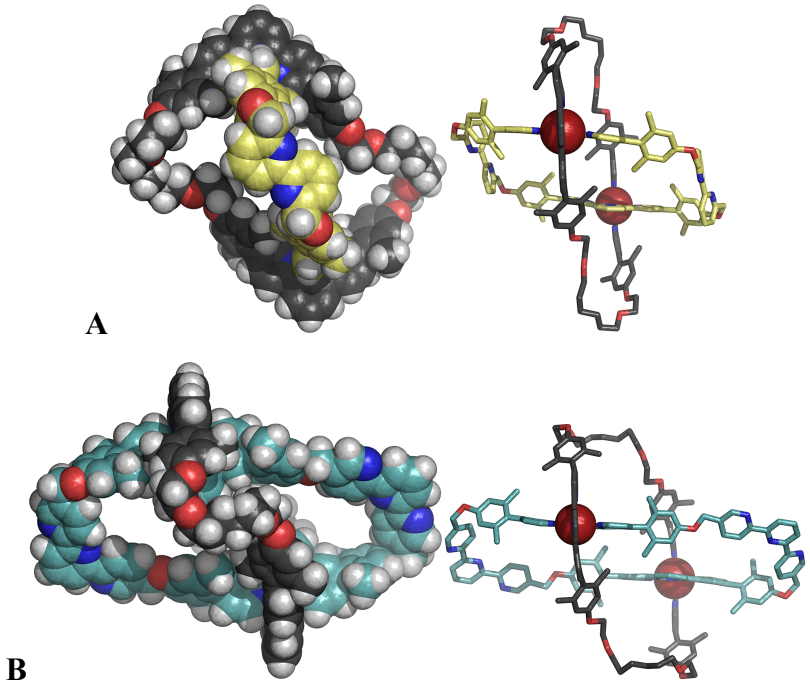

Figure 5.18. X-ray structures of **A.** Loren's ring-in-ring Ru(II) complex **91**.
B. Klosterman's ring-in-ring Ru(II) complex **93**[55,56].

Therefore, Loren synthesized the two-ring structure **92** with phenantroline binding sites already having the correct conformation of the bidentated pockets (Scheme 5.2). However, the threading was also not successful (Scheme 5.3).

Jeremy Klosterman was able to synthesize similar structures **93** and **94** with terpyridine cap to increase the cavity accessible for the threading (Scheme 5.2 and Figure 5.18, B.).[55] However, all attempts to obtain the desired threading products failed, too (Scheme 5.3).

Scheme 5.2. Ring-in-ring Structures Synthesized in Siegel Group

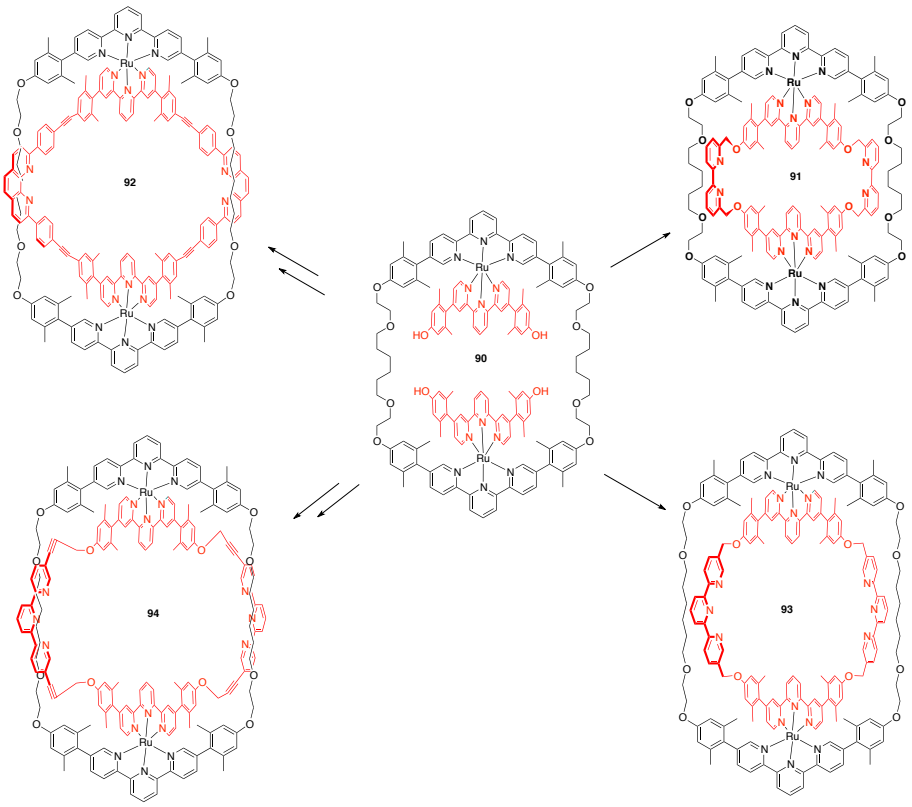

Scheme 5.3. Unsuccessful Attempts for the Introduction of The Third Ring Motif

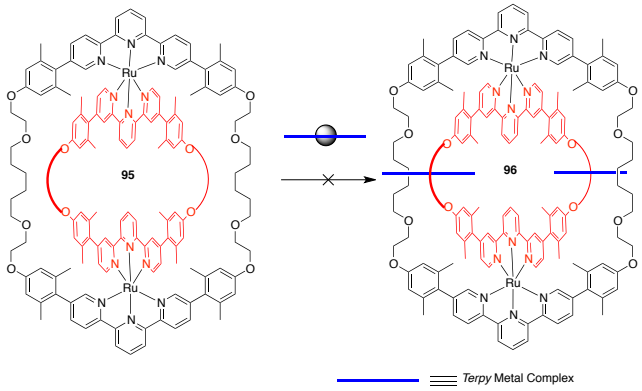

Klosterman proposed an alternative strategy to avoid the problematic threading step (Figure 5.19). This rout relies on an already preformed cap **D** which could be a heteroleptic Ru(II) complex.[55]

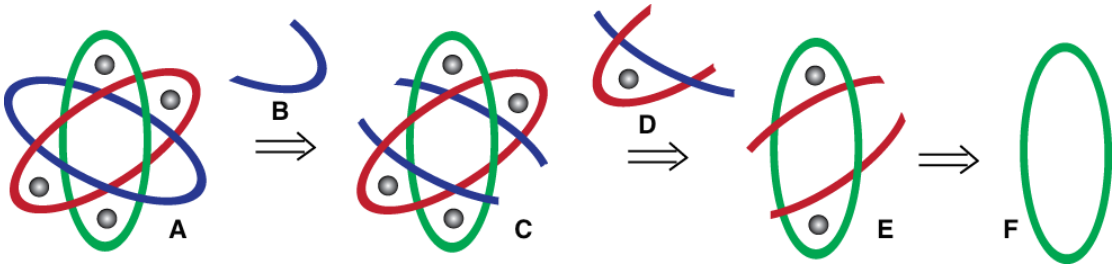

Figure 5.19. Klosterman's strategy based on the preformed hetereoleptic complex **D**.

This strategy would allow avoiding problems that are caused by the conformational change of polypyridine binding pockets. Unfortunately, the correct combination of the functional groups to successfully perform capping was never reached.[55]

Derik Frantz proposed to use an orthogonal thioketal cap as an alternative to the metal coordination (Figure 5.20). Thioketal functional group can be cleaved in the hydrogenolysis reaction[57], which would be helpful upon liberation of the interlocked rings. However, introduction of such cap on the threaded macrocycle **90** was unsuccessful.[58]

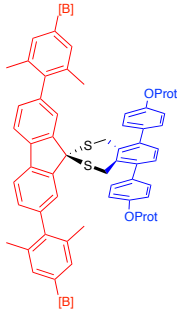

Figure 5.20. Thioketal cap proposed by Derik Frantz.[58]

Helen Seifert was able to modify the original Jon Loren's double threaded macrocycle **90** by replacing "W"-terpyridine ligands with linear bilateral extended *terpy* (Scheme 5.4)[59]. The complex **98** was characterized by the single crystal X-ray diffraction analysis (Figure 5.21), which revealed that the distance between both flanking hydroxyl groups on the opposite ligands is around 19 Å – it is twice as much as for the Loren's macrocycle **90** (8 Å). This opened the doors for the further investigation towards the kinetic synthesis of the Borromean link.

Scheme 5.4. Seifert's Threaded Ru(II) Macrocycle 98

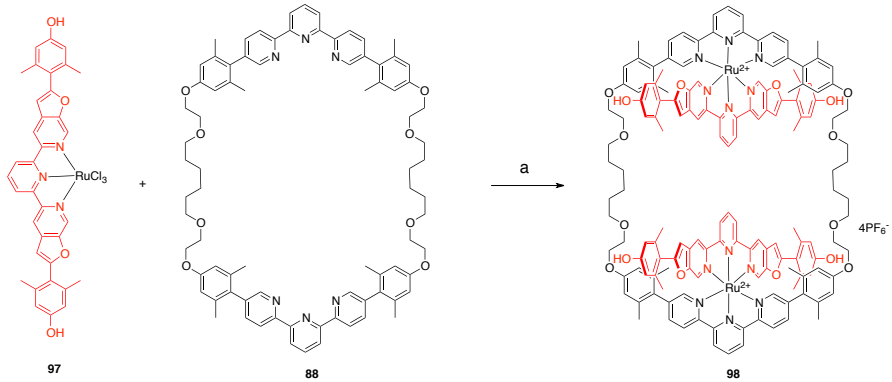

Reaction conditions: a) 1,2-dichloroethane/EtOH/ethylene glycol 3:3:2, 120 °C, 3 d, 26%.

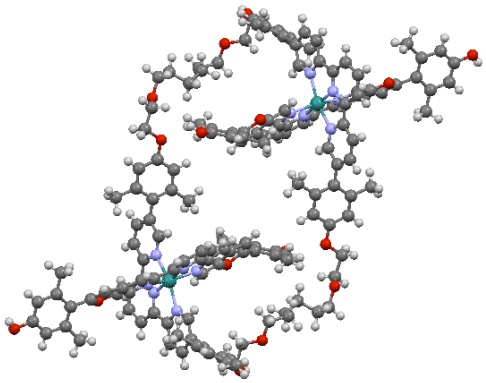

Figure 5.21. X-ray structure of Seifert's double threaded macrocycle **98**.[59]

5.2. Current Work

The landmark of thermodynamic assembly and topological chemistry is the Stoddard's approach towards the molecular Borromean link.[51] However, there are several limitations to this approach; for example, the Borromean link consisting of three different rings cannot be obtained by the above described methodology. The control over the thermodynamic assembly is usually limited to specific substrates, and subtle modifications of such dynamic systems can bring an unexpected outcome; therefore, serendipity often plays the major role.[60] The stepwise kinetic synthesis of the molecular Borromean link is still an open problem. However, this chapter describes a significant leap towards this long-standing goal.

The goal of the current work is to combine all the knowledge that has been accumulated in Siegel group[44,54,55,58,59] regarding the synthesis of extended ring-structures and extract the most promising directions towards the kinetic synthesis of the molecular Borromean link. Several problems "crystallized" out of the huge synthetic efforts performed before in the group (Figure 5.22):

- Unsuccessful threading of the ring 3 motifs;
- Insufficient cavity available for threading;
- Limited flexibility of the ring 2;
- Conformation change of *terpy* or *bipy* upon metal complexation, which causes a strain on the whole structure;
- Correct choice of the denticity and size of the binding motif of the ring 2;
- Selection of proper functional groups compatible with the further chemical manipulations.

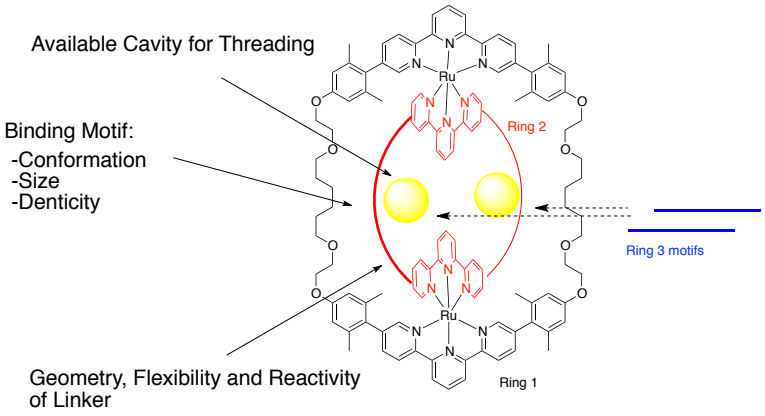

Figure 5.22. Important parameters for the introduction of the third ring.

Several objectives were set in our pursuit towards the improvement of the synthesis:

- The linear bilateral extended *terpy* ligands could be further used to construct the rings 2 and 3 to gain larger cavities available for threading;
- A flexible chain motif could be incorporated in the ring 2, so that it could adjust a proper conformation when the third ring is constructed;
- Synthetic route should be as convergent as possible;
- Number of synthetic steps should be reduced, especially those that are applied on the highly advanced intermediates;
- The final step of the synthesis should be reliable, efficient, and high yielding.

The extended geometry of the linear bilateral extended terpyridine ligands make them a valuable building block for the further synthesis. Klosterman's proposed strategy based on the pretemplated Ru(II) cap[55] in combination with Seifert's threaded ring **98**[59], offering potentially larger void space, seemed to be a promising approach to our pursuit towards the kinetic synthesis of the molecular Borromean link. However, the major challenge was expected when dealing with bigger structures that have more degrees of freedom – the potential formation of exo-/endocyclic stereoisomers. This chapter shows the feasibility of chemistry selected for the synthesis of the molecular Borromean link, but the control over stereochemistry is still an open problem.

5.2.1. Sonogashira Coupling Strategy

Initially, the synthetic route via heteroleptic Ru(II) complex was chosen, originally proposed by Klosterman[55]. A schematic representation of the retrosynthesis is shown in Figure 5.23. The pretemplated heteroleptic Ru(II) complex **D** should bear ligands with two different functional groups to discriminate reactivity necessary for the coupling with the

threaded macrocycle **E** and macrocyclization of the third ring with linker **B**. Therefore, the heteroleptic Ru(II) complex **99** (cap **D**) was chosen as the first synthetic target (Figure 5.24). The first ligand of the complex **99** could be functionalized with flexible linkers and good leaving groups suitable for the alkylation reactions[61], but the second ligand could bear aryl bromide moieties suitable for the cross coupling chemistry[62].

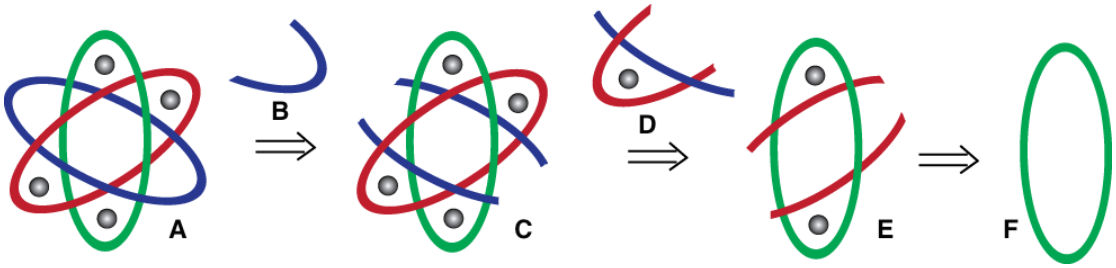

Figure 5.23. Schematic retrosynthesis of the Borromean link via pretemplated Ru(II) cap **D**.

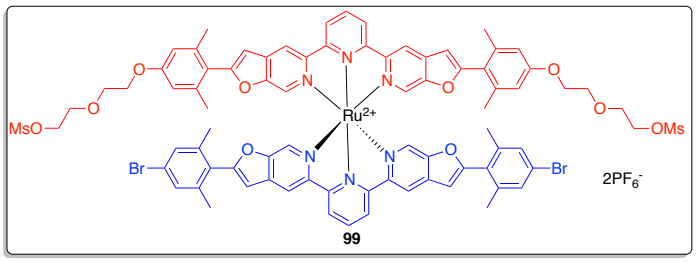

Figure 5.24. Heteroleptic Ru(II) complex **99** as a potential pretemplated cap.

The synthesis of necessary ligands was started from the diiodoterpyridine **69** (Scheme 5.5) which was coupled to the corresponding acetylenes **59** under the standard Sonogashira coupling conditions[62] to give either bromo- or methoxy- substituted diacetylenes **78**. The following one-pot MOM deprotection and cycloisomerization gave linear bilateral extended terpyridines **L8** and **L12**.

Scheme 5.5. Synthesis of Ligands L8 and L12

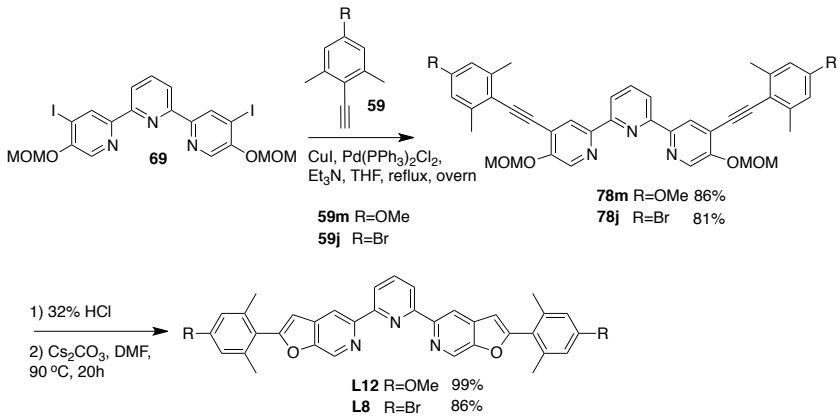

The corresponding methoxy-derivative **L12** in the presence of neat pyridinium chloride was converted to the dihydroxyl-substituted terpyridine **L16** under microwave radiation[59] (Scheme

5.6). Subsequent alkylation of the phenolic hydroxyl groups with 2-(2-chloroethoxy)ethanol in DMF, using Cs_2CO_3 as a base, resulted in the diethylene glycol substituted ligand **L17**.

Scheme 5.6. Synthesis of L17

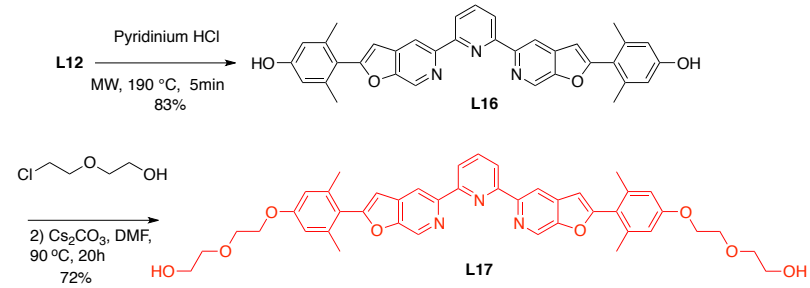

The dibromo derivative **L8** was heated with $RuCl_3 \cdot 3H_2O$ in ethanol to give the $RuCl_3$ complex **100** (Scheme 5.7) which, due to the extremely poor solubility, was used in the next step without further purification[63].

Scheme 5.7. Synthesis of 100

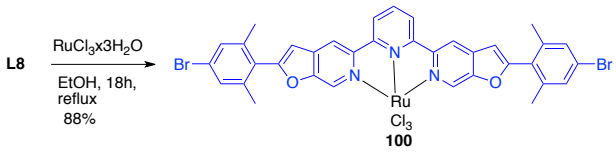

The reaction between stoichiometric amounts of the ruthenium complex **100** and the ligand **L17** in ethanol, using *N*-ethylmorpholine as the additive[64], afforded the heteroleptic complex **101** (Scheme 5.8). Treatment of **101** with methanesulfonyl chloride afforded the mesylate **99**.

Scheme 5.8. Synthesis of 99

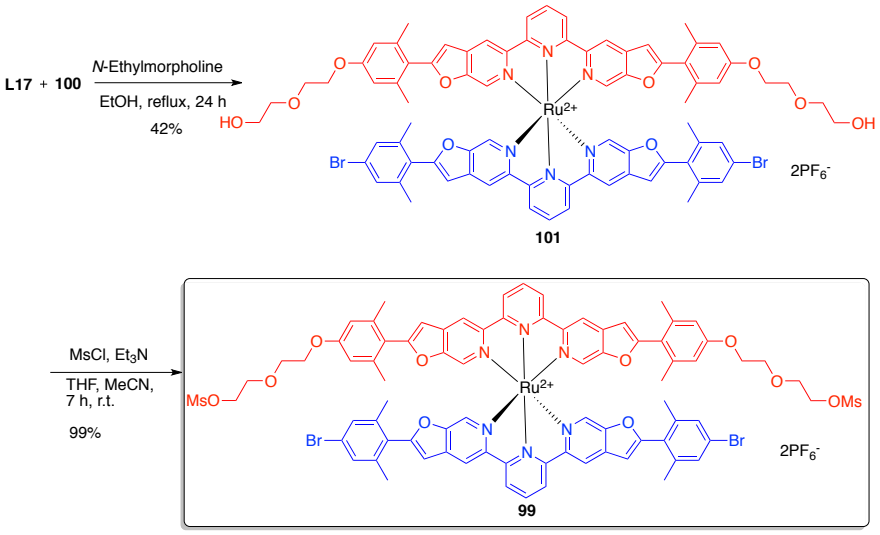

Furthermore, the work involved attempts to obtain a X-crystal structure for the heteroleptic Ru(II) cap in order to assess its suitability for the construction of the Borromean link. The crystals of the dihydroxyl intermediate **101** suitable for the X-ray analysis were obtained by a slow diethyl ether vapor diffusion into an acetonitrile solution. The crystal quality appeared to be good; however, the poor diffraction of the crystals on the in-house diffractometer did not

give an unambiguous solution of the structure. A synchrotron radiation was used to elucidate the structure, and the results are presented in Figure 5.25 and 5.26. The crystal structure was elucidated in space group $P2_1/n$. As expected, the molecular structure confirms the coordination of two different ligands around the ruthenium(II) center.

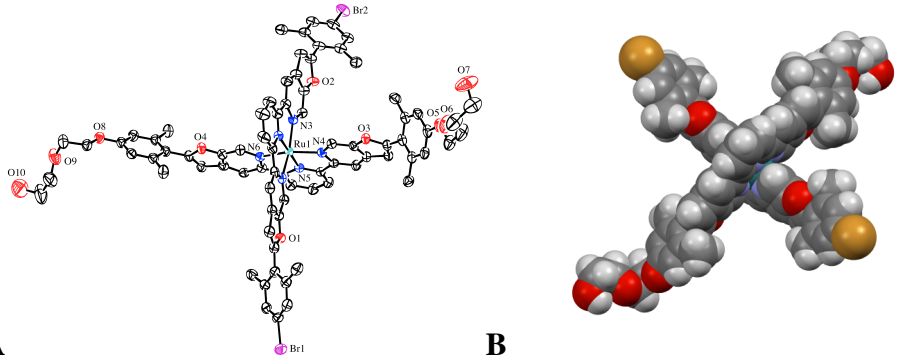

A **B**

Figure 5.25. A. ORTEP drawing (50% probability) and **B.** spacefill representation of heteroleptic Ru(II) complex **101**. Hydrogen atoms and PF_6^- removed for clarity.

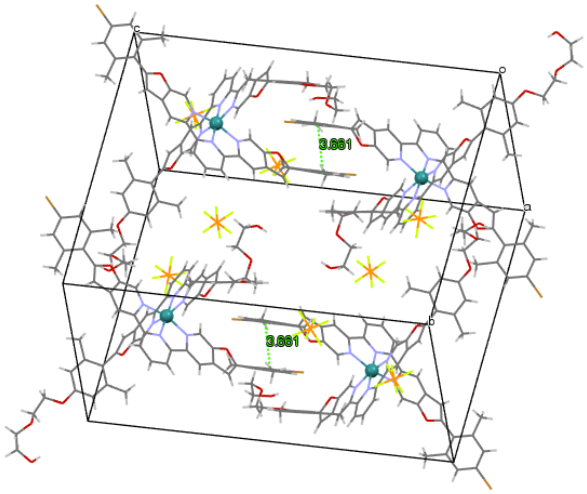

Figure 5.26. Unit cell of the heteroleptic Ru(II) complex **101**

A unit cell and packing of the complex **101** is drawn in Figure 5.26. The 4-bromo-2,6-dimethylphenyl groups of the neighboring cations are arranged antiparallel, and the distance between the both is ~3.7 Å, which suggests the intermolecular π-stacking within the crystal lattice.

The bite angles for the bromoaryl and diethylene glycol substituted ligands are C(1)-N(2)-C(15) =145.94(5)° and C(36)-N(2)-C(15)=144.96(6)°, respectively (Figure 5.27).

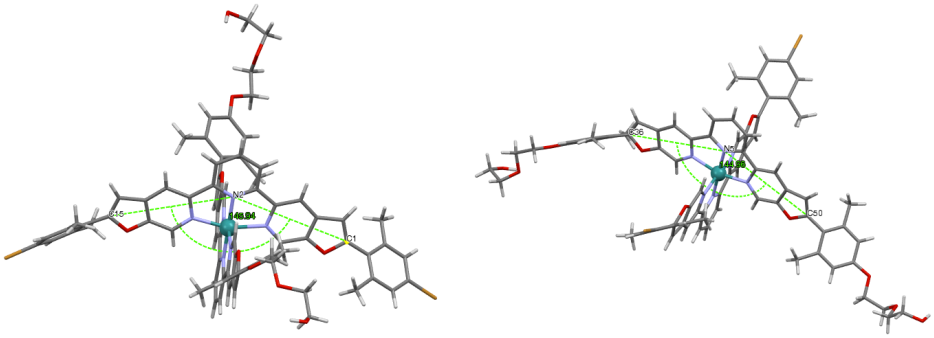

Figure 5.27. The bite angles of the bilateral *terpy* ligands in the complex **101**.

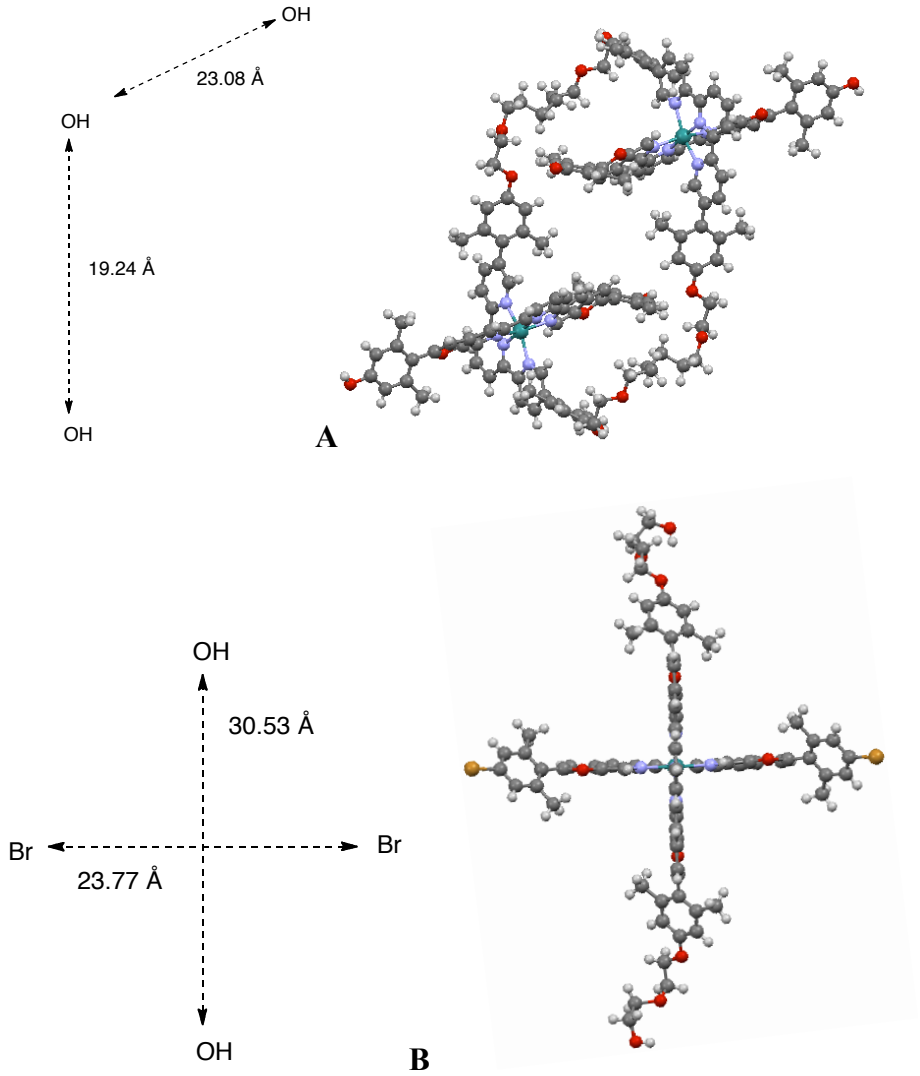

Figure 5.28. Dimensions of **A.** Seifert's threaded macrocycle **98**[59] and **B.** heteroleptic Ru(II) complex **101**.

The comparison of the dimensions of Seifert's threaded macrocycle **98**[59] and the heteroleptic complex **101** is shown in Figure 5.28. The distances between both hydroxyl groups and bromines in **101** are around 30.5 Å and 23.8 Å, respectively. Furthermore, the distances between phenolic hydroxyl groups of the opposite and the same ligands in the threaded

macrocycle **98** are around 19.2 Å and 23.1 Å, respectively. The flexible character of the first macrocycle[55] allows the combination of these two building blocks. Therefore, Williamsons ether synthesis[61] between the threaded macrocycle **98** and the mesylate cap **99** was tested (Table 5.1).

To establish the initial reaction conditions with a limited amount of the starting material, a rapid survey of the reaction conditions was performed on the microscale (Table 5.1, entries 1-3). The reaction was controlled by the on-flow ESI-MS analysis. It was found out that the reaction is extremely sensitive to temperature; therefore, careful adjustment of the heating regime was necessary. The product formation was observed at 75 °C (Table 5.1, entry 3).

Table 5.1. Screening of Reaction Conditions for Synthesis of the Threaded Ring-in-Ring Complex 102

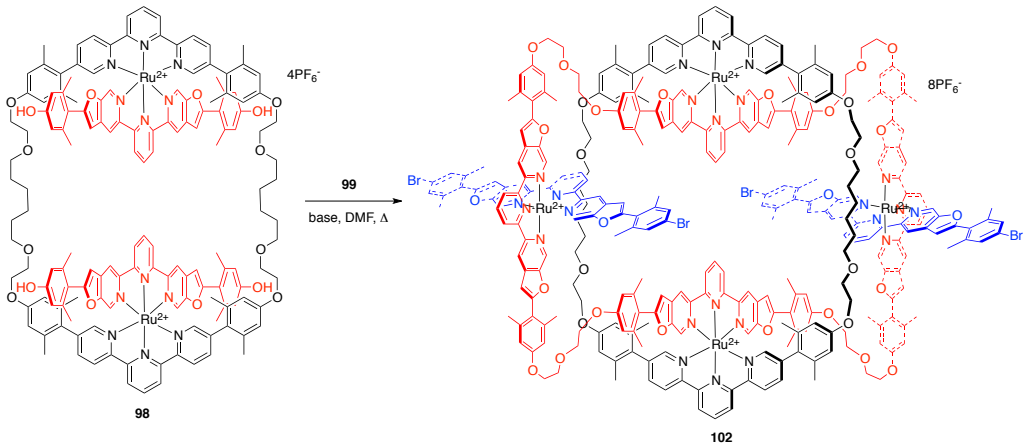

entry	conc. **98** (mM)	cap	eq	base	eq.	T, °C	t, h	results
1 [c]	0.320	**99**	2.3	K_2CO_3	20	83	42	ESI-MS: **101**, polym./decomp. of SM. No product **102**
2 [c]	0.315	**99**	2.2	K_2CO_3	20	65	24	ESI-MS: mostly unreacted **98**, **99** and traces of product **102**
3 [c]	0.315	**99**	2.2	K_2CO_3	20	75	24	ESI-MS: ~1:1 product **102** and **98**
4	0.310	**99**	2.2	K_2CO_3	26	75	72	ESI-MS: product **102** and traces of **98**. Isolated yield:24%
5	0.315	**99**	2.2+0.2 [a]	K_2CO_3	20	75+80 [b]	24+18 [b]	ESI-MS: product **102** and traces of **98**. Isolated yield: 36%
6	0.431	**99**	1+0.65+0.65 [a]	K_2CO_3	25	75+75+75 [b]	18+8+18 [b]	ESI-MS: product **102** and **99**. Isolated yield:41%

[a] Stepwise addition of **99**. [b] Heating was continued at specified temperature for indicated time after the next portion of **99** was added. [c] Reaction was run on microscale to indentify critical parameters for the reaction. The reaction products were not isolated.

Higher temperature caused decomposition and polymerization of starting materials **99** and **98** (entry 1), whereas lower temperature resulted in a very slow conversion and gave only traces of the desired product **102** apart from mostly unreacted starting materials (entry 2). Stepwise addition and the higher excess of the mesylate **99** turned out to improve the outcome of the reaction (Table 5.1, entries 5 and 6).

The formation of the product with the expected composition was supported by HRMS-ESI (Figure 5.29). The ion series characteristic to the highly charged Ru(II) complexes with sequential loss of PF_6^- anions can be observed in mass spectrum.

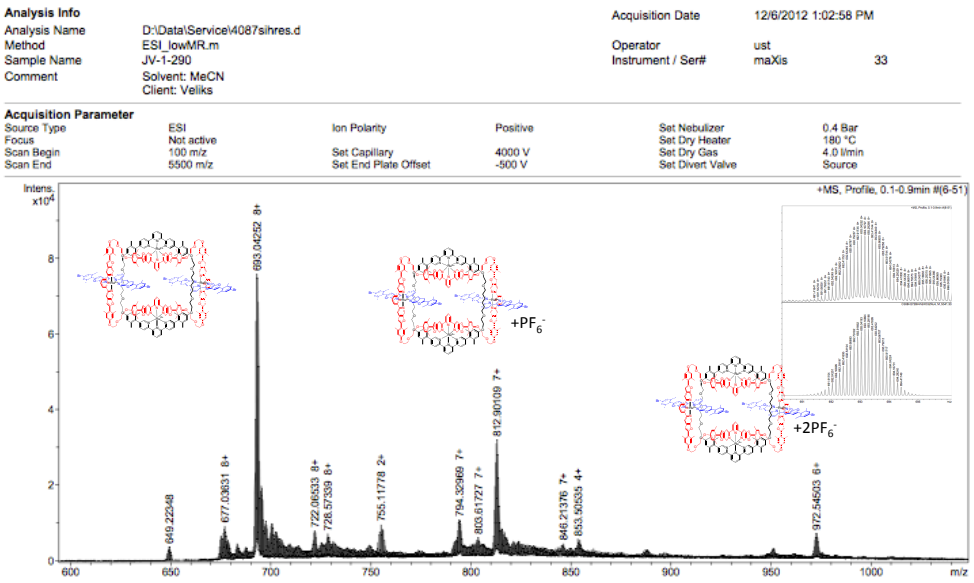

Figure 5.29. HRMS-ESI spectrum of the threaded ring-in-ring complex **102**.

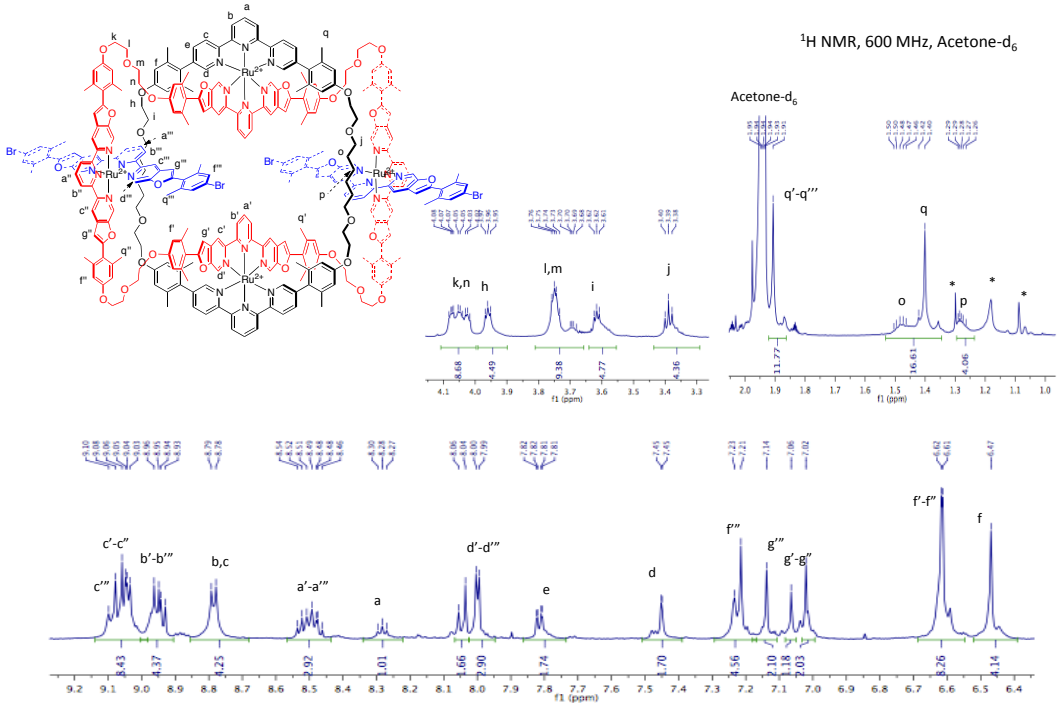

Figure 5.30. ^{1}H-NMR (600 MHz, Acetone-d_6) spectrum of the threaded ring-in-ring complex **102**.

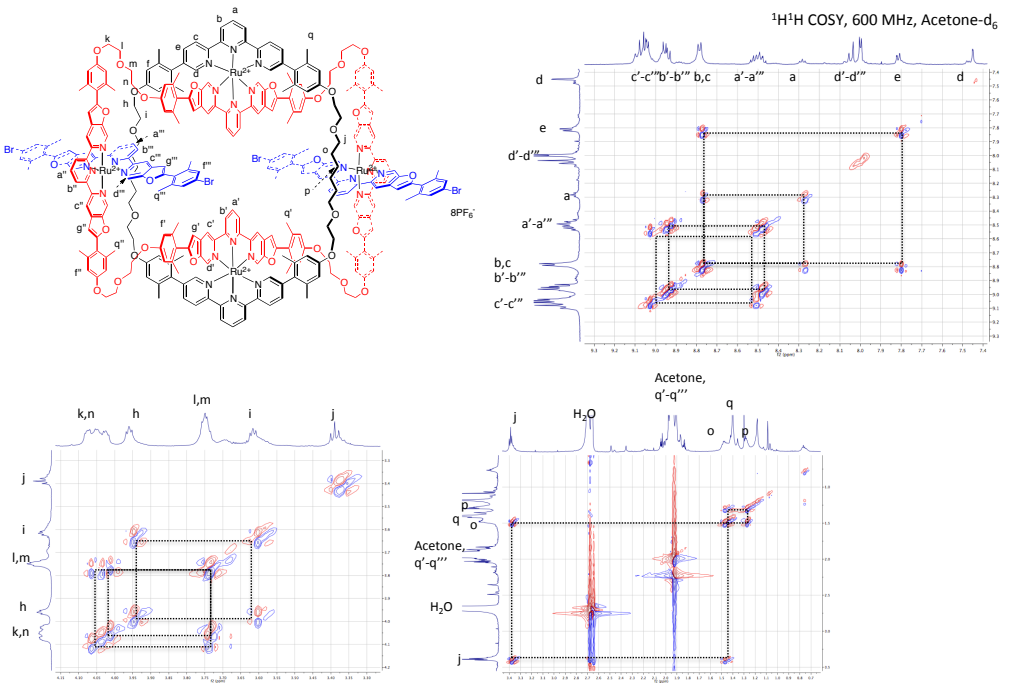

Figure 5.31. ^{1}H-^{1}H COSY (600 MHz, Acetone-d$_6$) spectrum of the threaded ring-in-ring complex **102**.

The ^{1}H and ^{1}H-^{1}H COSY NMR spectra (Figure 5.30 and 5.31) show all the expected signal clusters of the desired product; however, the symmetry observed in NMR is lower then expected and the overlap of several signals with similar nature can be seen. This suggests that more than one isomeric species are present in the mixture. Besides the desired D_{2h} symmetric endo/endo product **102**, D_{2h} symmetric exo/exo and C_{2v} symmetric exo/endo could be also envisioned (Figure 5.32). The significant overlap of the signals did not allow the identification of the exact stereochemistry of all the involved species. So far, the separation of these isomeric species was not successful.

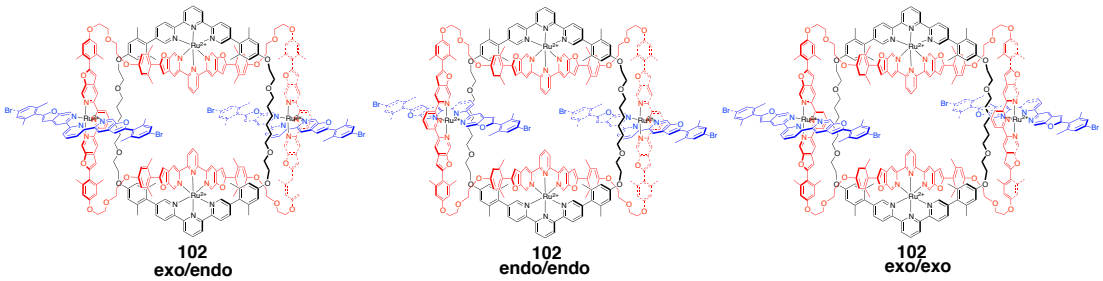

Figure 5.32. Theorecitcal stereoisomers of the threaded ring-in-ring complex **102**.

Nevertheless, the product mixture **102** was subjected to the next step. The long enough linker **103** having two acetylene groups at the terminal positions, suitable for the Sonogashira coupling[62], theoretically could complete the synthesis of the Borromean link (Scheme 5.9). After screening various bases, Pd catalysts and ligands[65-68], the formation of the desired

coupling product was not observed. Instead, either there was no reaction, partial decomposition, or polymerization of the starting materials took place.

Scheme 5.9. Unsuccessful attempts to complete the Borromean Link Synthesis via the Sonogashira Coupling

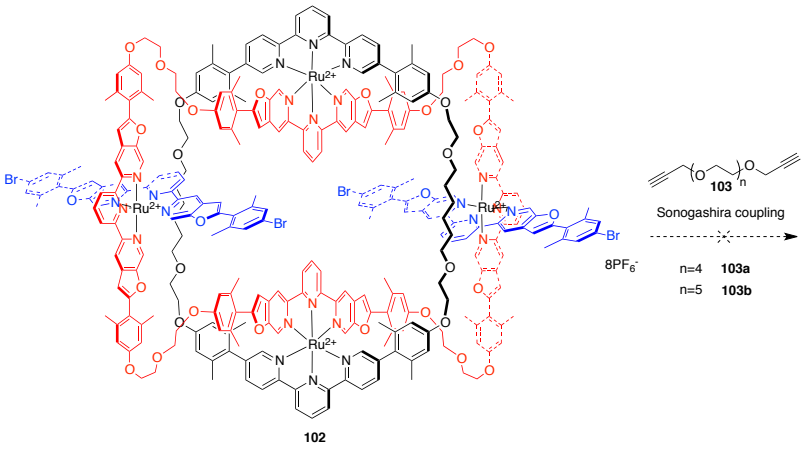

Therefore, another approach was considered to overcome the problematic coupling reaction, and the structure of the heteroleptic Ru(II) cap was reconsidered.

5.2.2. Eglinton Reaction Strategy

The emphasis was placed on the creation of a more convergent route, reducing the total synthetic steps and the number of chemical manipulations with already advanced ring-in-ring structures. It was decided to construct the preformed Ru(II) templated cap which in combination with the threaded ring **98** would contain all the necessary carbon atoms for the final Borromean link structure (Figure 5.33).

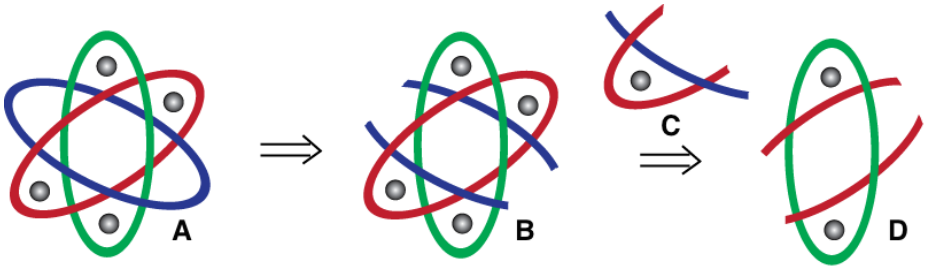

Figure 5.33. Reconsidered retrosynthesis of the molecular Borromean link.

The RCM reaction[69,70] and Eglinton reaction[71,72] turned out to be efficient final macrocycilzation steps in many total syntheses of natural products[73,74] and supramolecular architectures[47,75]. The ethylene or acetylene groups are also chemically compatible with the basic conditions of the Williamson's ether synthesis[61]. Therefore, the pretemplated cap **99** could be modified in such a way that, instead of bromines, linkers of the proper length, functionalized with either olefin or acetylene groups, could be introduced at the terminal

positions (Figure 5.34). However, the olefin RCM reaction in large macrocycles can form a mixture of cis/trans isomers[76]; therefore, it was decided to use the acetylene homocoupling – Eglinton reaction – as the final cyclization step. Based on the estimated dimensions of all the involved building blocks, 2-(2-(4-ethynylphenoxy)ethoxy)ethanol (**106**) was selected as a suitable linker with the length of ~14.3 Å.

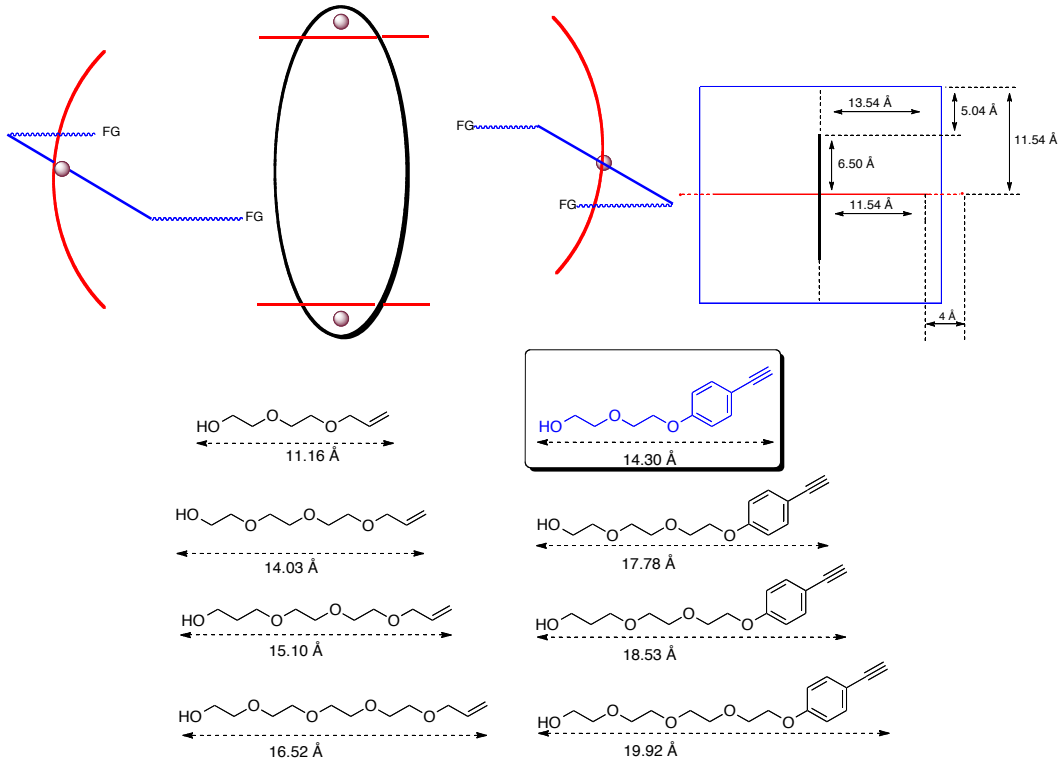

Figure 5.34. The new design of the pretemplated cap and estimation of the length of linkers.

The synthesis of the corresponding linker **107** was started from 4-iodophenol (**104**), which was alkylated with 2-(2-chloroethoxy)ethanol to afford **105** (Scheme 5.10).[77,78] Subsequently, the Sonogashira coupling with trimethylsilyl acetylene[79] and one-pot deprotection gave the acetylene **106**, and after tosylation afforded the product **107**.

Scheme 5.10. Synthesis of the linker 107

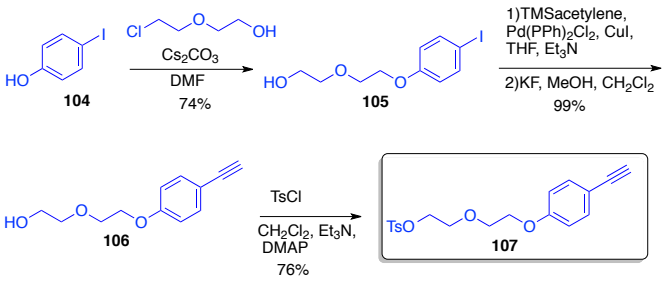

Scheme 5.11. Synthesis of 108

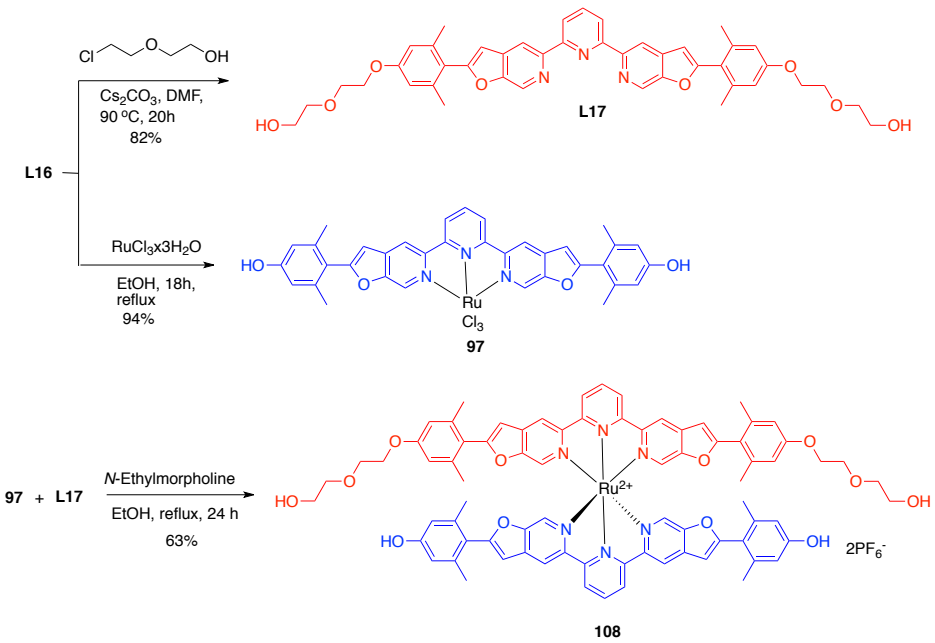

The heteroleptic complex **108** was synthesized (Scheme 5.11) from the ligand **L17** and the ruthenium trichloride complex **97**[59]. The heteroleptic complex **108** has four hydroxyl groups; however, the phenolic OH groups are more acidic. This allowed performing selective alkylation of the complex **108** with two equivalents of the tosylate **107** in DMF, using Cs_2CO_3 as a base, to afford the compound **109** (Scheme 5.12). The treatment of the Ru(II) complex **109** with the corresponding sulfonyl chloride afforded either mesylate **110a** or tosylate **110b**.

Scheme 5.12. Synthesis of the Pretemplated Cap 110

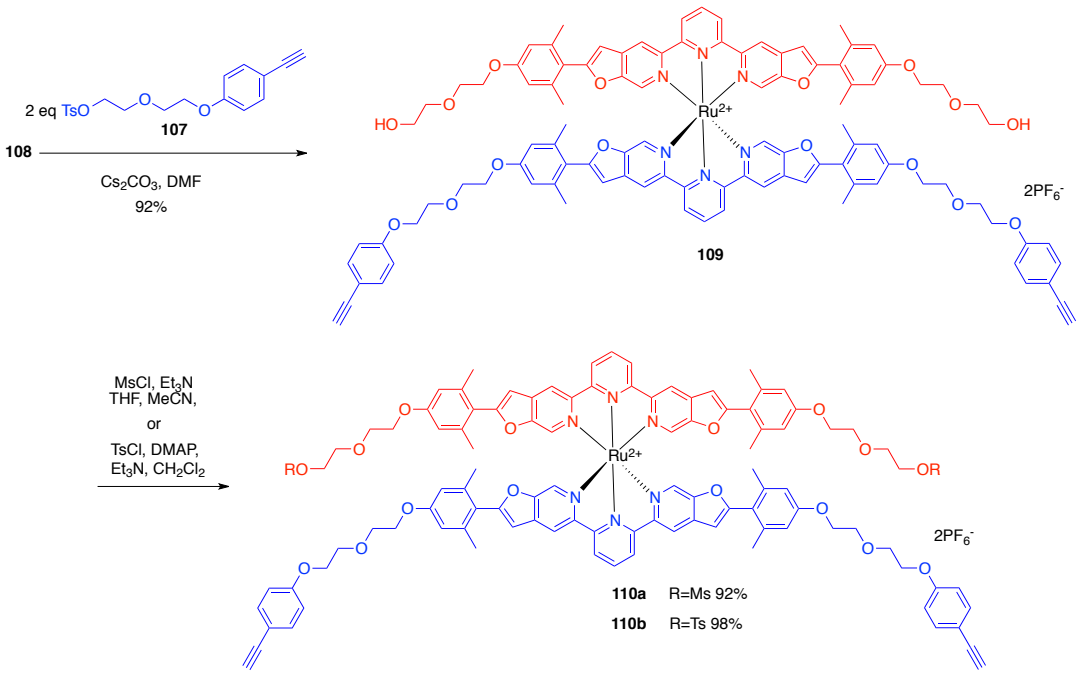

Alkylation of the threaded macrocycle **98** with the cap **110** turned out to be extremely challenging. A survey of the reaction conditions on microscale was performed to identify the

initial parameters such as base, leaving group, temperature, and way of addition of the pseudohalide **110** (Table 5.2). The reaction control was performed by on-flow ESI-MS. The best result for the synthesis of **111** was reached, when K_2CO_3 was used as a base, the mesylate **110a** as a nucleophile, and the activated 4 Å molecular sieve powder as an additive (Table 5.2, entry 7). However, the yield is still rather low. Similarly to the synthesis of tetrabromo-complex **102**, this reaction is extremely sensitive to temperature variations. Higher temperatures (80~83 °C) caused polymerization and decomposition of the starting materials giving no desired product **111** (entry 1). Whereas heating at lower temperature (70 °C) resulted in an extremely slow conversion of the starting materials, but it helped to decrease the rate of polymerization (Table 5.2, entry 6 and 7). Mass spectra showed that the desired product forms via several intermediates, such as **112**, **113** and **114** (Scheme 5.13), which accumulated in the course of the reaction at 70 °C. However, at this temperature the formation of the product **111** is extremely slow. Therefore, after a certain time, when most of the starting materials were consumed, the reaction temperature had to be increased to 78 °C. This facilitated the formation of the desired product **111**. The switching of the temperature regime during the reaction turned out to be crucial.

Analytical data (MS, NMR, IR) support the formation of the product **111**. ^{1}H NMR spectrum suggests that the isomeric species with lower symmetry are also present in the mixture, but, due to the strong overlap of the signals, stereochemistry of all involved species (exo/exo, endo/endo, endo/exo, or the mixture of all isomers) could not been determined.

Table 5.2. Screening of Reaction Conditions for Synthesis of the Threaded Ring-in-Ring Complex 111

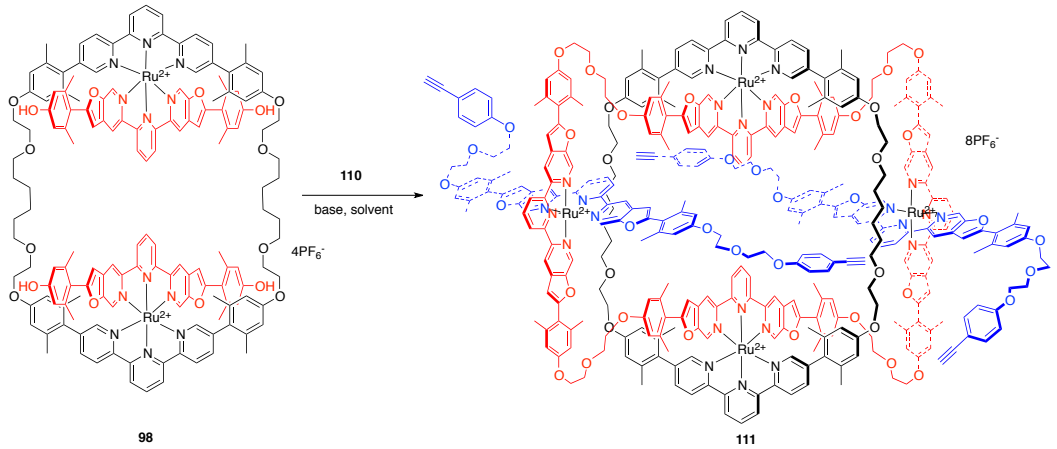

entry	conc. **98** (mM)	solvent	cap	eq.	base	eq.	T, °C	t, h	results
1	0.323	DMF	**110a**	2.2	K_2CO_3	26	84	29	ESI-MS: **109**, polym./decomp. of SM, no product
2	0.193	DMF	**110b**	2.1	Cs_2CO_3	10	75	32	ESI-MS: **98**, polym./decomp. of SM, no product
3	0.189	DMF	**110b**	5.6[a]	Cs_2CO_3	10	60	72	ESI-MS: **109**, **98**, mono alkylated side product, product **111**. Isolated yield: 9%
4[b]	0.270	DMF	**110b**	2.7[a]	Cs_2CO_3	10	72	27	ESI-MS: **110b**, **98**, product **111**. Isolated yield: 10%
5[b]	0.630	DMSO	**110b**	2.2	Cs_2CO_3	15	70	24	ESI-MS: polym./decomp. of SM, no product
6[c]	0.520	DMF	**110a**	2.2+0.5[d]	K_2CO_3	26	70+83[d]	36+24[d]	ESI-MS: mostly product **111**, traces of **98**. Isolated yield: 5%
7	0.525	DMF	**110a**	2.2+0.5[d]	K_2CO_3	26	70+78+81[d]	34+24+32[d]	ESI-MS: mostly product **111**, traces of **98**. Isolated yield 20%

[a] Stepwise addition. [b] 3 Å molecular sieves added. [c] 4 Å molecular sieves (powder) added. [d] Additional **110a** was added, continued heating at specified temperature for the indicated time.

Scheme 5.13. Intermediates Observed in the Reaction Between 98 and 110

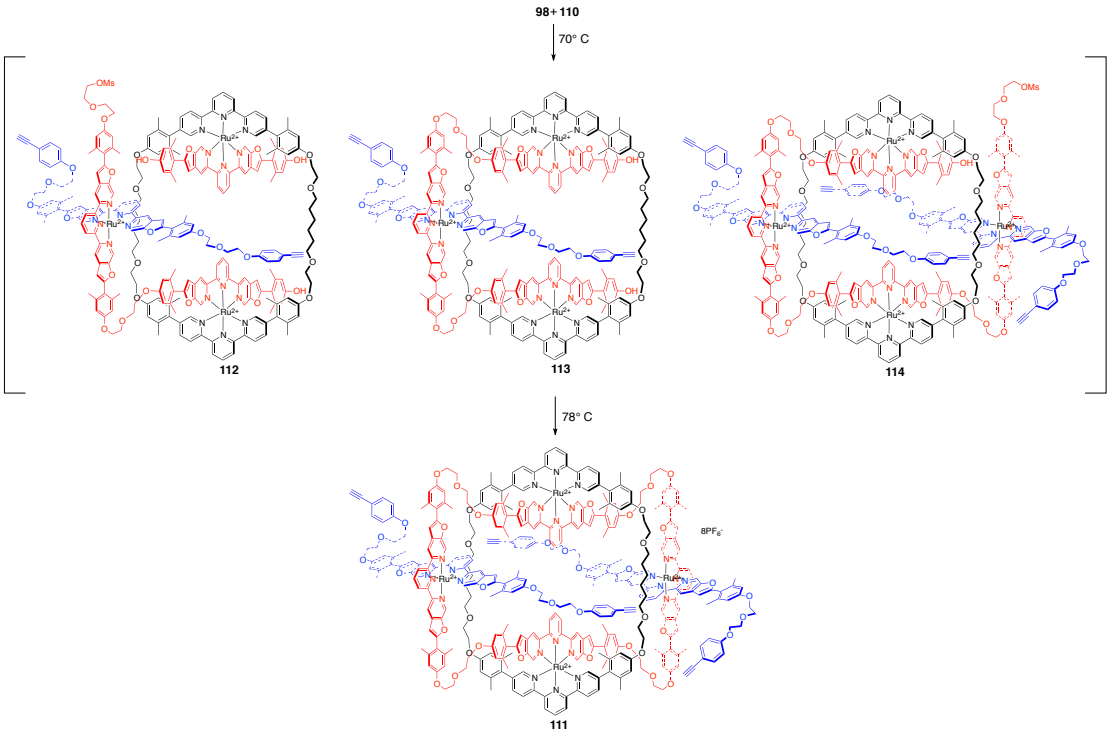

Despite the uncertain stereochemistry, the ring-in-ring complex **111** was introduced in the Eglinton reaction[71,75] to form the third and the final ring. The complex **111** was heated under reflux in acetonitrile together with excess of $Cu(OAc)_2$ (Scheme 5.14).

Scheme 5.14. The Final Macrocyclization Reaction Towards the Borromean Link

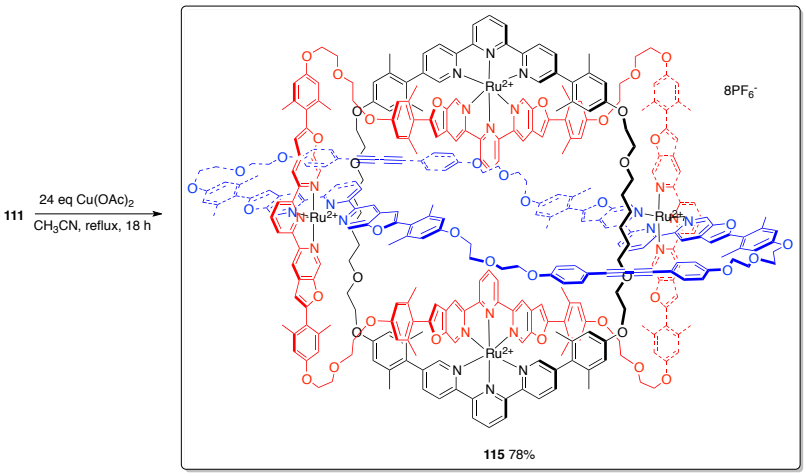

The reaction progress was controlled by on-flow ESI-MS, which showed that after 18 h all the starting material was consumed. The MS data of the reaction product support the expected composition of **115** – the calculated isotope pattern corresponds to the experimental (Figure 5.35). Sequential loss of PF_6^- counterions can be also observed, which is characteristic for such highly charged complexes.

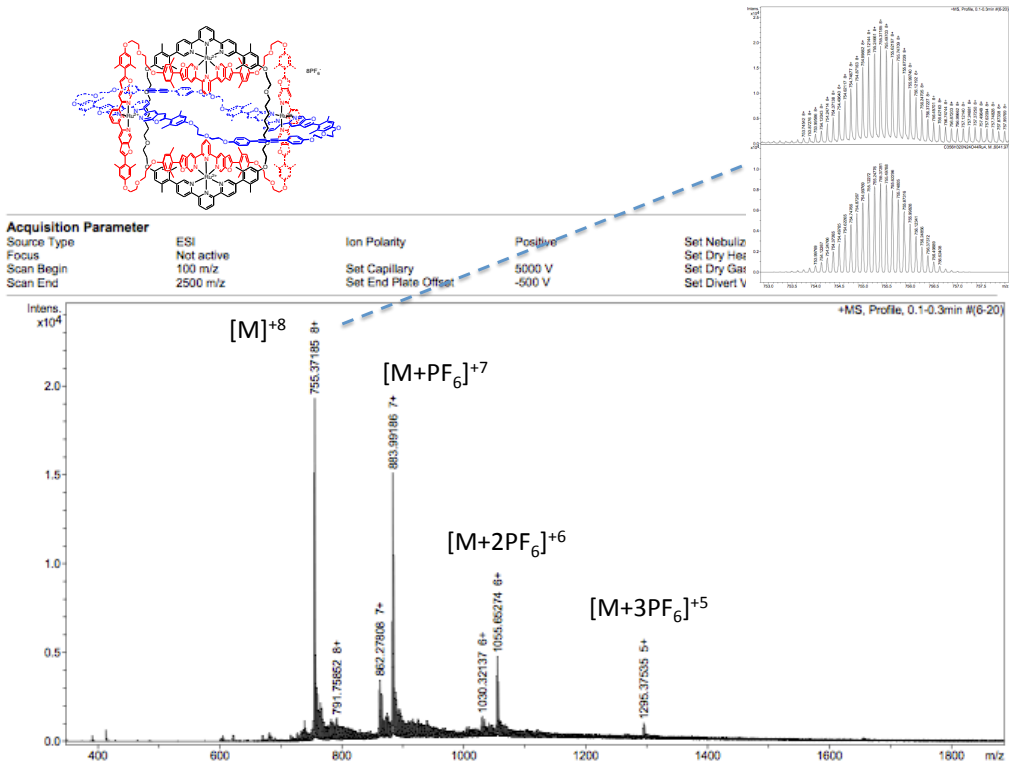

Figure 5.35. Mass spectrum of the reaction product (or mixture of isomers) **115**.

Infrared spectroscopy also proves that all terminal acetylenes were consumed in the course of the reaction. The spectrum of **115** shows that the characteristic bands for the terminal acetylenes at ~3280 cm^{-1} are absent as compared to the spectrum of the starting material **111** (Figure 5.36).

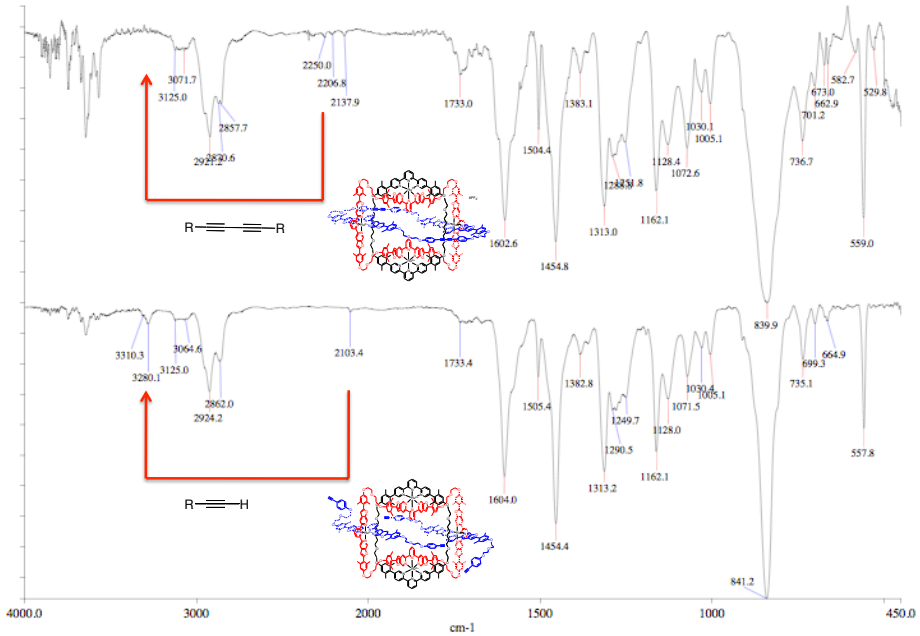

Figure 5.36. Comparison of IR-spectra of **111** and **115**.

The ^{1}H NMR spectrum contains all the expected signal clusters necessary for the desired product; however, they are extremely broadened (Figure 5.36 and 5.37). ^{1}H-^{1}H COSY spectrum indicates that more than one chemical species of similar structure are present in the mixture (Figure 5.38). This might suggest, that in the course of the reaction, other topological isomers of the Borromean link are formed. As an exact stereochemistry and isomeric purity of the starting material **111** was not clear, after macrocyclization totally nine isomeric exo- and endo- structures **115**, **116** and **117** can be envisioned, consisting of 3-, 4- and 5- rings Figure 5.39.

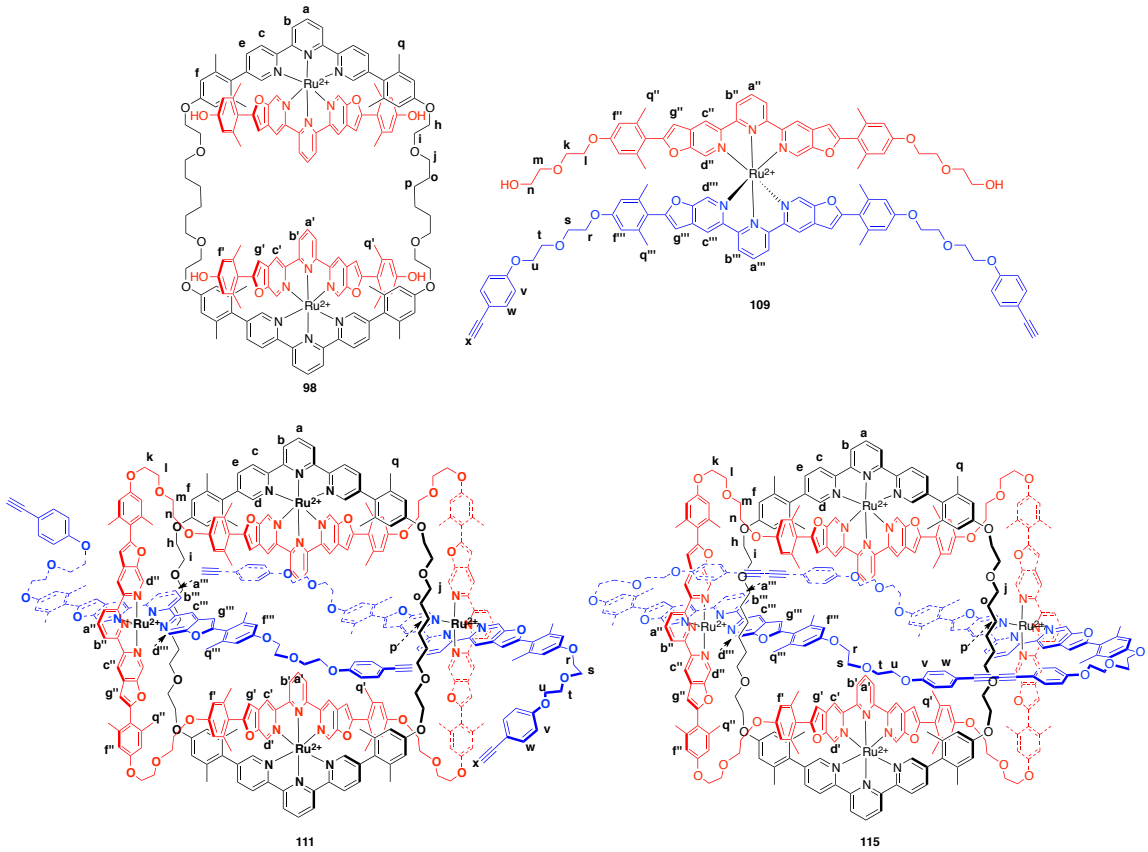

Figure 5.36. Labels for assignment of ^{1}H NMR spectra.

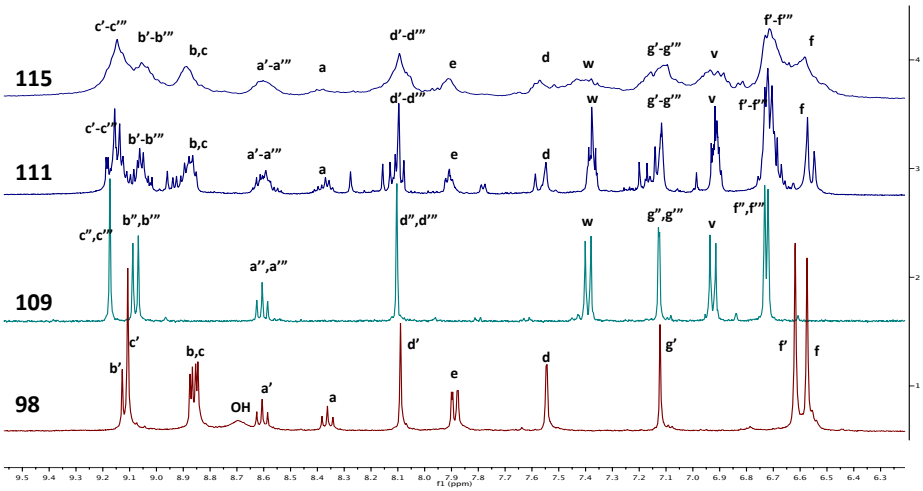

Figure 5.37. The aromatic regions in ^{1}H NMR of **98**, **109**, **111**, and **115**.

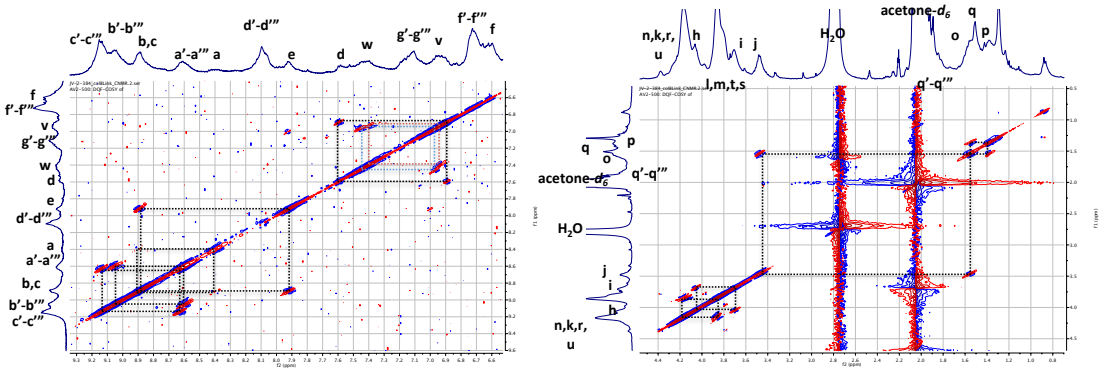

Figure 5.38. ^{1}H-^{1}H COSY (500 MHz, Acetone-d_6) spectrum of **115**.

So far, all attempts to isolate these isomeric structures by means of chromatography, HPLC, or recrystallizations were not successful. The correct topology of the Borromean link should be supported by X-ray crystallography; however, there has been no success in obtaining suitable crystals for this purpose. *In silico* calculations could also be helpful for establishing the composition of the mixture by excluding the least probable isomers. This has not been achieved yet due to time constraints.

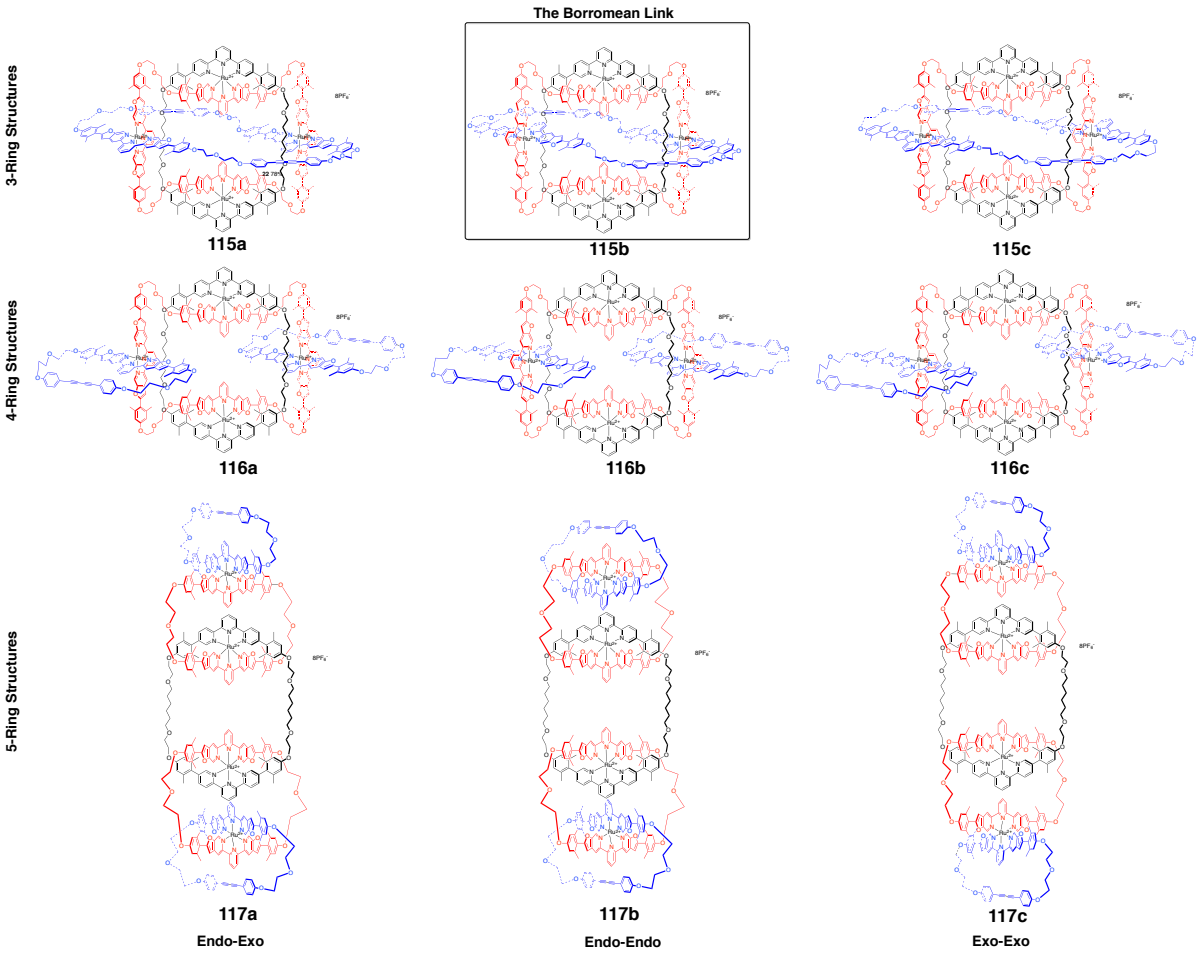

Figure 5.39. Theoretical isomers of the molecular Borromean link Ru(II) complex.

5.3. Conclusions and Outlook

The kinetic or stepwise synthesis of the Borromean link consisting of three different rings is still a problem with some unanswered questions. However, this work shows that the new route via the pretemplated Ru(II) cap and Eglinton reaction is chemically feasible; however, the important stereocontrol element for obtaining the expected topology still remains a future challenge. The analytical data support the formation of the isomeric product mixture, and, presumably, it contains the desired Borromean link Ru(II) complex, but further evidences should be provided to prove this unambiguously. Nevertheless, this is a real breakthrough towards the kinetic synthesis of the Borromean link and establishes a solid base for further investigations.

In order to gain more control over the desired topology, we propose the following improvements for the synthesis:

- More rigid linkers for the construction of the “ring two” could be used to force the formation of only endocyclic product;

- Functionalization of a pretemplated cap with a bulky functional group at the “ring two” ligand might block the approach to it from the undesired side, again forcing the formation of the expected endocyclic product.

With this work it has been shown that linear bilateral extended terpyridine ligands possess valuable geometric features for the construction of extended macrocyclic structures; therefore, there is great potential for designing other topologically challenging supramolecular architectures using this motif.

5.4. Experimental Section

5.4.1. Materials and Methods

All reagents and solvents used for reactions were reagent grade and used without further purification unless otherwise noted. Anhydrous THF and toluene was supplied from an Mbraun solvent purification system. Analytical thin-layer chromatography was performed with Macherey–Nagel POLYGRAM SIL N-HR/UV254 or ALOX N/UV254. Flash silica gel column chromatography was performed with Merck silica gel 60 (particle size 0.040–0.063 mm). Flash alumina column chromatography was performed with deactivated (5% water) Fluka alumina (particle size 0.05–0.15 mm, pH 7.0±0.5). Melting points were recorded on a Büchi B-540 melting point apparatus. For characterization purposes, proton nuclear magnetic resonance (^{1}H-NMR) spectra were all recorded on Bruker instruments (AV-300 and ARX-300 at 300 MHz, AV2- 400 at 400 MHz, and AV-500 at 500 MHz). Chemical shifts are reported in ppm relative to $CHCl_3$ (δ 7.26), CD_2Cl_2 (δ 5.31), CD_3CN (δ 1.94) or DMSO-d_6 (2.50). Multiplicity and shape are indicated by one or more of the following abbreviations: s (singlet); d (doublet); t (triplet); q (quartet); dd (doublet of doublets); td (triplet of doublets); m (multiplet); br (broad). Carbon-13 nuclear magnetic resonance (^{13}C- NMR) spectra were recorded on Bruker instruments (ARX-300 at 75 MHz, AV2-400 at 100 MHz, and AV-500 at 125 MHz). Chemical shifts are reported relative to $CDCl_3$ (δ 77.2), CD_2Cl_2 (δ 53.8), CD_3CN (δ 1.3) or DMSO-d_6 (δ 39.5). Infrared spectroscopic data were recorded on NaCl plates as thin films, as KBr pellets or neat sample on a Perkin Elmer Spectrum One (PE) or Jasco FT/IR-4100 spectrophotometer. The intensities are given as follows: *s* = strong, *m* = medium, and *w* = weak. An Agilent 8453 UV/Vis spectrophotometer was used to record all UV/Vis spectra. Emission spectra and lifetimes (ns) were recorded on an Edinburgh Instruments FLS920 spectrometer. Solid-state quantum yields were measured using an integrating sphere accessory for FLS920 spectrometer. X-ray structures were carried out by the Laboratorium für Computerchemie und Röntgenstructuranalyse of the Institute of Organic Chemistry of the University of Zurich using a Nonius KappaCCD diffractometer with MoKα radiation (λ = 0.71037 Å). Dr. Philip Pattison collected the diffraction data for compound **101** on the Swiss Norwegian Beamlines at the European Synchrotron Radiation Facility.

5.4.2. Experimental Procedures

2,6-bis-[2-(4-methoxy-2,6-dimethylphenyl)furo[2,3-c]pyridin-5-yl]pyridine (L12)

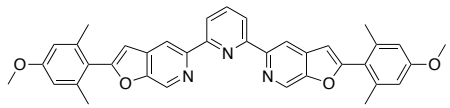

Prepared according to the procedure by Helen Seifert[59].

2,6-bis-[2-(4-hydroxy-2,6-dimethylphenyl)furo[2,3-c]pyridin-5-yl]pyridine (L16)

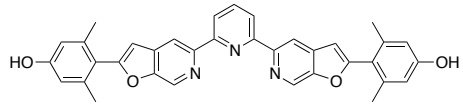

Prepared according to the procedure by Helen Seifert[59].

2,6-bis(2-(4-bromo-2,6-dimethylphenyl)furo[2,3-c]pyridin-5-yl)pyridine (L8)

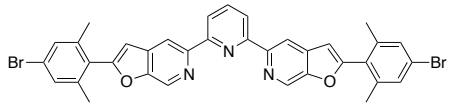

To a solution of 5,5″-bis-(methoxymethoxy)-4,4″-bis-((4-bromo-2,6-dimethylphenyl)ethynyl)-2,2′:6′,2″-terpyridine (**78j**) (543 mg, 0.707 mmol, 1.00 eq) in DMF (25 mL) was added 32% aq. HCl (0.347 mL, 3.54 mmol, 5.0 eq). The reaction mixture was heated to 80 °C for 20 h, then Cs_2CO_3 (10.4 g, 31.8 mmol, 45.0 eq) was added portion-wise. The resulting mixture was heated to 90 °C for 18 h. Evaporation of DMF gave the residue that was suspended in water (200 ml). The resulting solid was collected by filtration, washed on the filter with excess water and re-dissolved with CH_2Cl_2 (200 ml) into a clean flask. Evaporation of solvent gave a crude product, which was dissolved in minimum amount of CH_2Cl_2, introduced on a plug of neutral Al_2O_3 (deact. with 5% w/w H_2O) and eluted with hexane:EtOAc 3:1. The solvent was evaporated under reduced pressure to give desired product **L8** (414 mg, 86%) as an off-white solid.

Mp 283.3–284.0 °C.

^{1}H NMR (500 MHz, $CDCl_3$, δ): 8.95 (s, 4H), 8.47 (d, J = 7.8 Hz, 2H), 7.98 (t, J = 7.8 Hz, 1H), 7.35 (s, 4H), 6.84 (s, 2H), 2.26 (s, 12H).

^{13}C NMR (125 MHz, $CDCl_3$, δ): 157.9, 155.9, 152.6, 150.5, 140.7, 138.1, 136.2, 132.7, 130.8, 128.8, 124.1, 120.6, 113.7, 106.8, 20.5.

IR (film on NaCl, cm^{-1}): 2957*w*, 2924*w*, 2853*w*, 1604*m*, 1571*s*, 1447*vs*, 1398*m*, 1307*w*, 1291*w*, 1251*w*, 1239*w*, 1145*m*, 1112*w*, 1075*w*, 1010*m*, 914*m*, 856*m*, 824*s*, 802*w*, 733*m*, 651*w*.

HRMS (ESI) *m/z*: $[M + H]^+$ calcd for $C_{35}H_{26}Br_2N_3O_2$: 678.03863; found: 680.03747.

2,2′-(2,2′-(4,4′-(5,5′-(pyridine-2,6-diyl)bis(furo[2,3-*c*]pyridine-5,2-diyl))bis(3,5-dimethyl-4,1-phenylene))bis(oxy)bis(ethane-2,1-diyl))bis(oxy)diethanol (L17)

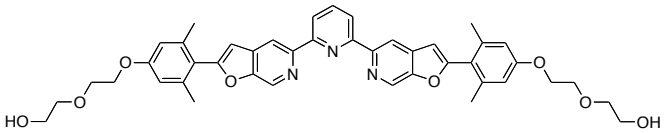

To a mixture of 2,6-bis-[2-(4-hydroxy-2,6-dimethylphenyl)furo[2,3-c]pyridin-5-yl]- pyridine (**L16**) (100 mg, 1.0 eq, 0.181 mmol) and anhydrous Cs_2CO_3 (177 mg, 3.0 eq, 0.542 mmol) in dry DMF (4 mL) under N_2 atmosphere was added 2-(2-chloroethoxy)ethanol (0.055 mL, 2.9 eq, 0.521 mmol). The reaction mixture was heated to 100 °C for 18 h. The reaction mixture was allowed to cool to room temperature and DMF was evaporated under reduced pressure. The resulting residue was treated with water and extracted with CH_2Cl_2 (4 × 80 ml). The combined organic layers were washed with brine, dried over $MgSO_4$, filtered and evaporated. The resulting crude product was purified by silica gel column chromatography (eluent gradient CH_2Cl_2:MeOH 100:0 to 95:5) to give desired compound **L17** (96 mg, 72%) as a sticky amorphous solid. (Treatment of the product with Et_2O and evaporation under reduced pressure helped to obtain easy transferable, flocky solid).

Mp 85.6–86.7 °C.

^{1}H NMR (400 MHz, $CDCl_3$, δ): 8.94 (d, *J* = 1.0 Hz, 2H), 8.93 (t, *J* = 0.9 Hz, 2H), 8.45 (d, *J* = 7.9 Hz, 2H), 7.97 (t, *J* = 7.9 Hz, 1H), 6.80 (d, *J* = 0.9 Hz, 2H), 6.74 (s, 4H), 4.21-4.18 (m, 4H), 3.91-3.89 (m, 4H), 3.81-3.76 (m, 4H), 3.72-3.69 (m, 4H), 2.26 (s, 12H).

^{13}C NMR (125 MHz, $CDCl_3$, δ): 159.6, 159.3, 155.9, 152.5, 150.2, 140.4, 138.0, 136.5, 132.4, 122.6, 120.5, 113.9, 113.6, 106.5, 72.7, 69.8, 67.5, 61.9, 21.0.

IR (film on NaCl, cm^{-1}): 3356*br*, 2925*m*, 2866*w*, 1607*s*, 1570*m*, 1449*s*, 1400*s*, 1318*m*, 1285*w*, 1161*m*, 1132*m*, 1070*w*, 1007*w*, 907*m*, 858*w*, 824*m*, 733*m*, 642*w*.

HRMS (ESI) *m/z*: $[M + H]^+$ calcd for $C_{43}H_{44}N_3O_8$: 730.31229; found: 730.31240.

2,2′-(2,2′-(4,4′-(5,5′-(pyridine-2,6-diyl)bis(furo[2,3-*c*]pyridine-5,2-diyl))bis(3,5-dimethyl-4,1-phenylene))bis(oxy)bis(ethane-2,1-diyl))bis(oxy)bis(ethane-2,1-diyl) dimethanesulfonate (L18)

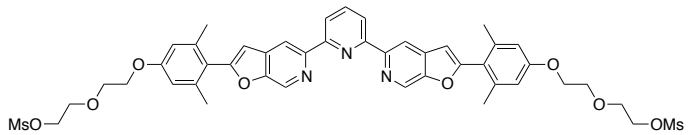

To a solution of 2,2′-(2,2′-(4,4′-(5,5′-(pyridine-2,6-diyl)bis(furo[2,3-*c*]pyridine-5,2-diyl))bis(3,5-dimethyl-4,1-phenylene))bis(oxy)bis(ethane-2,1-diyl))bis(oxy)diethanol (**L17**) (30 mg, 1.0 eq, 0.0411 mmol) in anhydrous CH_2Cl_2 (1.5 mL) under N_2 atmosphere was added

methanesulfonyl chloride (0.0112 ml, 3.5 eq, 0.144 mmol). The reaction mixture was stirred for 2 h at room temperature, quenched with water (3 ml) and extracted with CH_2Cl_2 (3 × 3 ml). The combined organic layers were dried over $MgSO_4$, filtered and evaporated under reduced pressure. The obtained product was dried under vacuum to give desired compound **L18** (36.2 mg, 99%) as a white amorphous solid.

Mp >170 °C dec.

^{1}H NMR (400 MHz, $CDCl_3$, δ): 8.95 (s, 2H), 8.94 (s, 2H), 8.46 (d, *J* = 7.9 Hz, 2H), 7.97 (t, *J* = 7.9 Hz, 1H), 6.81 (s, 2H), 6.71 (s, 4H), 4.43-4.41 (m, 4H), 4.19-4.17 (m, 4H), 3.91-3.89 (m, 4H), 3.87-3.85 (m, 4H), 3.07 (s, 6H), 2.26 (s, 12H).

^{13}C NMR (125 MHz, $CDCl_3$, δ): 159.5, 159.3, 155.8, 152.5, 150.1, 140.4, 138.0, 136.6, 132.4, 122.6, 120.6, 113.9, 113.6, 106.5, 69.9, 69.4, 69.3, 67.4, 37.9, 21.0.

IR (film on NaCl, cm^{-1}): 2923*w*, 2875*w*, 1607*s*, 1570*m*, 1449*s*, 1400*m*, 1352*s*, 1319*s*, 1175*s*, 1140*s*, 1074*m*, 1011*m*, 973*m*, 913*s*, 825*m*, 733*m*.

HRMS (ESI) *m/z*: $[M + H]^+$ calcd for $C_{45}H_{48}N_3O_{12}S_2$: 886.26739; found: 886.26701.

2,6-bis(2-(4-(2-(2-iodoethoxy)ethoxy)-2,6-dimethylphenyl)furo[2,3-*c*]pyridin-5-yl)pyridine (L19)

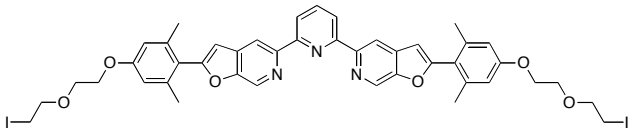

To a mixture of 2,2′-(2,2′-(4,4′-(5,5′-(pyridine-2,6-diyl)bis(furo[2,3-*c*]pyridine-5,2-diyl))bis(3,5-dimethyl-4,1-phenylene))bis(oxy)bis(ethane-2,1-diyl))bis(oxy)diethanol (**L17**) (25.5 mg, 1.0 eq, 0.0349 mmol), imidazole (12.8 mg, 5.4 eq, 0.189 mmol), iodine (30.2 mg, 3.4 eq, 0.119 mmol) and triphenylphosphine (12.8 mg, 5.4 eq, 0.189 mmol) under Ar atmosphere was added anhydrous DCM (1.5 mL). The reaction mixture was stirred for 2 h at room temperature. After completion (followed by LC-MS) the mixture was quenched with 10% aqueous $Na_2S_2O_3$ (6 mL) and extracted with CH_2Cl_2 (3 × 10 mL). The combined organic extracts were dried over $MgSO_4$, filtered and evaporated under reduced pressure. The residue was purified by neutral Al_2O_3 (deact. with 5% w/w H_2O) column chromatography (eluent hexane:EtOAc 3:1) to give desired product **L19** (25.7 mg, 76%) as an off white amorphous solid.

Mp 123–126 °C.

^{1}H NMR (500 MHz, $CDCl_3$, δ): 8.95 (s, 2H), 8.94 (s, 2H), 8.46 (d, *J* =7.8 Hz, 2H), 7.98 (t, *J* = 7.8 Hz, 1H), 6.81 (s, 2H), 6.74 (s, 4H), 4.20-4.18 (m, 4H), 3.91-3.89 (m, 4H), 3.86 (t, *J* =6.7 Hz, 4H), 3.31 (t, *J* =6.8 Hz, 4H), 2.27 (s, 12H).

^{13}C NMR (125 MHz, $CDCl_3$, δ): 159.5, 159.3, 155.8, 152.4, 150.0, 140.2, 137.9, 136.5, 132.3, 122.4, 120.4, 113.9, 113.5, 106.4, 72.2, 69.3, 67.4, 20.9, 2.7.

IR (film on NaCl, cm^{-1}): 2952*w*, 2923*w*, 2866*w*, 1607*s*, 1569*m*, 1448*s*, 1399*m*, 1318*s*, 1285*m*, 1160*s*, 1127*m*, 1074*w*, 1035*w*, 1007*w*, 904*w*, 824*m*.

HRMS (ESI) *m/z*: $[M + H]^+$ calcd for $C_{43}H_{42}I_2N_3O_6$: 950.11575; found: 950.11528.

Ru(2,6-bis-(2-(4-hydroxy-2,6-dimethylphenyl)furo[2,3-c]pyridin-5-yl)- pyridine)Cl_3 (97)

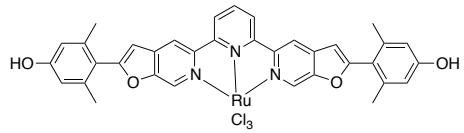

Prepared according to the procedure by Helen Seifert[59].

Ru(2,6-bis(2-(4-bromo-2,6-dimethylphenyl)furo[2,3-c]pyridin-5-yl)pyridine)Cl_3 (100)

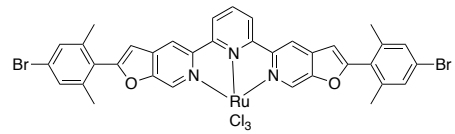

A mixture of 2,6-bis(2-(4-bromo-2,6-dimethylphenyl)furo[2,3-c]pyridin-5-yl)pyridine (**L8**) (150 mg, 1.0 eq, 0.221 mmol) and $RuCl_3 \cdot 3H_2O$ (57.7 mg, 1.0 eq, 0.221 mmol) in ethanol (27 mL) under N_2 atmosphere was heated to reflux for 18 h. The dark brown suspension was allowed to cool to room temperature, and the solvent was evaporated under reduced pressure. The resulting brown solid was suspended in water (50 ml), collected by filtration, washed on the filter with addition amount of water (till filtrate colorless) and acetonitrile (till filtrate colorless). The product was dried under vacuum to give desired compound **100** (173 mg, 88%) as an insoluble, dark brown solid.

Mp >350 °C

IR (KBr, cm^{-1}): 3042*w*, 2920*w*, 2851*w*, 1617*m*, 1573*s*, 1456*s*, 1384*m*, 1318*w*, 1245*m*, 1011*m*, 914*m*, 888*w*, 857*m*, 814*w*, 738*w*, 661*w*.

bis-(5′,5″-bis-(4-(2-propoxyethoxy)-2,6-dimethylphenyl)-2,2′:6′,2″-terpyridine) macrocycle⊃bis-(Ru(2,6-bis-(2-(4-hydroxy-2,6-dimethylphenyl)furo[2,3-c]pyridin-5-yl)-pyridine))$(PF_6)_4$ (98)

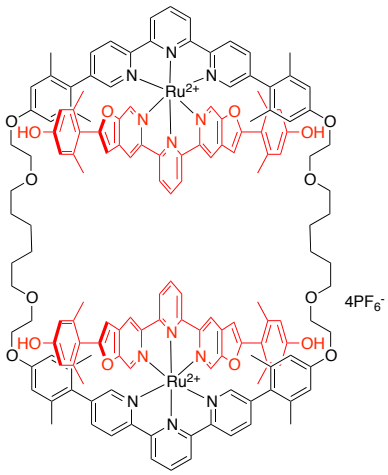

Prepared according to the improved literature procedure[59].

In dry 25 ml two-necked flask equipped with magnetic stirring bar, reflux condenser and septum a solid mixture of macrocycle **88**[44] (40 mg, 1.0 eq, 0.0311 mmol) and Ru(2,6-bis-(2-(4-hydroxy-2,6-dimethylphenyl)furo[2,3-c]pyridin-5-yl)-pyridine)Cl_3 (**97**) was 3 × degassed and refilled with Ar. To the mixture degassed EtOH (13 mL) was added through the septum. The reaction mixture was brought to reflux and *N*-ethylmorpholine (~4 drops or 6.3 μL, 1.6 eq, 0.049 mmol) was added through the septum. The reaction mixture was heated to reflux for 24 h and allowed to cool to room temperature. To the mixture sat. aq. KPF_6 (20 ml) was added. The resulting brown precipitate was filtered over Celite, washed on the filter with excess water and Et_2O, and then re-dissolved with acetone into a clean flask (green solid remains on Celite). The obtained red solution was evaporated under reduced pressure to give brown residue that was purified by silica gel column chromatography– first, a brown/green band was eluted by using the 1st eluent (MeCN:CH_2Cl_2:H_2O:aq.KPF_6 320:100:10:1), then it was switch to the 2nd eluent (MeCN:CH_2Cl_2:H_2O:aq.KPF_6 345:90:15:4) to move a red band which contained the desired product **98**. The product fractions were evaporated, re-dissolved in acetone, and to the solution sat. aq. KPF_6 was added. The resulting precipitate was collected by filtration over Celite, washed with excess water, Et_2O and re-dissolved with acetone into a clean flask. After evaporation of solvent and drying under vacuum the desired product **98** (28.6 mg, 29%) was obtained as a red solid.

Mp >295 °C dec.

^{1}H NMR (500 MHz, Acetone-d_6, δ): 9.13 (d, J = 8.0 Hz, 4H), 9.12 (s, 4H), 8.88 (d, J = 8.3 Hz, 4H), 8.87 (d, J = 8.4 Hz, 4H), 8.62 (t, J = 8.2 Hz, 2H), 8.37 (t, J =8.2 Hz, 2H), 8.10 (s, 4H),

7.90 (dd, J = 8.3, 1.9 Hz, 4H), 7.56 (d, J = 1.4 Hz, 4H), 7.12 (s, 4H), 6.62 (s, 8H), 6.58 (s, 8H), 4.07 (t, J = 4.6 Hz, 8H), 3.70 (t, J = 4.4 Hz, 8H), 3.48 (t, J = 6.5 Hz, 8H), 2.01 (s, 24H), 1.58-1.52 (m, 8H), 1.50 (s, 24H), 1.40-1.35 (m, 8H).

^{13}C NMR (125 MHz, Acetone-d_6, δ) 163.7, 160.0, 159.8, 157.9, 156.9, 156.5, 153.5, 152.7, 152.5, 141.1, 140.8, 140.3, 137.9, 137.8, 137.3, 137.2, 136.8, 128.3, 125.1, 124.6, 122.9, 120.0, 117.8, 115.7, 114.6, 107.8, 71.7, 69.8, 68.2, 30.5, 26.7, 20.6, 20.4.

IR (neat, cm^{-1}): 3524*w*, 2929*w*, 2865*w*, 1705*w*, 1605*w*, 1454*m*, 1361*w*, 1313*m*, 1277*w*, 1158*w*, 1075*w*, 1031*w*, 1007*w*, 840*s*, 739*w*, 558*m*.

HRMS (ESI) m/z: $[M]^{4+}$ calcd for $C_{152}H_{144}N_{12}O_{16}Ru_2$: 649.22362; found: 649.22274.

Ru(2,6-bis(2-(4-bromo-2,6-dimethylphenyl)furo[2,3-c]pyridin-5-yl)pyridine)⊃(2,2′-(2,2′-(4,4′-(5,5′-(pyridine-2,6-diyl)bis(furo[2,3-*c*]pyridine-5,2-diyl))bis(3,5-dimethyl-4,1-phenylene))bis(oxy)bis(ethane-2,1-diyl))bis(oxy)diethanol))$(PF_6)_2$ (101)

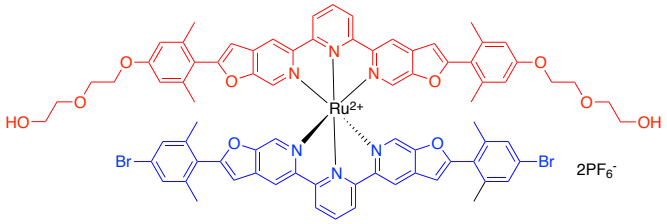

A mixture of Ru(2,6-bis(2-(4-bromo-2,6-dimethylphenyl)furo[2,3-c]pyridin-5-yl)pyridine)Cl_3 (**100**) (134 mg, 1.0 eq, 0.151 mmol), 2,2′-(2,2′-(4,4′-(5,5′-(pyridine-2,6-diyl)bis(furo[2,3-*c*]pyridine-5,2-diyl))bis(3,5-dimethyl-4,1-phenylene))bis(oxy)bis(ethane-2,1-diyl))bis(oxy)diethanol (**L17**) (110 mg, 1.0 eq, 0.151 mmol) and *N*-ethylmorpholine (44.6 μL, 2.3 eq, 0.350 mmol) in EtOH (36 mL) was heated to reflux for 24 h. The reaction mixture was allowed to cool down to room temperature and sat. aq. KPF_6 was added. The resulting brown precipitate was filtered over Celite, washed on the filter with excess water, EtOAc, Et_2O and re-dissolved with acetonitrile into a clean flask. After evaporation of solvent the resulting brown solid was purified by silica gel column chromatography – first, a brown band was eluted by using the 1st eluent (MeCN:H_2O:aq.KPF_6 97:3:0.3), then it was switched to the 2nd eluent (MeCN:H_2O:aq.KPF_6 95:5:1) to move a red band which contained the desired product **101**. The combined product fractions were evaporated under reduced pressure, re-dissolved in acetonitrile and sat. aq. KPF_6 was added. The resulting precipitate was collected by filtration over Celite, washed with excess water, Et_2O and re-dissolved with acetonitrile into a clean flask. After evaporation the desired product **101** (114 mg, 42%) was obtained as a red solid. Recrystallization by slow Et_2O vapor diffusion into the acetone solution of **101** gave single crystals suitable for X-ray diffraction analysis.

Mp >320 °C dec.

^{1}H NMR (400 MHz, CD_3CN): 8.85 (d, J = 0.8 Hz, 2H), 8.82 (d, J = 0.8 Hz, 2H), 8.75 (d, J = 8.2 Hz, 2H), 8.75 (d, J = 8.2 Hz, 2H), 8.43 (t, J = 8.1 Hz, 1H), 8.43 (t, J = 8.1 Hz, 1H), 7.72 (s, 2H), 7.69 (s, 2H), 7.35 (s, 4H), 7.05 (d, J = 0.8 Hz, 2H), 6.98 (d, J = 0.8 Hz, 2H), 6.71 (s, 4H), 4.14-4.06 (m, 4H), 3.84-3.73 (m, 4H), 3.65-3.57 (m, 4H), 3.56-3.50 (m, 4H), 2.69 (br. s, 2H), 2.04 (s, 12H), 2.04 (s, 12H).

^{13}C NMR (126 MHz, CD_3CN): 163.0, 161.3, 161.1, 156.9, 156.8, 153.1, 152.9, 152.7, 152.5, 141.8, 141.3, 137.7, 137.5, 137.3, 137.2, 136.8, 136.8, 131.6, 128.4, 125.0, 123.2, 123.1, 121.6, 117.8, 114.8, 108.4, 107.8, 73.5, 70.1, 68.5, 62.0, 20.7, 20.3.

IR (film on NaCl, cm^{-1}): 3427*s*, 2925*w*, 2866*w*, 1603*m*, 1454*s*, 1384*w*, 1313*m*, 1251*w*, 1162*w*, 1127*w*, 1068*w*, 1007*w*, 842*vs*, 558*m*.

HRMS (ESI) *m/z*: $[M]^{2+}$ calcd for $C_{78}H_{68}Br_2N_6O_{10}Ru$: 755.12012; found: 755.12074.

Ru(2,6-bis(2-(4-bromo-2,6-dimethylphenyl)furo[2,3-c]pyridin-5-yl)pyridine) ⊃(2,2′-(2,2′-(4,4′-(5,5′-(pyridine-2,6-diyl)bis(furo[2,3-*c*]pyridine-5,2-diyl))bis(3,5-dimethyl-4,1-phenylene))bis(oxy)bis(ethane-2,1-diyl))bis(oxy)bis(ethane-2,1-diyl) dimethanesulfonate)(PF_6)$_2$ (99)

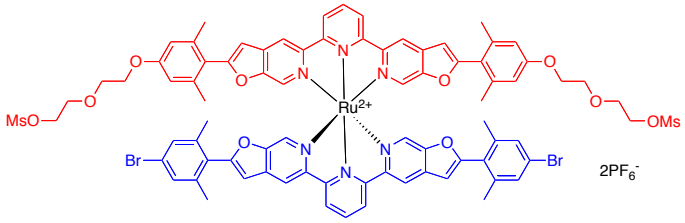

To a solution of **101** (44.2 mg, 1.0 eq, 0.0246 mmol) in a mixture of anhydrous THF (3.5 mL) and acetonitrile (1.5 mL) under Ar atmosphere were added triethylamine (0.137 mL, 40 eq, 0.982 mmol) and methanesulfonyl chloride (0.048 mL, 20 eq, 0.491 mmol). The reaction mixture was stirred for 1 h at room temperature. To the mixture was added sat. aq. KPF_6 to cause precipitation. The resulting red solid was collected by filtration over Celite, washed on the filter with excess water, Et_2O and 1:1 hexane:EtOAc then re-dissolved with acetonitrile into a clean flask. After evaporation of solvent and drying under vacuum the desired product **99** (47.5 mg, 99%) was obtained as a red solid.

Mp >230 °C.

^{1}H NMR (400 MHz, CD_3CN): 8.85 (d, J = 0.8 Hz, 2H), 8.82 (d, J = 0.8 Hz, 2H), 8.75 (d, J = 8.2 Hz, 2H), 8.74 (d, J = 8.2 Hz, 2H), 8.44 (t, J = 8.2 Hz, 1H), 8.43 (t, J = 8.2 Hz, 1H), 7.72 (s, 2H), 7.69 (s, 2H), 7.35 (s, 4H), 7.05 (d, J = 0.8 Hz, 2H), 6.98 (d, J = 0.8 Hz, 2H), 6.70 (s, 4H), 4.35-4.28 (m, 4H), 4.15-4.07 (m, 4H), 3.83-3.76 (m, 4H), 3.79-3.72 (m, 4H), 3.02 (s, 6H), 2.04 (s, 12H), 2.04 (s, 12H).

^{13}C NMR (125 MHz, CD_3CN): 162.0, 160.3, 160.0, 155.9, 155.9, 152.1, 151.9, 151.7, 151.6, 140.8, 140.3, 136.7, 136.5, 136.3, 136.2, 135.8, 135.8, 130.6, 127.4, 124.1, 122.2, 122.1, 120.7, 116.8, 113.8, 107.4, 106.8, 69.9, 69.3, 68.8, 67.3, 36.7, 19.7, 19.3.

IR (film on NaCl, cm^{-1}): 2957*w*, 2925*w*, 2858*w*, 1603*m*, 1455*s*, 1351*w*, 1313*m*, 1251*w*, 1175*m*, 1164*m*, 1072*w*, 1008*w*, 840*vs*, 558*m*.

HRMS (ESI) *m/z*: $[M]^{2+}$ calcd for $C_{80}H_{72}Br_2N_6O_{14}RuS_2$: 833.09763; found: 833.09738.

2-(2-(4-ethynylphenoxy)ethoxy)ethanol (106)

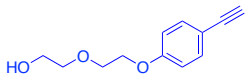

To a mixture of 2-(2-(4-iodophenoxy)ethoxy)ethanol (**105**)[77,78] (2.5 g, 1.0 eq, 8.11 mmol), $Pd(PPh_3)_2Cl_2$ (171 mg, 3 mol%, 0.243 mmol) and CuI (46 mg, 3 mol%, 0.243 mmol) in triethylamine (30 mL) under N_2 atmosphere was added trimethylsilylacetylene (2.3 mL, 2.0 eq, 16 mmol). The reaction mixture was heated to 75 °C for 18 h. The mixture was allowed to cool to room temperature, and the solvent was evaporated under reduced pressure. The resulting residue was dissolved in minimum amount of CH_2Cl_2 and filtered through a plug of silica gel eluting with EtOAc. The filtrate was evaporated under reduced pressure to give crude 2-(2-(4-((trimethylsilyl)ethynyl)phenoxy)ethoxy)ethanol.

^{1}H NMR (400 MHz, $CDCl_3$) 7.39 (AA′BB′ spin system, 2H), 8.83 (AA′BB′ spin system, 2H), 4.16-4.08 (m, 2H), 3.89-3.82 (m, 2H), 3.78-3.72 (m, 2H), 3.70-3.62 (m, 2H), 0.23 (s, 9H).

The obtained product was dissolved in a mixture of MeOH (32 mL) and CH_2Cl_2 (5 mL). To the solution KF (4.7 g, 10 eq, 81 mmol) was added and the mixture was heated to 50 °C for 4 h. The solvent was evaporated under reduced pressure and the resulting residue was filtered through a plug of silica gel eluting with CH_2Cl_2. The solvent from the filtrate was evaporated under reduced pressure to give desired 2-(2-(4-ethynylphenoxy)ethoxy)ethanol (**106**) (1.65 g, 99%) as a yellowish oil.

^{1}H NMR (500 MHz, $CDCl_3$): 7.42 (AA′BB′ spin system, 2H), 6.86 (AA′BB′ spin system, 2H), 4.15-4.13 (m, 2H), 3.87-3.85 (m, 2H), 3.77-3.75 (m, 2H), 3.68-3.66 (m, 2H), 3.00 (s, 1H), 2.09 (s, 1H).

^{13}C NMR (125 MHz, $CDCl_3$): 159.2, 133.7, 114.7, 114.7, 83.7, 76.1, 72.7, 69.7, 67.6, 61.9.

IR (film on NaCl, cm^{-1}): 3418*br*, 3285*s*, 3043*w*, 2931*s*, 2877*s*, 2537*w*, 2105*m*, 1605*s*, 1572*m*, 1505*s*, 1455*s*, 1356*m*, 1289*s*, 1250*s*, 1173*s*, 1131*s*, 1059*s*, 929*m*, 888*m*, 837*m*, 538*w*.

HRMS (ESI) *m/z*: $[M+Na]^+$ calcd for $C_{12}H_{14}NaO_3$: 229.08352; found: 229.08328.

2-(2-(4-ethynylphenoxy)ethoxy)ethyl 4-methylbenzenesulfonate (107)

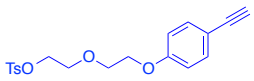

To a solution of 2-(2-(4-ethynylphenoxy)ethoxy)ethanol (**106**) (1.49 g, 1.0 eq, 7.22 mmol), DMAP (26 mg, 0.3 eq, 0.22 mmol) and triethylamine (3.0 mL, 3.0 eq, 21 mmol) in CH_2Cl_2 (50 mL) was added 4-toluenesulfonyl chloride (2.20 g, 1.5 eq, 11.6 mmol) in one portion. The reaction mixture was stirred for 2.5 h at room temperature. The reaction was quenched with water (100 ml), organic layer was separated, washed with water (2 × 50 ml), dried over $MgSO_4$, filtered and evaporated under reduced pressure. The resulting crude product was purified by silica gel column chromatography (eluent hexane:EtOAc 3:1) to give 2-(2-(4-ethynylphenoxy)ethoxy)ethyl 4-methylbenzenesulfonate (**107**) (1.99 g, 76%) as a yellowish oil.

^{1}H NMR (500 MHz, $CDCl_3$): 7.79 (AA′BB′ spin system, 2H), 7.41 (AA′BB′ spin system, 2H), 7.30 (AA′BB′ spin system, 2H), 6.82 (AA′BB′ spin system, 2H), 4.20-4.18 (m. 2H), 4.05-4.04 (m, 2H), 3.79-3.77 (m, 2H), 3.76-3.74 (m, 2H), 3.00 (s, 1H), 2.41 (s, 3H).

^{13}C NMR (126 MHz, $CDCl_3$): 159.1, 145.0, 133.7, 133.1, 129.9, 128.1, 125.5, 114.7, 83.7, 76.1, 69.9, 69.3, 69.1, 67.6, 21.8.

IR (film on NaCl, cm^{-1}): 3281*m*, 3065*w*, 3045*w*, 2922*w*, 2877*w*, 2105*w*, 1605*m*, 1572*w*, 1506*s*, 1454*w*, 1399*w*, 1355*s*, 1289*m*, 1249*m*, 1189*m*, 1176*s*, 1138*m*, 1018*w*, 919*m*, 836*m*, 815*m*, 775*w*, 663*m*, 554*w*.

HRMS (ESI) *m/z*: $[M+Na]^+$ calcd for $C_{19}H_{20}NaO_5S$: 383.09237; found: 383.09267.

Ru(2,6-bis-(2-(4-hydroxy-2,6-dimethylphenyl)furo[2,3-c]pyridin-5-yl)- pyridine)⊃(2,2′-(2,2′-(4,4′-(5,5′-(pyridine-2,6-diyl)bis(furo[2,3-*c*]pyridine-5,2-diyl))bis(3,5-dimethyl-4,1-phenylene))bis(oxy)bis(ethane-2,1-diyl))bis(oxy)diethanol))$(PF_6)_2$ (108)

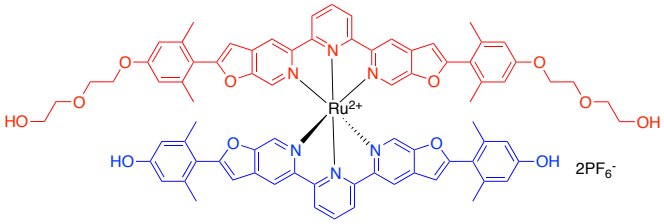

To a mixture of 2,2′-(2,2′-(4,4′-(5,5′-(pyridine-2,6-diyl)bis(furo[2,3-*c*]pyridine-5,2-diyl))bis(3,5-dimethyl-4,1-phenylene))bis(oxy)bis(ethane-2,1-diyl))bis(oxy)diethanol (**L17**) (200 mg, 1.0 eq, 0.274 mmol) and Ru(2,6-bis-(2-(4-hydroxy-2,6-dimethylphenyl)furo[2,3-c]pyridin-5-yl)- pyridine)Cl_3 (**97**) (209 mg, 1.0 eq, 0.274 mmol) in degassed EtOH (100 mL) under N_2 atmosphere was added *N*-ethylmorpholine (0.081 mL, 2.3 eq, 0.636 mmol). The reaction mixture was heated to reflux for 20 h. The mixture was allowed to cool to room

temperature and sat. aq. KPF_6 was added. The resulting precipitate was collected by filtration over Celite, washed on the filter with excess water, Et_2O, hexane:EtOAc 1:1 and re-dissolved with acetonitrile into a clean flask. The solvent was evaporated and resulting residue was purified by silica gel column chromatography– first, a brown/green band was eluted by using the 1st eluent (MeCN:H_2O:aq.KPF_6 97:3:0.3), then it was switched to the 2nd eluent (MeCN:CH_2Cl_2:H_2O:aq.KPF_6 51:9:3:1) to move a red band which contained the product **108**. The combined product fractions were evaporated under reduced pressure, re-dissolved in acetonitrile and re-precipitated by addition of sat. aq. KPF_6. The resulting precipitate was collected over Celite, washed on the filter with excess water, Et_2O and re-dissolved into a clean flask. After evaporation of solvent the desired product **108** (288 mg, 63%) was obtained as a red solid.

Mp >200 °C dec.

^{1}H NMR (500 MHz, CD_3CN): 8.82 (s, 2H), 8.82 (s, 2H), 8.75 (d, *J* = 8.2 Hz, 2H), 8.75 (d, *J* = 8.1 Hz, 2H), 8.43 (t, *J* = 8.2 Hz, 1H), 8.43 (t, *J* = 8.1 Hz, 1H), 7.69 (s, 2H), 7.68 (s, 2H), 7.16 (s, 2H), 6.97 (s, 2H), 6.94 (s, 2H), 6.70 (s, 4H), 6.56 (s, 4H), 4.15-4.06 (m, 4H), 3.79-3.74 (m, 4H), 3.64-3.57 (m, 4H), 3.57-3.49 (m, 4H), 2.83 (t, *J* = 5.4 Hz, 2H), 2.03 (s, 12H), 1.99 (s, 12H).

^{13}C NMR (125 MHz, CD_3CN): 163.2, 162.9, 161.0, 159.4, 156.9, 153.0, 153.0, 152.6, 152.6, 141.3, 141.3, 137.5, 137.5, 137.3, 137.3, 136.7, 123.1, 123.1, 121.8, 120.8, 117.8, 117.8, 115.6, 114.8, 107.9, 107.8, 73.3, 70.1, 68.5, 61.9, 20.7, 20.6.

IR (KBr, cm^{-1}): 3431*br*, 3125*w*, 2953*w*, 2921*w*, 2871*w*, 1607*m*, 1454*s*, 1384*w*, 1313*m*, 1288*w*, 1276*w*, 1158*m*, 1128*w*, 1065*w*, 1031*w*, 1005*w*, 843*s*, 739*w*, 558*m*.

HRMS (ESI) *m/z*: $[M]^{2+}$ calcd for $C_{78}H_{70}N_6O_{12}Ru$: 692.20529; found: 692.20595.

Ru(2,6-bis(2-(4-(2-(2-(4-ethynylphenoxy)ethoxy)ethoxy)-2,6-dimethylphenyl)furo[2,3-*c*]pyridin-5-yl)pyridine)⊃(2,2′-(2,2′-(4,4′-(5,5′-(pyridine-2,6-diyl)bis(furo[2,3-*c*]pyridine-5,2-diyl))bis(3,5-dimethyl-4,1-phenylene))bis(oxy)bis(ethane-2,1-diyl))bis(oxy)diethanol))$(PF_6)_2$ (109)

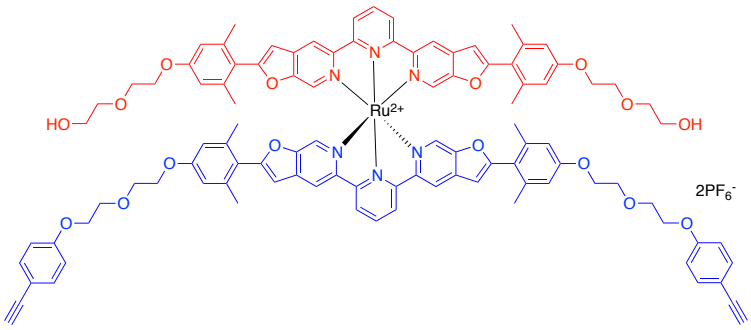

To a mixture of heteroleptic Ru(II) complex **108** (200 mg, 1.0 eq, 0.119 mmol), 2-(2-(4-ethynylphenoxy)ethoxy)ethyl 4-methylbenzenesulfonate (**107**) (94.7 mg, 2.2 eq, 0.263 mmol)

and anhydrous Cs_2CO_3 (117 mg, 3.0 eq, 0.358 mmol) under N_2 atmosphere was added anhydrous DMF (37 mL). The reaction mixture was heated to 80 °C for 9.5 h, allowed to cool to room temperature and sat. aq. KPF_6 was added. The resulting red precipitate was collected by filtration over Celite, washed on the filter with excess water, Et_2O, hexane:EtOAc 3:1 and re-dissolved in a clean flask. After evaporation of solvent and drying under vacuum the desired complex (**109**) was obtained as a red solid (226 mg, 92%).

Mp >247 °C dec.

^{1}H NMR (500 MHz, CD_3CN): 8.82 (s, 4H), 8.74 (d, J = 8.2 Hz, 4H), 8.43 (t, J = 8.2 Hz, 2H), 7.69 (d, J = 0.9 Hz, 4H), 7.39 (AA′BB′ spin system, 4H), 6.98 (d, J = 0.9 Hz, 2H), 6.97 (d, J = 0.9 Hz, 2H), 6.88 (AA′BB′ spin system, 4H), 6.71 (s, 4H), 6.68 (s, 4H), 4.13-4.09 (m, 12H), 3.86-3.79 (m, 8H), 3.79-3.73 (m, 4H), 3.61-3.58 (m, 4H), 3.56-3.51 (m, 4H), 3.25 (s, 2H), 2.67 (t, J = 5.6 Hz, 2H), 2.04 (s, 12H), 2.03 (s, 12H).

^{13}C NMR (125 MHz, CD_3CN): 163.0, 161.1, 161.1, 160.3, 156.9, 153.0, 152.6, 141.3, 141.2, 137.4, 137.3, 136.7, 134.5, 123.1, 121.6, 117.8, 115.7, 115.1, 114.8, 114.8, 107.8, 84.2, 77.5, 73.5, 70.3, 70.3, 70.1, 68.6, 68.5, 68.4, 62.0, 20.7.

IR (film on NaCl, cm^{-1}): 3744*w*, 3310*w*, 3282*w*, 2953*w*, 2919*w*, 2871*w*, 2103*w*, 1604*s*, 1506*m*, 1384*w*, 1313*m*, 1289*m*, 1250*m*, 1162*m*, 1130*m*, 1067*w*, 1031*w*, 1004*w*, 841*s*, 808*w*, 735*w*, 558*m*.

HRMS (ESI) *m/z*: $[M]^{2+}$ calcd for $C_{102}H_{94}N_6O_{16}Ru$: 880.28820; found: 880.28864.

Ru(2,6-bis(2-(4-(2-(2-(4-ethynylphenoxy)ethoxy)ethoxy)-2,6-dimethylphenyl)furo[2,3-*c*]pyridin-5-yl)pyridine)⊃(2,2′-(2,2′-(4,4′-(5,5′-(pyridine-2,6-diyl)bis(furo[2,3-*c*]pyridine-5,2-diyl))bis(3,5-dimethyl-4,1-phenylene))bis(oxy)bis(ethane-2,1-diyl))bis(oxy)bis(ethane-2,1-diyl) dimethanesulfonate)(PF_6)$_2$ (110a)

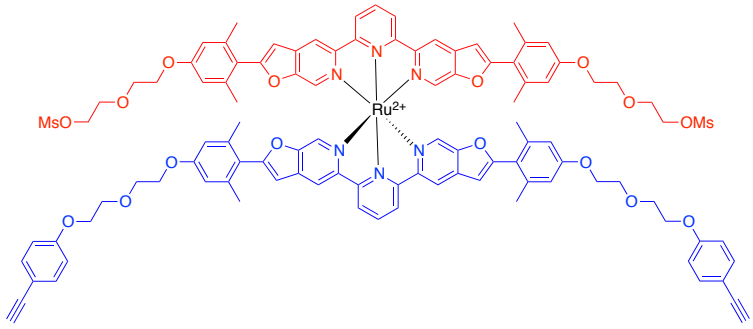

To a solution of heteroleptic Ru(II) complex **109** (40.0 mg, 1.0 eq, 0.0195 mmol) in mixture of anhydrous THF (3 mL) and acetonitrile (0.5 mL) under Ar atmosphere was added triethylamine (163 μL, 60 eq, 1.17 mmol) and methanesulfonyl chloride (45 μL, 30 eq, 0.58 mmol) that caused formation of precipitate. The reaction mixture was stirred for 2 h at room temperature. To the mixture sat. aq. KPF_6 was added, and the resulting red precipitate was

collected by filtration over Celite, washed with excess water, Et_2O, hexane:Et_2O 1:1 and re-dissolved into a clean flask. After evaporation of solvent and drying under vacuum the desired product **110a** (39.4 mg, 92%) was obtained as a red solid.

Mp >239 °C dec.

^{1}H NMR (400 MHz, CD_3CN): 8.82 (s, 4H), 8.74 (d, J = 8.2 Hz, 4H), 8.43 (t, J = 8.1 Hz, 2H), 7.69 (s, 2H), 7.69 (s, 4H), 7.39 (AA′BB′ spin system, 4H), 6.98 (d, J = 0.9 Hz, 2H), 6.97 (d, J = 0.9 Hz, 2H), 6.88 (AA′BB′ spin system, 4H), 6.70 (s, 4H), 6.68 (s, 4H), 4.35-4.28 (m, 4H), 4.14-4.09 (m, 12H), 3.87-3.76 (m, 12H), 3.79-3.71 (m, 4H), 3.25 (s, 2H), 3.02 (s, 6H), 2.04 (s, 12H), 2.03 (s, 12H).

^{13}C NMR (125 MHz, CD_3CN): 163.0, 163.0, 161.1, 161.0, 160.3, 156.9, 153.0, 152.6, 141.3, 141.2, 137.4, 137.3, 136.7, 134.5, 123.1, 121.7, 121.6, 117.8, 115.7, 115.1, 114.8, 114.8, 107.8, 84.2, 77.5, 70.9, 70.3, 70.3, 70.3, 69.8, 68.6, 68.4, 68.3, 37.7, 20.7.

IR (film on NaCl, cm^{-1}): 3310*w*, 3281*w*, 3125*w*, 3043*w*, 2957*w*, 2919*w*, 2875*w*, 2103*w*, 1604*m*, 1508*m*, 1455*s*, 1351*m*, 1313*s*, 1289*m*, 1251*m*, 1163*m*, 1133*m*, 1071*w*, 1005*w*, 974*w*, 923*w*, 914*w*, 841*s*, 807*w*, 735*w*, 558*w*.

HRMS (ESI) *m/z*: $[M]^{2+}$ calcd for $C_{104}H_{98}N_6O_{20}RuS_2$: 958.26572; found: 958.26570.

Ru(2,6-bis(2-(4-(2-(2-(4-ethynylphenoxy)ethoxy)ethoxy)-2,6-dimethylphenyl)furo[2,3-*c*]pyridin-5-yl)pyridine)⊃(2,2′-(2,2′-(4,4′-(5,5′-(pyridine-2,6-diyl)bis(furo[2,3-*c*]pyridine-5,2-diyl))bis(3,5-dimethyl-4,1-phenylene))bis(oxy)bis(ethane-2,1-diyl))bis(oxy)bis(ethane-2,1-diyl) bis(4-methylbenzenesulfonate))$(PF_6)_2$ (110b)

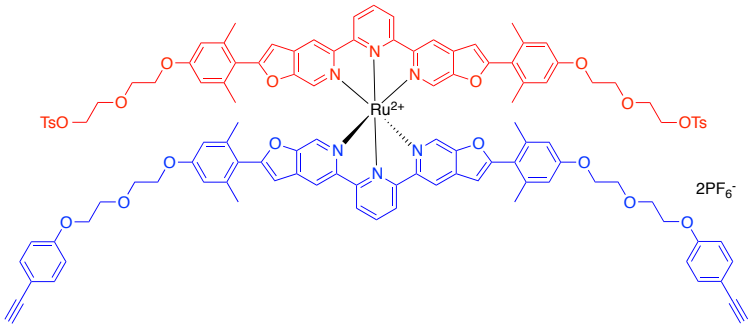

To a mixture of heteroleptic Ru(II) complex **109** (40.0 mg, 1.0 eq, 0.0195 mmol), 4-toluenesulfonyl chloride (54.7 mg, 14.7 eq, 0.286 mmol) and DMAP (1.4 mg, 0.6 eq, 0.012 mmol) in anhydrous CH_2Cl_2 (3.5 mL) under Ar atmosphere was added triethylamine (65 µL, 24 eq, 0.47 mmol). The reaction mixture was stirred at room temperature for 3.5 h. To the mixture sat. aq. KPF_6 was added, and the resulting precipitate was filtered over Celite, washed with excess water, Et_2O, hexane:EtOAc and re-dissolved into a clean flask. After evaporation of solvent and drying under vacuum the desired product **110b** (45.2 mg, 98%) was obtained as red solid.

Mp >259 °C dec.

^{1}H NMR (500 MHz, Acetone-d_6): 9.17 (s, 4H), 9.06 (d, J = 8.2 Hz, 4H), 8.60 (t, J = 8.2 Hz, 2H), 8.10 (s, 2H), 8.10 (s, 2H), 7.78 (AA′BB′ spin system, 4H), 7.42 (AA′BB′ spin system, 4H), 7.38 (AA′BB′ spin system, 4H), 7.13 (d, J = 0.9 Hz, 2H), 7.12 (d, J = 0.9 Hz, 2H), 6.92 (AA′BB′ spin system, 4H), 6.72 (s, 4H), 6.71 (s, 4H), 4.20-4.14 (m, 12H), 4.11-4.05 (m, 4H), 3.91-3.85 (m, 8H), 3.78-3.69 (m, 8H), 3.47 (s, 2H), 2.40 (s, 6H), 2.05 (s, 12H, overlap with acetone-d_6 signal), 2.03 (s, 12H).

^{13}C NMR (125 MHz, Acetone-d_6): 163.1, 163.1, 161.2, 161.1, 160.3, 157.1, 152.9, 152.9, 152.9, 145.8, 140.9, 140.9, 137.6, 137.2, 137.0, 134.3, 134.2, 130.8, 128.7, 123.2, 121.4, 121.3, 118.0, 115.6, 115.3, 114.8, 107.9, 84.2, 77.6, 70.7, 70.4, 70.4, 70.2, 69.4, 68.6, 68.4, 68.2, 21.5, 20.8.

IR (film on NaCl, cm^{-1}): 3310*w*, 3281*w*, 3125*w*, 3073*w*, 2953*w*, 2921*w*, 2879*w*, 2103*w*, 1604*s*, 1506*m*, 1455*s*, 1355*w*, 1313*m*, 1289*m*, 1250*m*, 1190*w*, 1176*m*, 1163*m*, 1134*w*, 1005*w*, 913*w*, 841*vs*, 736*w*, 557*m*.

HRMS (ESI) *m/z*: $[M]^{2+}$ calcd for $C_{116}H_{106}N_6O_{20}RuS_2$: 1034.29704; found: 1034.29805.

Synthesis of Threaded Ring-in-Ring Complex 102

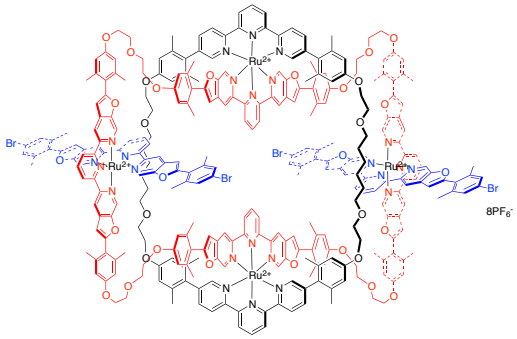

A mixture of threaded macrocycle **98** (5.48 mg, 1.0 eq, 0.001725 mmol), mesylate Ru(II) cap **99** (3.38 mmol, 1.0 eq, 0.001725 mmol) and anhydrous K_2CO_3 (5.96 mg, 25 eq, 0.0431 mmol) in anhydrous DMF (4.0 mL) under Ar atmosphere was heated to 75 °C for 18 h, and then additional portion of mesylate **99** (2.20 mg, 0.65 eq, 0.00112 mmol) in DMF (0.5 mL) was added. The heating of the mixture was continued for 8 h, after which the final portion of **99** (2.20 mg, 0.65 eq, 0.00112 mmol) in DMF (0.5 mL) was added. The reaction mixture was heated for another 18 h, allowed to cool to room temperature and sat. aq. KPF_6 was added. The resulting red precipitate was collected by filtration over Celite, washed on the filter with excess water, Et_2O, hexane:EtOAc 3:1 and re-dissolved with acetonitrile into a clean flask. After evaporation of solvent the red residue was purified by silica gel column chromatography (eluent MeCN:CH_2Cl_2:H_2O:aq.KPF_6 97:67:3:0.3). The combined product

fractions were evaporated; the residue was treated with CH_2Cl_2 filtered and evaporated to give the product (could also contain exo/exo and endo/exo isomers) **102** (4.7 mg, 41%) as a red solid.

Mp >200 °C.

^{1}H NMR (600 MHz, Acetone-d_6): 9.10-9.05 (m, 16H), 8.99-8.93 (m, 8H), 8.79 (s, 4H), 8.78 (s, 4H), 8.54-8.46 (m, 6H), 8.28 (t, J = 8.1 Hz, 2H), 8.04 (s, 4H), 8.00 (s, 4H), 7.99 (s, 4H), 7.81 (dd, J = 8.3, 1.8 Hz, 4H), 7.45 (d, J = 1.5 Hz, 4H), 7.21 (s, 8H), 7.14 (s, 4H), 7.06 (s, 4H), 7.02 (s, 4H), 6.62 (s, 8H), 6.61 (s, 8H), 6.47 (s, 8H), 4.08-4.02 (m, 16H), 3.97-3.95 (m, 8H), 3.76-3.68 (m, 16H), 3.62-3.58 (m, 8H), 3.40-3.36 (m, 8H), 1.95 (overlap with signal of acetone-d_6, 48H), 1.91 (s, 24H), 1.50-1.42 (m, 8H), 1.40 (s, 24H), 1.29-1.26 (m, 8H).

^{13}C NMR (125 MHz, Acetone-d_6): 163.3, 163.2, 163.1, 163.1, 161.3, 159.8, 158.0, 157.1, 157.1, 157.0, 156.6, 153.6, 153.1, 153.0, 152.9, 152.8, 152.6, 141.6, 141.3, 140.9, 140.9, 140.8, 138.0, 137.9, 137.8, 137.6, 137.6, 137.4, 137.3, 137.3, 137.3, 137.1, 137.1, 131.5, 128.4, 128.3, 125.2, 125.0, 124.7, 123.3, 123.2, 123.2, 121.4, 121.3, 118.3, 118.1, 114.9, 114.7, 114.7, 108.6, 108.0, 107.8, 71.9, 70.5, 70.4, 69.9, 68.7, 68.5, 68.1, 29.2, 26.9, 20.8, 20.7, 20.5, 20.3.

IR (film on NaCl, cm^{-1}): 3091*w*, 2957*w*, 2919*w*, 2853*w*, 1603*m*, 1313*m*, 1280*m*, 1263*m*, 1163*m*, 1009*w*, 842*s*, 807*m,* 701*w*, 558*w*.

HRMS (ESI) *m/z*: $[M]^{8+}$ calcd for $C_{308}H_{272}Br_4N_{24}O_{32}Ru_4$: 692.66692; found: 692.66787; $[M+PF_6]^{7+}$ calcd for $C_{308}H_{272}Br_4F_6N_{24}O_{32}PRu_4$: 812.32858; found: 812.32970.

Synthesis of Threaded Ring-in-Ring Complex 111

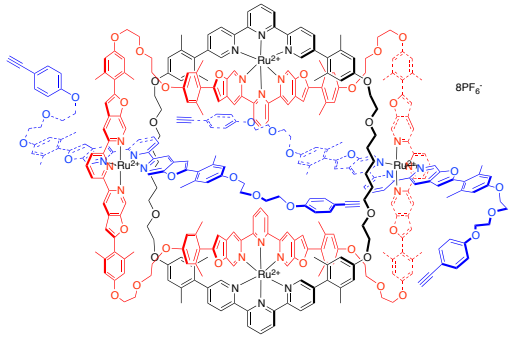

A mixture of threaded macrocycle **98** (17.8 mg, 1.0 eq, 0.00560 mmol), mesylate Ru(II) cap **110a** (27.7 mg, 2.2 eq, 0.0125 mmol), anhydrous K_2CO_3 (20.1 mg, 26 eq, 0.146 mmol) and activated 4 Å molecular sieve powder (~30 mg) in anhydrous DMF (11 mL) under Ar atmosphere was heated to 70 °C for 34 h. Then the reaction temperature was increased to 78 °C, and the heating was continued for another 24 h. To the mixture additional mesylate Ru(II) cap **110a** (6.2 mg, 0.5 eq, 0.0028 mmol) in anhydrous DMF (1 mL) was added and the

mixture was heated to 80 °C for 32 h. The reaction mixture was allowed to cool to room temperature, and sat. aq. KPF_6 was added. The resulting precipitate was collected by filtration over Celite, washed on the filter with excess water, Et_2O, hexane:EtOAc 3:1 and re-dissolved with acetonitrile into a clean flask. After evaporation of solvent the red residue was purified by silica gel column chromatography– first, a band containing a mixture of unreacted **110a** and hydrolysation product **109** was moved by using 1st eluent (MeCN:CH_2Cl_2:H_2O:sat.KPF_6 139:11:5:1), then it was switched to 2nd eluent (MeCN:CH_2Cl_2:H_2O:sat.KPF_6 139:36:7:2) to elute band which contained the desired product **111**. The fractions containing **111** were evaporated and the residue was subjected to the 2nd column chromatography (eluent MeCN:CH_2Cl_2:H_2O:sat.KPF_6 139:47:4:0.4). The desired product moved as a first band. After evaporation of product fractions, the residue was dissolved in CH_2Cl_2, filtered and evaporated under reduced pressure to give a desired product **111** (8.2 mg, 20%) as a red solid.

Mp >250 °C dec.

^{1}H NMR (600 MHz, Acetone-d_6): 9.19-9.10 (m, 16H), 9.09-9.02 (m, 8H), 8.91-8.85 (m, 8H), 8.64-8.56 (m, 6H), 8.41-8.34 (m, 2H), 8.10 (s, 12H), 7.92 (dd, J = 8.2, 1.8 Hz, 4H), 7.55 (m, 4H), 7.39-7.36 (m, 8H), 7.20-7.12 (m, 12H), 6.91-6.90 (m, 8H), 6.73 (s, 8H), 6.72 (s, 8H), 6.70 (s, 8H), 6.57 (s, 8H), 4.18-4.14 (m, 32H), 4.06-4.05 (m, 8H), 3.89-3.83 (m, 32H), 3.73-3.67 (m, 8H), 3.50-3.47 (m, 8H), 3.47 (s, 4H), 2.03 (s, 24H), 2.02 (s, 24H), 2.01 (s, 24H), 1.62-1.52 (m, 8H), 1.50 (s, 24H), 1.40-1.36 (m, 8H).

^{13}C NMR (150 MHz, Acetone-d_6): 163.1, 163.1, 161.6, 161.5, 161.2, 160.3, 159.8, 157.9, 157.3, 157.1, 157.0, 153.6, 152.9, 152.8, 152.8, 152.6, 141.2, 140.9, 140.9, 140.8, 140.3, 137.9, 137.9, 137.7, 137.6, 137.3, 137.2, 137.2, 137.0, 134.2, 128.4, 125.2, 124.7, 123.3, 123.2, 123.0, 121.3, 118.0, 115.6, 115.3, 115.1, 115.0, 114.8, 114.7, 107.9, 84.2, 77.7, 71.9, 71.7, 71.0, 71.0, 70.5, 70.4, 69.9, 68.6, 68.4, 30.3, 26.8, 20.8, 20.7, 20.7, 20.5.

IR (film on NaCl, cm^{-1}): 3315w, 3280w, 3122w, 3073w, 2924m, 2867w, 2103w, 1604s, 1505w, 1454s, 1383w, 1313m, 1291m, 1279m, 1252m, 1162m, 1128w, 1072w, 1005w, 841vs, 735w, 558m.

HRMS (ESI) *m/z*: $[M]^{8+}$ calcd for $C_{356}H_{324}N_{24}O_{44}Ru_4$: 755.75166; found: 755.75142; $[M+PF_6]^{7+}$ calcd for $C_{356}H_{324}F_6N_{24}O_{44}PRu_4$: 884.42544; found: 884.42499; $[M+2PF_6]^{6+}$ calcd for $C_{356}H_{324}F_{12}N_{24}O_{44}P_2Ru_4$: 1055.99046; found: 1055.98883.

Synthesis of the Borromean Link Ru(II) Complex 115

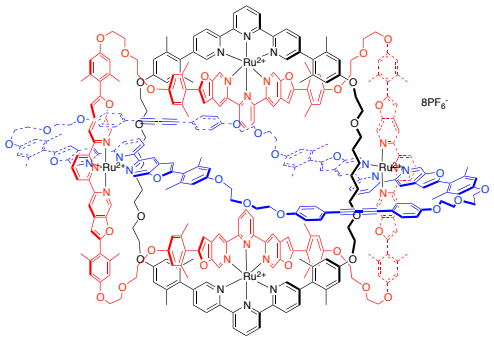

A mixture of threaded ring-in-ring Ru(II) complex **111** (1.64 mg, 1.0 eq, 0.000228 mmol) and $Cu(OAc)_2 \cdot H_2O$ (1.30 mg, 29 eq, 0.00651 mmol) in acetonitrile (2.0 mL) was heated to reflux for 23 h. The reaction mixture was allowed to cool to room temperature, and the solvent was evaporated under reduced pressure. The resulting residue was dissolved in CH_2Cl_2, filtered and the solvent was evaporated under reduced pressure. The residue was dissolved in acetonitrile and re-precipitated by additions of conc. aq. KPF_6. The precipitate was collected by filtration, washed on the filter with excess water, Et_2O, hexane:EtOAc 1:1 and re-dissolved into a clean flask. After evaporation of solvent and drying under vacuum the isomeric mixture of **115** was obtained (1.28 mg, 78%) as a red solid.

Mp > 286 °C dec.

^{1}H NMR (400 MHz, Acetone-d_6): 9.21-8.96 (m, 24H), 8.94-8.82 (m, 8H), 8.65-8.54 (m, 6H), 8.43-8.36 (m, 2H), 8.09 (s, 12H), 7.94-7.89 (m, 4H), 7.60-7.55 (m, 4H), 7.43-7.38 (m, 8H), 7.17-7.10 (m, 12H), 6.97-6.89 (m, 8H), 6.73-6.65 (m, 24H), 6.60-6.57 (m, 8H), 6.77-6.48 (m, 32H), 4.26-4.02 (m, 40H), 3.93-3.65 (m, 40H), 3.53-3.40 (m, 8H), 2.00 (s, 24H, overlap with acetone-d_6), 1.99 (s, 24H), 1.96 (s, 24H), 1.64-1.46 (m, 8H), 1.51 (s, 24H), 1.43-1.33 (m, 8H).

^{13}C NMR (125 MHz, Acetone-d_6): 163.1, 161.5, 161.3, 161.1, 160.0, 159.8, 157.9, 157.3, 157.0, 156.6, 153.7, 153.1, 152.8, 152.5, 140.8, 140.7, 140.6, 140.3, 137.8, 137.6, 137.2, 137.0, 134.8, 128.3, 123.1, 121.3, 118.0, 115.9, 114.8, 107.9, 71.7, 70.5, 70.4, 69.8, 68.6, 68.3, 32.6, 23.3, 20.8, 20.5.

IR (film on NaCl, cm^{-1}): 3125*w*, 3091*w*, 2953*w*, 2921*w*, 2254*w*, 2211*w*, 2138*w*, 1603*m*, 1504*w*, 1455*s*, 1383*w*, 1313*m*, 1289*w*, 1252*w*, 1162*m*, 1128*w*, 1073*w*, 1005*w*, 840*vs*, 737*w*, 559*m*.

HRMS (ESI) *m/z*: $[M]^{8+}$ calcd for $C_{356}H_{320}N_{24}O_{44}Ru_4$: 755.24775; found: 755.24661; $[M+PF_6]^{7+}$ calcd for $C_{356}H_{320}F_6N_{24}O_{44}PRu_4$: 883.84953; found: 883.84914; $[M+2PF_6]^{6+}$ calcd for $C_{356}H_{320}F_{12}N_{24}O_{44}P_2Ru_4$: 1055.31858; found: 1055.31955.

5.5. References

(1) Shankar, R. *Principles of Quantum Mechanics*; Springer US, **1994**.

(2) Gullberg, J. *Mathematics: From the Birth of Numbers*; 1st ed.; W. W. Norton & Company, **1997**.

(3) Goss, R. J.; Shankar, S.; Fayad, A. A. *Nat. Prod. Rep.* **2012**, *29*, 870–889.

(4) Perry, J.; Bratman, M.; Fischer, J. M. *Introduction to Philosophy: Classical and Contemporary Readings*; 6th ed.; Oxford University Press: USA, **2012**.

(5) Lehn, J.-M. *Supramolecular Chemistry*; VCH: Wein-heim, Germany, **1995**.

(6) Safont-Sempere, M. M.; Fernandez, G.; Wurthner, F. *Chem. Rev.* **2011**, *111*, 5784–5814.

(7) Flapan, E. *When Topology Meets Chemistry: A Topological Look at Molecular Chirality*; Cambridge University Press: New York, **2000**.

(8) Dean, F. B.; Stasiak, A.; Koller, T.; Cozzarelli, N. R. *J. Biol. Chem.* **1985**, *260*, 4975–4983.

(9) Spengler, S.; Stasiak, A.; Cozzarelli, N. *Cell* **1985**, *42*, 325–334.

(10) Chambron, J.-C.; Sauvage, J.-P. *New J. Chem.* **2013**, *37*, 49–57.

(11) Iijima, S. *J. Cryst. Growth* **1980**, *50*, 675–683.

(12) Kroto, H. W.; Heath, J. R.; O'Brien, S. C.; Curl, R. F.; Smalley, R. E. *Nature* **1985**, *318*, 162–163.

(13) http://en.wikipedia.org/wiki/File:C60a.png *GNU Free Documentation License*.

(14) http://en.wikipedia.org/wiki/File:Graph_of_60-fullerene_w-nodes.svg *GNU Free Documentation License*.

(15) Liang, C.; Mislow, K. *J. Math. Chem.* **1995**, *18*, 1–24.

(16) Adams, C. C. *The Knot Book: An Elementary Introduction to the Mathematical Theory of Knots*; American Mathematical Society, 2004.

(17) Walba, D. M. *Tetrahedron* **1985**, *41*, 3161–3212.

(18) http://en.wikipedia.org/wiki/File:Blue_Unknot.png *reproduced according to GNU Free Documentation License*.

(19) http://en.wikipedia.org/wiki/File:Blue_Trefoil_Knot.png *reproduced according to GNU Free Documentation License*.

(20) http://en.wikipedia.org/wiki/File:Hopf_Link.png *reproduced according to GNU Free Documentation License*.

(21) Kuratowski, K. *Fund. Math.* **1930**, *15*, 271–283.

(22) Wasserman, E. *J. Am. Chem. Soc.* **1960**, *82*, 4433–4434.

(23) Schill, G. *Chem. Ber.* **1965**, *98*, 2906–2915.

(24) Schill, G. *Chem. Ber.* **1967**, *100*, 2021–2037.

(25) Frisch, H. L.; Wasserman, E. *J. Am. Chem. Soc.* **1961**, *83*, 3789–3795.

(26) Walba, D. M.; Richards, R. M.; Haltiwanger, R. C. *J. Am. Chem. Soc.* **1982**, *104*, 3219–3221.

(27) Simmons, H. E.; Maggio, J. E. *Tetrahedron Lett.* **1981**, *22*, 287–290.

(28) Paquette, L. A.; Vazeux, M. *Tetrahedron Lett.* **1981**, *22*, 291–294.

(29) Walba, D. M.; Homan, T. C.; Richards, R. M.; Haltiwanger, R. C. *New J. Chem.* **1993**, *17*, 661–681.

(30) Chen, C.-T.; Gantzel, P.; Siegel, J. S.; Baldridge, K. K.; English, R. B.; Ho, D. M. *Angew. Chem. Int. Ed. Engl.* **1996**, *34*, 2657–2660.

(31) Dietrich-Buchecker, C. O.; Sauvage, J. P.; Kintzinger, J. P. *Tetrahedron Lett.* **1983**, *24*, 5095–5098.

(32) Dietrich-Buchecker, C. O.; Sauvage, J. P.; Kern, J. M. *J. Am. Chem. Soc.* **1984**, *106*, 3043–3045.

(33) Amabilino, D. B.; Stoddart, J. F. *Chem. Rev.* **1995**, *95*, 2725–2828.

(34) Beves, J. E.; Blight, B. A.; Campbell, C. J.; Leigh, D. A.; McBurney, R. T. *Angew. Chem. Int. Ed.* **2011**, *50*, 9260–9327.

(35) Tian, H.; Wang, Q. C. *Chem. Soc. Rev.* **2006**, *35*, 361–376.

(36) Ruben, M.; Rojo, J.; Romero-Salguero, F. J.; Uppadine, L. H.; Lehn, J. M. *Angew. Chem. Int. Ed.* **2004**, *43*, 3644–3662.

(37) Shen, Y.; Chen, C. F. *Chem. Rev.* **2012**, *112*, 1463–1535.

(38) Hubin, T. J.; Busch, D. H. *Coord. Chem. Rev.* **2000**, *200-202*, 5–52.

(39) Aucagne, V.; Hanni, K. D.; Leigh, D. A.; Lusby, P. J.; Walker, D. B. *J. Am. Chem. Soc.* **2006**, *128*, 2186–2187.

(40) Goldup, S. M.; Leigh, D. A.; Long, T.; McGonigal, P. R.; Symes, M. D.; Wu, J. *J. Am. Chem. Soc.* **2009**, *131*, 15924–15929.

(41) *Image created with KnotPlot software*.

(42) (a) Liang, C.; Mislow, K. *J. Math. Chem.* **1994**, *16*, 27–35. (b) Huylebrouck, D.; Cromwell, P.; Beltrami, E.; Rampichini, M. *Math. Intelligencer* **1998**, *20*, 53–62.

(43) Rolfsen, D. *Knots and links*; Publish or Perish Press: Houston, **1990**.

(44) Loren, J. C.; Yoshizawa, M.; Haldimann, R. F.; Linden, A.; Siegel, J. S. *Angew. Chem. Int. Ed.* **2003**, *42*, 5702–5705.

(45) Baron, M. E. *Math. Gaz.* **1969**, *53*, 113–125.

(46) Woods, C. R.; Benaglia, M.; Toyota, S.; Hardcastle, K.; Siegel, J. S. *Angew. Chem. Int. Ed.* **2001**, *40*, 749–751.

(47) Arias, K. I.; Zysman-Colman, E.; Loren, J. C.; Linden, A.; Siegel, J. S. *Chem. Commun.* **2011**, *47*, 9588–9590.

(48) Watson, J. D.; Crick, F. H. C. *Nature* **1953**, *171*, 737–738.

(49) Mao, C.; Sun, W.; Seeman, N. C. *Nature* **1997**, *386*, 137–138.

(50) Lehn, J.-M. *Angew. Chem. Int. Ed. Engl.* **1990**, *29*, 1304–1319.

(51) Chichak, K. S.; Cantrill, S. J.; Pease, A. R.; Chiu, S. H.; Cave, G. W.; Atwood, J. L.; Stoddart, J. F. *Science* **2004**, *304*, 1308–1312.

(52) Peters, A. J.; Chichak, K. S.; Cantrill, S. J.; Stoddart, J. F. *Chem. Commun.* **2005**, 3394–3396.

(53) Pentecost, C. D.; Peters, A. J.; Chichak, K. S.; Cave, G. W.; Cantrill, S. J.; Stoddart, J. F. *Angew. Chem. Int. Ed.* **2006**, *45*, 4099–4104.

(54) Loren, J. C. PhD thesis, University of California, San Diego, **2004.**

(55) Klosterman, J. K. PhD thesis, University of Zurich, **2007**.

(56) Klosterman, J. K.; Frantz, D.; Veliks, J.; Yasui, Y.; Löpfe, M.; Zysman-Coleman, E.; Linden, A.; Siegel, J. S. *Manuscript in preparation*.

(57) Yus, M.; Nájera, C.; Foubelo, F. *Tetrahedron* **2003**, *59*, 6147–6212.

(58) Frantz, D. K. PhD thesis, University of Zurich, **2012**.

(59) Seifert, H. MS thesis, University of Zurich, **2012**.

(60) Saalfrank, R. W.; Maid, H.; Scheurer, A. *Angew. Chem. Int. Ed.* **2008**, *47*, 8794–8824.

(61) Williamson, A. *Philos. Mag.* **1850**, *37*, 350–356.

(62) Sonogashira, K.; Tohda, Y.; Hagihara, N. *Tetrahedron Lett.* **1975**, *16*, 4467–4470.

(63) Sullivan, B. P.; Calvert, J. M.; Meyer, T. J. *Inorg. Chem.* **1980**, *19*, 1404–1407.

(64) Maestri, M.; Armaroli, N.; Balzani, V.; Constable, E. C.; Thompson, A. M. W. C. *Inorg. Chem.* **1995**, *34*, 2759–2767.

(65) Chinchilla, R.; Najera, C. *Chem. Rev.* **2007**, *107*, 874–922.

(66) Chinchilla, R.; Najera, C. *Chem. Soc. Rev.* **2011**, *40*, 5084–5121.

(67) Huang, H.; Liu, H.; Jiang, H.; Chen, K. *J. Org. Chem.* **2008**, *73*, 6037–6040.

(68) Schilz, M.; Plenio, H. *J. Org. Chem.* **2012**, *77*, 2798–2807.

(69) Schrock, R. R. *Acc. Chem. Res.* **1986**, *19*, 342–348.

(70) Hong, S. H.; Sanders, D. P.; Lee, C. W.; Grubbs, R. H. *J. Am. Chem. Soc.* **2005**, *127*, 17160–17161.

(71) Eglinton, G.; Galbraith, A. R. *J. Chem. Soc.* **1959**, 889–896.

(72) Glaser, C. *Ber. Dtsch. Chem. Ges.* **1869**, *2*, 422–424.

(73) Chausset-Boissarie, L.; Arvai, R.; Cumming, G. R.; Besnard, C.; Kundig, E. P. *Chem. Commun.* **2010**, *46*, 6264–6266.

(74) Cheng, B.; Sunderhaus, J. D.; Martin, S. F. *Org. Lett.* **2010**, *12*, 3622–3625.

(75) Karim, A. R.; Linden, A.; Baldridge, K. K.; Siegel, J. S. *Chem. Sci.* **2010**, *1*, 102–110

(76) Fürstner, A. *Chem. Commun.* **2011**, *47*, 6505–5611.

(77) James, D.; Escudier, J.-M.; Amigues, E.; Schulz, J.; Vitry, C.; Bordenave, T.; Szlosek-Pinaud, M.; Fouquet, E. *Tetrahedron Lett.* **2010**, *51*, 1230–1232.

(78) Chandra, R.; Oya, S.; Kung, M. P.; Hou, C.; Jin, L. W.; Kung, H. F. *J. Med. Chem.* **2007**, *50*, 2415–2423.

(79) Takahashi, S.; Kuroyama, Y.; Sonogashira, K.; Hagihara, N. *Synthesis* **1980**, 627–630.